Copyright is owned by the author of the thesis. Permission is given for a copy to be downloaded by an individual for the purpose of research and private study only. This thesis may not be reproduced elsewhere without the permission of the Author.

Biofilm Formation of *Pseudomonas* spp. at the Air-Liquid Interface, EPS Matrix Composition and Resistance to CIP Cleaning.

A thesis presented in partial fulfilment of the requirements for the degree of

Doctor of Philosophy

In

Food Technology

At Massey University, Palmerston North, New Zealand

Srinithi Muthuraman

2026

Highlights

- The temperature and substrate surface type strongly influenced biofilm formation of the dairy isolates in this study. The crystal violet values and cell counts were significantly ($p < 0.05$) higher at 4°C than 30°C and on biofilms formed on polystyrene surfaces than stainless steel for the strong biofilm-forming isolates.

- The surface differences strongly influenced the biofilm formation of the isolates. On a stainless-steel surface, the cells to EPS ratio was significantly ($p < 0.05$) higher compared to the polystyrene surface. These differences are reflected in the biofilm architecture. Compared to 30ºC, the cold temperatures encouraged significantly ($p < 0.05$) higher secretion of EPS components.

- The biofilm formation at the air-liquid interface encourages more cells, EPS production, and biofilm thickness compared with the submerged biofilm formation. *algK* and *bcsA* genes were upregulated 2-fold higher in the air-liquid interface biofilm cells.

- Psychrotrophic pseudomonads leave EPS footprints after cleaning with hot water (55ºC) and 1% NaOH (70ºC). The remaining footprints encouraged the early appearance of biofilm growth at the air-liquid interface of the strong biofilm formers. The growth of the biofilms on the footprints was more rapid than the growth on clean surfaces.

- Enzyme cleaners did not disperse the biofilms completely. The sequential treatment of NaOH and enzyme cleaners removed both cells and EPS. The regrowth was significantly ($p < 0.05$) less than that on acid-treated control coupons.

Abstract

Pseudomonads are known for their spoilage potential due to the production of thermostable enzymes and pigments. Pseudomonads can affect a wide range of processing environments, including dairy, poultry, meat, fish, and vegetable processing. The proteolytic, lipolytic and pectolytic enzyme production associated with pseudomonads was witnessed in the past. The high persistence of pseudomonads is observed due to their biofilm formation on food contact surfaces, especially under cold temperatures (e.g. 4°C) and at the air-liquid interface and submerged conditions. Despite the incidences reported of pseudomonad spoilage, limited information exists on their biofilm formation at cold temperatures, matrix compositional differences on food contact surfaces, and how the biofilm formation at cold temperatures affects the cleaning processes. This thesis addresses these research gaps by studying the biofilm formation and matrix composition of pseudomonads at cold temperatures and their control strategies.

Among the eleven isolates studied, two isolates, *P. lundensis* and *P. cedrina* were identified as strong biofilm formers at cold temperatures with higher biomass and cell counts. This study identified that these two isolates are cellulose-only producers and can form strong biofilms in the absence of curli fibres. The characterization of the extracellular polymeric substances EPS composition revealed that the cold temperatures encouraged increased matrix production with polysaccharides, proteins, and extracellular DNA, which resulted in complex biofilm architecture. The cell-to-EPS ratio was much higher in the biofilms formed on stainless-steel surfaces compared with those on polystyrene surfaces, explaining the influence of temperature and surface type on the biofilm formation of these isolates.

The air-liquid interface promoted higher EPS production, as confirmed by the overexpression of EPS-encoding genes in air-liquid interface biofilm cells compared to their submerged counterparts. These findings demonstrate the air-liquid interface as a favourable niche in the biofilm formation of pseudomonads. The cleaning simulation with traditional CIP revealed the EPS footprints left on the stainless-steel surface. The potential of these footprints during recolonisation was shown in both strong and weak biofilm formers. The removal of these footprints using commercial enzyme cleaners resulted in less aggressive biofilm formation during recolonisation.

Overall, this thesis addresses the critical research gaps in the biofilm formation of psychrotrophic pseudomonads under cold temperatures. Linking the EPS composition, biofilm architecture and at the different surfaces and interfaces provides practical insights improving cleaning and sanitation and finally reduces the spoilage incidents of these pseudomonad isolates.

Acknowledgments

I am profoundly grateful to my supervisor, Dr. Steve Flint, for accepting my PhD application and for his invaluable guidance and support throughout this journey. His insightful feedback and critical questions have significantly shaped this thesis. I want to express my sincere gratitude to Dr. Jon Palmer, without whom the SDS-PAGE experiment would not have been possible. Thank you for your expert guidance and continued support during my PhD.

My heartfelt thanks go to our Lab Manager, Ann-Marie Jackson, for her unwavering support throughout my PhD, even during the final writing stage. I have always admired her patience and exceptional organisational skills. This journey would not have been possible without you, Ann-Marie. I am deeply grateful to Baizura Zain, who patiently taught me the basics of molecular biology. Thank you, Baizura, for your generous help and encouragement. Special thanks to Anja Schieman for her valuable guidance in qPCR experiments.

Special thanks to Inge Mertz for her numerous occasions of assistance with the freeze dryer. I also extend my thanks to Rob, without your stainless-steel coupons, my experiments would not have been possible, and to Simon for providing the laser-cut polystyrene coupons.

To Krisha and Ili, thank you for being the amazing lab mates, officemates, and friends. I'll always cherish our daily venting sessions and the PhD memes we shared. I was fortunate to have such a wonderful team with whom I could share and discuss research ideas. Thanks to our seniors, Dana and Farah, for sharing their experiences, which helped me find my way. Thank you, Gloria, for all the tips and tricks with the microscope. To Dilushi, Hansani, and Van, thank you for the many memories. Thanks also to my officemates, Sujirtha and Prishanthi, for their friendship and support.

I am eternally grateful to my beloved Amma and Appa; I always feel your presence. Your words have shaped my life and driven me forward. I would also like to thank my Chithapa and Chithi, Santhana Krishnan and Chithra Devi, without whose support I would not have survived the initial years of my PhD and motherhood.

To Ammu, thank you for your constant support and for always being by my side through every challenge. To Dhamu, thank you for being an amazing (brother)-in-law and being with

us through all the struggles. A big thanks to the kids Aarav and Aarish for their delightful smiles, which brightened my days. Special thanks to Dhanya for the big smile, warm hugs and lots of love. Thanks to Bhuvana and Dinisha for being my best friends from school days and for all the supportive words during tough times. Lastly, thank you, Karthick, for your endless love, care, and support, the late-night lab visits, the delicious food, and for standing by me every step of the way.

Declaration

The presented thesis comprises eight chapters, including five with research work in this study. The partial contents of chapters 2, 3, 4, 5, 6, and 7 are structured as manuscripts that have either been published, submitted, or intended to be submitted to a journal.

Poster and Oral presentations

- Characterization of Pseudomonas biofilm Matrix. Oral Presentation, 2024 NZIFST conference, Hamilton, New Zealand.

- Biofilm formation of Psychrotrophic pseudomonads with different media. Poster Presentation 2024 NZIFST conference, Hamilton, New Zealand.

Publications

- Muthuraman, S., Flint, S., & Palmer, J. (2025). Characterization of the extracellular polymeric substances matrix of *Pseudomonas* biofilms formed at the air-liquid interface. *Food Bioscience*, *64*, 105918. https://doi.org/10.1016/j.fbio.2025.105918.

- Muthuraman, S., Flint, S., & Palmer, J. (2025). Extracellular polymeric substances – a real target in eliminating pseudomonad biofilms. *Food Bioscience*, (In press) DOI: https://doi.org/10.1016/j.fbio.2025.107330.

- Muthuraman, S., Palmer, J., & Flint, S. (2025). Enzymatic Dispersion of Pseudomonad Biofilms Grown at Psychrotrophic Temperature. *Food and Bioproducts Processing*, S0960308525002718. https://doi.org/10.1016/j.fbp.2025.12.015.

- Muthuraman, S., Palmer, J., & Flint, S. (2026). Air-liquid interface biofilm formation of pseudomonads and the impact of traditional clean-in-place on biofilm removal. *Food Research International*, *226*, 118215. https://doi.org/10.1016/j.foodres.2025.118215.

- Muthuraman, S., Palmer, J., & Flint, S. (2026). Sequential treatment of psychrotrophic pseudomonad biofilms with sodium hydroxide and commercial enzyme cleaners. *Food Control*, *182*, 111858 https://doi.org/10.1016/j.foodcont.2025.111858.

Table of Contents

Highlights ..... **iii**

Abstract ..... **iv**

Acknowledgments ..... **vi**

Poster and Oral presentations ..... **ix**

Publications ..... **ix**

List of Figures ..... **xvi**

List of Tables ..... **xx**

Abbreviations ..... **xxi**

Chapter 1. Introduction **1**

1.1 Background 2

1.2 Research questions 3

1.3 Research objectives 3

1.4 Research hypotheses 3

1.5 References 4

Chapter 2. Literature Review: EPS is a Real Target in Eliminating Pseudomonad Biofilms. **6**

2.1 Pseudomonads 7

2.2 Spoilage potential of pseudomonads 8

2.3 Biofilm formation of pseudomonads 9

2.4 Biofilm formation of the pseudomonads at the air-liquid interface 10

2.5 Robust biofilm formation at psychrotrophic temperatures 12

2.6 EPS produced by pseudomonads 13

2.7 Pseudomonads produce public goods 19

2.8 Biofilm-related genes in pseudomonads 20

2.9 Biofilm removal strategies 22
2.10 Pseudomonad biofilm footprints 31
2.11 Future research 33
2.12 Conclusion 34
2.13 References 34
Chapter 3 Biofilm-Forming Abilities of Psychrotrophic Pseudomonads 56
3.1 Introduction 58
3.2 Materials and methods 59
3.2.1 Bacterial isolates and culture conditions 59
3.2.2 Identification using PCR and 16S rDNA sequencing. 59
3.2.3 Biofilm formation 60
3.2.4 Congo Red Assay (CRA) 62
3.2.5 Levan production 62
3.2.6 Cellulose production 63
3.2.7 Data analysis 63
3.3 Results 64
3.3.1 Identification by PCR and partial 16S rDNA sequencing 64
3.3.2 Biofilm formation 64
3.3.3 Congo red assay (CRA) 74
3.3.4 Levan production 76
3.3.5 Quantification of Cellulose 76
3.4 Discussion 78
3.5 Conclusions 81
3.6 References 81
3.7 Supplementary Information 86
3.7.1 Composition of Tri Gene 86

Chapter 4 Characterisation of Biofilm Extracellular Polymeric Substances Matrix (EPS) Composition of Psychrotrophic Pseudomonads.....87

4.1 Introduction 89

4.2 Materials and Methods 90

4.2.1 Bacterial isolates and culture conditions 90

4.2.1.2 Biofilm formation on Stainless-steel coupons 91

4.2.2 Biofilm and planktonic growth 91

4.2.3 Microscopic observation 91

4.2.4 Isolation of EPS 93

4.2.5 Cellulose quantification 94

4.2.6 Polysaccharide Quantification 94

4.2.7 Protein quantification 95

4.2.8 Protein identification (LC-MS) 95

4.2.9 eDNA isolation and quantification 95

4.2.10 Data analysis 96

4.3 Results 96

4.3.1 Biofilm growth 96

4.3.2 Biofilm and planktonic cell enumeration 100

4.3.3 Biofilm EPS matrix composition 101

4.4 Discussion 111

4.5 Conclusion 116

4.6 References 116

4.7 Supplementary file 125

4.7.1 Cell counts over 14 days. 125

4.7.1 Microscopic observations. 128

Chapter 5 Air-Liquid Interface Biofilm Formation of Pseudomonads. 136

5.1 Introduction 138

5.2 Materials and Methods 139
5.2.1 Bacterial isolates and Culture conditions 139
5.2.2 CDC reactor conditions 139
5.2.3 Enumeration of biofilm cells 140
5.2.4 Quantification of Polysaccharides 141
5.2.5 Microscopic observations 141
5.2.6 Expression of EPS producing genes. 141
5.3 Results 144
5.3.1 Visible biofilm formation 144
5.3.2 Biofilm cell enumeration 145
5.3.3 Quantification of the polysaccharides 146
5.3.4 Microscopic observations 147
5.3.5 Expression of EPS producing genes. 148
5.4 Discussion 149
5.5 Conclusion 151
5.6 References 151
5.7 Supplementary Information 154
5.7.1 Doubling time and flow rate 154
5.7.2 EPS producing genes in this study and their functions 154
Chapter 6 Cleaning with NaOH, Footprints and Regrowth 155
6.1 Introduction 157
6.2 Materials and Methods 158
6.2.1 Bacterial isolates and Culture conditions 158
6.2.2 CDC reactor conditions 158
6.2.3 Enumeration of biofilm cells 158
6.2.4 Cleaning -in- Place (ClP) system 158
6.2.5 Microscopic observations 159

6.2.6 Attenuated Total Reflection – Fourier-transform infrared spectroscopy (ATR-FTIR) 159
6.2.7 Regrowth of the strong biofilm formers 159
6.2.8 Regrowth of the weak biofilm former 160
6.2.9 Data analysis 160
6.3 Results 161
6.3.1 Cell counts after CIP 161
6.3.2 Microscopic observations 162
6.3.3 ATR-FTIR spectra on EPS isolated from untreated and cleaned coupons 167
6.3.4 Regrowth of the strong biofilm former after CIP cleaning 169
6.3.5 Regrowth of the weak biofilm former after CIP cleaning 171
6.4 Discussion 174
6.5 Conclusion 176
6.6 References 176
6.7 Supplementary information 179
6.7.1. Elemental analysis of EPS and NaOH crystals. 179
6.7.2 Calcofluor white staining 181
6.7.3 The control coupons that underwent CIP were included in the FTIR observations 181
6.7.4 Congo red assay confirmation for weak biofilm formers 182
Chapter 7 Sequential Treatment of Biofilms with NaOH and Enzyme Cleaners 183
7.1 Introduction 185
7.2 Materials and methods 186
7.2.1 Bacterial isolates 186
7.2.2 Biofilm formation 186
7.2.3 Treating the biofilms with enzyme cleaners. 186
7.2.4 Treating the biofilms with NaOH and Enzyme cleaners 187
7.2.5 Microscopical observations 187

7.2.6 Attenuated Total Reflection- Fourier Transform Infrared Spectroscopy (ATR-FTIR) 187
7.2.7 Regrowth after CIP+ enzymatic cleaners 188
7.2.8 Data analysis 188
7.3 Results 189
7.3.1 Treating the biofilms with enzyme cleaners 189
7.3.2 NaOH + Enzyme cleaners 192
7.3.3 ATR-FTIR observations of EPS after treating with enzyme cleaners 196
7.3.4 Regrowth 198
7.4 Discussion 199
7.5 Conclusion 202
7.6 References 202
7.7 Supplementary File 206
7.7.1 ATR-FTIR observations of enzyme cleaners, and EPS isolated after cleaning with enzyme cleaners. 206
Chapter 8 Final Discussion 207
8.1 Final discussion 208
8.2 Limitations 209
8.3 Future work 211
8.4 Final conclusions 212
Appendices 216
Appendix I. Statement of contribution- Chapter 2 216
Appendix II. Statement of contribution- Chapter 3 217
Appendix III. Statement of contribution- Chapter 4 218
Appendix IV. Statement of contribution- Chapters 5&6 219
Appendix V. Statement of contribution- Chapters 5&7 220

List of Figures

Figure 2.1 Biofilm formation of pseudomonads at the air-liquid and liquid-liquid interfaces (Created in https://BioRender.com). 12

Figure 2.2 Biofilm formation of pseudomonads at psychrotrophic temperatures by reducing motility and matrix overproduction (Created in https://BioRender.com). 13

Figure 2.3 The ci-di-GMP regulation pathways in biofilm EPS synthesis in pseudomonads 21

Figure 2.4 Biofilm prevention and eradication strategies of pseudomonads (Created in https://BioRender.com). 31

Figure 2.5 Biofilm footprints of pseudomonads after antimicrobial treatment or cleaning and the robust biofilm formation on the footprints by new occupant cells (Created in https://BioRender.com). 32

Figure 3.1(A) OD570 values from the crystal violet assay at 30°C with half-strength TSB and (B) the cell counts at 30°C with half-strength TSB 68

Figure 3.2 (A) OD_{570} values from the crystal violet assay at 4°C with half-strength TSB and (B) the cell counts at 4°C ith half-strength TSB 70

Figure 3.3 (A) OD_{570} values from the crystal violet assay at 30°C with half-strength TSB on a stainless-steel surface and (B) the cell counts at 30°C with half-strength TSB. 72

Figure 3.4 (A) OD_{570} values from the crystal violet assay at 4°C with half-strength TSB on a stainless-steel surface and (B) the cell counts at 4°C with half-strength TSB 73

Figure 3.5 (A) Pink, dry, and rough colonies (*Pdar*, Isolate 3SM), (B) Brown, dry, and rough colonies (*Bdar*, Isolate 1SM), White and smooth colonies (44SM), (D) Blue coloured colonies (Isolate 6SM). 75

Figure 3.6 (A) mucoid colonies indicating Levan (Isolate 6SM), (B) non-mucoid colonies (Isolate 2SM), (C) sticky when touched with an inoculation loop, (D) non-mucoid colonies. 76

Figure 3.7 (A) Standard curve with microcrystalline cellulose concentration 25 to 100 mg/ mL, (B) Cellulose quantification 78

Figure 4.1 Visible biofilms on polystyrene surface at 30°C, 7°C, and 4°C at the end of two weeks. Blue arrows indicate the air-liquid interface biofilms. (A) represents the visible biofilms formed by isolate 3SM, while (B) shows the visible biofilms formed by isolate 20SM. 97

Figure 4.2 Visible biofilm formation on stainless-steel surface at 30°C, 7°C, and 4°C at the end of two weeks. (A)shows the visible biofilms formed by isolate 3SM, while (B) shows the biofilms of isolate 20SM. 97
Figure 4.3 The biofilm growth on polystyrene surface, (A) Biofilm of isolate 3SM at 24h, which shows the ringlike structures, while (B) biofilm of isolate 3SM on the 14th day, which shows the cells grown around the ringlike structure (Scale bar 10µm).....98
Figure 4.4 Filamentous cells in the biofilm. (A) Filamentous cells grown in a semi-solid medium,(B) Semi-solid medium (TSB with 0.2% agar) with culture (C) Biofilms grown on stainless-steel surface for the isolates 3SM (Scale bar 10µm). 99
Figure 4.5 Pellicles stained with Acridine Orange at 30°C, 7°C, and 4°C from the planktonic cultures of the isolate 3SM(Scale bar 10µm). 100
Figure 4.6 Graph A shows the standard microcrystalline cellulose curve from 30 mg/mL to 100mg/mL. Graph B shows the quantity of cellulose isolated from the EPS of biofilms and the planktonic cell-free supernatant after two weeks of incubation 102
Figure 4.7 Graph A shows the standard curve for D-Glucose from 200µg/mL to 1mg/mL. Graph B shows the total polysaccharide concentration from the biofilm EPS and Planktonic cell-free supernatant 104
Figure 4.8 (A) Isolate 3SM on a polystyrene surface at the end of two weeks, White arrows indicate the spots where EPS entirely covered the cells(Scale bar 10µm). (B) Isolate 3SM on a polystyrene surface (Scale bar 100µm).....105
Figure 4.9 The graph here represents the concentration of eDNA present in the biofilms grown on stainless-steel and polystyrene surfaces and the planktonic cell-free supernatant.....106
Figure 4.11 Graph A shows the standard curve for Bovine serum albumin from 50µg/mL to 1mg/mL. Graph B shows the total protein concentrations from the biofilm EPS formed on stainless-steel and polystyrene surfaces and the proteins from planktonic CFS 109
Figure 4.12 (A) represents the proteins isolated from Gel electrophoresis of isolate 3SM while (B)shows the bands from isolate 20SM.....110
Figure 5.1 The CDC reactor setup in this study at 4ºC.....140
Figure 5.2 The visible biofilm formation of isolate 3SM observed on A-L, L1, and L2 coupons at 168 h at 4ºC. 144
Figure 5.3 Graph A shows the cell counts from isolate 3SM over seven days. Graph B shows the cell counts from isolate 20SM 146

Figure 5.4 Graph A shows the quantity of EPS recovered from the A-L, L1, and L2 coupons. Graph B shows the total polysaccharides from the isolated EPS recovered from A-L, L1, and L2 coupons.....147
Figure 5.5 Epifluorescence microscopic images of (A) Isolate 3SM at the end of 168 h, (B) Isolate 20SM at the end of 168 h (Scale bar 10µm).....147
Figure 5.6 SEM images of (A) Isolate 3SM at the end of 168 h, (B) Isolate 20SM at the end of 168 h (Scale bar 10µm).....148
Figure 5.7 Gene expression differences in EPS producing genes between air-liquid interface and submerged biofilm cells.....149
Figure 6.1 Schematic representation of the CIP process and regrowth 160
Figure 6.2 The cell counts from untreated control coupons, hot water-treated coupons (55ºC for 10 min), and NaOH-treated (70ºC for 10 min) coupons.....161
Figure 6.3 (A)& (B) SEM images of 3SM and 20SM untreated coupons, (C) & (D)SEM images of hot water-treated coupons of isolates 3SM and 20SM, and (D) & (F) SEM images of NaOH-treated coupons of isolates 3SM and 20SM.....164
Figure 6.5 (A) ATR-FTIR images of the EPS isolated from untreated, hot water washed, and NaOH washed coupons from isolate 3SM and (B) 20SM.....168
Figure 6.6 Graph A shows the regrowth of isolate 3SM after CIP cleaning, while Graph B shows the isolate 20SM after CIP cleaning 170
Figure 6.7 (A) shows the cell counts of the weak biofilm former 44SM on control clean coupons A-L, L1, and L2 after a week of incubation. (B) shows the coupons at 24 h and 48 h, showing no visible biofilm formation. (C) shows the microscopic images of the weak biofilm former 44SM after a week of incubation.....172
Figure 6.7 (A) shows the cell counts from the control clean coupons and CIP coupons of the weak biofilm former 44SM. All the results are expressed as mean ± standard deviation.(B) Blue arrows show the appearance of air-liquid interface biofilms on the CIP cleaned coupons. (C) Microscopic images show the biofilms formed on the control and CIP cleaned coupons.....173
Figure 7.1 (A) Cell counts of biofilms formed by isolate 3SM after treating with commercial enzyme cleaners, (B) Cell counts of isolate 20SM biofilms after treating with commercial enzyme cleaners.....190
Figure 7.2 (A) & (B) EnduroZyme-treated coupons of isolate 3SM and 20SM, (C) & (D) DualZyme-treated coupons of isolates 3SM and 20SM, (E) & (F) TriZyme-treated coupons of isolates 3SM and 20SM. 192

Figure 7.3 Epifluorescence microscopic images of (A) & (B) NaOH + Enduro Zyme treated coupons of isolates 3SM and 20SM, (C) & (D) NaOH+Dua lZyme treated coupons of isolates 3SM and 20SM, (E) & (D) NaOH+Tri Zyme treated coupons of isolates 3SM and 20SM.....194

Figure 7.4 Scanning electron microscope images of (A) & (B) NaOH+ Enduro Zyme treated coupons of isolates 3SM and 20SM, (C) & (D) NaOH + Dual Zyme treated coupons of isolates 3SM and 20SM, (E) & (F) NaOH +Tri Zyme treated coupons of isolates 3SM and 20SM, (G) acid treated control coupons. 196

Figure 7.5 ATR-FTIR images of untreated, NaOH, and NaOH+ Enzyme treated coupons of isolates (A) 3SM and (B) 20SM. 198

Figure 7.6 Graph (A) shows the regrowth of isolate 3SM after CIP+EnduroZyme cleaning, while graph (B) shows the regrowth of isolate 20SM. 199

List of Tables

Table 2.1 Components of EPS present in the pseudomonad biofilms.....14

Table 3.1 Classification of biofilm formation. 61

Table 3.2 Identification by PCR and partial 16S rDNA sequencing 64

Table 3.3 Colony morphology observed with Congo Red Assay.....74

Table 4.1 Biofilm cell counts at the end of two weeks.....100

Table 4.2 Planktonic cell counts at the end of two weeks. 101

Table 4.3 Proteins identified from the biofilms of 3SM and 20SM grown at 4°C on stainless-steel coupons.....111

Table 6.1 Reynolds number.....159

Table 7.1 Enzyme cleaners used in this study 186

Abbreviations

A-L	Air-Liquid Interface coupons
ANOVA	Analysis of variance
ATR- FTIR	Attenuated Total Reflectance – Fourier Transform Infra-Red spectroscopy
CDC	Centre for Disease Control
CFU	Colony Forming Unit
CIP	Clean- In- Place
cm	Centimetre
CRA	Congo Red Assay
CV	Crystal Violet
DAPI	4′,6-Diamidino-2-Phenylindole
DNA	Deoxyribonucleic Acid
eDNA	Extracellular DNA
EPS	Extracellular Polymeric Substances
FITC	Fluorescein Isothiocyanate
h	Hours
kDa	Kilo Daltans
L1	Submerged coupon 1
L2	Submerged coupon 2
LC-MS/MS	Liquid Chromatography coupled with Mass Spectrometry

mg	Milligrams
min	Minutes
mL	Milli litre
RNA	Ribo Nucleic Acid
SDS- PAGE	Sodium Dodecyl Sulphate Poly Acrylamide Gel Electrophoresis
SEM	Scanning Electron Microscopy
SLAM	Surface Localised Antimicrobial Microparticles
TRITC	Tetramethyl Rhodamine Iso Thio Cyanate
TSA	Tryptic Soy Agar
TSB	Tryptic Soy Broth

Chapter 1. Introduction

1.1 Background

Pseudomonads are unicellular rod-shaped bacteria with polar flagella. Pseudomonads belong to the group of Gammaproteobacteria (Molina et al., 2013; Raposo et al., 2016). The genus *Pseudomonas* is a non-spore-forming and non-pathogenic bacterium; however, some species of pseudomonads are opportunistic pathogens (*P. aeruginosa*) and phytopathogens (*P. syringae*) (Silby et al., 2011) but are not a food safety issue. A complex enzyme system enables these organisms to have metabolic versatility. Pseudomonads can be fluorescent or non-fluorescent, and most species are psychotropic (Franzetti & Scarpellini, 2007). There have been incidents of *Pseudomonas* spp. contamination affecting the food quality in dairy, poultry, and meat processing conditions (Nychas et al., 2008).

Thermostable proteolytic and lipolytic enzymes produced by pseudomonads can cause curdling and gelation of milk even after pasteurization, due to post-pasteurisation contamination (Weidmann et al.,2000). These bacteria can produce thermostable pigments, which cause discoloration of foods (Chiesa et al., 2014). Pseudomonads can form biofilms that can accommodate some pathogenic bacteria, which pose a food safety risk (Puga et al., 2018).

Biofilms are dense aggregations of cells and an extracellular polymeric substance (EPS) matrix that attach to a surface. Biofilm formation occurs whenever there are situations unsuitable for planktonic growth (Flemming & Wingender, 2010). Pseudomonads can form biofilms in a wide range of temperatures (Wickramasinghe et al., 2019; Kim et al., 2020). Pseudomonad biofilms are hard to eliminate from the food processing surfaces. The interaction between bacterial cells and the substrate is significantly stronger than the cohesive forces between individual cells and is difficult to remove by the cleaning-in-place (CIP) process, remaining a source of continuous contamination in food processing environments (Bénézech & Faille, 2018).

Understanding the mechanisms behind the biofilm formation of pseudomonads and their EPS composition will help to develop strategies to combat these biofilms. This research aims to overcome the limitations of the current CIP process and explore strategies to ensure better biofilm removal in food industries.

1.2 Research questions

(a) What phenotypes of pseudomonads form robust biofilms at cold temperatures and at the air-liquid interface?
(b) What are all the compositional differences in the EPS between different surfaces and temperatures?
(c) Can the surface type affect biofilm architecture of pseudomonads?
(d) What are the key differences between the air-liquid interface and submerged biofilms?
(e) What is the mechanism behind the persistence of pseudomonad biofilms after CIP?
(f) What are the available strategies to eliminate these biofilms?

1.3 Research objectives

(a) Explore the biofilm-forming abilities of psychrotrophic pseudomonads on different surface types under optimal and cold temperatures.
(b) Explore the compositional differences in EPS between the different temperatures
(c) Compare the air-liquid interface and submerged biofilm formation.
(d) Explore whether the leftover EPS after cleaning can enhance the biofilm formation

1.4 Research hypotheses

Despite considerable research on pseudomonad biofilms, food spoilage and product loss by these bacteria still exist. Studies demonstrated the robust biofilm formation of pseudomonads at cold temperatures and the failure of cleaning chemicals due to the reduced diffusivity of the EPS. From the literature, the biofilm formation of pseudomonads is mostly studied in the submerged systems, and the air-liquid interface biofilm formation of these bacteria is not much considered in the food biofilm studies. Our preliminary experiments revealed that these isolates form strong biofilms at the air-liquid interface. Based on the findings and gaps identified from the literature, the following hypotheses were formulated.

(a) Dairy isolates of *Pseudomonas* spp. form the most biofilms under refrigeration, at the air-liquid interface and on stainless-steel surfaces.

(b) EPS overproduction is enhanced in cold temperatures more than simply increased bacterial numbers.

(c) Residual EPS after cleaning enhances subsequent biofilm formation, and this can be improved with enzyme cleaning.

1.5 References

Bénézech, T., & Faille, C. (2018). Two-phase kinetics of biofilm removal during CIP. Respective roles of mechanical and chemical effects on the detachment of single cells vs cell clusters from a *Pseudomonas fluorescens* biofilm. *Journal of Food Engineering*, *219*, 121–128. https://doi.org/10.1016/j.jfoodeng.2017.09.013.

Chiesa, F., Lomonaco, S., Nucera, D., Garoglio, D., Dalmasso, A., & Civera, T.(2014). distribution of *Pseudomonas* species in a dairy plant affected by occasional blue discoloration. *Italian Journal of Food Safety*, *3*(4). https://doi.org/10.4081/ijfs.2014.1722.

Flemming, H.-C., & Wingender, J. (2010). The biofilm matrix. *Nature Reviews Microbiology*, *8*(9), 623–633. https://doi.org/10.1038/nrmicro2415

Franzetti, L., & Scarpellini, M. (2007). Characterisation of *Pseudomonas* spp. Isolated from foods. *Annals of Microbiology*, *57*(1), 39–47. https://doi.org/10.1007/BF03175048

Kim, S., Li, X.-H., Hwang, H.-J., & Lee, J.-H. (2020). Thermoregulation of *Pseudomonas aeruginosa* Biofilm Formation. *Applied and Environmental Microbiology*, *86*(22), e01584-20. https://doi.org/10.1128/AEM.01584-20

Molina, G., Pimentel, M. R., & Pastore, G. M. (2013). *Pseudomonas*: A promising biocatalyst for the bioconversion of terpenes. *Applied Microbiology and Biotechnology*, *97*(5), 1851–1864. https://doi.org/10.1007/s00253-013-4701-8

Nychas, G.-J. E., Skandamis, P. N., Tassou, C. C., & Koutsoumanis, K. P. (2008). Meat spoilage during distribution. *Meat Science*, *78*(1–2), 77–89. https://doi.org/10.1016/j.meatsci.2007.06.020

Puga, C. H., Dahdouh, E., SanJose, C., & Orgaz, B. (2018). *Listeria monocytogenes* Colonizes *Pseudomonas fluorescens* Biofilms and Induces Matrix Over-Production. *Frontiers in Microbiology*, *9*, 1706. https://doi.org/10.3389/fmicb.2018.01706

Raposo, A., Pérez, E., De Faria, C. T., Ferrús, M. A., & Carrascosa, C. (2016). Food Spoilage by *Pseudomonas* spp.—An Overview. In O. V. Singh (Ed.), *Foodborne Pathogens and Antibiotic Resistance* (1st ed., pp. 41–71). Wiley. https://doi.org/10.1002/9781119139188.ch3.

Silby, M. W., Winstanley, C., Godfrey, S. A. C., Levy, S. B., & Jackson, R. W. (2011). *Pseudomonas* genomes: Diverse and adaptable. *FEMS Microbiology Reviews*, *35*(4), 652–680. https://doi.org/10.1111/j.1574-6976.2011.00269.x

Wickramasinghe, N. N., Ravensdale, J. T., Coorey, R., Dykes, G. A., & Scott Chandry, P. (2019). *In situ* characterisation of biofilms formed by psychrotrophic meat spoilage pseudomonads. *Biofouling*, *35*(8), 840–855. https://doi.org/10.1080/08927014.2019.1669021

Wiedmann, M., Weilmeier, D., Dineen, S. S., Ralyea, R., & Boor, K. J.,2000. Molecular and phenotypic characterization of *Pseudomonas* spp. isolated from milk. *Applied and EnvironmentalMicrobiology*, *66*(5)20852095. https://doi.org/10.1128/AEM.66.5.2085-2095.2000.

Chapter 2. Literature Review: EPS is a Real Target in Eliminating Pseudomonad Biofilms.

This chapter is an adaptation of material that was published as a peer-reviewed article:

Muthuraman, S., Flint, S., & Palmer, J. (2025). Extracellular polymeric substances – a real target in eliminating pseudomonad biofilms. *Food Bioscience*, DOI: 10.1016/j.fbio.2025.107330.

2.1 Pseudomonads

Food spoilage by microbial contamination affects the final quality of food products, interferes with processing time, and sometimes leads to economic loss (Teh et al., 2011). Pseudomonads are one such bacterial genus dominating the cold food processing conditions. In Italy, 70,000 packs of Mozzarella cheese were withdrawn from the market due to contamination and blue pigment production with *Pseudomonas fluorescens* during June 2010 (Del Olmo et al., 2018). A recent study on isolating pseudomonads from the minced and frozen meat from supermarkets revealed that pseudomonads are the predominant bacteria in minced beef (76%) and imported frozen meat (48%) (Wehedy et al., 2025). Biofilms formed by these bacteria are a source of thermostable enzymes, pigments that affect the quality of food and provide nutrients to the cells (Teh et al., 2012). The ability to grow and form biofilms at psychrotrophic temperatures, resistance to environmental stress, thrive on simple nutrients, and adhere to both biotic and abiotic surfaces are the reasons for their persistence in the food processing environments (Sterniša et al., 2023; Saá Ibusquiza et al., 2012). The robust EPS (Extracellular Polymeric Substances) matrix can accommodate low EPS producers and pathogens, which can be a food safety threat (Puga et al., 2018).

Pseudomonas spp. are non-spore-forming, Gram-negative rods with flagella. *Pseudomonas* spp. are the most studied bacterial genera among gram-negative bacteria (Silby et al., 2011). Pseudomonads fail to grow under pH 4.5 (acidic conditions), are chemoorganotrophs, oxidase-positive or negative, and catalase-positive (Lalucat et al., 2022). Some of the pseudomonads are opportunistic pathogens and phytopathogens. However, most pseudomonads are non-pathogenic (Molina et al., 2013). Pseudomonads are strict aerobic bacteria with respiratory metabolism, where oxygen is the terminal electron acceptor. However, in some pseudomonads, nitrogen can act as a terminal electron acceptor and allow them to grow under anaerobic conditions (Lalucat et al., 2022). Arginine fermentation via the arginine deiminase pathway (ADI) provides energy and glucose fermentation to ethanol via the Entner-Doudoroff pathway and contributes to long-term survival under anaerobic conditions (Kolbeck et al., 2021). Group 1 pseudomonads are psychrotrophic, fluorescent, or non-fluorescent and known for their history of food spoilage. The well-known fluorescent species are *P. fluorescens*, *P. putida*, *P. aeruginosa,* and *P. chlororaphis* (Kumar et al., 2019).

A complex enzymatic system enables good metabolic versatility among these *Pseudomonas* species (Silby et al., 2011).

The optimum growth temperatures for most *Pseudomonas* species are between 25°C and 30°C. However, some pseudomonads can grow up to 45°C and as low as 0°C (Tribelli & López, 2022). Pseudomonads produce a range of proteolytic, lipolytic, and pectolytic enzymes. Proteolytic and lipolytic enzymes are often associated with the spoilage of meat, poultry, and dairy, where they break down the proteins and lipids and produce rancid odours. *P. fluorescens*, *P. viridiflava* are responsible for the spoilage of fresh fruits and vegetables due to pectolytic enzymes (Kumar et al., 2019). *Pseudomonas* spp. secretes pigments such as pyoverdine (Fluorescein), a yellow pigment, and pyocyanin, a blue pigment (Lau et al., 2004). The prevalence of *P. fluorescens* in the milk indicates the possible spoilage of milk (Ahmed & Hassan, 2024). Pseudomonads form biofilms on both biotic and abiotic surfaces. Biofilms provide a source of bacteria and enzymes contributing to spoilage in food (Machado et al.,2017). *P. aeruginosa* is considered a model organism for biofilm formation studies (McDougald et al., 2008). This chapter focuses on different aspects of biofilm formation of psychrotrophic pseudomonads and how pseudomonad biofilms persist in food processing environments.

2.2 Spoilage potential of pseudomonads

The presence of the *aprX* gene is positively correlated with the proteolytic activity of spoilage pseudomonads isolated from dairy, meat, and vegetable processing sources (Kumar et al., 2019; Caldera et al., 2016). The important extracellular protease in *Pseudomonas* spp is alkaline metalloprotease (apr), which is controlled by the *aprX* genes (Wang et al., 2021). The casein degradation in milk is solely achieved by the protease enzymes through the *aprX* genes (Woods et al.,2001). Many of the proteases from pseudomonads belong to the class of metallopeptidases (EC 3.4.24) (Caldera et al., 2016). Pseudomonads isolated from raw milk with high protease activity have a greater number of functional protease genes (including *aprX*) encoding carbohydrate transport and metabolism, signal transduction, synthesis, transport, and metabolism of secondary metabolites, polysaccharide lytic enzymes, sugar esterase, and show a higher multidrug resistance index (Du et al., 2023).

Pseudomonads produce high levels of peptidases at 25°C, followed by 10, 7, 4 and 2°C. However, the peptidase activity is reduced from 10 to 2°C; consequently, storing and

transporting milk between 1 to 3°C is recommended since the proteolytic activity is lower around this temperature range (Meng et al., 2017). The dairy isolates of *P. aeruginosa* and *P. fluorescens* showed no proteolytic and lipolytic activity at 4 °C and higher activity at 20°C. In one published study of *Pseudomonas* spp, two isolates showed only proteolytic activity, three showed lipolytic activity, and five showed both proteolytic and lipolytic activity (Hoda Mahrous, 2012).

Another homologous gene to *aprX* identified in *P. fragi* is *aprD*, which is known to affect biofilm formation. In *P. fragi, aprD* regulates the protease secretion and inversely affects auto-aggregation, swimming motility, and biofilm formation (Wang et al., 2021). The mutants still produce slime and off-flavour, while with the *aprD* gene, the proteolytic effect was well pronounced (Wang et al., 2021). In sheep milk stored at 4°C, a higher expression of the *aprX* gene is found in *P. putida*, *P. fluorescens,* and *P. aeruginosa,* showing the spoilage potential of these psychrotrophs at cold temperatures. Sheep milk stored at 9°C facilitated the lipolytic activity of *P. putida* (Bruzaroski et al., 2023).

AHLs (N-acyl-homoserine lactones) are known as autoinducers in the quorum-sensing system, which can also modulate the spoilage characteristics of pseudomonads. When the Exogenous AHLs (C6-HSL N-hexanoyl homoserine lactone) were added to the growth medium of *P. korensis* PS1, it increased the protease and lipase activity, cell density, accelerated the decomposition of chilled pork (4ºC), and increased production of total volatile base nitrogen content (TVB-N) (Dai et al., 2022b). The ability of pseudomonads to produce the AHLs is weaker than *Aeromonas, Acetobacter* and *Serratia* (Li et al., 2019). However, pseudomonads can utilise the AHLs from the environment, which may accelerate the decomposition of chilled products, as confirmed by Dai et al.(2022b). AHLs are involved in quorum sensing (Li et al., 2019). However, the molecular mechanisms behind AHL-mediated quorum sensing and spoilage enzymes need to be studied.

2.3 Biofilm formation of pseudomonads

Biofilm formation by pseudomonads consists of a series of sequential stages. Stressed cells attach to the biotic or abiotic surface, which is known as the reversible attachment (Stage 1) (Hinsa et al.,2003). High levels of intracellular c-di-GMP facilitate the production of adhesins and the initial attachment (Fazli et al., 2014). This stage of biofilm formation is usually considered weak and can be easily disrupted (Hinsa et al.,2003). When cells attach to the long axis, a monolayer of cells is formed, which is known as irreversible attachment (Stage 2)

(O'Toole et al.,2000; Hinsa et al.,2003). Microcolonies (Stage 3) will be formed from the monolayer of cells and develop into mature biofilms (Stage 4). Finally, the low levels of cyclic c-di-GMP downregulate the production of adhesins and extracellular polymeric substances and lead to dispersion (Stage 5) (Fazli et al., 2014).

The timeline to reach the 5 stages of biofilm formation varies among the species, and this variation is even observed across strains. A study based on biofilm formation of isolates from the meat industry showed that the initial attachment of *P. lundensis* occurred after 2 h of post-inoculation, and most of the population adhered after 4 h of inoculation. After initial attachment, the cells started producing extracellular matrix substances, which produced notable biofilm structures (Liu et al.,2015). The biofilm formation of *P. putida* increases after 4 to 6 h of incubation, and this gradually decreases when the biofilm attains maturity (24 h) (Puhm et al.,2022).

Pseudomonads form biofilms on both biotic such as sprouts, spinach, lettuce, meat, seafood and abiotic surfaces, such as floors, walls, pipes, drains and foot contact surfaces (Meliani & Bensoltane, 2015). Pseudomonads form biofilms on meat surfaces, as reported by several studies (Liu et al., 2015; Wickramasinghe et al., 2020). *P. fragi* and *P. lundensis* form biofilms on the meat surface and produce a slimy layer (Wickramasinghe et al., 2019). Several studies reported the biofilm formation of pseudomonads on stainless steel, which is a common surface in the food processing environment (Zarei et al., 2022; Liu et al., 2023; Santos Rosado Castro et al., 2021).

Biofilm EPS acts as a nutrient reservoir, protects the cells from desiccation and resists other antimicrobials (Mann & Wozniak, 2012). *P. fluorescens* C224 planktonic cells showed proteolytic activity at 20 and 30°C, and no growth at 37°C, while the biofilm cells grown on a stainless-steel surface showed proteolytic activity at 20, 30, and 37°C. Biofilm formation facilitated the growth of this pseudomonad at 37ºC (Teh et al., 2012).

2.4 Biofilm formation of the pseudomonads at the air-liquid interface

Surfaces and different interfaces affect the biofilm formation, including initial attachment, biofilm maturation, detachment, and interaction with environmental factors (Ye et al., 2022). Pseudomonads can form biofilms on different interfaces, such as air-liquid interface, liquid-liquid interface, and solid-liquid interfaces (Meliani & Bensoltane, 2015). The spoiled-meat-

associated *Pseudomonas* spp. show 88% of the isolates form biofilms at the air-liquid interface, indicating the deep-rooted ability within the genus (Robertson et al., 2013). Flagella play an important role in the air-liquid interface biofilm formation of pseudomonads. The thick air-liquid interface biofilm formation appeared from 48-144h (Sung et al.,2024). Proteins involved in flagellar structure, type I and IV secretion systems, alginate/siderophore synthesis, quorum sensing, and c-di-GMP signalling exhibited significant upregulation between 48 h to 72 h in the air-liquid interface biofilms of *P. aeruginosa,* indicating the importance of the air-liquid interfaces (Sung et al.,2024). Cellulose is an insoluble polymer involved in the air-liquid interface biofilm formation. Secretion of cellulose and other polymers in the meniscus is seen in wrinkly spreaders (Wps), the air-water surface (Aws), and the micro-water-surface (Mws) biofilm formation in *P. fluorescens* SBW25 (Ardré et al., 2019). When the shear stress was introduced (Tw=0.3 Pa), the cell counts of *P. aeruginosa* on the air-liquid interface biofilms were not affected, while the submerged biofilms showed lower cell counts compared to stress-free conditions (Zhang et al., 2022). The morphology of the biofilms formed at the liquid -liquid interface (with shear stress) was heterogeneous with ridges and dome-like structures, while on the air-liquid interface, it was multiple layers of cells. This morphological difference affects the biofilm permeability; the submerged biofilms were 2-fold more permeable than the air-liquid interface biofilms (Zhang et al., 2022). The biofilms formed at the air-liquid interface can be a hundred times more resistant to antimicrobials than the submerged biofilms due to the EPS overproduction acting as a physical barrier (Tan et al., 2024). The air-liquid interface biofilms provide the bacteria with oxygen and nutrients, while the submerged conditions provide nutrients with limited oxygen (Fig. 2.1) (Ye et al., 2022). Most of the biofilm formation models, such as microtiter plates, CDC (Centre for Disease Control) biofilm reactors, Calgary devices, and rotating biofilm reactors, often focus on biofilm formation at the solid-liquid interface or submerged conditions. However, the air-liquid interface biofilm formation influences attachment, nutrient uptake, and mass exchange (Zhang et al., 2022). Cleaning of the air-liquid interface and submerged biofilms of *P. aeruginosa* PAO1 revealed that the air-liquid interface biofilms require twice the MBEC (Minimal biofilm eradication concentration) of cleaning chemicals than the liquid-liquid biofilms (Ye et al., 2022). The physical disruption of these air-liquid interface biofilms results in fragments, flocs, and slimes. Compared to individual bacteria, these aggregates will be more effective in new colonisation after dispersion (Robertson et al., 2013). The air-liquid interface is often seen in food processing environments such as partly

filled tanks, storage silos, and residual liquid after cleaning. Biofilm formation at the air-liquid interface leads to serious contamination and resistance to cleaning (Jha et al., 2020).

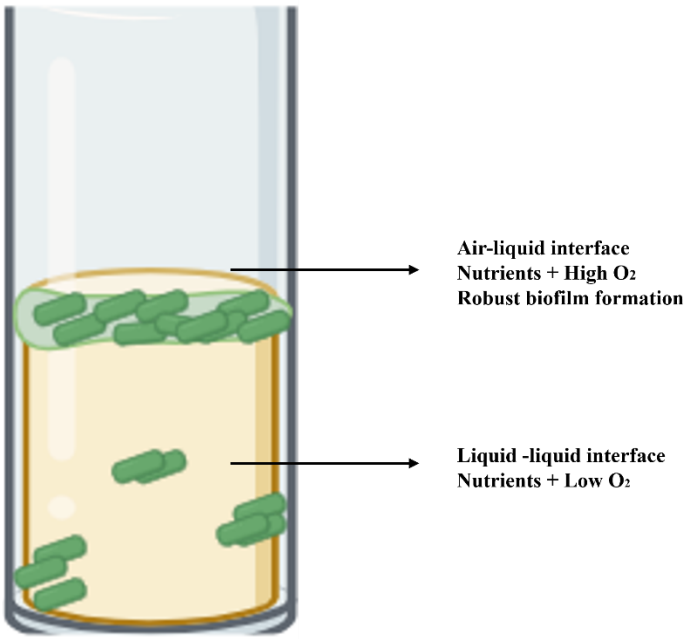

Figure 2.1 Biofilm formation of pseudomonads at the air-liquid and liquid-liquid interfaces (Created in https://BioRender.com).

2.5 Robust biofilm formation at psychrotrophic temperatures

Cold temperatures in food processing are used to limit microbial activity. However, the pseudomonads can form robust biofilms in cold processing conditions (Liu et al., 2023). Cold temperatures result in reduced motility, caused by the downregulation of flagellar genes and encourage the switch from planktonic cells to biofilms (Fig. 2.2). At 4°C, the swimming motility was completely repressed, and higher biofilm formation was observed (Guttenplan & Kearns, 2013). While the metabolic rate is lowered at refrigerated temperatures, the bacteria can still survive, multiply, and form uniform layers of biofilms. When the pseudomonads were allowed to form biofilms at 4°C and 10°C, the planktonic cells were completely absent after 7 days for 4°C-grown biofilms and 3 days at 10 °C. This indicates the absence of planktonic cells in the mature biofilms (Wickramasinghe et al., 2019). Another important molecule in biofilm formation is cyclic di-GMP, which can suppress flagella-mediated swimming and promote matrix overproduction (McDougald et al., 2012). Genes regulating the biosynthesis of alginate, cellulose, and colonic acid are highly expressed in *P. fragi* biofilms grown in meat processing conditions at 10°C (Wagner et al., 2021). Psychrotrophic

pseudomonads overcome cold stress by different mechanisms such as over-expression of Cap, Csp proteins, cell membrane adaptations, dense and rigid biofilm formation, down-regulation of flagellar motility, overexpression of antioxidant enzymes, no mitochondrial swelling, accumulation of osmotic solutes and amino acids and, upregulation of cryoprotective amines (Chauhan et al., 2013).

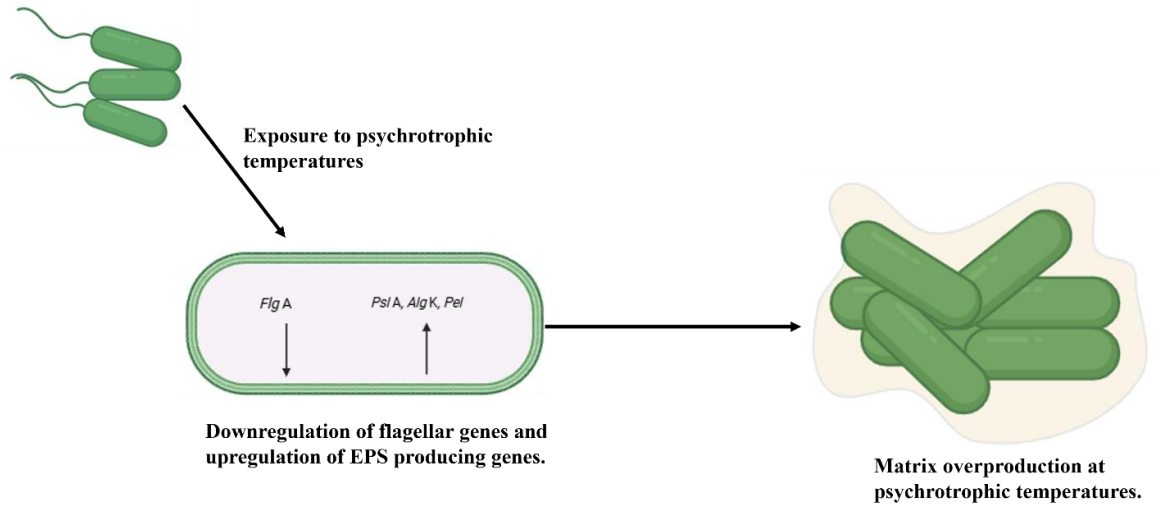

Figure 2.2 Biofilm formation of pseudomonads at psychrotrophic temperatures by reducing motility and matrix overproduction (Created in https://BioRender.com).

The robust biofilm formation at low temperatures is achieved by reducing the growth rate and matrix overproduction. The psychrotrophic pseudomonad biofilms grown at 25 °C (6.5 days) and 4°C (5 days) reached similar cell counts in the matured phase, but at 4°C, the overproduction of exopolysaccharides and proteins was observed (Wickramasinghe et al., 2020). The stress created by low temperatures can stimulate the EPS production of these psychrotrophic pseudomonads. The matrix overproduction is achieved by upregulating the exopolysaccharides-producing genes such as *algK* and *pslA* at 4°C (Liu et al., 2023).

2.6 EPS produced by pseudomonads

Pseudomonad biofilm EPS is composed of insoluble, soluble, and capsular polysaccharides, proteins, and eDNA (Table 2.1), and the matrix overproduction is observed at the psychrotrophic temperatures (Wickramasinghe et al., 2020; Liu et al., 2023; Muthuraman et al., 2025). Psl, Pel, alginate, and cellulose are the common polysaccharides found in pseudomonad biofilms (Chung et al., 2023). Adhesins, curli fibres, polysaccharide binding proteins, eDNA binding proteins, and flagellin are the proteins found in the matrix of

pseudomonad biofilms. Pseudomonads also produce lectins and extracellular enzymes such as arginine deiminase in their biofilms (Flemming & Wingender, 2010). The functional amyloid-like fibres in pseudomonads are termed curli fibres. The strain *Pseudomonas fluorescens* UK4 exhibits curli production and imparts robust biofilm formation (Zeng et al., 2015). In densely packed biofilms of *P. fragi* and *Vibrio cholera*, a protein called RbmA was isolated, which may have a role in keeping molecules together (Drescher K et al.,2016). Extracellular DNA, also known as eDNA, can be actively secreted by the bacteria or formed from the dead biofilm cells involved in biofilm functions. However, the secretion mechanisms of eDNA still need to be explored. (Wickramasinghe et al., 2020; Flemming & Wingender, 2010).

Table 2.1: Components of EPS present in the pseudomonad biofilms

Components	Role	Isolate	Reference
Polysaccharides			
Alginate	Structural stability, Water and Nutrient retention	*Pseudomonas aeruginosa*, Mucoid variants of *Pseudomonas fluorescens* *P. putida and P. syringae*	Mann & Wozniak, 2012. Chung et al., 2023.
Levan	Nutrient reservoir	*P. syringae*	Laue et al.,2006.
Polysaccharide synthesis locus (Psl)	Biofilm architecture, Protection against neutrophils and immune effectors	*P. aeruginosa* *P. syringae* *P. medocina* *P. fluorescens*	Starkey et al.,2009. Winsor et al.,2009. Chung et al., 2023
Pel	Pellicle formation. Compensate for the role of Psl during its absence.	*P. aeruginosa* *P. fluorescens* Pf5	Jennings et al., 2015 Le Mauff et al., 2022

	Aggregation in the broth culture.		
Cellulose	Air-liquid interface biofilms.	*P. aeruginosa* *P. lundensis* *P. cedrina* *P. fluorescens*	Winsor et al.,2009 Ardré et al., 2019 Muthuraman et al., 2025
Proteins			
CdrA	Interact with the Psl polysaccharide	*P. aeruginosa*	Reichhardt, 2023.
Lap A and Lap D	Cell interconnection Surface adhesion	*P. aeruginosa* *P. fluorescens* *P. putida* *P. syringae*	Gjermanson et al.,2010.
Cell appendages	Flagella and type IV pili. Forms mushroom-like structures	Most of the Pseudomonads	(Patel & Gajjar, 2022)
Functional amyloid-like proteins	Initial adhesion and aggregation	*P. fluorescens* *P. aeruginosa*	Dueholm et al.,2015.
Lipids			
Rhamnolipids	Biofilm remodelling and Dispersion	Most of the pseudomonads	Abdel-Magowd et al.,2010.
eDNA	Intracellular connector Nutrient reservoir Mediate biofilms in the absence of polysaccharides	Most of the pseudomonads	Muthuraman et al., 2025 Dai et al., 2024b, Flemming & Wingender, 2010.

2.6.1 Distinct polysaccharides and proteins in the EPS matrix of pseudomonads

Pseudomonads are known to produce more polysaccharides in their EPS matrix compared to planktonic cells. A study comparing the biofilm EPS composition of *B. subtilis* and *P. aeruginosa* showed that the biofilm EPS produced by *Bacillus* spp. contains proteinaceous substances when observed with Fourier Transform Infrared Spectroscopy (FTIR), while the pseudomonad biofilms showed signals for lipopolysaccharides, alginate, Pel and Psl. The presence of polysaccharides in the EPS matrix promoted more adhesion strength of the EPS (Harimawan & Ting, 2016). The Pel and Psl polysaccharides are responsible for the biofilm architecture of pseudomonads. Deletion of the Psl gene in *P. aeruginosa* resulted in no macrocolony (mushroom-shaped structures with both motile and non-motile cells) formation, and deletion of both *pel* and *psl* genes resulted in the absence of both micro (localised clusters of small cell aggregates) and macrocolony formation (Yang et al., 2011). The absence of micro and macro colonies lowered the antimicrobial resistance (Yang et al., 2011). Another distinct polysaccharide produced by mucoid pseudomonads is alginate, and the interaction of alginate with divalent cations can result in the formation of a gel. The increase in alginate and Pel content will increase the yield strain of the biofilms under mechanical stress (Di Martino et al., 2018). The Psl, Pel, and alginate were absent in the *S. aureus* and *L. monocytogenes* biofilms; instead, the EPS matrix of these bacteria consists of lipoteichoic acid (LTA) and poly-N-acetyl glucosamine (PNAG) (Colagiorgi et al., 2016). The differences in their matrix composition are reflected in the biomass. Monospecies biofilms of *P. fluorescens* produced 2-fold higher biomass than monospecies *L. monocytogenes* biofilms (Puga et al., 2018).

The protein Cdr A in the biofilms can bind cells to Psl and cause aggregation and biofilm stability. In the absence of Psl, it can bind with Pel and promote biofilm formation (Reichhardt et al., 2020). The Cdr A and Psl are present in the biofilm matrix of pseudomonads, consisting of robust, tightly packed aggregates that keep the matrix protease resistant (Reichhardt et al., 2018). While the other bacteria possess different proteins and polysaccharides in their matrix, pseudomonads possess Cdr A, type IV pili and lectins (Lec A/ Lec B) (Karygianni et al., 2020).

Compared with the two-day-old biofilms of *S. aureus, P. aeruginosa* PAO1 forms flat, tightly packed biofilms with more coverage and exhibits resistance to phagocytosis (Yang et al., 2011). All three strains of *S. aureus* tested formed loosely packed, irregular microcolony

structures with less surface coverage than *P. aeruginosa* PAO1. The binding of eDNA and type IV pili in the pseudomonads supported the co-culture of *S. aureus* and improved the density (Yang et al., 2011). When comparing the EPS production between *P. fluorescens* PF2 and *S. Typhimurium* N25, *P. fluorescens* produced more polysaccharides and proteins on both stainless-steel and polystyrene surfaces (Yuan et al., 2025). Compared to other bacteria, *Pseudomonas* spp. possesses distinct polysaccharides in the EPS matrix, which strengthen the biofilm.

2.6.2 Interaction between EPS components

The different EPS components balance each other and maintain the integrity of the biofilms. In *P. putida*, the mutants lacking major adhesin genes *Lap* A and *Lap* F resulted in overproduction of EPS. Even though the exact overproduced component is unknown, this study indicates that biofilm formation does not depend on a single factor. The absence of a specific factor mostly results in overproduction of other components in the EPS (Martínez-Gil et al., 2013). In *P. aeruginosa*, the absence of Psl polysaccharide induces the overexpression of Pel. Whereas the absence of Pel induces the overproduction of alginate, and these mechanisms protect the cells from adverse conditions (Ghafoor et al., 2013). The interaction of Psl and Pel is responsible for microcolony formation, and the type IV pili and eDNA interaction is essential for less heterogeneous, tightly packed flat biofilms (Yang et al., 2011). The eDNA and Psl interaction results in a thick rope-like structure, which is essential for resisting enzymatic dispersion and provides a framework for the biofilms in *P. aeruginosa* (Wang et al., 2015).

Differences in the EPS composition were observed even between the different species of pseudomonads. The monosaccharides present in the *P. aeruginosa* are mannose and mannitol, while in *P. putida*, galactose and glucose were present when forming biofilms on xylose-based growth medium (Celik et al., 2008). In mucoid strains, alginate is overexpressed, and in the non-mucoid pseudomonads, Psl takes over the role of alginate (Di Martino et al., 2018). Levan is a unique polysaccharide produced by soil pseudomonads. Levan acts as a nutrient reservoir in the biofilms and was seen to fill the voids of the biofilms and not participate in the biofilm architecture as a structural component (Laue et al.,2006; Mann & Wozniak, 2012). When the biofilms of *P. lundensis* and *P. fragi* were grown at 25°C and 10ºC, the EPS production was higher at 10ºC for both bacteria. *P. lundensis* produced

significantly higher proteins in the EPS matrix, while *P. fragi* produced higher polysaccharides at 10°C (Wickramasinghe et al., 2020). The polysaccharide proportion in the EPS was higher in *P. fluorescens* (PF07) biofilms compared to *P. lundensis* (PL28) and *P. psychrophile* (PP26) when grown at 4ºC. This difference is reflected in the biomass residue after treatment with sodium hypochlorite. The residues left by PF07 (93.76%) were higher than those of PL28 (73.29%) and PP26 (85.65%), but the protein concentrations in the untreated EPS were similar (Liu et al., 2023).

2.6.3 Factors affecting the EPS production

Variables such as temperature, pH and the presence of cations can affect the biofilm formation of pseudomonads. A study comparing the biofilm formation of *P. fluorescens* and *L. monocytogenes* under cold and acidic conditions found that *P. fluorescens* produced higher amounts of proteins and polysaccharides when grown at 4ºC (both pH 5.4 and 7.0), which is reflected in the highest biomass (crystal violet values). This study suggests that cold and acidic stress together facilitate strong biofilm formation of *P. fluorescens* (Zhou et al., 2024). A mild acidic pH (5.0) environment encouraged thicker biofilm formation and overexpression of rhamnolipid and alginate-producing genes, which resulted in increased biomass production compared to the neutral (7.0) pH environment in *P. aeruginosa* biofilms (Mozaheb et al., 2023). When comparing the EPS production by *P. aeruginosa*, *Micrococcus* sp. and *Ochrobacterium* sp. at three different pH levels (7.0, 8.0, 9.0), *P. aeruginosa* (> 300 mg/mL) EPS production was not affected by pH and was higher than the other two bacteria (<300 mg/mL) at all the pH levels. Cations are present in all food processing environments. For example, the presence of Ca^{2+} in dairy processing, and the presence of Na and Mg^{2+} in seafood processing. Supplementation of 5 and 10 mM Ca^{2+} ions resulted in higher polysaccharide production in the EPS and complex biofilm structures with more cell clusters in *P. fluorescens* PF4 (Yuan et al., 2024). The addition of Mg^{2+} ions increased the biofilm depth, surface colonisation and induced the formation of large aggregates (Song & Leff, 2006). The robust biofilm formation on meat and in dairy processing environments indicates that pseudomonads can thrive in protein-rich environments together with ions (Wickramasinghe et al., 2019).

2.7 Pseudomonads produce public goods

Public goods are metabolically expensive products secreted by one bacterium and utilized by other bacteria in the same community without being involved in production. Siderophores, exoproteases, rhamnolipids, and cyclic lipopeptides are the molecules produced by *Pseudomonas* spp. as public goods (Loarca et al., 2019; O'Brien et al., 2017). EPS, eDNA, and some biofilm proteins can be exploited as public goods as they enable protection from adverse conditions and aid in the adhesion and attachment process (Guadarrama-Orozco et al., 2023). Bacterial volatile compounds from *P. fluorescens* act as a public good and interact with *L. monocytogenes* across the physical barriers, promote motility, and encourage biofilm formation (Zhou et al., 2024). Diffusion of public goods in planktonic form is much more effective than diffusing in tightly packed, spatially structured biofilms. In *P. aeruginosa* biofilms, maximum concentrations of pyoverdine are observed at the centre of the biofilms, and this local trafficking of public goods modulates the growth of the community. However, the molecular mechanisms that regulate the public goods need to be addressed (Julou et al., 2013). When specialisation is enforced in the production of public goods (siderophores) results in mutual cheating rather than efficient division of labour in *P. aeruginosa* under iron-limiting conditions (Mridha & Kümmerli, 2022).

L. monocytogenes is a "cheater" when co-cultured with *P. fluorescens* as it's a poor EPS producer and shelters under pre-formed pseudomonad biofilm, and this highlights the sharing of EPS as a public good (Puga et al.,2018). Scanning electron microscopy of *Listeria* and *P. aeruginosa* biofilms showed that after 24 h, *Listeria* spp. was still in its adhesion stage, while *P. aeruginosa* formed denser biofilms, and the structure of the co-culture biofilms is the same as the *P. aeruginosa* biofilms. Since EPS is a major architectural compound, these observations reveal the dominance of *Pseudomonas* spp. in the EPS production (Dong et al., 2022). The advantages of this EPS for *Listeria* spp. are providing nutrients, protection from external stress, reduced diffusivity of chemicals, and prolonged survival. This cooperative behaviour depends on the species and their concentration (Dong et al., 2022). Rhamnolipid is a biosurfactant produced by pseudomonads that can be exploited by other bacteria for swarming motility, mediate assimilation of hydrocarbons as nutrients, and change the biofilm architecture. However, *P. aeruginosa* controls the rhamnolipid production based on the growth rate rather than cell density, which regulates the rhamnolipid biosynthesis genes (Guadarrama-Orozco et al., 2023). By producing surfactants, pseudomonads achieve

phyllosphere (aerial habitat in plants which supports the microbial colonisation) colonisation during fluctuating humidity. The surfactant produced by *Pseudomonas* sp.FF1 encouraged the co-swarming of *Pantoeafiji eucalypti* 299R. *P. eucalypti* biomass was significantly increased in the dual species biofilms compared to its monoculture, and dual species with biosurfactant mutant pseudomonads (Kunzler et al., 2024).

2.8 Biofilm-related genes in pseudomonads

A ubiquitous second messenger in proteobacteria is known as cyclic dimeric GMP (c-di-GMP), which upregulates biofilm formation (Fig. 2.3). Putrescine and arginine enhance the biofilm formation of *P. aeruginosa* PAO1 with increased levels of c-di-GMP (Liu et al., 2022). Flagella (*flgA*), quorum sensing (luxR), exopolysaccharides (*algK, pslA*), and stress response (*rpoS*) are found in *P. fluorescens* PF07, *P. lundensis* PL28, and *P. psychrophile* PP26 and their relative expression is higher at 4°C compared to 25°C (Liu et al., 2023). The gene *aprD* is known for controlling the protease secretion in pseudomonads. However, the deletion of the *aprD* genes leads to a disorganised biofilm structure and reduced production of EPS matrix components such as proteins and polysaccharides. The deletion of *apr*D increased the motility of *P. fragi* and resulted in sparsely distributed cell aggregates (Wu et al., 2022). The functional amyloid (*fap*) in *P. fluorescens* PF07 is required for the formation of microcolonies, pellicles, and solid surface-associated biofilms. The bacterial enhancer-binding protein *brf*A regulates the fap-dependant biofilm formation by sensing c-di-GMP (Guo et al., 2024) (Fig. 2.3). The gene r*po*N and *rpoN-dependent* promoters regulate the *fap ABCDE* operon, which is responsible for the Fap amyloids in *P. fluorescens* PF07 biofilms and are regulated by *Rpo*N and *Brf*A (Guo et al., 2022).

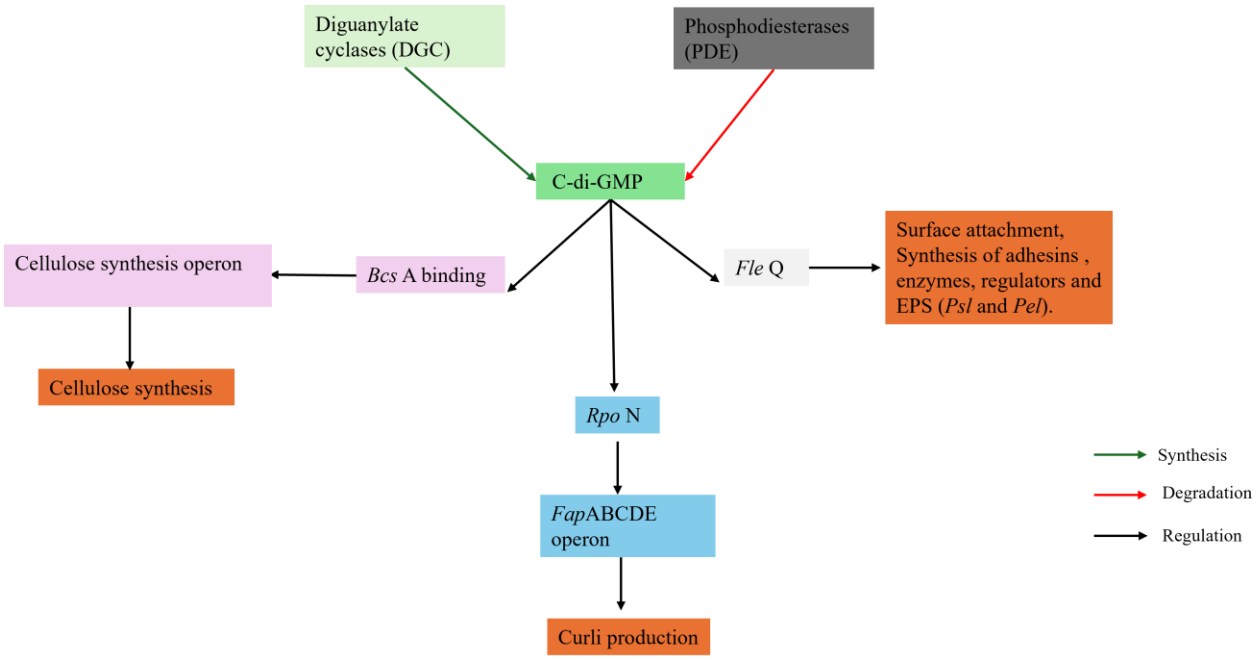

Figure 2.3 The ci-di-GMP regulation pathways in biofilm EPS synthesis in pseudomonads

Bacterial cellulose is also a part of biofilm formation in some Gram-negative proteobacteria. *bcsAB* tandem is responsible for cellulose synthesis in *Pseudomonas* spp. biofilms. Cellulose has exceptional water retention capacity, porosity, and mechanical resistance. It also interacts with other polysaccharides or proteinaceous compounds and is an architectural element for biofilms (Abidi et al., 2022). *P. putida*, *P. syringae,* and *P. fluorescens* subsp. *cellulosa* are the common cellulose producing pseudomonads (Nielsen et al., 2011).

Cellulose production is an important aspect of air-liquid interface biofilm-forming pseudomonads. The *algD, psl,* and *pel* are the genes involved in the exopolysaccharide production of pseudomonads (Rajabi et al., 2022). FleQ is a bacterial enhancer binding protein and responds to c-di-GMP signalling by controlling surface attachment and biofilm formation, stimulating the synthesis of enzymes, regulators, adhesins, EPS, and other envelope components in a wide range of pseudomonads (Fig. 2.3). FleQ controls the flagellin synthesis, which controls the flagella production. FleN is the anti-activator FleQ, and the deletion of FleN leads to a hyperflagellated phenotype (Martínez-Rodríguez et al., 2023).

2.9 Biofilm removal strategies

2.9.1 Enzymes

The biofilm EPS matrix comprises proteins, polysaccharides, lipids, and eDNA. The enzymatic removal of these biofilms must hydrolyse the components of the EPS matrix. The enzymes (α-amylase, protease, DNase I, dispersin B) hydrolyse biofilm EPS and convert the cells into their planktonic form, which increases their susceptibility toward antimicrobials (Wang et al., 2023). The biofilms of *P. aeruginosa* are hard to remove by DNase I as the enzyme gets inactivated by the over-produced EPS matrix and proteolytic exoenzymes in mature biofilms (Algburi et al., 2017). However, the combination of DNase I,α-amylase, and dispersin B reduced the EPS biomass (Algburi et al., 2017). The α-amylase derived from *Bacillus subtilis* is effective against *S. aureus* and *P. aeruginosa* biofilms compared to the amylases from human saliva and sweet potato, indicating the importance of bacterial enzymes in biofilm removal (Kalpana et al., 2012). The biofilm removal (82%) of *P. aeruginosa* is achieved by α-amylase (Singh et al., 2016). In vitro studies have demonstrated the effects of dispersin B against *S. aureus, S. epidermis, A. baumanni, K. pneumoniae, E.coli* and *P. fluorescens* (Wang et al., 2023). Purified marine alginate enzyme (AlyP1400) can degrade the *P. aeruginosa* biofilms and enhance the cidal activity of tobramycin (Blanco-Cabra et al., 2020). PslG is a glycoside hydrolase capable of hydrolysing Psl polysaccharide in *P. aeruginosa* in its early stages but not mature biofilms (Baker et al., 2015). $PelA_h$ is another glycoside hydrolase that targets the Pel polysaccharide in the biofilm matrix of *P. aeruginosa* and encourages significant biofilm dispersal within 24 hrs (Baker et al., 2016). However, PslG and PelAh cannot disperse the mature biofilms due to the higher EPS concentration and interaction between the EPS components (Baker et al., 2016). Treating *P. aeruginosa* biofilms with proteinase K (2,5 and 10μL) shows that proteinase K is biphasic and promotes or inhibits biofilm formation at different concentrations (Eladawy et al., 2020). Mechmechani et al. (2023) combined trypsin with pepsin and carvacrol, and this combination was able to disperse the biofilms of *P. aeruginosa* and *Enterococcus faecalis*. The main disadvantage of these enzymes is that when administered, they facilitate the dispersion without bactericidal activity, and this may lead to new biofilm formation from the dispersed cells (Wang et al., 2023). However, the emphasis on the enzymatic dispersion studies mostly focused on *P. aeruginosa* and many other spoilage pseudomonads in the food industry, which

may not show a similar response to enzymatic treatments, needs to be studied. Alkaline and enzymatic detergents improve the efficacy of disinfectants tested against strong biofilms of a poultry strain *P. fluorescens* (Merino et al., 2024). Enzymes such as DNase I, cellulase, and α-amylase, when immobilised with silver nanoparticles, can disperse the biofilms and reduce the cell viability. However, the antibacterial activity is achieved by silver rather than the enzymes (Rubio-Canalejas et al., 2022). The single or combination of enzymes cannot disperse the biofilms completely. The enzyme cleaners may be included in the sequential cleaning process rather than applied alone.

2.9.2 Ultrasound

Ultrasound affects the biofilms by three different mechanisms: mechanical effects by cavitation (formation, growth, and collapse of a microscopic gas bubble in a liquid), chemical effects including the generation of free radicals (hydroxyl and superoxide radicals), and heat effects by generation of local hotspots with very high temperatures (5000 K, inside cavitation bubbles). However, the biofilm deformation is mainly achieved through mechanical effects (Lambert et al., 2010). A study on the removal of *P. fluorescens* in a dairy environment showed that 2% lactic acid with ultrasound treatment can remove the biofilm cells below the detection limit (Dai et al., 2024a). Another study with ultrasound (power > 80 W) combined with mild heat treatment at 50°C can successfully remove the biofilm of *P. fluorescens,* with a large disruption of the biofilm structure occurring after 15 min of treatment (Su et al., 2022). Ultrasound treatment on *P. fluorescens* biofilms altered around 27 metabolites (metabolomics and UPLC-MS/MS) involved in carbohydrate, lipid, amino acid, and nucleotide metabolism. Ultrasound at 15.79 W/cm^2 disrupted the energy and genetic information of biofilms, while at 26.32 W/cm^2 resulted in disruption of the metabolic activity and osmotic pressure of biofilms (Wang et al., 2024).

2.9.3 Quorum-quenching (QQ) molecules

Quorum-quenching (QQ) enzymes or molecules should suppress the AHL quorum-sensing molecule and cut down the cell-to-cell communication in the biofilms. QQ enzymes belong to two classes: (i) AHL lactone and (ii) AHL acylases. A novel quorum quenching enzyme, LrsL, isolated from the red sea sediment bacteria *Labrenzia* sp. VG12 effectively suppressed the biofilm formation of *P. aeruginosa*. However, the elimination of established biofilms was

not studied. The authors conclude that, with QQ enzymes, complete elimination is not possible, but the amount of antimicrobials and cleaning chemicals may be lowered (Rehman et al., 2022). The QQ strains isolated from a sludge membrane bioreactor, which belonged to the genera *Bacillus* and *Pseudomonas,* successfully prevented the biofilm formation of *P. aeruginosa* by 60% (Khalid et al., 2022).

2.9.4 Sanitizers

Sanitizers are substances that reduce but do not necessarily eliminate all the microbial contaminants on inanimate surfaces. The commonly used industrial sanitizers are oxidative (halogens), hydrogen peroxide-based (peracetic acid, peracids, chlorine dioxide, and ozone), surfactant-based (quarternary ammonium compounds), phenolics, and aldehydes (Marriott et al., 2018).

Didecyl Dimethyl Ammonium Bromide (DDAB) and Slightly Acidic Electrolysed Water (SAEB) remove the biofilms of *P. aeruginosa*. DDAB 16 MIC and SAEW completely cleared the biofilm formation of *P. aeruginosa* on a stainless-steel surface (Li et al., 2022). Among the four sanitizers tested, benzalkonium chloride (BAC) and glycolic acid (GA) increased the levels of persister cells of *P. fluorescens* during regrowth. In contrast, peracetic acid (PAA) and glyoxal (GO) did not alter the susceptibility of the persister cells, and similar levels of persister cells were detected after several rounds of treatment. It is important to consider the sanitizer that should not induce a change in the antimicrobial susceptibility of persister cells. Persister cells are dormant variants of regular cells and are highly tolerant to antimicrobials but do not grow in the presence of antimicrobials (Wood, 2016; Lewis, 2010).

Application of ozonated water (gas inlet concentration of 20mg/L, airflow rate of 1.0 L/min, water temperature 6±1°C) under flow conditions for *P. parancis* biofilms effectively removed 0.510 log CFU/cm^2 compared to static removal at 0.22 log CFU/cm^2 (Santos et al., 2025). Panebianco et al. (2022) reported that gaseous ozone application (50ppm for 6h) is ineffective in removing the established biofilms of *Pseudomonas* spp. The ineffectiveness is due to the presence of biofilm biomass with dead cells acting as a protective shield (Panebianco et al., 2022). However, ozone is more effective under high relative humidity conditions, and high levels of ozone are dangerous to human health (Panebianco et al., 2021).

The next generation QAC (Quaternary Ammonium Chloride) known as Decon 7 achieved approximately 4-5 log reduction in *S. aureus* and *P. aeruginosa* dual-species biofilms (Shah

& Muriana, 2021). When the pseudomonad biofilms formed at 25°C, 10°C, and 4°C were treated with sodium hypochlorite at 65°C, the log reductions with the biofilms grown at 4°C were lower than the biofilms grown at 25 °C and 10°C (Liu et al., 2023). This shows the importance of EPS produced by pseudomonads at lower temperatures in resistance to antimicrobials. The Pel and Psl polysaccharides in *P. aeruginosa* exhibit protective functions against oxidative stress induced by sodium hypochlorite and hydrogen peroxide (H_2O_2). The interaction between the antimicrobials and Pel provides time for the biofilm cells to grow and produce detoxifying enzymes in pseudomonads (Da Cruz Nizer et al., 2024).

2.9.5 Biosurfactants

Biosurfactants are surface-active, amphipathic biomolecules with emulsifying properties that are microbial secondary metabolites. These molecules can alter the cell surface morphology and cell adhesiveness, and can disrupt the bacterial membranes (Bhadra et al., 2023). Surfactant derived from *Lactiplantibacillus plantarum* reduced the biofilm formation of *P. aeruginosa* by 59.8%, and at the sub-MIC concentration, QS inhibitory effects, such as reduction in pyocyanin, total protease, LasA, and LasB, were also observed (Patel et al., 2022b). Similarly, when the *Lactobacillus* cell-free supernatant (CFS) is supplemented with the biofilm formation medium with *P. aeruginosa,* this results in 99.99±0.003% of the cells failing to adhere. Additionally, the application of *Lactobacillus* CFS on preformed pseudomonad biofilms also results in an 83.83±6.28% decrease in metabolic activity. These results suggest the promising ability of biosurfactants of lactic acid bacteria for antiadhesive and antibiofilm activities against *P. aeruginosa* (Jeyanathan et al., 2021). Crude biosurfactant from *L. plantarum* showed disruption in bacterial cell walls and reduction in thickness of multilayered biofilms under SEM (Patel et al., 2021). Biosurfactants from *B. niabensis* reduce growth and biofilm formation of the marine biofouling bacteria *P. stutzeri* by upregulating metabolites such as glucose, acetic acid, histidine, lactic acid, phenylalanine, uracil, and NADP+ and downregulating trehalose and histamine (Sánchez-Lozano et al., 2023).

2.9.6 Photodynamic Inactivation (PDI)

Photodynamic inactivation involves photosensitizers (non-toxic dyes) that are activated by absorption of visible light, resulting in the formation of reactive oxygen species (hydroxyl ions and singlet oxygen) that inactivate the microbial cells (Hamblin, 2016). Octyl Gallate

and Blue light, when used to treat *P. fluorescens* biofilms, exhibit synergistic bactericidal and antibiofilm activity by reactive oxygen species produced by oxidative stress (Shi et al., 2022). Berberine, when combined with a blue LED at 450 nm, can destroy biofilm cells at concentrations of 150 and 500 μg/mL through oxidative stress, whereas without the blue LED, the effects on biofilm removal are significantly lower (Safai et al., 2022). The photodynamic inactivation of *P. fluorescens* in milk demonstrated that curcumin, combined with a blue LED at 450 nm, reduced around approximately 7 log CFU/mL cells, whereas riboflavin had no effect. SEM shows that photodynamic inhibition causes changes in cell shape, cell damage, and membrane rupture, resulting in cytoplasmic contents around the cells. However, this study focused on the planktonic cells in milk media, and the interference of biomolecules in the milk and the observed cell reduction cannot be discounted (Saraiva et al., 2024). The interference from biofilm EPS is another aspect to consider when designing PDI.

2.9.7 Cold atmospheric plasma (CAP)

Cold plasma is a new emerging technology proven to be efficient against bacteria with antibiotic resistance (Mai-Prochnow et al., 2015). Cold plasma is a mixture of photons, electrons, charged ions, atoms, free radicals, and excited molecules with bactericidal activities at temperatures below 40°C (Mai-Prochnow et al., 2021). The single and dual species biofilms of *P. aeruginosa* and *B. cereus* revealed that *Bacillus* (38% remained after 120 s of CAP treatment) is more tolerant to cold plasma than *P. aeruginosa* (33% remained after 120 s of CAP treatment). However, in the dual-species biofilms, the tolerance was higher (36% after 120 s of CAP treatment) for both bacteria involved (Lavrikova, 2025). Moisture in the biofilms reduces the efficiency of CAP treatment. Desiccation before treatment is recommended to have better penetration of reactive species such as O_2 and NO_2 generated by cold plasma (Lavrikova, 2025). When the biofilms were allowed to regrow after being treated with CAP for 300s, regrowth of the *P. aeruginosa* biofilms occurred both in wet and dry conditions, whereas the *B. cereus* failed to regrow under dry conditions. The authors concluded that to avoid the regrowth, the debris still needs to be washed away after CAP (Lavrikova, 2025).

Table 2.2: Comparison of the biofilm elimination strategies of pseudomonads

Biofilm eradication strategies	Target	Cost effectiveness	Efficacy	Challenges	References
Traditional CIP involves the use of hot water, alkali, and acid treatments.	Cells	Low	Industry standard Remove food debris Remove minerals	High energy and water use Salt residues EPS remnants Corrosion of metal by acid treatment Crews and crevices can accommodate biofilms	Parkar et al., 2004 Simões et al., 2010 Pant et al., 2023
Chlorination	Cells	High	High oxidation capacity (Chlorine dioxide)	Chlorate deposition and health risk Impact on food matrix Corrosion Chlorate resistance	Pant et al., 2023 Gagnon et al., 2005
Enzyme cleaners	EPS	Low (Require a combination of enzymes or surfactants, or other	Disperse the biofilms Environment friendly Biodegradable	Possible recolonisation The interaction between the matrix components can keep the matrix resistant to enzymes	Nahar et al.,2018

		molecules that increase the production cost).		Residual enzymes can react with food matrices.	
Biosurfactants	Cells	Low (High production cost)	Prevent the cell attachment and biofilm formation Biodegradable Prevent corrosion	Cannot eliminate mature biofilms. Only a few, such as sophorolipids, possess bactericidal activities. Loss of activity and low stability.	Bhadra et al., 2023 Jimoh et al., 2023 Díaz De Rienzo et al., 2015
Ultrasound	Cells	Low (High operational cost and treatment time)	Prevents bacterial adhesion Mechanical disruption of the EPS matrix	Stimulated alginate production in *P. aeruginosa* due to mechanical stress. The effects on food quality are not well known	Yu et al., 2020 Erriu et al., 2014 Lambert et al., 2010
Quorum-quenching molecules	Cells	Low (Longer treatment time)	Reduction in bacterial adhesion Inhibit microcolony formation Biodegradable	Possibilities of developing resistance towards quorum-quenching molecules. Not a universal solution.	Paluch et al., 2020 Krzyżek, 2019

				High temperatures in dairy processing, the complexity of food matrices can affect the effectiveness of QQ molecules.	
Sanitizers	Cells	Moderate to high (However, the biodegradable sanitizers require high concentration).	Prevents biofilm formation. Targets (peracetic acid and hydrogen peroxide) include a broad spectrum of bacteria.	Reduced diffusivity due to EPS Not all sanitizers are environmentally friendly Risk of biocide-induced antimicrobial resistance. Some sanitizers are corrosive, unstable, and explosive.	Fernandes et al., 2024 Jones & Joshi, 2021 Dawan et al., 2025 Chowdhury et al., 2025 Yuan et al., 2021
Photodynamic inactivation	Cells	Low (Scaling up needs to be considered from an industrial point of view)	Rapid microbial killing. The reactive oxygen species can target cells and some molecules (polysaccharides are susceptible to photodamage) in the EPS. No effects on Food matrices.	Reactive oxygen species can affect the food quality. Minimal effects on the EPS matrix. Require combined treatment to eradicate the biofilms. Limited penetration depth. Indirect application by water treated with PDI is possible in	Wang et al., 2021 Cieplik et al., 2014 De Melo et al., 2013

				industries with confined spaces, such as dairy. Direct application is not possible.	
Cold atmospheric plasma (CAP)	Cells	Low (Requires double the cost compared to chlorination, as it relies completely on electricity).	Preserving bioactive components in food matrices. No added chemicals. Minimal adverse effects on the organoleptic properties of food.	Reactive species can break down the lipid bonds and have an impact on food quality. CAP. The dairy system often involves wet surfaces, and the reactive species work better on dry surfaces.	Zhu et al., 2020 Naicker et al., 2023

2.10 Pseudomonad biofilm footprints

The term “Footprints” represents the polymeric material left on the surface while the bacterial cells have been removed. These footprints can be seen on a surface after cell removal, and the polymeric material is clumped together due to hydrophobicity (Neu & Marshall, 1991). Biosurfactants, quorum-quenching (QQ) molecules, and photodynamic inactivation (PDI) mostly target the prevention of biofilm formation. Other strategies, such as sanitizers, ultrasound, and enzymes, focus on preventing and removing biofilms. Among these strategies, enzymes that target the biofilm EPS rather than the cells is and effective strategy (Fig. 2.4). However, Baker et al.,2015; Baker et al.,2016, concluded that the polysaccharides and protein targeting enzymes cannot completely disperse the biofilms.

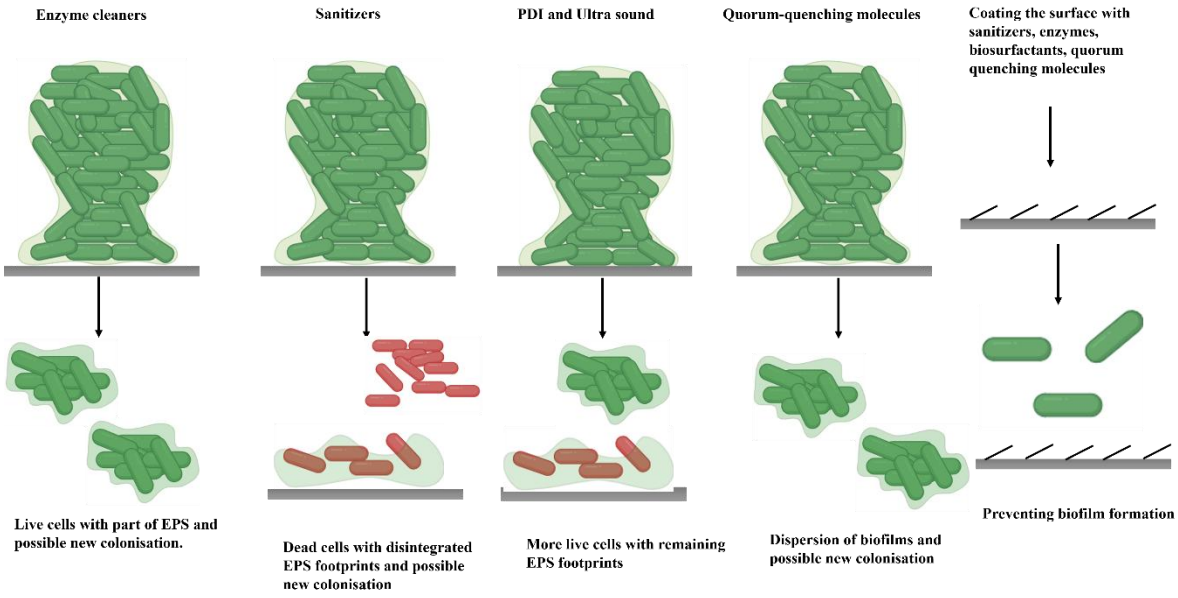

Figure 2.4 Biofilm prevention and eradication strategies of pseudomonads (Created in https://BioRender.com).

The cleaners and sanitizers such as sodium hydroxide (NaOH), ozone, and peracetic acid can eliminate the cells, but the remaining EPS footprints can accommodate new occupant cells and encourage new microcolonies and biofilm formation (Fig. 2.5).

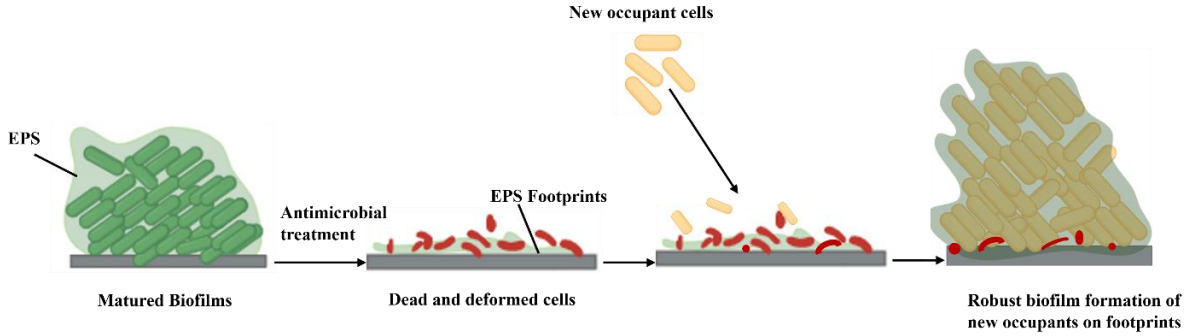

Figure 2.5 Biofilm footprints of pseudomonads after antimicrobial treatment or cleaning and the robust biofilm formation on the footprints by new occupant cells (Created in https://BioRender.com).

Didecyl Dimethyl Ammonium Bromide (DDAB) combined with slightly acidic electrolysed water (SAEW) showed less prominent FTIR (Fourier Transform Infrared Spectroscopy) peaks for polysaccharides, proteins, and lipids than control biofilms. This confirms the remaining EPS footprints after cleaning (Li et al., 2022). The footprints remaining after cleaning depends on the also depend on the type of biofilm formed. The air-liquid interface (ALI) biofilms of *P. fluorescens* Pf1 after CIP resulted in dead cells and EPS debris found on the coupons with no viable cells (Jha et al., 2020). A study with multispecies biofilms cleaned with antimicrobials resulted in early and aggressive regrowth of subsequent biofilms, and this observation was thought to be due to fresh cells attaching to the footprints, leading to faster biofilm formation post cleaning (Han et al., 2019). *P. aeruginosa* biofilms treated with 3% hydrogen peroxide (H_2O_2) and peracetic acid (PAA) were able to reduce the biofilm cell numbers to undetectable levels. However, with SEM, the EPS residues that remained on the surface could be observed. The EPS remnants significantly increased the proliferation of cells in the next 24 h. This observation suggests that EPS produced by pseudomonads and not removed by cleaning is the main culprit in biofilm regrowth (Deng et al., 2025). The viscoelastic properties of EPS produced by pseudomonads remained unchanged when mechanical (high shear stress), chemical (addition of NaCl, $FeCl_3$, and others), and both forces were applied, which reflects the resilience of the EPS. The EPS produced by most of the pseudomonads can recover from the damage, as the degree of recovery measured after high shear stress and chemical treatments is high (Lieleg et al., 2011). The FTIR observations showed peaks for proteins, polysaccharides, and phospholipids after cleaning with DDAB and SAEW, indicating the EPS's complexity (the proteins, polysaccharides, and phospholipids) remained the same (with lower peak intensity in FTIR) after cleaning with

DDAB and SAEW (Li et al., 2022). However, there is no information about the eDNA present in the footprints derived from FTIR data.

Self-locomotive antimicrobial microrobot known as SLAM, when combined with peracetic acid (PAA) and hydrogen peroxide (H_2O_2), shows promising results against *P. aeruginosa* biofilms and prevents regrowth over time by reducing the EPS volume and preventing the regrowth of biofilms for more than two months (Deng et al., 2025). Pseudomonads are strong EPS producers and can accommodate other pathogens in their EPS matrix, as EPS can be exploited as a public good (Puga et al., 2018). Thus, the removal of their EPS is important to keep the food processing surface contamination-free. Not only pseudomonads, but many other strong EPS producers could leave the biofilm footprints.

2.11 Future research

Pseudomonads are public good producers and can accommodate other bacteria in their matrix. Thus, the biofilm eradication studies in the future should focus on community biofilms. The traditional sequential treatment of cleaning chemicals targets both cells and EPS, and improved strategies need to be developed to target the biofilm EPS footprints left behind after cleaning. In a study on multispecies biofilm (*Pseudomonas* spp., *E. coli*, *Bacillus* spp., *Staphylococcus* spp., and *Enterococcus* spp) removal, sequential treatment steps included alkali, surfactant 1, acid, enzyme, surfactant 2, and sanitizers (Singh & Anand, 2022). Among the tested bacteria in the multispecies consortia, around 1.13 ±0.03 log CFU/cm^2 *Bacillus* spp. remaining cells were difficult to eliminate (Singh & Anand, 2022).

- Processing equipment modifications with removable parts may enhance the biofilm removal.
- Bacteriophages show promising effects in killing biofilm cells and disrupting the EPS matrix. However, most studies are limited to laboratory conditions; scaling up and standardisation need to be developed (Yin et al., 2022).
- Enzyme immobilization can reduce the particle size, increase the zeta potential, and enhance the penetrability of the enzymes (Rubio-Canalejas et al., 2022). However, the immobilized enzymes still target the EPS matrix and disperse the live cells. To achieve complete elimination of biofilms, many studies suggest combined treatments.

- Combined treatment of enzymes with ultrasound, shear stress, chelating agents, buffers, surfactants, and detergents can achieve complete removal. However, cost-effectiveness is the biggest burden here (Nahar et al.,2018).
- Physical, chemical, and biological disinfection methods in combination with each other are also a strategy to combat the pseudomonad biofilms. Formulation of such strategies needs more research to find the right combinations that eradicate biofilm (Yuan et al., 2021).
- Nanocomposites can eliminate pseudomonad biofilms by inhibiting bacterial adhesion to the surface, disrupting the EPS matrix, and dispersing the bacterial cells. Cost-effective production and biocompatibility need to be addressed (Omran et al., 2024).

2.12 Conclusion

Pseudomonads are strong EPS producers, and the incomplete removal of the biofilm results in continuous contamination in food processing environments. Despite so many eradication methods to control the biofilm removal of psychrotrophic pseudomonads, the removal is complicated due to exopolysaccharides and matrix overproduction at low temperatures. Herein, the biofilm formation of psychrotrophic pseudomonads and their EPS matrix is discussed. This review compared the different eradication strategies focused on cells and the EPS matrix and found that the strategies need to be combined for complete biofilm removal. This review emphasises the need for more studies to investigate the elimination strategies for cost-effective production, minimization of the adverse effects, and safe application on food matrices.

2.13 References

Abdel-Mawgoud, A. M., Lépine, F., & Déziel, E. (2010). Rhamnolipids: Diversity of structures, microbial origins and roles. *Applied Microbiology and Biotechnology*, *86*(5), 1323–1336. https://doi.org/10.1007/s00253-010-2498-2

Abidi, W., Torres-Sánchez, L., Siroy, A., & Krasteva, P. V. (2022). Weaving of bacterial cellulose by the Bcs secretion systems. *FEMS Microbiology Reviews*, *46*(2), fuab051. https://doi.org/10.1093/femsre/fuab051

Ahmed, A., & Hassan, M. (2024). Monitoring the prevalence of Pseudomonas fluorescens as a spoilage indicator in cow raw milk, teat surfaces and milk tanks. *Open Veterinary Journal*, *14*(8), 1983. https://doi.org/10.5455/OVJ.2024.v14.i8.27.

Algburi, A., Comito, N., Kashtanov, D., Dicks, L. M. T., & Chikindas, M. L. (2017). Control of Biofilm Formation: Antibiotics and Beyond. *Applied and Environmental Microbiology*, *83*(3), e02508-16. https://doi.org/10.1128/AEM.02508-16.

Ardré, M., Dufour, D., & Rainey, P. B. (2019). Causes and Biophysical Consequences of Cellulose Production by *Pseudomonas fluorescens* SBW25 at the Air-Liquid Interface. *Journal of Bacteriology*, *201*(18). https://doi.org/10.1128/JB.00110-19.

Baker, P., Hill, P. J., Snarr, B. D., Alnabelseya, N., Pestrak, M. J., Lee, M. J., Jennings, L. K., Tam, J., Melnyk, R. A., Parsek, M. R., Sheppard, D. C., Wozniak, D. J., & Howell, P. L. (2016). Exopolysaccharide biosynthetic glycoside hydrolases can be utilized to disrupt and prevent *Pseudomonas aeruginosa* biofilms. *Science Advances*, *2*(5), e1501632. https://doi.org/10.1126/sciadv.1501632.

Baker, P., Whitfield, G. B., Hill, P. J., Little, D. J., Pestrak, M. J., Robinson, H., Wozniak, D. J., & Howell, P. L. (2015). Characterization of the *Pseudomonas aeruginosa* Glycoside Hydrolase PslG Reveals That Its Levels Are Critical for Psl Polysaccharide Biosynthesis and Biofilm Formation. *Journal of Biological Chemistry*, *290*(47), 28374–28387. https://doi.org/10.1074/jbc.M115.674929.

Bhadra, S., Chettri, D., & Kumar Verma, A. (2023). Biosurfactants: Secondary Metabolites Involved in the Process of Bioremediation and Biofilm Removal. *Applied Biochemistry and Biotechnology*, *195*(9), 5541–5567. https://doi.org/10.1007/s12010-022-03951-3

Blanco-Cabra, N., Paetzold, B., Ferrar, T., Mazzolini, R., Torrents, E., Serrano, L., & LLuch-Senar, M. (2020). Characterization of different alginate lyases for dissolving *Pseudomonas aeruginosa* biofilms. *Scientific Reports*, *10*(1), 9390. https://doi.org/10.1038/s41598-020-66293-2.

Bruzaroski, S. R., Correia, S. D. S., Devara, L. F. D. S., Poli-Frederico, R. C., Fagnani, R., & Santana, E. H. W. D. (2023). Influence of the storage temperature of raw sheep milk on the spoilage potential of *Pseudomonas* spp. *Small Ruminant Research*, *224*, 106998. https://doi.org/10.1016/j.smallrumres.2023.106998.

Caldera, L., Franzetti, L., Van Coillie, E., De Vos, P., Stragier, P., De Block, J., & Heyndrickx, M. (2016). Identification, enzymatic spoilage characterization and proteolytic activity quantification of *Pseudomonas* spp. Isolated from different foods. *Food Microbiology*, *54*, 142–153. https://doi.org/10.1016/j.fm.2015.10.004.

Celik, G. Y., Aslim, B., & Beyatli, Y. (2008). Characterization and production of the exopolysaccharide (EPS) from *Pseudomonas aeruginosa* G1 and *Pseudomonas putida* G12 strains. *Carbohydrate Polymers*, *73*(1), 178–182. https://doi.org/10.1016/j.carbpol.2007.11.021.

Cellular levels of c-di-GMP are regulated by two enzyme classes: diguanylate cyclases (DGC) that synthesise c-di-GMP and phosphodiesterases that degrade the c-di-GMP (Jenal et al., 2017).

Chauhan, M., Kimothi, A., Sharma, A., & Pandey, A. (2013). Cold adapted Pseudomonas: Ecology to biotechnology. *Frontiers in Microbiology*.https://doi.org/10.3389/fmicb.2023.1218708.

Chen, J., Sun, Z., Jin, J., Wang, F., Yang, Q., Yu, H., Yu, J., & Wang, Y. (2023). Role of siderophore in *Pseudomonas fluorescens* biofilm formation and spoilage potential function. *Food Microbiology*, *109*, 104151. https://doi.org/10.1016/j.fm.2022.104151.

Chowdhury, M. A. H., Reem, C. S. A., Ashrafudoulla, M., Rahman, M. A., Shaila, S., Jie-Won Ha, A., & Ha, S. D. (2025). Role of advanced cleaning and sanitation techniques in biofilm prevention on dairy equipment. *Comprehensive reviews in food science and food safety*, *24*(3), e70176. https://doi.org/10.1111/1541-4337.70176.

Chung, J., Eisha, S., Park, S., Morris, A. J., & Martin, I. (2023). How Three Self-Secreted Biofilm Exopolysaccharides of *Pseudomonas aeruginosa*, Psl, Pel, and Alginate, Can Each Be Exploited for Antibiotic Adjuvant Effects in Cystic Fibrosis Lung Infection. *International Journal of Molecular Sciences*, *24*(10), 8709. https://doi.org/10.3390/ijms24108709.

Cieplik, F., Tabenski, L., Buchalla, W., & Maisch, T. (2014). Antimicrobial photodynamic therapy for inactivation of biofilms formed by oral key pathogens. *Frontiers in Microbiology*, *5*. https://doi.org/10.3389/fmicb.2014.00405.

Colagiorgi, A., Di Ciccio, P., Zanardi, E., Ghidini, S., & Ianieri, A. (2016). A Look inside the *Listeria monocytogenes* Biofilms Extracellular Matrix. *Microorganisms*, *4*(3), 22. https://doi.org/10.3390/microorganisms4030022.

Da Cruz Nizer, W. S., Allison, K. N., Adams, M. E., Vargas, M. A., Ahmed, D., Beaulieu, C., Raju, D., Cassol, E., Howell, P. L., & Overhage, J. (2024). The role of exopolysaccharides Psl and Pel in resistance of *Pseudomonas aeruginosa* to the oxidative stressors sodium hypochlorite and hydrogen peroxide. *Microbiology Spectrum*, *12*(10), e00922-24. https://doi.org/10.1128/spectrum.00922-24.

Dai, H., Zhang, Y., Xu, Z., Stoteyome, T. and Yuan, L. (2024a), Ultrasound promoted the inactivation efficacy of lactic acid against calcium-mediated biofilm formation by *Pseudomonas fluorescens*. Int J Dairy Technol, 77: 773-783. https://doi.org/10.1111/1471-0307.13108

Dai, J., Fang, L., Wu, Y., Liu, B., Cheng, X., Yao, M., & Huang, L. (2022). Effects of exogenous AHLs on the spoilage characteristics of *Pseudomonas koreensis* PS1. *Journal of Food Science*, *87*(2), 819–832. https://doi.org/10.1111/1750-3841.16038.

Dai, J., Luo, W., Hu, F., & Li, S. (2024b). In vitro inhibition of *Pseudomonas aeruginosa* PAO1 biofilm formation by DZ2002 through regulation of extracellular DNA and alginate production. *Frontiers in Cellular and Infection Microbiology*, *13*, 1333773. https://doi.org/10.3389/fcimb.2023.1333773.

Dawan, J., Zhang, S., & Ahn, J. (2025). Recent Advances in Biofilm Control Technologies for the Food Industry. *Antibiotics*, *14*(3), 254. https://doi.org/10.3390/antibiotics14030254.

De Melo, W. C., Avci, P., De Oliveira, M. N., Gupta, A., Vecchio, D., Sadasivam, M., Chandran, R., Huang, Y.-Y., Yin, R., Perussi, L. R., Tegos, G. P., Perussi, J. R., Dai, T., & Hamblin, M. R. (2013). Photodynamic inactivation of biofilm: Taking a lightly colored approach to stubborn infection. *Expert Review of Anti-Infective Therapy*, *11*(7), 669–693. https://doi.org/10.1586/14787210.2013.811861.

Del Olmo, A., Calzada, J., & Nuñez, M. (2018). The blue discoloration of fresh cheeses: A worldwide defect associated to specific contamination by *Pseudomonas fluorescens. Food Control*, *86*, 359–366. https://doi.org/10.1016/j.foodcont.2017.12.001.

Deng, Y.-H., Lee, J. H., Kim, M.-J., & Kong, H. (2025). Biofilm comes back: Controlling regrowth by mitigating the cell-matrix interaction. *Chemical Engineering Journal*, *508*, 160947. https://doi.org/10.1016/j.cej.2025.160947.

Di Martino, P. (2018). Extracellular polymeric substances, a key element in understanding biofilm phenotype. *4*(2), 274–288. https://doi.org/10.3934/microbiol.2018.2.274.

Díaz De Rienzo, M. A., Banat, I. M., Dolman, B., Winterburn, J., & Martin, P. J. (2015). Sophorolipid biosurfactants: Possible uses as antibacterial and antibiofilm agent. *New Biotechnology*, *32*(6), 720–726. https://doi.org/10.1016/j.nbt.2015.02.009.

Dong, Q., Sun, L., Fang, T., Wang, Y., Li, Z., Wang, X., Wu, M., & Zhang, H. (2022). Biofilm Formation of *Listeria monocytogenes* and *Pseudomonas aeruginosa* in a Simulated Chicken Processing Environment. *Foods*, *11*(13), 1917. https://doi.org/10.3390/foods11131917 .

Drescher, K., Dunkel, J., Nadell, C. D., Van Teeffelen, S., Grnja, I., Wingreen, N. S., Stone, H. A., & Bassler, B. L. (2016). Architectural transitions in *Vibrio cholerae* biofilms at single-cell resolution. *Proceedings of the National Academy of Sciences*, *113*(14). https://doi.org/10.1073/pnas.1601702113.

Du, B., Lu, M., Liu, H., Wu, H., Zheng, N., Zhang, Y., Zhao, S., Zhao, Y., Gao, T., & Wang, J. (2023). Pseudomonas isolates from raw milk with high-level proteolytic activity display reduced carbon substrate utilization and higher levels of antibiotic resistance. *LWT*, *181*, 114766. https://doi.org/10.1016/j.lwt.2023.114766.

Dueholm, M. S., Petersen, S. V., Sønderkær, M., Larsen, P., Christiansen, G., Hein, K. L., Enghild, J. J., Nielsen, J. L., Nielsen, K. L., Nielsen, P. H., & Otzen, D. E. (2010). Functional amyloid in *Pseudomonas*. *Molecular Microbiology*, *77*(4), 1009–1020. https://doi.org/10.1111/j.1365-2958.2010.07269.x

Eladawy, M., El-Mowafy, M., El-Sokkary, M. M. A., & Barwa, R. (2020). Effects of Lysozyme, Proteinase K, and Cephalosporins on Biofilm Formation by Clinical Isolates of *Pseudomonas aeruginosa*. *Interdisciplinary Perspectives on Infectious Diseases*, *2020*, 1–9. https://doi.org/10.1155/2020/6156720.

Erriu, M., Blus, C., Szmukler-Moncler, S., Buogo, S., Levi, R., Barbato, G., Madonnaripa, D., Denotti, G., Piras, V., & Orrù, G. (2014). Microbial biofilm modulation by ultrasound:

Current concepts and controversies. *Ultrasonics Sonochemistry*, *21*(1), 15–22. https://doi.org/10.1016/j.ultsonch.2013.05.011.

Extracellular polymeric substances, a key element in understanding biofilm phenotype. *AIMS Microbiology*, Ghafoor, A., Jordens, Z., & Rehm, B. H. A. (2013). Role of PelF in Pel Polysaccharide Biosynthesis in *Pseudomonas aeruginosa*. *Applied and Environmental Microbiology*, *79*(9), 2968–2978. https://doi.org/10.1128/AEM.03666-12.

Fazli, M., Almblad, H., Rybtke, M. L., Givskov, M., Eberl, L., & Tolker-Nielsen, T. (2014). Regulation of biofilm formation in *P seudomonas* and *B urkholderia* species. *Environmental Microbiology*, *16*(7), 1961–1981. https://doi.org/10.1111/1462-2920.12448.

Fernandes, S., Gomes, I. B., Simões, M., & Simões, L. C. (2024). Novel chemical-based approaches for biofilm cleaning and disinfection. *Current Opinion in Food Science*, *55*, 101124. https://doi.org/10.1016/j.cofs.2024.101124.

Fleming, D., Chahin, L., & Rumbaugh, K. (2017). Glycoside Hydrolases Degrade Polymicrobial Bacterial Biofilms in Wounds. *Antimicrobial Agents and Chemotherapy*, *61*(2), e01998-16. https://doi.org/10.1128/AAC.01998-16.

Flemming, H.-C., & Wingender, J. (2010). The biofilm matrix. *Nature Reviews Microbiology*, *8*(9), 623–633. https://doi.org/10.1038/nrmicro2415.

Gagnon, G. A., Rand, J. L., O'Leary, K. C., Rygel, A. C., Chauret, C., & Andrews, R. C. (2005). Disinfectant efficacy of chlorite and chlorine dioxide in drinking water biofilms. *Water Research*, *39*(9), 1809–1817. https://doi.org/10.1016/j.watres.2005.02.004.

Gjermansen, M., Nilsson, M., Yang, L. and Tolker-Nielsen, T. (2010). Characterization of starvation-induced dispersion in *Pseudomonas putida* biofilms: genetic elements and molecular mechanisms. Molecular Microbiology, 75: 815-826. https://doi.org/10.1111/j.1365-2958.2009.06793.x.

Guadarrama-Orozco, K. D., Perez-Gonzalez, C., Kota, K., Cocotl-Yañez, M., Jiménez-Cortés, J. G., Díaz-Guerrero, M., Hernández-Garnica, M., Munson, J., Cadet, F., López-Jácome, L. E., Estrada-Velasco, Á. Y., Fernández-Presas, A. M., & García-Contreras, R. (2023). To cheat or not to cheat: Cheatable and non-cheatable virulence factors in

Pseudomonas aeruginosa. *FEMS Microbiology Ecology*, *99*(11), fiad128. https://doi.org/10.1093/femsec/fiad128.

Guo, M., Tan, S., Wu, Y., Zheng, C., Du, P., Zhu, J., Sun, A., & Liu, X. (2024). BrfA functions as a bacterial enhancer-binding protein to regulate functional amyloid Fap-dependent biofilm formation in *Pseudomonas fluorescens* by sensing cyclic diguanosine monophosphate. *Microbiological Research*, *287*, 127864. https://doi.org/10.1016/j.micres.2024.127864.

Guo, M., Tan, S., Zhu, J., Sun, A., Du, P., & Liu, X. (2022). Genes Involved in Biofilm Matrix Formation of the Food Spoiler *Pseudomonas fluorescens* PF07. *Frontiers in Microbiology*, *13*, 881043. https://doi.org/10.3389/fmicb.2022.881043.

Guttenplan, S. B., & Kearns, D. B. (2013). Regulation of flagellar motility during biofilm formation. *FEMS Microbiology Reviews*, *37*(6), 849–871. https://doi.org/10.1111/1574-6976.12018.

Hamblin, M. R. (2016). Antimicrobial photodynamic inactivation: A bright new technique to kill resistant microbes. *Current Opinion in Microbiology*, *33*, 67–73. https://doi.org/10.1016/j.mib.2016.06.008.

Han, Q., Jiang, Y., Brandt, B. W., Yang, J., Chen, Y., Buijs, M. J., Crielaard, W., Cheng, L., & Deng, D. (2019). Regrowth of Microcosm Biofilms on Titanium Surfaces After Various Antimicrobial Treatments. *Frontiers in Microbiology*, *10*, 2693. https://doi.org/10.3389/fmicb.2019.02693.

Harimawan, A., & Ting, Y.-P. (2016). Investigation of extracellular polymeric substances (EPS) properties of *P. aeruginosa* and *B. subtilis* and their role in bacterial adhesion. *Colloids and Surfaces B: Biointerfaces*, *146*, 459–467. https://doi.org/10.1016/j.colsurfb.2016.06.039.

Hinsa, S. M., Espinosa-Urgel, M., Ramos, J. L., & O'Toole, G. A. (2003). Transition from reversible to irreversible attachment during biofilm formation by *Pseudomonas fluorescens* WCS365 requires an ABC transporter and a large secreted protein. *Molecular Microbiology, 49*(4), 905–918. https://doi.org/10.1046/j.1365-2958.2003.03615.

Hoda Mahrous. (2012). Proteolytic and lipolytic activities of *Pseudomonas* spp. Isolated from pasteurized milk. *African Journal of Food Science*, *6*(6). https://doi.org/10.5897/AJFS11.152.

Jennings, Laura K., Kelly M. Storek, Hannah E. Ledvina, Charlène Coulon, Lindsey S. Marmont, Irina Sadovskaya, Patrick R. Secor, et al. 'Pel Is a Cationic Exopolysaccharide That Cross-Links Extracellular DNA in the *Pseudomonas Aeruginosa* Biofilm Matrix'. *Proceedings of the National Academy of Sciences* 112, no. 36 (8 September 2015): 11353–58. https://doi.org/10.1073/pnas.1503058112.

Jeyanathan A, Ramalhete R, Blunn G, et al. *Lactobacillus* cell-free supernatant as a novel bioagent and biosurfactant against *Pseudomonas aeruginosa* in the prevention and treatment of orthopedic implant infection. *J Biomed Mater Res*. 2021; 109: 1634–1643. https://doi.org/10.1002/jbm.b.34821.

Jha, P. K., Dallagi, H., Richard, E., Benezech, T., & Faille, C. (2020). Formation and resistance to cleaning of biofilms at air-liquid-wall interface. Influence of bacterial strain and material. *Food Control*, *118*, 107384. https://doi.org/10.1016/j.foodcont.2020.107384.

Jimoh, A. A., Booysen, E., Van Zyl, L., & Trindade, M. (2023). Do biosurfactants as anti-biofilm agents have a future in industrial water systems? *Frontiers in Bioengineering and Biotechnology*, *11*. https://doi.org/10.3389/fbioe.2023.1244595.

Jones, I. A., & Joshi, L. T. (2021). Biocide Use in the Antimicrobial Era: A Review. *Molecules*, *26*(8), 2276. https://doi.org/10.3390/molecules26082276.

Joseph, B., Otta, S. K., Karunasagar, I., & Karunasagar, I. (2001). Biofilm formation by *Salmonella* spp. On food contact surfaces and their sensitivity to sanitizers. *International Journal of Food Microbiology*, *64*(3), 367–372. https://doi.org/10.1016/S0168-1605(00)00466-9.

Julou, T., Mora, T., Guillon, L., Croquette, V., Schalk, I. J., Bensimon, D., & Desprat, N. (2013). Cell–cell contacts confine public goods diffusion inside *Pseudomonas aeruginosa* clonal microcolonies. *Proceedings of the National Academy of Sciences*, *110*(31), 12577–12582. https://doi.org/10.1073/pnas.1301428110.

Kalpana, B. J., Aarthy, S., & Pandian, S. K. (2012). Antibiofilm Activity of α-Amylase from *Bacillus subtilis* S8-18 Against Biofilm Forming Human Bacterial Pathogens. *Applied*

Biochemistry and Biotechnology, *167*(6), 1778–1794. https://doi.org/10.1007/s12010-011-9526-2.

Karygianni, L., Ren, Z., Koo, H., & Thurnheer, T. (2020). Biofilm Matrixome: Extracellular Components in Structured Microbial Communities. *Trends in Microbiology*, *28*(8), 668–681. https://doi.org/10.1016/j.tim.2020.03.016.

Khalid, S. J., Ain, Q., Khan, S. J., Jalil, A., Siddiqui, M. F., Ahmad, T., Badshah, M., & Adnan, F. (2022). Targeting Acyl Homoserine Lactones (AHLs) by the quorum quenching bacterial strains to control biofilm formation in Pseudomonas aeruginosa. *Saudi Journal of Biological Sciences*, *29*(3), 1673–1682. https://doi.org/10.1016/j.sjbs.2021.10.064.

Kolbeck, S., Abele, M., Hilgarth, M., & Vogel, R. F. (2021). Comparative Proteomics Reveals the Anaerobic Lifestyle of Meat-Spoiling *Pseudomonas* Species. *Frontiers in Microbiology*, *12*, 664061. https://doi.org/10.3389/fmicb.2021.664061.

Krzyżek, P. (2019). Challenges and Limitations of Anti-quorum Sensing Therapies. *Frontiers in Microbiology*, *10*. https://doi.org/10.3389/fmicb.2019.02473.

Kumar, H., Franzetti, L., Kaushal, A., & Kumar, D. (2019). *Pseudomonas fluorescens*: A potential food spoiler and challenges and advances in its detection. *Annals of Microbiology*, *69*(9), 873–883. https://doi.org/10.1007/s13213-019-01501-7.

Kunzler, M., Schlechter, R. O., Schreiber, L., & Remus-Emsermann, M. N. P. (2024). Hitching a Ride in the Phyllosphere: Surfactant Production of *Pseudomonas spp*. Causes Co-swarming of Pantoea eucalypti 299R. *Microbial Ecology*, *87*(1), 62. https://doi.org/10.1007/s00248-024-02381-4.

Lalucat, J., Gomila, M., Mulet, M., Zaruma, A., & García-Valdés, E. (2022). Past, present and future of the boundaries of the *Pseudomonas* genus: Proposal of *Stutzerimonas* gen. Nov. *Systematic and Applied Microbiology*, *45*(1), 126289. https://doi.org/10.1016/j.syapm.2021.126289

Lambert, N., Rediers, H., Hulsmans, A., Joris, K., Declerck, P., De Laedt, Y., & Liers, S. (2010). Evaluation of ultrasound technology for the disinfection of process water and the prevention of biofilm formation in a pilot plant. *Water Science and Technology*, *61*(5), 1089–1096. https://doi.org/10.2166/wst.2010.735.

Lau, G. W., Hassett, D. J., Ran, H., & Kong, F. (2004). The role of pyocyanin in *Pseudomonas aeruginosa* infection. *Trends in Molecular Medicine*, *10*(12), 599–606. https://doi.org/10.1016/j.molmed.2004.10.002.

Laue, H., Schenk, A., Li, H., Lambertsen, L., Neu, T. R., Molin, S., & Ullrich, M. S. (2006). Contribution of alginate and levan production to biofilm formation by *Pseudomonas syringae*. *Microbiology*, *152*(10), 2909-2918.https://doi.org/10.1099/mic.0.28875-0

Lavrikova, A., Janda, M., Bujdáková, H., & Hensel, K. (2025). Eradication of single- and mixed-species biofilms of *Pseudomonas aeruginosa* and *Staphylococcus aureus* by pulsed streamer corona discharge cold atmospheric plasma. *Science of The Total Environment, 916*, 178184. https://doi.org/10.1016/j.scitotenv.2024.178184.

Le Mauff, F., Razvi, E., Reichhardt, C., Sivarajah, P., Parsek, M. R., Howell, P. L., & Sheppard, D. C. (2022). The Pel polysaccharide is predominantly composed of a dimeric repeat of α-1,4 linked galactosamine and N-acetylgalactosamine. *Communications Biology*, *5*(1), 502. https://doi.org/10.1038/s42003-022-03453-2.

Lewis, K. (2010). Persister Cells. *Annual Review of Microbiology*, *64*(1), 357–372. https://doi.org/10.1146/annurev.micro.112408.134306.

Li, Y., Wang, H., Zheng, X., Li, Z., Wang, M., Luo, K., Zhang, C., Xia, X., Wang, Y., & Shi, C. (2022). Didecyldimethylammonium bromide: Application to control biofilms of *Staphylococcus aureus* and *Pseudomonas aeruginosa* alone and in combination with slightly acidic electrolyzed water. *Food Research International*, *157*, 111236. https://doi.org/10.1016/j.foodres.2022.111236.

Lieleg, O., Caldara, M., Baumgärtel, R., & Ribbeck, K. (2011). Mechanical robustness of *Pseudomonas aeruginosa* biofilms. *Soft Matter*, *7*(7), 3307. https://doi.org/10.1039/c0sm01467b.

Liu, J., Wu, S., Feng, L., Wu, Y., & Zhu, J. (2023). Extracellular matrix affects mature biofilm and stress resistance of psychrotrophic spoilage *Pseudomonas* at cold temperature. *Food Microbiology*, *112*, 104214. https://doi.org/10.1016/j.fm.2023.104214.

Liu, X., Ye, Y., Zhu, Y., Wang, L., Yuan, L., Zhu, J., & Sun, A. (2021). Involvement of RpoN in Regulating Motility, Biofilm, Resistance, and Spoilage Potential of Pseudomonas

fluorescens. *Frontiers in Microbiology*, *12*, 641844. https://doi.org/10.3389/fmicb.2021.641844.

Liu, Y., Xie, J., Zhao, L., Qian, Y., Zhao, Y., & Liu, X. (2015). Biofilm Formation Characteristics of *Pseudomonas lundensis* Isolated from Meat. *Journal of Food Science*, *80*(12). https://doi.org/10.1111/1750-3841.13142.

Liu, Z., Hossain, S. S., Morales Moreira, Z., & Haney, C. H. (2022). Putrescine and Its Metabolic Precursor Arginine Promote Biofilm and c-di-GMP Synthesis in Pseudomonas aeruginosa. *Journal of Bacteriology*, *204*(1), e00297-21. https://doi.org/10.1128/JB.00297-21.

Loarca, D., Díaz, D., Quezada, H., Guzmán-Ortiz, A. L., Rebollar-Ruiz, A., Presas, A. M. F., Ramírez-Peris, J., Franco-Cendejas, R., Maeda, T., Wood, T. K., & García-Contreras, R. (2019). Seeding Public Goods Is Essential for Maintaining Cooperation in Pseudomonas aeruginosa. *Frontiers in Microbiology*, *10*, 2322. https://doi.org/10.3389/fmicb.2019.02322.

Machado, S. G., Baglinière, F., Marchand, S., Van Coillie, E., Vanetti, M. C. D., De Block, J., & Heyndrickx, M. (2017). The Biodiversity of the Microbiota Producing Heat-Resistant Enzymes Responsible for Spoilage in Processed Bovine Milk and Dairy Products. *Frontiers in Microbiology*, *8*. https://doi.org/10.3389/fmicb.2017.00302.

Mai-Prochnow, A., Bradbury, M., Ostrikov, K., & Murphy, A. B. (2015). *Pseudomonas aeruginosa* biofilm response and resistance to cold atmospheric pressure plasma is linked to the redox-active molecule phenazine. *PLOS ONE, 10*(6), e0130373. https://doi.org/10.1371/journal.pone.0130373.

Mai-Prochnow, A., Zhou, R., Zhang, T., Ostrikov, K., Mugunthan, S., Rice, S. A., & Cullen, P. J. (2021). Interactions of plasma-activated water with biofilms: Inactivation, dispersal effects and mechanisms of action. *Npj Biofilms and Microbiomes*, *7*(1), 11. https://doi.org/10.1038/s41522-020-00180-6.

Mann, E. E., & Wozniak, D. J. (2012). *Pseudomonas* biofilm matrix composition and niche biology. *FEMS Microbiology Reviews*, *36*(4), 893–916. https://doi.org/10.1111/j.1574-6976.2011.00322.xhttps://doi.org/10.3389/fcimb.2023.1333773.

Marriott, N. G., Schilling, M. W., & Gravani, R. B. (2018). *Principles of Food Sanitation*. Springer International Publishing. https://doi.org/10.1007/978-3-319-67166-6.

Martínez-Gil, M., Quesada, J. M., Ramos-González, M. I., Soriano, M. I., De Cristóbal, R. E., & Espinosa-Urgel, M. (2013). Interplay between extracellular matrix components of Pseudomonas putida biofilms. *Research in Microbiology*, *164*(5), 382–389. https://doi.org/10.1016/j.resmic.2013.03.021.

Martínez-Rodríguez, L., López-Sánchez, A., García-Alcaide, A., Govantes, F., & Gallegos, M.-T. (2023). FleQ, FleN and c-di-GMP coordinately regulate cellulose production in Pseudomonas syringae pv. Tomato DC3000. *Frontiers in Molecular Biosciences*, *10*, 1155579. https://doi.org/10.3389/fmolb.2023.1155579.

McDougald, D., Klebensberger, J., Tolker-Nielsen, T., Webb, J. S., Conibear, T., Rice, S. A., Kirov, S. M., Matz, C., & Kjelleberg, S. (2008). *Pseudomonas aeruginosa: A model for biofilm formation*. In B. H. A. Rehm (Ed.), *Pseudomonas: Model organism, pathogen, cell factory* (pp. 215–254). https://doi.org/10.1002/9783527622009.ch9.

McDougald, D., Rice, S. A., Barraud, N., Steinberg, P. D., & Kjelleberg, S. (2012). Should we stay or should we go: Mechanisms and ecological consequences for biofilm dispersal. *Nature Reviews Microbiology*, *10*(1), 39–50. https://doi.org/10.1038/nrmicro2695.

Mechmechani, S., Gharsallaoui, A., Karam, L., El Omari, K., Fadel, A., Hamze, M., & Chihib, N.-E. (2023). Pepsin and Trypsin Treatment Combined with Carvacrol: An Efficient Strategy to Fight *Pseudomonas aeruginosa* and *Enterococcus faecalis* Biofilms. *Microorganisms*, *11*(1), 143. https://doi.org/10.3390/microorganisms11010143.

Meng, L., Zhang, Y., Liu, H., Zhao, S., Wang, J., & Zheng, N. (2017). Characterization of *Pseudomonas* spp. And Associated Proteolytic Properties in Raw Milk Stored at Low Temperatures. *Frontiers in Microbiology*, *8*, 2158. https://doi.org/10.3389/fmicb.2017.02158.

Merino, N., García-Castillo, C., Berdejo, D., Pagán, E., García-Gonzalo, D., & Pagán, R. (2024). Comparative analysis of commercial cleaning and disinfection formulations and protocols for effective eradication of biofilms formed by a *Pseudomonas fluorescens* strain isolated from a poultry meat plant. *Food Control*, *164*, 110614. https://doi.org/10.1016/j.foodcont.2024.110614.

Molina, G., Pimentel, M. R., & Pastore, G. M. (2013). *Pseudomonas:* A promising biocatalyst for the bioconversion of terpenes. *Applied Microbiology and Biotechnology*, *97*(5), 1851–1864. https://doi.org/10.1007/s00253-013-4701-8.

Mozaheb, N., Rasouli, P., Kaur, M., Van Der Smissen, P., Larrouy-Maumus, G., & Mingeot-Leclercq, M.-P. (2023). A Mildly Acidic Environment Alters *Pseudomonas aeruginosa* Virulence and Causes Remodeling of the Bacterial Surface. *Microbiology Spectrum*, *11*(4), e04832-22. https://doi.org/10.1128/spectrum.04832-22.

Mridha, S., & Kümmerli, R. (2022). Enforced specialization fosters mutual cheating and not division of labour in the bacterium *Pseudomonas aeruginosa*. *Journal of Evolutionary Biology*, *35*(5), 719–730. https://doi.org/10.1111/jeb.14001.

Muthuraman, S., Flint, S., & Palmer, J. (2025). Characterization of the extracellular polymeric substances matrix of *Pseudomonas* biofilms formed at the air-liquid interface. *Food Bioscience*, *64*, 105918. https://doi.org/10.1016/j.fbio.2025.105918.

Nahar, S., Mizan, M. F. R., Ha, A. J., & Ha, S. D. (2018). Advances and future prospects of enzyme-based biofilm prevention approaches in the food industry. *Comprehensive Reviews in Food Science and Food Safety,* *17*(6), 1484–1502. https://doi.org/10.1111/1541-4337.12382.

Naicker, K.-I., Kaweesa, P., Daramola, M. O., & Iwarere, S. A. (2023). Non-Thermal Plasma Review: Assessment and Improvement of Feasibility as a Retrofitted Technology in Tertiary Wastewater Purification. *Applied Sciences*, *13*(10), 6243. https://doi.org/10.3390/app13106243.

Neu, T. R., & Marshall, K. C. (1991). Microbial "footprints"—A new approach to adhesive polymers. *Biofouling*, *3*(2), 101–112. https://doi.org/10.1080/08927019109378166.

Nielsen, L., Li, X., & Halverson, L. J. (2011). Cell–cell and cell–surface interactions mediated by cellulose and a novel exopolysaccharide contribute to *Pseudomonas putida* biofilm formation and fitness under water-limiting conditions. *Environmental Microbiology*, *13*(5), 1342–1356. https://doi.org/10.1111/j.1462-2920.2011.02432.x.

O'Brien, S., Luján, A. M., Paterson, S., Cant, M. A., & Buckling, A. (2017). Adaptation to public goods cheats in *Pseudomonas aeruginosa*. *Proceedings of the Royal Society B: Biological Sciences*, *284*(1859), 20171089. https://doi.org/10.1098/rspb.2017.1089.

O'Toole, G., Kaplan, H. B., & Kolter, R. (2000). Biofilm Formation as Microbial Development. *Annual Review of Microbiology*, *54*(1), 49–79. https://doi.org/10.1146/annurev.micro.54.1.49.

Omran, B. A., Tseng, B. S., & Baek, K.-H. (2024). Nanocomposites against Pseudomonas aeruginosa biofilms: Recent advances, challenges, and future prospects. *Microbiological Research*, *282*, 127656. https://doi.org/10.1016/j.micres.2024.127656.

Paluch, E., Rewak-Soroczyńska, J., Jędrusik, I., Mazurkiewicz, E., & Jermakow, K. (2020). Prevention of biofilm formation by quorum quenching. *Applied Microbiology and Biotechnology*, *104*(5), 1871–1881. https://doi.org/10.1007/s00253-020-10349-w.

Panebianco, F., Rubiola, S., Chiesa, F., Civera, T., & Di Ciccio, P. A. (2022). Effect of gaseous ozone treatment on biofilm of dairy-isolated *Pseudomonas* spp. Strains. *Italian Journal of Food Safety*, *11*(2). https://doi.org/10.4081/ijfs.2022.10350.

Pant, K. J., Cotter, P. D., Wilkinson, M. G., & Sheehan, J. J. (2023). Towards sustainable Cleaning-in-Place (CIP) in dairy processing: Exploring enzyme-based approaches to cleaning in the Cheese industry. *Comprehensive Reviews in Food Science and Food Safety*, 22, 3602–3619. **https://doi.org/10.1111/1541-4337.13206**.

Parkar, S. G., Flint, S. H., & Brooks, J. D. (2004). Evaluation of the effect of cleaning regimes on biofilms of thermophilic bacilli on stainless steel. *Journal of Applied Microbiology*, *96*(1), 110–116. https://doi.org/10.1046/j.1365-2672.2003.02136.x.

Patel, H., & Gajjar, D. (2022a). Cell adhesion and twitching motility influence strong biofilm formation in *Pseudomonas aeruginosa*. *Biofouling*, *38*(3), 235–249. https://doi.org/10.1080/08927014.2022.2054703

Patel, M., Siddiqui, A. J., Ashraf, S. A., Surti, M., Awadelkareem, A. M., Snoussi, M., Hamadou, W. S., Bardakci, F., Jamal, A., Jahan, S., Sachidanandan, M., & Adnan, M. (2022b). *Lactiplantibacillus plantarum*-Derived Biosurfactant Attenuates Quorum Sensing-Mediated Virulence and Biofilm Formation in *Pseudomonas aeruginosa* and *Chromobacterium violaceum*. *Microorganisms*, *10*(5), 1026. https://doi.org/10.3390/microorganisms10051026.

Patel, M., Siddiqui, A. J., Hamadou, W. S., Surti, M., Awadelkareem, A. M., Ashraf, S. A., Alreshidi, M., Snoussi, M., Rizvi, S. M. D., Bardakci, F., Jamal, A., Sachidanandan, M., & Adnan, M. (2021). Inhibition of Bacterial Adhesion and Antibiofilm Activities of a Glycolipid Biosurfactant from *Lactobacillus rhamnosus* with Its Physicochemical and Functional Properties. *Antibiotics*, *10*(12), 1546. https://doi.org/10.3390/antibiotics10121546.

Puga, C. H., Dahdouh, E., SanJosé, C., & Orgaz, B. (2018). *Listeria monocytogenes* colonizes *Pseudomonas fluorescens* biofilms and induces matrix over-production. *Frontiers in Microbiology, 9*, 1706. https://doi.org/10.3389/fmicb.2018.01706.

Puhm, M., Ainelo, H., Kivisaar, M., & Teras, R. (2022). Tryptone in Growth Media Enhances *Pseudomonas putida* Biofilm. *Microorganisms*, *10*(3), 618. https://doi.org/10.3390/microorganisms10030618.

Rajabi, H., Salimizand, H., Khodabandehloo, M., Fayyazi, A., & Ramazanzadeh, R. (2022). Prevalence of *algD* , *pslD* , *pelF* , *Ppgl* , and *PAPI-1* Genes Involved in Biofilm Formation in Clinical *Pseudomonas aeruginosa* Strains. *BioMed Research International*, *2022*(1), 1716087. https://doi.org/10.1155/2022/1716087.

Rehman, Z. U., Momin, A. A., Aldehaiman, A., Irum, T., Grünberg, R., & Arold, S. T. (2022). The exceptionally efficient quorum-quenching enzyme LrsL suppresses *Pseudomonas aeruginosa* biofilm production. *Frontiers in Microbiology*, *13*, 977673. https://doi.org/10.3389/fmicb.2022.977673.

Reichhardt, C. (2023). The Pseudomonas aeruginosa Biofilm Matrix Protein CdrA Has Similarities to Other Fibrillar Adhesin Proteins. *Journal of Bacteriology*, *205*(5), e00019-23. https://doi.org/10.1128/jb.00019-23.

Reichhardt, C., Jacobs, H. M., Matwichuk, M., Wong, C., Wozniak, D. J., & Parsek, M. R. (2020). The Versatile *Pseudomonas aeruginosa* Biofilm Matrix Protein CdrA Promotes Aggregation through Different Extracellular Exopolysaccharide Interactions. *Journal of Bacteriology*, *202*(19). https://doi.org/10.1128/JB.00216-20.

Reichhardt, C., Wong, C., Passos Da Silva, D., Wozniak, D. J., & Parsek, M. R. (2018). CdrA Interactions within the *Pseudomonas aeruginosa* Biofilm Matrix Safeguard It from Proteolysis and Promote Cellular Packing. *mBio*, *9*(5), e01376-18. https://doi.org/10.1128/mBio.01376-18.

Robertson, M., Hapca, S. M., Moshynets, O., & Spiers, A. J. (2013). Air–liquid interface biofilm formation by psychrotrophic pseudomonads recovered from spoiled meat. *Antonie van Leeuwenhoek*, *103*(1), 251–259. https://doi.org/10.1007/s10482-012-9796-x

Rubio-Canalejas, A., Baelo, A., Herbera, S., Blanco-Cabra, N., Vukomanovic, M., & Torrents, E. (2022). 3D spatial organization and improved antibiotic treatment of a *Pseudomonas aeruginosa–Staphylococcus aureus* wound biofilm by nanoparticle enzyme delivery. *Frontiers in Microbiology*, *13*, 959156. https://doi.org/10.3389/fmicb.2022.959156.

Saá Ibusquiza, P., Herrera, J. J. R., Vázquez-Sánchez, D., & Cabo, M. L. (2012). Adherence kinetics, resistance to benzalkonium chloride, and microscopic analysis of mixed biofilms formed by *Listeria monocytogenes* and *Pseudomonas putida. Food Control*, *25*(1), 202–210. https://doi.org/10.1016/j.foodcont.2011.10.002.

Safai, S. M., Khorsandi, K., & Falsafi, S. (2022). Effect of Berberine and Blue LED Irradiation on Combating Biofilm of *Pseudomonas aeruginosa* and *Staphylococcus aureus*. *Current Microbiology*, *79*(12), 366. https://doi.org/10.1007/s00284-022-03063-5.

Sánchez-Lozano, I., Muñoz-Cruz, L. C., Hellio, C., Band-Schmidt, C. J., Cruz-Narváez, Y., Becerra-Martínez, E., & Hernández-Guerrero, C. J. (2023). Metabolomic Insights of Biosurfactant Activity from Bacillus niabensis against Planktonic Cells and Biofilm of Pseudomonas stutzeri Involved in Marine Biofouling. *International Journal of Molecular Sciences*, *24*(4), 4249. https://doi.org/10.3390/ijms24044249.

Santos, T. M., Lopes, M. E. T., De Alencar, E. R., Silva, M. V. D. A., & Machado, S. G. (2025). Ozonized water as a promising strategy to remove biofilm formed by *Pseudomonas* spp. On polyethylene and polystyrene surfaces. *Biofouling*, *41*(2), 144–156. https://doi.org/10.1080/08927014.2024.2444387.

Saraiva, B. B., Campanholi, K. D. S. S., Machado, R. R. B., Nakamura, C. V., Silva, A. A., Caetano, W., & Pozza, M. S. D. S. (2024). Reducing *Pseudomonas fluorescens* in milk through photodynamic inactivation using riboflavin and curcumin with 450 nm blue light-emitting diode. *International Dairy Journal*, *148*, 105787. https://doi.org/10.1016/j.idairyj.2023.105787.

Scarpellini, M., Franzetti, L., & Galli, A. (2004). Development of PCR assay to identify *Pseudomonas fluorescens* and its biotype. *FEMS Microbiology Letters*, *236*(2), 257–260. https://doi.org/10.1111/j.1574-6968.2004.tb09655.x.

Shah, K., & Muriana, P. (2021). Efficacy of a Next Generation Quaternary Ammonium Chloride Sanitizer on Staphylococcus and *Pseudomonas* Biofilms and Practical Application in a Food Processing Environment. *Applied Microbiology*, *1*(1), 89–103. https://doi.org/10.3390/applmicrobiol1010008.

Shi, Y., Jiang, L., Lin, S., Jin, W., Gu, Q., Chen, Y., Zhang, K., & Ettelaie, R. (2022). Ultra-efficient antimicrobial photodynamic inactivation system based on blue light and octyl gallate for ablation of planktonic bacteria and biofilms of *Pseudomonas fluorescens*. *Food Chemistry*, *374*, 131585. https://doi.org/10.1016/j.foodchem.2021.131585.

Silby, M. W., Winstanley, C., Godfrey, S. A. C., Levy, S. B., & Jackson, R. W. (2011). *Pseudomonas* genomes: Diverse and adaptable. *FEMS Microbiology Reviews*, *35*(4), 652–680. https://doi.org/10.1111/j.1574-6976.2011.00269.x.

Simões, M., Simões, L. C., & Vieira, M. J. (2010). A review of current and emergent biofilm control strategies. *LWT - Food Science and Technology*, *43*(4), 573–583. https://doi.org/10.1016/j.lwt.2009.12.008.

Singh, D., & Anand, S. (2022). Efficacy of a typical clean-in-place protocol against in vitro membrane biofilms. *Journal of Dairy Science*, *105*(12), 9417–9425. https://doi.org/10.3168/jds.2022-21712.

Singh, V., Haque, S., Singh, H., Verma, J., Vibha, K., Singh, R., Jawed, A., & Tripathi, C. K. M. (2016). Isolation, Screening, and Identification of Novel Isolates of Actinomycetes from India for Antimicrobial Applications. *Frontiers in Microbiology*, *7*. https://doi.org/10.3389/fmicb.2016.01921.

Song, B., & Leff, L. G. (2006). Influence of magnesium ions on biofilm formation by Pseudomonas fluorescens. *Microbiological Research*, *161*(4), 355–361. https://doi.org/10.1016/j.micres.2006.01.004.

Starkey, M., Hickman, J. H., Ma, L., Zhang, N., De Long, S., Hinz, A., Palacios, S., Manoil, C., Kirisits, M. J., Starner, T. D., Wozniak, D. J., Harwood, C. S., & Parsek, M. R. (2009). *Pseudomonas aeruginosa* rugose small-colony variants have adaptations that

likely promote persistence in the cystic fibrosis lung. *Journal of Bacteriology, 191*(11), 3492–3503. https://doi.org/10.1128/JB.00119-09.

Sterniša, M., Gradišar Centa, U., Drnovšek, A., Remškar, M., & Smole Možina, S. (2023). *Pseudomonas fragi* biofilm on stainless steel (at low temperatures) affects the survival of *Campylobacter jejuni* and *Listeria monocytogenes* and their control by a polymer molybdenum oxide nanocomposite coating. *International Journal of Food Microbiology*, *394*, 110159. https://doi.org/10.1016/j.ijfoodmicro.2023.110159.

Su, Y., Jiang, L., Chen, D., Yu, H., Yang, F., Guo, Y., Xie, Y., & Yao, W. (2022). In vitro and in silico approaches to investigate antimicrobial and biofilm removal efficacies of combined ultrasonic and mild thermal treatment against *Pseudomonas fluorescens*. *Ultrasonics Sonochemistry*, *83*, 105930. https://doi.org/10.1016/j.ultsonch.2022.105930.

Sung, K., Park, M., Chon, J., Kweon, O., & Khan, S. (2024). Unraveling the molecular dynamics of *Pseudomonas aeruginosa* biofilms at the air–liquid interface. *Future Microbiology*, *19*(8), 681–696. https://doi.org/10.2217/fmb-2023-0234.

Tan, X., Huang, Y., Rana, A., Singh, N., Abbey, T. C., Chen, H., Toth, P. T., & Bulman, Z. P. (2024). Optimization of an in vitro *Pseudomonas aeruginosa* Biofilm Model to Examine Antibiotic Pharmacodynamics at the Air-Liquid Interface. *Npj Biofilms and Microbiomes*, *10*(1), 16. https://doi.org/10.1038/s41522-024-00483-y.

Teh, K. H., Flint, S., Palmer, J., Andrewes, P., Bremer, P., & Lindsay, D. (2012). Proteolysis produced within biofilms of bacterial isolates from raw milk tankers. *International Journal of Food Microbiology*, *157*(1), 28–34. https://doi.org/10.1016/j.ijfoodmicro.2012.04.008.

Tribelli, P. M., & López, N. I. (2022). Insights into the temperature responses of Pseudomonas species in beneficial and pathogenic host interactions. *Applied Microbiology and Biotechnology*, *106*(23), 7699–7709. https://doi.org/10.1007/s00253-022-12243-z.

Ueda, A., & Saneoka, H. (2015). Characterization of the Ability to Form Biofilms by Plant-Associated *Pseudomonas* Species. *Current Microbiology*, *70*(4), 506–513. https://doi.org/10.1007/s00284-014-0749-7.

Wagner, E. M., Fischel, K., Rammer, N., Beer, C., Palmetzhofer, A. L., Conrady, B., Roch, F.-F., Hanson, B. T., Wagner, M., & Rychli, K. (2021). Bacteria of eleven different species

isolated from biofilms in a meat processing environment have diverse biofilm-forming abilities. *International Journal of Food Microbiology*, *349*, 109232. https://doi.org/10.1016/j.ijfoodmicro.2021.109232.

Wang, D., Fletcher, G. C., Gagic, D., On, S. L. W., Palmer, J. S., & Flint, S. H. (2023). Comparative genome identification of accessory genes associated with strong biofilm formation in Vibrio parahaemolyticus. *Food Research International*, *166*, 112605. https://doi.org/10.1016/j.foodres.2023.112605.

Wang, D., Kyere, E., & Ahmed Sadiq, F. (2021a). New Trends in Photodynamic Inactivation (PDI) Combating Biofilms in the Food Industry—A Review. *Foods*, *10*(11), 2587. https://doi.org/10.3390/foods10112587.

Wang, G., Qing Li, Tang, W., Ma, F., Wang, H., Xu, X., & Qiu, W. (2021b). AprD is important for extracellular proteolytic activity, physicochemical properties, and spoilage potential in meat-borne *Pseudomonas fragi*. *Food Control*, *124*, 107868. https://doi.org/10.1016/j.foodcont.2021.107868.

Wang, M., Jiang, L., Liu, M., Yuan, S., Guo, Y., Yao, W., & Yu, H. (2024). Effects of ultrasound on disrupting metabolite profiles of *Pseudomonas fluorescens* biofilms cultured on the surface of lettuce. *Food Control*, *155*, 110103. https://doi.org/10.1016/j.foodcont.2023.110103.

Wang, S., Liu, X., Liu, H., Zhang, L., Guo, Y., Yu, S., Wozniak, D. J., & Ma, L. Z. (2015). The exopolysaccharide Psl-eDNA interaction enables the formation of a biofilm skeleton in *Pseudomonas aeruginosa*. *Environmental Microbiology Reports*, *7*(2), 330–340. https://doi.org/10.1111/1758-2229.12252.

Wang, S., Zhao, Y., Breslawec, A. P., Liang, T., Deng, Z., Kuperman, L. L., & Yu, Q. (2023). Strategy to combat biofilms: A focus on biofilm dispersal enzymes. *Npj Biofilms and Microbiomes*, *9*(1), 63. https://doi.org/10.1038/s41522-023-00427-y.

Wehedy, S., Elshafee, A., Helal, Z., Eldin, Y., Yassin, A., & Zaki, H. (2025). Contamination of meat and its products by *Pseudomonas* species and assessment of the antibacterial effect of clove (*Syzygium aromaticum*) essential oil on multidrug-resistant *P. aeruginosa*. *Open Veterinary Journal*, *0*, 1. https://doi.org/10.5455/OVJ.2025.v15.i4.34.

Wickramasinghe, N. N., Hlaing, M. M., Ravensdale, J. T., Coorey, R., Chandry, P. S., & Dykes, G. A. (2020). Characterization of the biofilm matrix composition of psychrotrophic, meat spoilage pseudomonads. *Scientific Reports*, *10*(1), 16457. https://doi.org/10.1038/s41598-020-73612-0.

Wickramasinghe, N. N., Ravensdale, J. T., Coorey, R., Dykes, G. A., & Scott Chandry, P. (2019). *In situ* characterisation of biofilms formed by psychrotrophic meat spoilage pseudomonads. *Biofouling*, *35*(8), 840–855. https://doi.org/10.1080/08927014.2019.1669021.

Wickramasinghe, N. N., Ravensdale, J., Coorey, R., Chandry, S. P., & Dykes, G. A. (2019). The Predominance of Psychrotrophic Pseudomonads on Aerobically Stored Chilled Red Meat. *Comprehensive Reviews in Food Science and Food Safety*, *18*(5), 1622–1635. https://doi.org/10.1111/1541-4337.12483.

Wickramasinghe, N. N., Ravensdale, J., Coorey, R., Dykes, G. A., & Chandry, P. S. (2021). Transcriptional profiling of biofilms formed on chilled beef by psychrotrophic meat spoilage bacterium, *Pseudomonas fragi* 1793. *Biofilm*, *3*, 100045. https://doi.org/10.1016/j.bioflm.2021.100045.

Winsor, G. L., Van Rossum, T., Lo, R., Khaira, B., Whiteside, M. D., Hancock, R. E., & Brinkman, F. S.(2009). Pseudomonas Genome Database: Facilitating user-friendly, comprehensive comparisons of microbial genomes. Nucleic Acids Research, 37(Suppl. 1), D483–D488. https://doi.org/10.1093/nar/gkn861.

Wood, T. K. (2016). Combatting bacterial persister cells. *Biotechnology and Bioengineering*, *113*(3), 476–483. https://doi.org/10.1002/bit.25721

Wu, Y., Ma, F., Pang, X., Chen, Y., Niu, A., Tan, S., Chen, X., Qiu, W., & Wang, G. (2022). Involvement of AprD in regulating biofilm structure, matrix secretion, and cell metabolism of meat-borne Pseudomonas fragi during chilled storage. *Food Research International*, *157*, 111400. https://doi.org/10.1016/j.foodres.2022.111400

Yang, L., Hu, Y., Liu, Y., Zhang, J., Ulstrup, J., & Molin, S. (2011). Distinct roles of extracellular polymeric substances in *Pseudomonas aeruginosa* biofilm development. *Environmental Microbiology*, *13*(7), 1705–1717. https://doi.org/10.1111/j.1462-2920.2011.02503.x

Yang, L., Liu, Y., Markussen, T., Høiby, N., Tolker-Nielsen, T., & Molin, S. (2011). Pattern differentiation in co-culture biofilms formed by *Staphylococcus aureus* and *Pseudomonas aeruginosa*. *FEMS Immunology & Medical Microbiology*, *62*(3), 339–347. https://doi.org/10.1111/j.1574-695X.2011.00820.x

Ye, Z., Silva, D. M., Traini, D., Young, P., Cheng, S., & Ong, H. X. (2022). An adaptable microreactor to investigate the influence of interfaces on Pseudomonas aeruginosa biofilm growth. *Applied Microbiology and Biotechnology*, *106*(3), 1067–1077. https://doi.org/10.1007/s00253-021-11746-5

Yin, R., Cheng, J., Wang, J., Li, P., & Lin, J. (2022). Treatment of *Pseudomonas aeruginosa* infectious biofilms: Challenges and strategies. *Frontiers in Microbiology*, *13*. https://doi.org/10.3389/fmicb.2022.955286

Yu, H., Liu, Y., Li, L., Guo, Y., Xie, Y., Cheng, Y., & Yao, W. (2020). Ultrasound-involved emerging strategies for controlling foodborne microbial biofilms. *Trends in Food Science & Technology*, *96*, 91–101. https://doi.org/10.1016/j.tifs.2019.12.010

Yuan, L., Liu, Y., Mi, Z., Xiong, D., Zhou, W., Xu, Z., Yang, Z., & Jiao, X. (2025). Dual-species biofilm and other profiles altered by interactions between Salmonella Typhimurium and Pseudomonas fluorescens isolated from meat. *Food Research International*, *203*, 115914. https://doi.org/10.1016/j.foodres.2025.115914

Yuan, L., Sadiq, F. A., Wang, N., Yang, Z., & He, G. (2021). Recent advances in understanding the control of disinfectant-resistant biofilms by hurdle technology in the food industry. *Critical Reviews in Food Science and Nutrition*, *61*(22), 3876–3891. https://doi.org/10.1080/10408398.2020.1809345

Yuan, L., Zhang, Y., Mi, Z., Zheng, X., Wang, S., Li, H., & Yang, Z. (2024). Calcium-mediated modulation of Pseudomonas fluorescens biofilm formation. *Journal of Dairy Science*, *107*(4), 1950–1966. https://doi.org/10.3168/jds.2023-23860

Zeng, G., Vad, B. S., Dueholm, M. S., Christiansen, G., Nilsson, M., Tolker-Nielsen, T., Nielsen, P. H., Meyer, R. L., & Otzen, D. E. (2015). Functional bacterial amyloid increases Pseudomonas biofilm hydrophobicity and stiffness. *Frontiers in Microbiology*, *6*. https://doi.org/10.3389/fmicb.2015.01099

Zhang, Y., Silva, D. M., Young, P., Traini, D., Li, M., Ong, H. X., & Cheng, S. (2022). Understanding the effects of aerodynamic and hydrodynamic shear forces on *Pseudomonas aeruginosa* biofilm growth. *Biotechnology and Bioengineering*, 119, 1483–1497. https://doi.org/10.1002/bit.28077

Zhou, G., Dong, P., Luo, X., Zhu, L., Mao, Y., Liu, Y., & Zhang, Y. (2024). Combined effects of cold and acid on dual-species biofilms of Pseudomonas fluorescens and Listeria monocytogenes under simulated chilled beef processing conditions. *Food Microbiology*, *117*, 104394. https://doi.org/10.1016/j.fm.2023.104394

Zhou, G., Liu, Y., Dong, P., Mao, Y., Zhu, L., Luo, X., & Zhang, Y. (2024). Airborne signals of Pseudomonas fluorescens modulate swimming motility and biofilm formation of Listeria monocytogenes in a contactless coculture system. *Food Microbiology*, *120*, 104494. https://doi.org/10.1016/j.fm.2024.104494

Zhu, Y., Li, C., Cui, H., & Lin, L. (2020). Feasibility of cold plasma for the control of biofilms in food industry. *Trends in Food Science & Technology*, *99*, 142–151. https://doi.org/10.1016/j.tifs.2020.03.001

Chapter 3 Biofilm-Forming Abilities of Psychrotrophic Pseudomonads

This chapter is an adaptation of material that was published as a peer-reviewed article:

Muthuraman, S., Palmer, J., & Flint, S. (2026). Enzymatic dispersion of pseudomonad biofilms grown at psychrotrophic temperature. *Food and Bioproducts Processing*, *155*, 179–188. https://doi.org/10.1016/j.fbp.2025.12.015.

Preface to Chapter 3

In Chapter 2, the biofilm formation of pseudomonads at the air-liquid interface, at psychrotrophic temperatures, and their control strategies have been discussed. In chapter 3, the strong biofilm formers were screened based on the crystal violet assay and cell counts at both 4°C and 30°C. The biofilms were allowed to form on polystyrene (PS) and stainless steel (SS) surfaces. The Congo Red Assay (CRA) and cellulose quantification were used to identify the isolates for cellulose and curli production.

3.1 Introduction

Pseudomonas spp. is a common psychrotrophic bacterium found in aerobically stored protein-rich foods such as red meat, poultry, and dairy. These gram-negative rods produce a wide range of thermostable proteolytic and lipolytic enzymes responsible for the curdling and gelation of milk (Weidmann et al.,2000; Parlapani et al.,2023). Pseudomonads such as *P. fluorescens* biovar I and II produce pyocyanin and pyoverdine and cause discoloration of foods (Dogan & Boor, 2003; Nychas et al., 2008; Chiesa et al., 2014).

Among the spoilage psychrotrophic bacteria present in milk, many isolates belong to the genus *Pseudomonas*, making it the most important genus in the dairy sector (Von Neubeck et al., 2015). Several studies report that pseudomonads form biofilms in dairy processing lines (Machado et al.,2017). Blue discoloration on the external surface of mozzarella cheese was caused by a blue branch cluster of pseudomonads (*P. fluorescens, P. korensis, P. carnis,* and *P. lactis*) (Andreani et al.,2019). *P. fluorescens*, *P. fragi*, *P. cedrina*, *P. lurida*, *P. psychrophila,* and *P. gessardii* are the common pseudomonads present in raw milk (Du et al., 2023).

Pseudomonads are known for their biofilm formation with EPS overproduction (Liu et al., 2023). Pseudomonads can form biofilms on biotic and abiotic surfaces and can be a source of continuous contamination in food processing environments. Due to reduced diffusivity, the biofilm can protect the bacterial cells from the cleaning chemicals (Aswath Narayan and Vittal, 2014). This group of bacteria can grow and form biofilms under a wide range of temperatures, especially at cold chain temperatures (Liu et al.,2015; Wickramasinghe et al.,2020). Comparing the biofilm formation under cold and ambient temperatures will be helpful in controlling these biofilms in food processing environments.

Cellulose and curli fibres are identified in the biofilm formation of Escherichia *coli*, *Salmonella, Pseudomonas* and some other proteobacteria and are involved in the strong biofilm formation (Wang et al., 2023; Abidi et al., 2022; Dueholm et al., 2010). Bacterial cellulose in biofilms is mainly seen in oxygen-dependent organisms that form an air-liquid interface (Cohen & Merzendorfer, 2019; Wahid & Zhong, 2021). Bacterial cellulose is known for its high-water retention and mechanical strength (Mbituyimana et al., 2021). Screening the biofilm formers based on cellulose and curli production is commonly observed with *E. coli* and *Salmonella* (Cimdins and Roger 2017). Studying the cellulose and curli production is important to identify the mechanism behind the biofilm formation.

The biofilm formation studies are usually done on the polystyrene microtiter plates. However, stainless steel is the common food contact surface in food processing industries (Oliveira et al., 2010). In Chapter 2, the biofilm formation abilities of pseudomonads in cold temperatures were discussed. This chapter focuses on comparing the biofilm formation abilities on both polystyrene and stainless-steel surfaces at different temperatures.

3.2 Materials and methods

3.2.1 Bacterial isolates and culture conditions

Eleven dairy isolates 1SM,2SM, 3SM, 4SM, 5SM, 6SM, 7SM, 16SM, 20SM, 38SM, 44SM were used in this study. All these isolates were obtained from raw milk collected from different dairy farms across New Zealand (Zhang et al., 2020).

Fresh, overnight cultures of these dairy isolates were prepared by streaking a stock culture (Stored at -80°C) on a Tryptic Soy agar plate (TSA, Difco^{TM}, Becton, Dickinson and Company, USA), incubating at 30°C, and inoculating a single colony in the Tryptic soy broth (TSB, Difco^{TM}, Becton, Dickinson and Company, USA) overnight at 30°C. This overnight culture (18 h) was used for further experiments.

To count the colony-forming units (CFU), the cultures were serially 10-fold diluted in physiological sterile saline (0.85% NaCl), and the dilutions were plated either by spread or drop plate on TSA.

3.2.2 Identification using PCR and 16S rDNA sequencing.

PCR amplification of 16S rDNA was used to confirm the identification of the isolates using universal primers Bac27F(5′-AGAGTTTGATCCTGGCTCAG-3′) and 1492R(5′-TACGGYTACCTTGTTACGACTT-3′) (Flint et al., 1999). The PCR amplification involved, 25µL of master mix (dNTPs, magnesium chloride, Taq polymerase) (Platinum Green Hot Start PCR Master mix, Invitrogen, Thermofisher Scientific, USA), 20µL of nuclease-free water, 1µL of forward primer, 1µL of reverse primer, and 3µL of overnight bacterial culture to a final volume of 50 µL. Amplification steps were as follows: denaturing at 94°C for 5 min, followed by 30 cycles of denaturing at 96°C for 25s, annealing at 50°C for 45s, and extension at 72°C for 2 min and final extension at 72°C for 7 min. The PCR assay was

carried out in a thermal cycler (Proflex PCR System, Thermofisher Scientific, USA). The PCR products were visualized (E-Gel iBASE™, Invitrogen, USA) using pre-made 2% agarose electrophoresis gel (E-Gel ® EX with SYBR Gold II, Invitrogen, USA). The PCR products were purified using a cleaning and concentration kit for DNA (DNA Clean and Concentrator, Zymo Research, USA). The DNA concentration after cleaning was checked using Nanodrop (Nanodrop Microvolume Spectrophotometers, Thermofisher Scientific, USA). The partial 16S rDNA sequencing was done at Massey genomics using Big Dye Terminator v3.1, and the results were analysed by Chromaslite and BLAST gene bank.

3.2.3 Biofilm formation

3.2.3.1 Polystyrene surface (PS)

The biofilms were allowed to grow on 96-well plates (cell culture plate with non-treated surface) (FALCON®, Corning Incorporated, Durham, USA). (Filloux & Ramos, 2014). A cell suspension was diluted to obtain an OD_{600} (Absorbance at 600nm) of 0.05±0.0015 (approximately 6 log CFU/mL) (Varioskan Lux 3020-1333, Thermo Fisher, USA) with 50% TSB (half-strength). Next, 200 µL of the adjusted inoculum was added to the wells of a 96-well microtiter plate. Two hundred microliters (200 µL) of half-strength TSB were added as a control. The plates were incubated at 4°C and 30°C for 24,48, 72,168, and 336 hours. Spent media was replaced, and fresh media was added to the wells every 72 h.

3.2.3.2 Stainless-steel surface (SS)

The biofilm formation on stainless-steel coupons was modified from (Wang et al., 2023). The stainless-steel coupons (SS) used in this study were 2.4 cm* 2.4 cm and 1mm in thickness (316 with 2B finish) (SS coupons, Advanced Sheet Metals, Palmerston North). The coupons were passivated (with 50% nitric acid at 70°C for 30 mins) to clean and generate an oxide coat on the surface (as is practiced in the food industry to reduce the possibility of corrosion) before being used for the biofilm formation assay. The used SS coupons were sonicated for 15 min to remove the adhering cells and cleaned with ethanol (Absolute ethanol, Thermo Fisher Scientific, USA) and Tri Gene (Tri Gene, Tristel Solutions Ltd, UK) (Composition listed in supplementary file 3.7). The cleaned coupons were allowed to dry overnight and autoclaved at 121°C for 15 min.

The SS coupons were placed diagonally in the vials (Plastic vials, Techno Plas Ltd, Australia**)** and filled with 4 mL of the inoculum to create an air-liquid interface on the surface of the coupons. The same culture concentration was maintained as on the PS surface. The vials were incubated at 30°C and 4°C for 24,48, 72,168, and 336 h. The biofilms were incubated from 24 to 336 h to test the biofilm formation from the early to the maturation stages. The coupons with 4 mL of half-strength TSB were used as a control. Spent media was replaced with fresh media every 72 h.

3.2.3.3 Crystal violet assay

After the required incubation time, the microtiter plates were taken out and gently inverted to remove the liquid from the wells. The wells were washed three times with sterile distilled water to remove all the planktonic and loosely attached cells and allowed to air-dry for 30 min. Two hundred microliters (200 µL) of 0.5% crystal violet (CV) (Crystal violet stain, Sigma-Aldrich, USA) were added to each well. After 15 min, the crystal violet-containing wells were washed three times with sterile distilled water. It was allowed to dry for 30 min. Next, 230 µL of 96% ethanol was added to the wells to dissolve the absorbed crystal violet and allowed to stand for 15 min at room temperature. After 15 min, the absorbance of the ethanol solution was read at 570 nm.

After the required incubation time, the SS coupons were taken out and washed three times with sterile distilled water and allowed to air-dry for 30 min. The dried coupons were added to the 6-well microtiter plates (FALCON®, Corning Incorporated, Durham, USA) filled with 4 mL of 0.5% crystal violet. After 15 min, the coupons were taken out and washed three times with sterile distilled water and allowed to air-dry for 30 min. The stained coupons were added to the 6-well plates containing 4 mL of 96% ethanol for 15 min. The contents were transferred to the 96-well plates and read at 570 nm.

Based on the CV values, the isolates were classified as strong, weak, and moderate biofilm formers based on the following criteria described by Xu et al. (2016) (Table 3.1).

Table 3.1: Classification of biofilm formation

No biofilm formation	$OD_{570} < OD_{570con}$
Weak biofilm formation	$OD_{570con} < OD_{570} \leq 2\ OD_{570con}$
Moderate biofilm formation	$2OD_{570con} < OD_{570} \leq 4\ OD_{570con}$

Strong biofilm formation	4 $OD_{570con} \leq OD_{570}$

*OD_{570con} – OD_{570} values from control wells with no biofilm formation

*OD_{570} - OD_{570} values from the wells with biofilms

3.2.3.4 Quantification of biofilm cells on PS wells and SS coupons

The wells of the PS microtiter plate and SS coupons were washed thrice with sterile distilled water after the required incubation period. Using sterile cotton swabs (CITOSWAB®, Wellkang Ltd, Northern Ireland), the wells, and coupons were swabbed and swirled in sterile saline. Then, 100 µL of the samples were serially diluted and 10 µL of drops were plated on TSA plates. The numbers of cells present in the wells and coupons were expressed as log $CFU/cm^{2.}$

3.2.4 Congo Red Assay (CRA)

The dairy isolates were screened by Congo red assay for biofilm formation (Cimdins and Roger 2017). Tryptone Agar (10g/L of tryptone and 15g/L of agar) was chosen due to the low interference with the results. Congo Red (Congo Red, Sigma-Aldrich, USA) 2g/L and Coomassie Brilliant Blue (Coomassie Brilliant Blue G-250, Sigma-Aldrich, USA)1g/L were prepared as aqueous solutions and autoclaved (121°C for 15 min). The above-mentioned stains were added later to the autoclaved T agar at 55°C (Köseoğlu et al.,2015; Cimdins and Roger, 2017), poured into agar plates, and allowed to set at room temperature. Overnight cultures (18 h) were streaked onto the agar plates and incubated at 30°C for 24 h to 120 h. Red, brown, pink, and white colonies indicate the production of curli and cellulose, curli, cellulose, and none, respectively.

3.2.5 Levan production

Levan is a capsular polysaccharide commonly found in the biofilms of *Pseudomonas* spp. Nutrient agar (NA, Difco™, Becton, Dickinson and Company, USA) with 5% sucrose (Sucrose, Sigma-Aldrich, USA) was used to screen the Levan producers. The bacteria with

the enzyme Levan sucrase convert sucrose into Levan, which was confirmed by the appearance of mucoid colonies (Lelliott and Stead,1987).

3.2.6 Cellulose production

Cellulose production was quantified using Anthrone colorimetry (Wang et al.,2023). The stock cultures of the isolates were streaked onto TSA plates and incubated at 30°C for 24 h and 48 h in triplicate. After incubation, approximately 3 g of wet-weight colonies were collected in a 15 mL centrifuge tube using a cell scraper. The extraction solution, consisting of an 8:2:1 ratio of acetic acid, nitric acid, and water, was added to the centrifuge tube. The mixture was boiled for 30 min and centrifuged at 11880 *g* for 5 min. The supernatant was discarded, and the pellet was washed with 1 mL of water and 1 mL of acetone and left overnight for drying. The dried pellet was dissolved in 1 mL of H_2SO_4. Then, 0.1 mL of the mixture was added to 0.5 mL of Anthrone (Anthrone ACS reagent, Sigma-Aldrich, USA) (0.2 g in 100 mL of H_2SO_4), and the absorbance was read at 620 nm. Microcrystalline cellulose (Cellulose, Sigma Aldrich, USA) solutions of 25mg/mL, 50mg/mL, and 100mg/mL were used as standards. From this, the strong cellulose producers were identified (Wang et al., 2023).

3.2.7 Data analysis

Viable colony counts were enumerated and transformed as log CFU/mL for planktonic cultures and log CFU/cm^2 for biofilms. The mean values and standard deviation (SD) for cell counts were based on three biological and three technical replicates. One-way analysis of variance (ANOVA) with a Tukey's test with a *p*-value below 0.05 indicated the significance of the results. The analysis was conducted using SPSS software (Version 29.0.2.0; IBM®, New York, United States).

3.3 Results

3.3.1 Identification by PCR and partial 16S rDNA sequencing

Identification of the presumptive *Pseudomonas* spp. isolates were confirmed with PCR and partial 16S rDNA sequencing, and the results are shown in Table 3.2 below.

Table 3.2 Identification by PCR and partial 16S rDNA sequencing

No.	Bacterial Identity	16S rDNA (% similarity)
1SM	*P. fluorescens*	99
2SM	*P. fragi*	97.12
3SM	*P. lundensis*	98
4SM	*P. fragi*	98
5SM	*P. psychrophilla*	98
6SM	*P. antartica*	98
7SM	*P. psychrophilla*	97.15
16SM	*P. fluorescens*	99
20SM	*P. cedrina*	98
38SM	*P. brenneri*	99
44SM	*P. fragi*	98

3.3.2 Biofilm formation

3.3.2.1 Biofilm formation on PS surface

Among the 11 isolates tested, only 2 isolates formed strong biofilms at both temperatures. Isolates 3SM and 20SM produced significantly ($p < 0.05$) higher cells and EPS compared to other isolates. However, the crystal violet values and cell counts were higher at 4°C than at 30°C.

At 30°C, the biofilm screening resulted in two strong biofilm formers, four moderate biofilm formers, and five weak biofilm formers (Fig. 3.1 A). The highest CV value reached was 1.38 ± 0.23 for isolate 3SM at 336 h and 1.34 ± 0.05 for isolate 20SM at 72 h. The cell counts of

the strong biofilm formers reached 6.60 ± 0.13 (3SM) and 6.58 ± 0.16 log CFU/cm^2 (20SM) (Fig. 3.1 B). The moderate biofilm formers were 1SM,4SM,7SM and 16SM and the weak biofilm formers were 2SM, 5SM,7SM, 38SM and 44SM.

At 4°C, the biofilm screening resulted in two strong biofilm formers and nine weak biofilm formers. The moderate biofilm formers at 30ºC failed to form biofilms at 4ºC. The crystal violet values for the strong biofilm formers reached 3.60 ± 0.27 (3SM)and 3.40 ± 0.36 (20SM) (Fig.3.2 A). The cell counts of the strong biofilm formers reached 8.60 ± 0.41 and 8.41 ± 0.10 log CFU/cm^2 (Fig. 3.2 B).

(A)

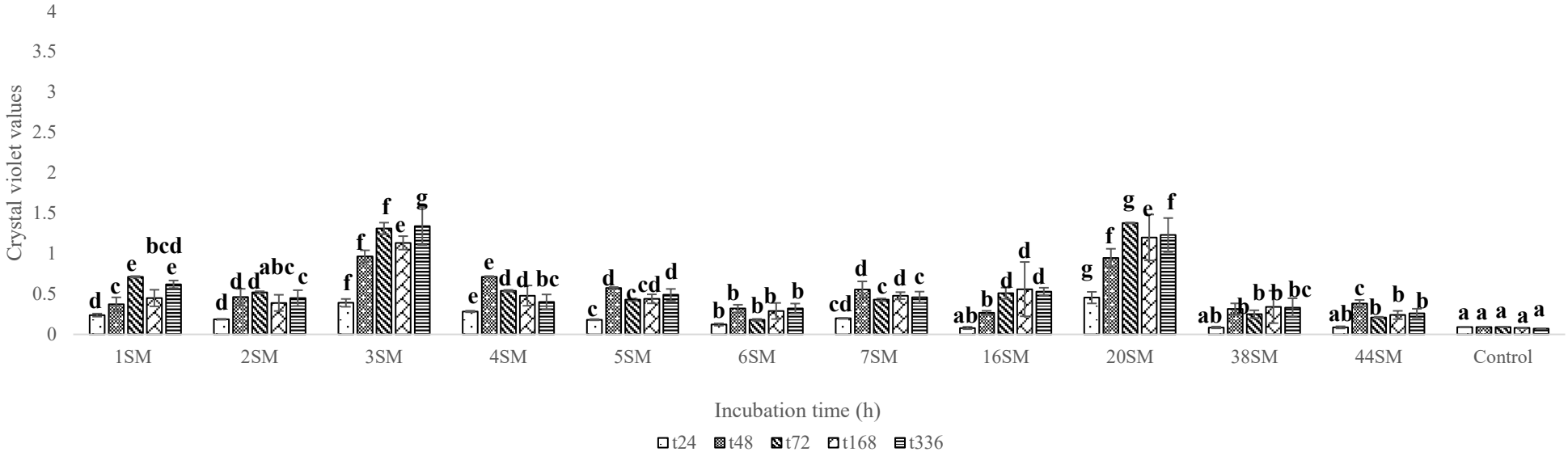
Crystal violet values
4
3.5
3
2.5
2
1.5
1
0.5
0
1SM
2SM
3SM
4SM
5SM
6SM
7SM
16SM
20SM
38SM
44SM
Control
Incubation time (h)
t24
t48
t72
t168
t336

(B)

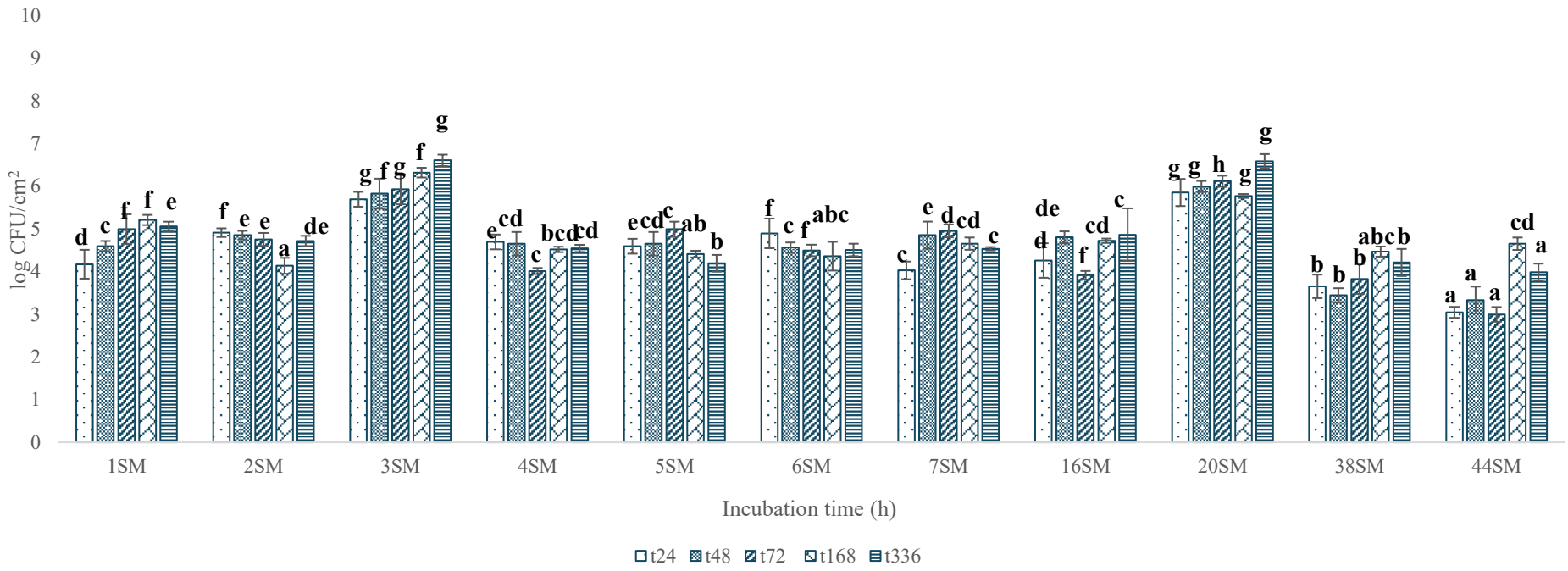

Figure 3.1 (A) OD570 values from the crystal violet assay as a function of time, at 30°C with half-strength TSB and (B) the cell counts at 30°C as a function of time with half-strength TSB. All the results are expressed as mean ± standard deviation. Different letters above the bars indicate significant differences ($p < 0.05$).

(A)

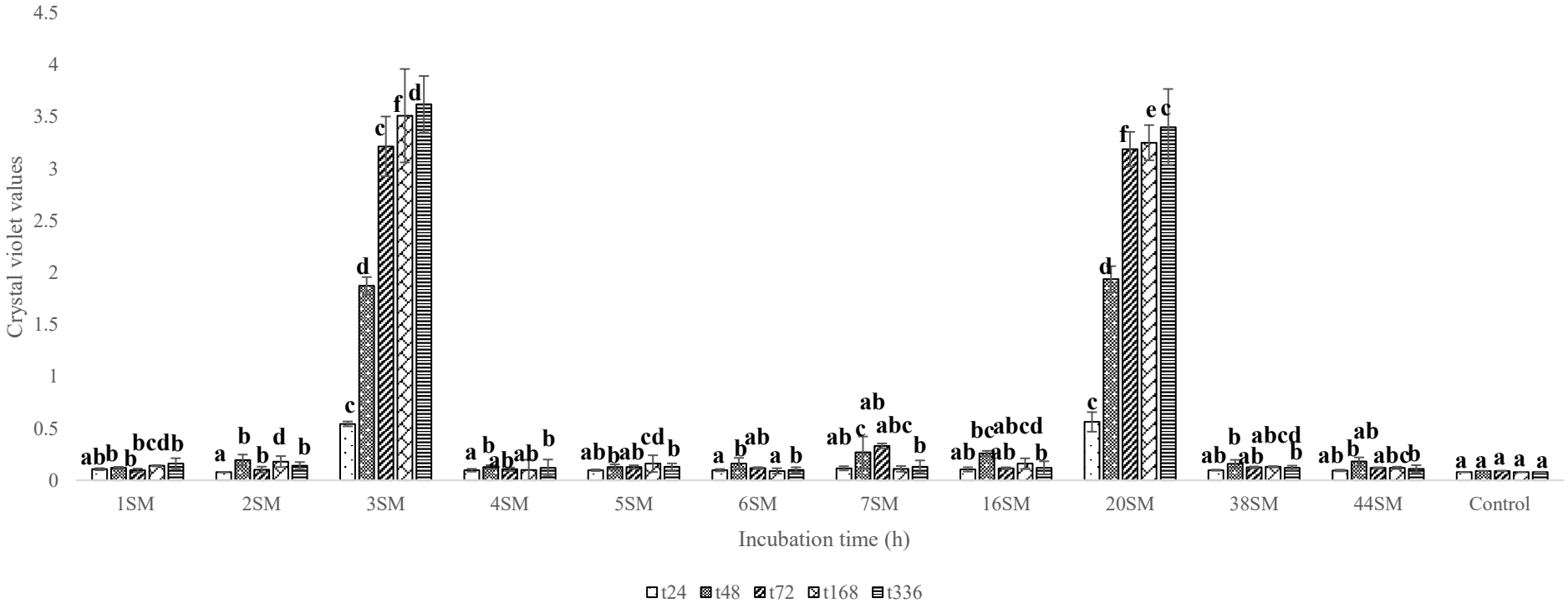
Crystal violet values
4.5
4
3.5
3
2.5
2
1.5
1
0.5
0
1SM
2SM
3SM
4SM
5SM
6SM
7SM
16SM
20SM
38SM
44SM
Control
Incubation time (h)
t24
t48
t72
t168
t336

(B)

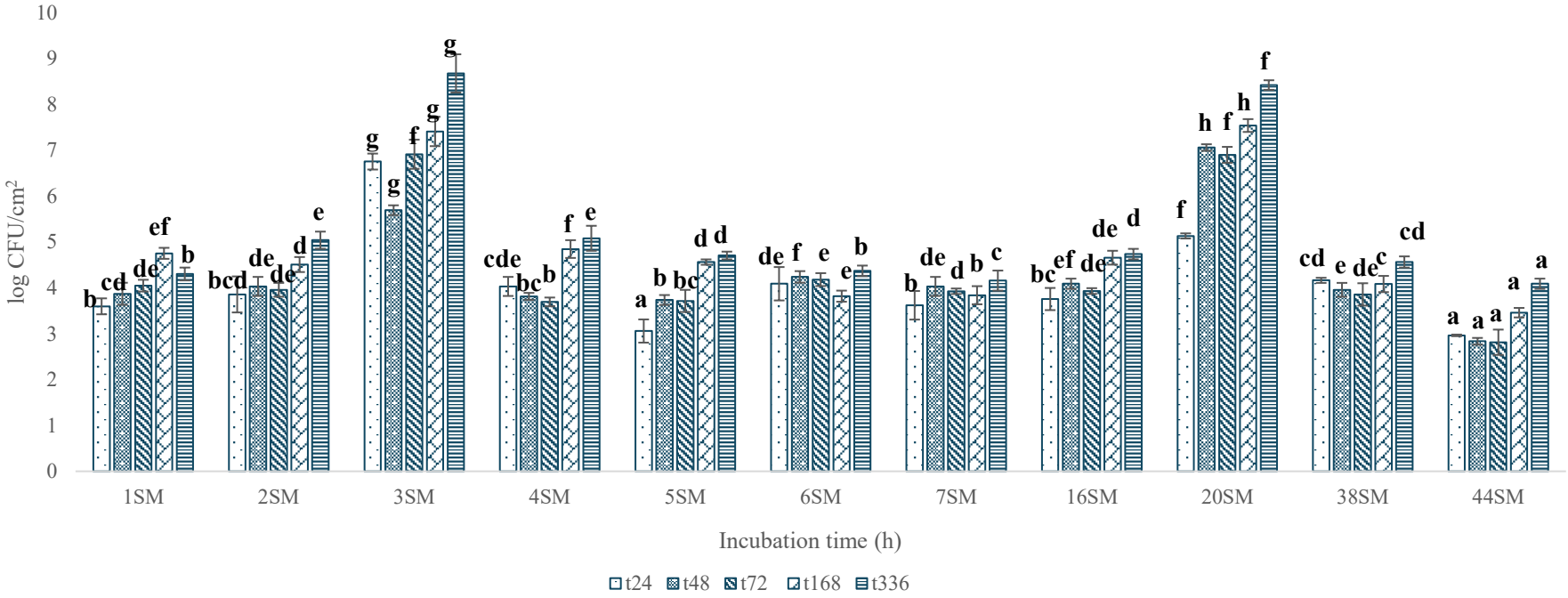

Figure 3.2 (A) OD_{570} values from the crystal violet assay as a function of timeat 4°C with half-strength TSB and (B) the cell counts as a function of time at 4°C with half-strength TSB. All the results are expressed as mean ± standard deviation. Different letters above the bars indicate significant differences (p <0.05).

3.3.2.2 Biofilm formation on SS coupons

Two strong and two weak biofilm formers were chosen for biofilm formation on the SS surface. The strong biofilm formers produced a visible air-liquid interface on the SS coupons that the weak ones did not form. There was a significant difference ($p < 0.05$) in OD_{570} values and cell counts between strong and weak biofilm formers, which agreed with the results from the PS surface. The crystal violet values and cell counts were significantly ($p < 0.05$) higher at 4°C compared to 30°C.

The highest crystal violet values reached by strong biofilm formers at 30°C on stainless steel were 0.94 ± 0.08 (3SM) and 0.91 ± 0.14 (20SM) OD_{570} at 336 h (Fig. 3.3 A). The cell counts reached 6.12 ± 0.21 (3SM) and 5.99 ± 0.15 log CFU/cm^2 (20SM) (Fig. 3.3 B). The highest crystal violet values reached by strong biofilm formers at 4ºC were 2.65 ± 0.18 (3SM) and 2.41 ± 0.14 (20SM) at 336 h (Fig.3.4 A). The cell counts reached by strong biofilm formers at 4°C were 7.21 ± 0.13 (3SM) and 7.23 ± 0.11(20SM) log CFU/cm^2 (Fig. 3.4 B).

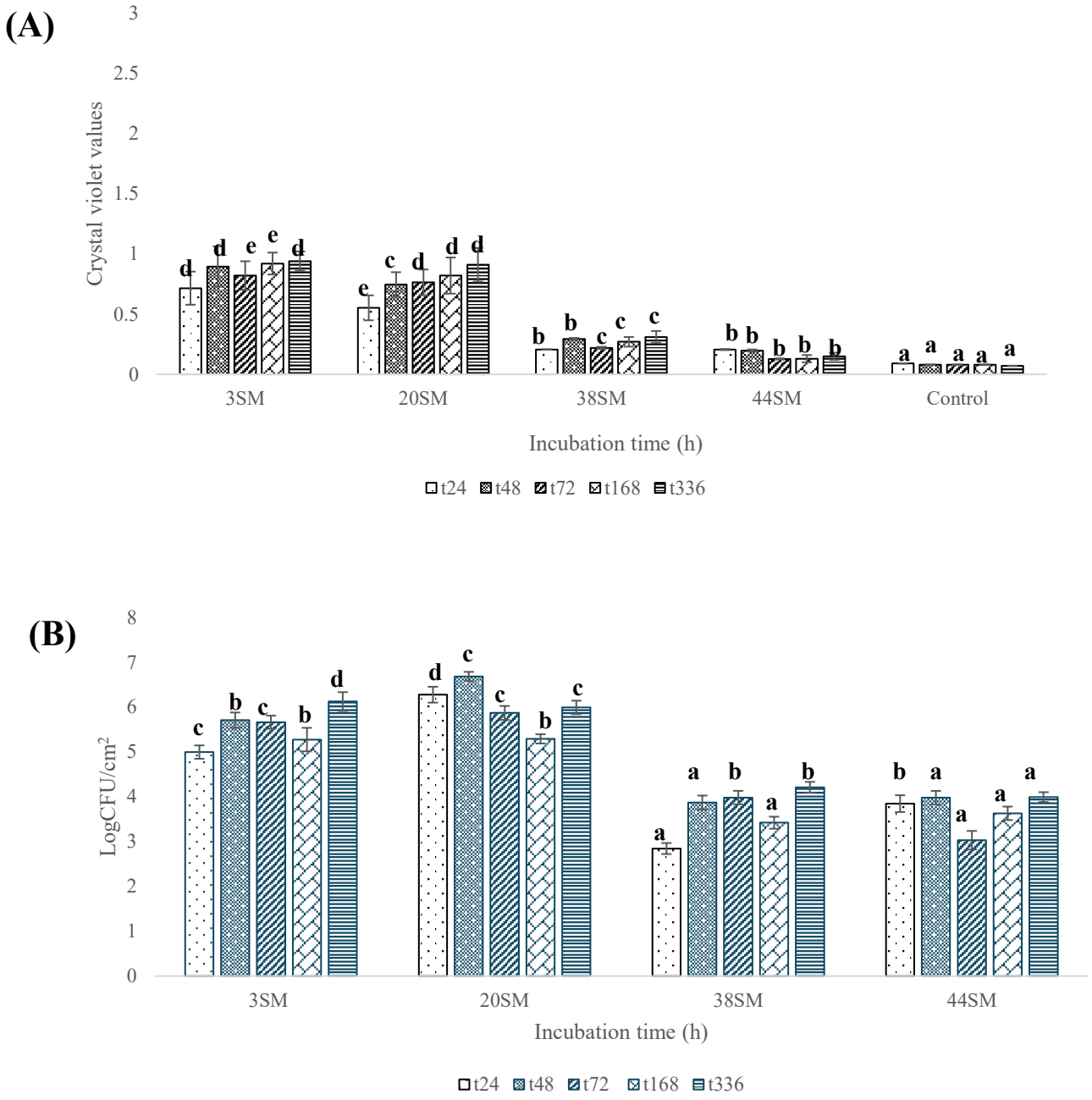

Figure 3.3 (A) OD_{570} values from the crystal violet assay as a function of time at 30°C with half-strength TSB on a stainless-steel surface and (B) the cell counts as a function of time at 30°C with half-strength TSB. All the results are expressed as mean ± standard deviation. Different letters above the bars indicate significant differences ($p < 0.05$).

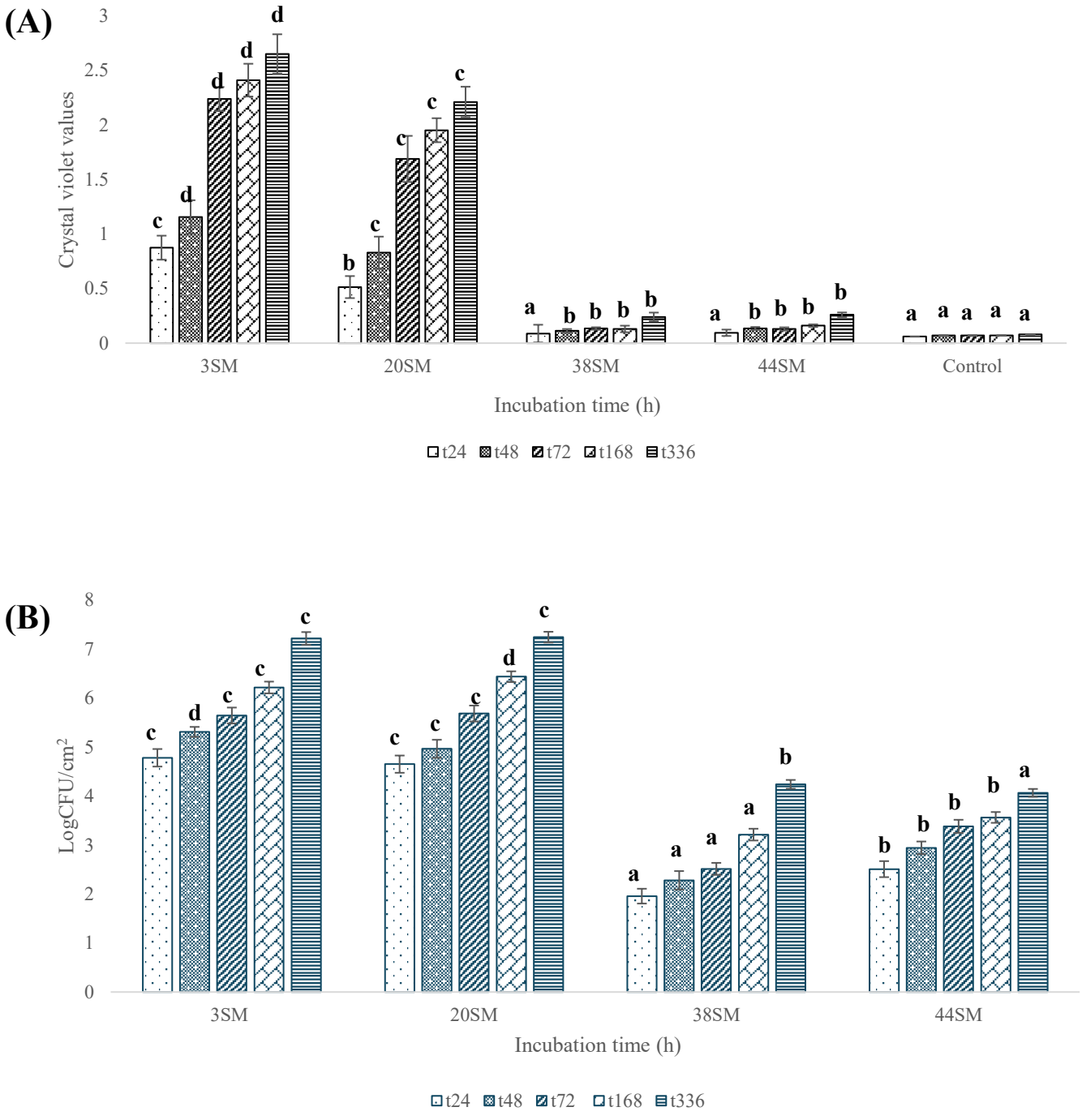

Figure 3.4 (A) OD_{570} values from the crystal violet assay as a function of time at 4°C with half-strength TSB on a stainless-steel surface and (B) the cell counts as a function of time at 4°C with half-strength TSB. All the results are expressed as mean ± standard deviation. Different letters above the bars indicate significant differences ($p < 0.05$).

3.3.3 Congo red assay (CRA)

The CRA plates were observed from 24 h to 120 h. Different colony morphologies were observed (Table 3.3) from the CRA. The pink, dry, and rough *(Pdar)* (Fig. 3.5 A) colonies indicate the production of cellulose only, the brown, dry, and rough *(Bdar)* (Fig. 3.5 B) colonies indicate the production of curli, while the red, dry, and rough *(Rdar)*colonies indicate the production of both cellulose and curli. The white, smooth colonies indicate neither curli nor cellulose production (Fig. 3.5 C). The rough colonies indicate higher levels of cellulose or curli, and the smooth colonies indicate lower levels.

Table 3.3: Colony morphology observed with Congo Red Assay

Strains	Colony morphology	Indication
1SM	Brown, dry, and rough colonies (*Bdar*)	Curli-only producer, impaired cellulose production
2SM	Red and smooth colonies	Low levels of cellulose and curli
3SM	Pink, dry, and rough colonies (*Pdar*)	Cellulose only producer and impairment of curli.
4SM	Brown and smooth colonies	Low levels of curli and impairment of Cellulose.
5SM	Red, dry, and rough colonies (*Rdar*)	Production of both cellulose and curli
6SM	Blue, dry, and rough colonies	Levan
7SM	Red and smooth colonies	Low levels of cellulose and curli
16SM	Brown and smooth colonies	Low levels of curli
20SM	Pink, dry, and rough colonies (*Pdar*)	Cellulose only producer and impairment of curli.
38SM	White, smooth colonies	Neither cellulose nor curli
44SM	White, smooth colonies	Neither cellulose nor curli

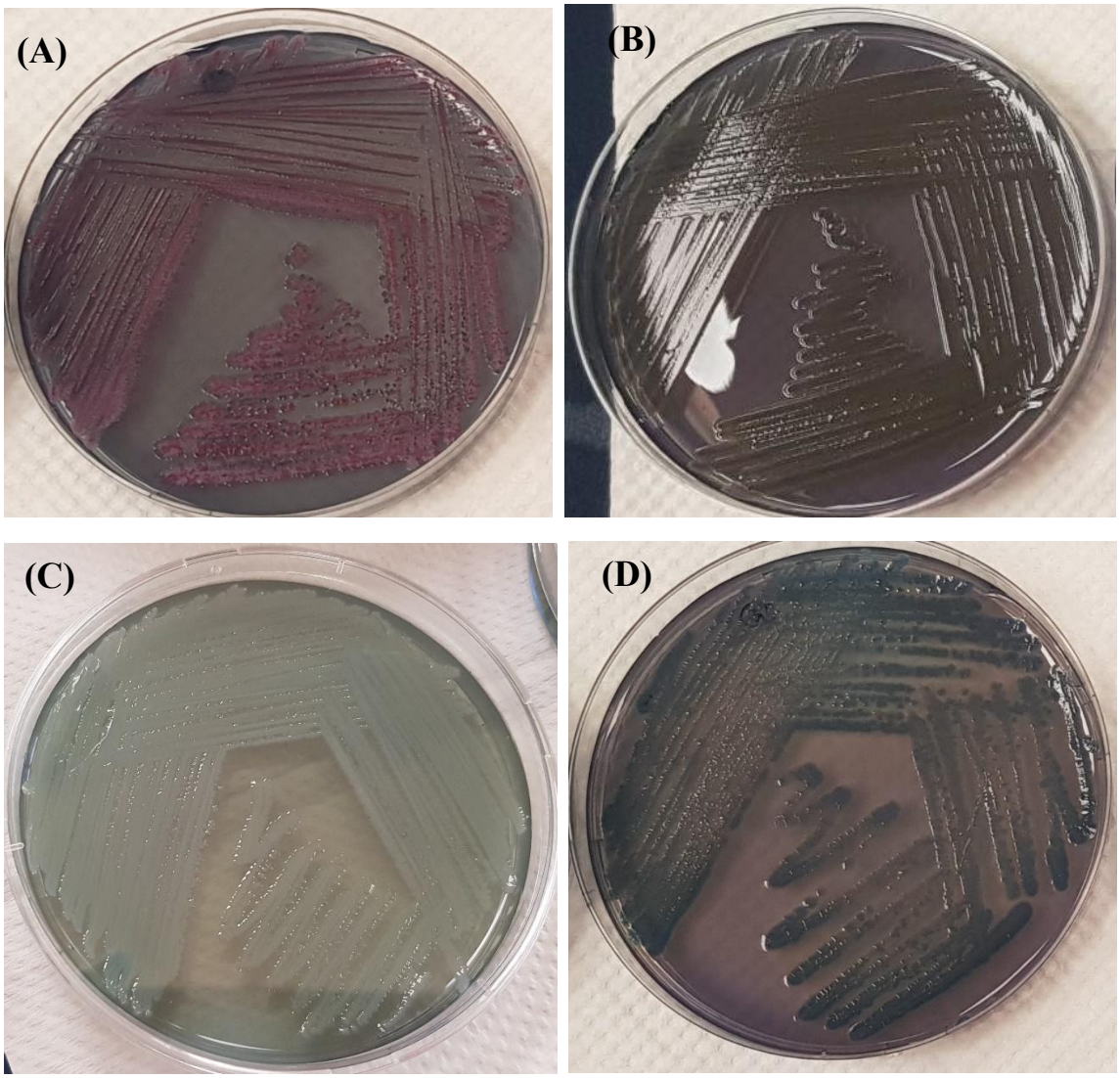

Figure 3.5 (A) Pink, dry, and rough colonies (*Pdar*, Isolate 3SM), (B) Brown, dry, and rough colonies (*Bdar*, Isolate 1SM), White and smooth colonies (44SM), (D) Blue coloured colonies (Isolate 6SM).

3.3.4 Levan production

The blue coloured colonies observed from CRA were never mentioned before. The isolate 6SM (*P. antarctica*) is a soil pseudomonad. Levan production is commonly observed with soil-based pseudomonads, and the Levan screening was done. Among the eleven isolates, strain 6SM produced mucoid colonies (Fig. 3.6 A & B), which were sticky when touched with the inoculation loop. The polysaccharide that produced a blue colour (Fig. 3.5 D) with Congo red in the previous experiment was identified as Levan.

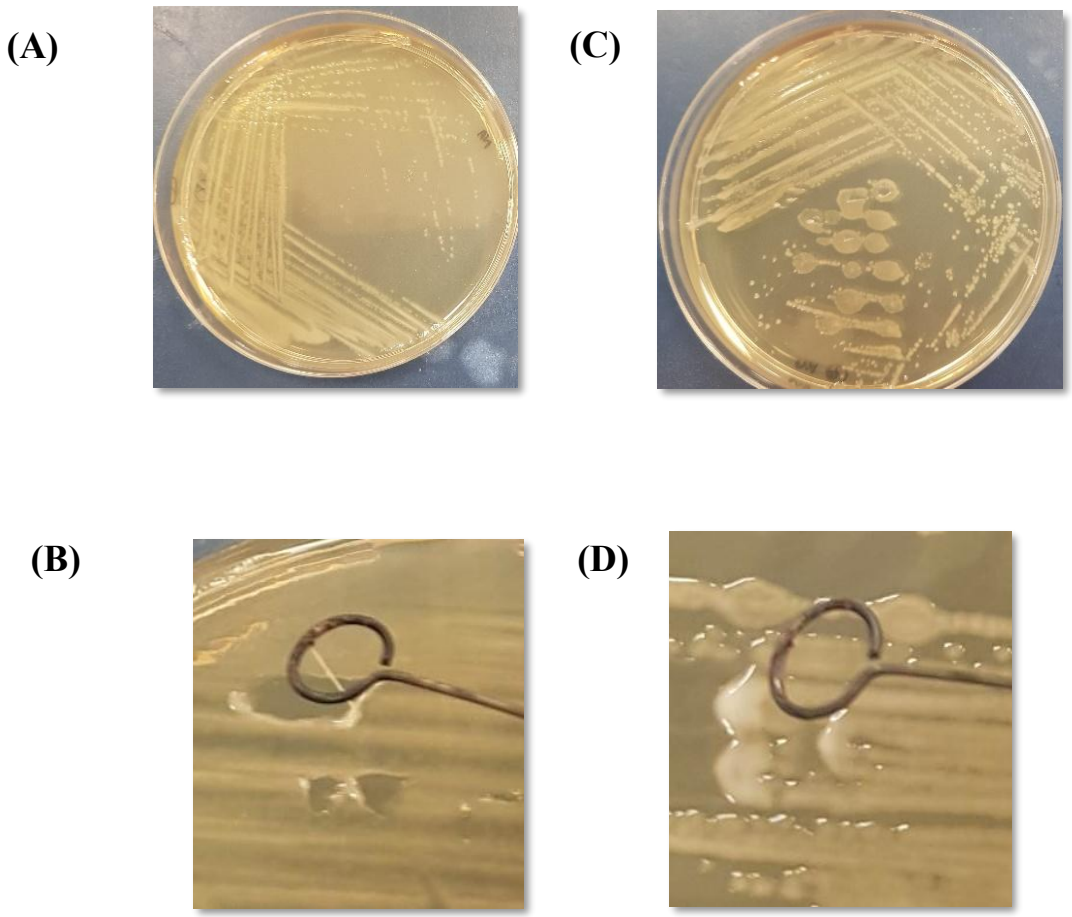

Figure 3.6 (A) mucoid colonies indicating Levan (Isolate 6SM), (B) non-mucoid colonies (Isolate 2SM), (C) sticky when touched with an inoculation loop, (D) non-mucoid colonies.

3.3.5 Quantification of Cellulose

The cells were scraped off after 24 h of incubation. The colonies were digested with acids, and the isolated cellulose was quantified using Anthrone colorimetry.

The amount of cellulose produced by isolates correlated with the results from the Congo Red Assay. The following isolates, 1SM, 6SM, 38SM, and 44SM, did not produce cellulosic colonies on CRA and showed zero OD_{620} with Anthrone colorimetry. The low cellulose producers indicated by CRA were 2SM, 4SM, 7SM, and 16SM produced cellulose 3.71 to 4 mg of cellulose per mL (Fig. 3.7). The cellulose-only producers 3SM and 20SM showed high amounts of cellulose among the 11 isolates. The only isolate that could produce both cellulose and curli, 5SM, produced 6.71 mg/mL of cellulose.

(A)

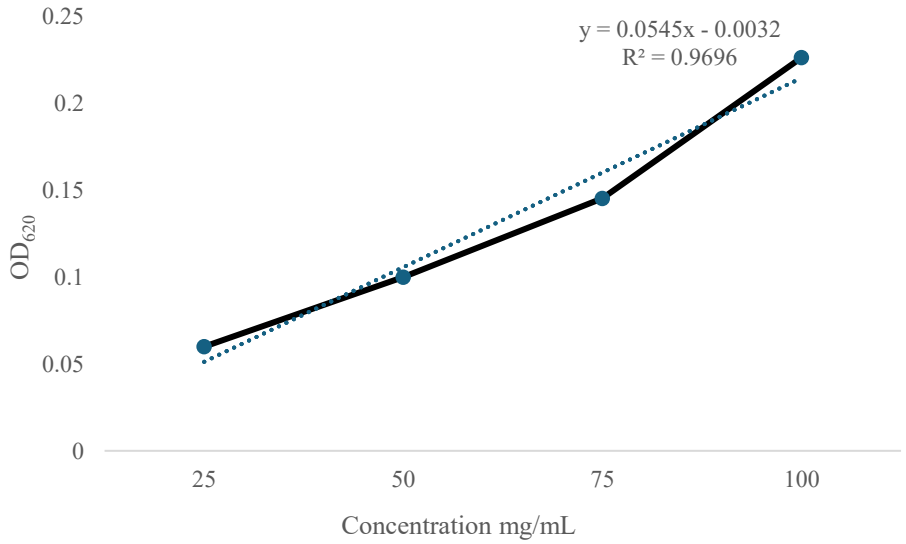

(B)

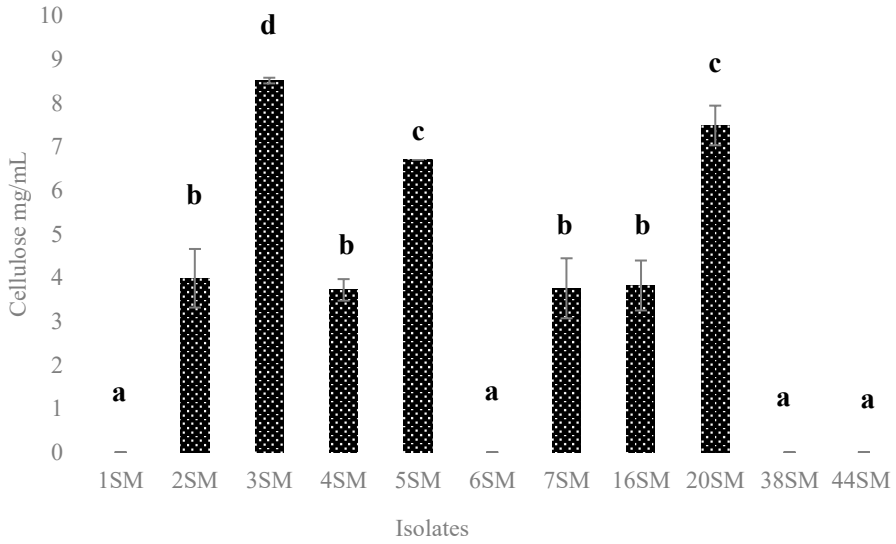

Figure 3.7 (A) Standard curve with microcrystalline cellulose concentration 25 to 100 mg/ mL, (B) Cellulose quantification, different letters above the bars indicate significant differences.

3.4 Discussion

The crystal violet assay (CV) was used to determine the biofilm formation of bacterial isolates in the present study. The CV assay is usually done with flat-bottom 96-well microtiter plates (Kamimura et al., 2022; Xu et al.,2016). However, in food processing conditions, stainless steel is the most used food contact surface due to easy cleaning and low reactivity with foods (Zaffora et al., 2021). Therefore, it is important to study biofilm formation on stainless-steel surfaces. This present study focused on the biofilm formation of psychrotrophic *Pseudomonas* spp. on both polystyrene and stainless-steel surfaces.

In this present study, the strong biofilm formers showed significantly ($p < 0.05$) higher cell counts/cm^2 and higher CV values compared to the stainless-steel surface. In another study on biofilm formation of *Listeria monocytogenes* on polystyrene and stainless-steel surfaces showed similar results. The authors tested cell surface properties and found that there is no correlation between cell surface properties and biofilm formation (Poimenidou et al., 2016). Whereas, in a study comparing the biofilm formation of *Escherichia coli* and *Salmonella* on polystyrene, polyethylene, and stainless-steel surfaces revealed that there is no significant difference between the surfaces (Carvalho et al.,2023). The polystyrene tissue culture plates are designed to encourage the adhesion of more cells or bacteria to the surface (Muazu et al., 2015), which could explain the higher cell numbers on the polystyrene surface. The influence of temperature on the cell hydrophobicity, surface roughness, and surface tension parameters influences the biofilm formation of *P. aeruginosa* and *Staphylococcus aureus* (Di Ciccio et al., 2015). Moreover, another study reported that stainless steel is hydrophilic, and polystyrene is hydrophobic, and that difference did not influence the biofilm formation of *S. aureus* (Da Silva Meira et al., 2012). However, the mechanism behind the biofilm formation of these two surfaces needs to be studied.

The processing and storage temperatures of perishable foods are from 4-7°C (Mercier et al., 2017), which help control the quality and safety of foods. However, there are incidents reported of food spoilage and poisoning even at cold temperatures, and therefore, it is important to study biofilm formation at cold temperatures. The temperatures used in this

study were 30°C and 4°C to represent an optimum growth temperature and a chilled temperature.

In this present study, among the 11 isolates, two of them (3SM and 20SM) could form strong biofilms at 4ºC (Fig. 3.2). Their biofilm formation at 30ºC was much lower when comparing the crystal violet values and cell counts at 4ºC. This significant difference indicates higher chances of persistent biofilm formation and continuous shedding of bacteria in the cold temperature environment, such as dairy, meat and seafood processing. *P. lundensis* from a meat source was reported to form higher biofilms and higher cell counts at 10 and 4°C compared with 25°C (Liu et al., 2015). Pseudomonads grown on meat surfaces form stronger biofilms at cold temperatures compared to ambient temperatures due to the response to cold stress (Wickramasinghe et al., 2019). When comparing the biofilm formation of *P. aeruginosa* at 23 and 37°C revealed that higher biomass is produced at 23°C, indicating the influence of lower temperatures on the biofilm formation (Bisht et al., 2021).

The biofilm formation of these isolates in this study focused on the early to mature stages. In this present study, the biofilm-forming duration did not affect the biofilm formation of strong and weak isolates. However, the CV values at the mature stage were significantly ($p < 0.05$) higher than 24 h for the strong biofilm formers at both 30°C and 4°C. The CV values and cell count followed an increasing trend from 24 to 336 h on both polystyrene and stainless-steel surfaces. The biofilm formation of meat isolates of pseudomonads reached higher CV values between 120 to 144 h at 4°C (72 h at 10°C) and decreased after 144 h (Liu et al., 2015). The increasing trend in the present study is due to the continuous supply of nutrients. In the study by Liu et al. (2015), the media were not refreshed. The time course assay on biofilms formed on the meat surface (continuous access to nutrients) showed significantly higher biovolume at day 7 compared to days 1 and 3 at both 10°C and 4°C (Wickramasinghe et al., 2019). This observation suggests that the biofilm formation of pseudomonads depends on the nutrient availability.

In this present study, the strong biofilm formers were the same on both stainless-steel and polystyrene surfaces. However, the crystal violet values and cell counts were higher on the polystyrene surface compared to the stainless-steel surface. The biofilm formation of *Salmonella enterica* strains on stainless steel and polystyrene surfaces showed differences between the surfaces in biofilm formation. Among thirteen strains, only eight formed strong

biofilms on the polystyrene surface, although all the strains form strong biofilms on the stainless-steel surface (Paz-Méndez et al., 2017).

Different morphotypes were identified from the CRA in this study: curli-only producer, cellulose-only producer, curli and cellulose producer, and low levels of cellulose or curli. The two strong biofilm formers were cellulose-only producers (Table 3.3). The isolate 5SM is a curli and cellulose producer, but the biofilm biomass was significantly lower than the strong biofilm formers 3SM and 20SM. In contrast, in *Salmonella* Typhimurium and *E. coli,* the co-production of cellulose and curli fibres results in a strong hydrophobic extracellular polymeric substance matrix. Either cellulose or curli production results in a fragile matrix (Flemming & Wingender, 2010).

In this present study, the strong biofilm formers are cellulose-only producers (*Pdar* morphotype), and the absence of curli fibres did not affect their biofilm formation. The divergent ability of *Rdar* and *Pdar* to produce cellulose leads to biofilm development and resistance of *S. typhimurium* biofilms (Kim et al., 2022).

According to Solano et al. (2002), the rich media require curli fibres or aggregative fimbriae to form biofilms. In this present study, half-strength TSB was used as a medium to evaluate the biofilm formation. TSB is a complex nutrient-rich general-purpose medium (Chen et al., 2020), and the curli producer morphotype was expected to form strong biofilms. In contrast with Solano et al. (2000), the cellulose-only producers formed strong biofilms in the present study. The cellulose production by the *Bdar* and *Pdar* morphotypes of *Vibrio parahaemolyticus* revealed that the pink colony formers produced cellulose, while there was no cellulose produced by the brown morphotypes. The brown morphotypes were also weak biofilm formers in that study (Wang et al., 2023).

The bacterial cellulose quantification in this present study showed similar results to CRA. Three isolates (3SM, 5SM, and 20SM) produced significantly ($p < 0.05$) than the other isolates. However, among these, only two (3SM and 20SM) formed strong biofilms. The absence of cellulose production in 1SM, 6SM, 38SM, and 44SM from CRA was also reflected in the cellulose quantification. CRA screening overall reflected the biofilm formation abilities of these pseudomonads (other than 5SM). However, the crystal violet assay and cell count remained important tools in the biofilm screening.

In Chapter 3, the cell counts were significantly ($p < 0.05$) higher on the polystyrene surface. However, the EPS production on different surfaces cannot be concluded only with the crystal

violet assay. The EPS production on these surfaces needs to be compared. When comparing the biofilm formation of these isolates, compared to surface types and nutrients, the biofilm formation of strong biofilm formers was temperature dependent. Similar studies confirmed that the temperature-driven biofilm formation occurs independently of surface type and nutrients (Bisht et al., 2021; Morimatsu et al., 2012). However, this study identified the influence of cellulose production on strong biofilm formation.

In Chapter 2, the robust biofilm formation of pseudomonads at cold temperatures was discussed. In this Chapter, the biofilm screening revealed strong biofilm formers with higher biomass at 4°C compared to 30°C. Not all the pseudomonads in this study formed strong biofilms. The link between cellulose production and strong biofilm formation needs to be explored. The strong biofilm formers produced higher biomass at 4°C on both stainless-steel and polystyrene surfaces. The air-liquid interface biofilm formation was focused on in this study to have a better comparison with polystyrene and stainless-steel surfaces. The comparison of submerged biofilms was not possible between microtiter plates and stainless-steel surfaces. However, the comparison of air-liquid interface and submerged biofilms needs to be made.

3.5 Conclusions

Pseudomonad isolates in this study showed variations in the biofilm formation on both polystyrene and stainless-steel surfaces. Previous studies reported the temperature dependency of the pseudomonad biofilm formation, and this study added that cellulose production is the key factor identified in the strong biofilm formers. The cell counts and crystal violet values were higher at 4°C. compared to 30°C, indicates the spoilage potential of these pseudomonads at cold storage and processing temperatures.

3.6 References

Abidi, W., Torres-Sánchez, L., Siroy, A., & Krasteva, P. V. (2022). Weaving of bacterial cellulose by the Bcs secretion systems. *FEMS Microbiology Reviews, 46*(2), fuab051. https://doi.org/10.1093/femsre/fuab051

Andreani N.A., Carraro L., Zhang L., Vos, M., Cardazzo, B. (2019). Transposon mutagenesis in *Pseudomonas fluorescens* reveals genes involved in blue pigment

production and antioxidant protection. Food Microbiol 82(9):497–503.https://doi: 10.1016/j.fm.2019-03-028.

Aswath Narayan JB., Vittal RR. (2014). Attachment and biofilm formation of *Pseudomonas fluorescens* PSD4 isolated from a dairy processing line. Food Sci Biotechnol 23(6):1903–1910. https://doi.org/10.1007/s10068-014-0260-8.

Carvalho, D., Chitolina, G. Z., Wilsmann, D. E., Lucca, V., de Emery, B. D., Borges, K. A., ... & do Nascimento, V. P. (2023). Adhesion capacity of Salmonella Enteritidis, Escherichia coli and Campylobacter jejuni on polystyrene, stainless steel, and polyethylene surfaces. *Food Microbiology*, *114*, 104280.

Chen, X., Thomsen, T. R., Winkler, H., & Xu, Y. (2020). Influence of biofilm growth age, media, antibiotic concentration and exposure time on Staphylococcus aureus and Pseudomonas aeruginosa biofilm removal in vitro. *BMC Microbiology*, *20*(1), 264. https://doi.org/10.1186/s12866-020-01947-9

Chiesa F., Lomonaco S., Nucera D., Garoglio D., Dalmasso A., & Civera T. (2014). distribution of *Pseudomonas* species in a dairy plant affected by occasional blue discoloration. *Italian Journal of Food Safety*, *3*(4). https://doi.org/10.4081/ijfs.2014.1722.

Cohen, E., & Merzendorfer, H. (Eds.). (2019). *Extracellular Sugar-Based Biopolymers Matrices* (Vol. 12). Springer International Publishing. https://doi.org/10.1007/978-3-030-12919-4

Dogan B., & Boor K. J. (2003). Genetic diversity and spoilage potentials among *Pseudomonas* spp. isolated from fluid milk products and dairy processing plants. *Applied and Environmental Microbiology*, *69*(1), 130–138. https://doi.org/10.1128/AEM.69.1.130-138.2003.

Dong Zhang, Jon Palmer, Koon Hoong Teh, Miranda Angeli Calinisan, and Steve Flint. (2020). “Milk fat influences proteolytic enzyme activity of dairy Pseudomonas species.” International Journal of Food Microbiology, 320.

Du, B., Lu, M., Liu, H., Wu, H., Zheng, N., Zhang, Y., Zhao, S., Zhao, Y., Gao, T., & Wang, J. (2023). Pseudomonas isolates from raw milk with high level proteolytic activity display reduced carbon substrate utilization and higher levels of antibiotic resistance. *LWT*, *181*, 114766. https://doi.org/10.1016/j.lwt.2023.114766

Dueholm, M. S., Petersen, S. V., Sønderkær, M., Larsen, P., Christiansen, G., Hein, K. L., Enghild, J. J., Nielsen, J. L., Nielsen, K. L., Nielsen, P. H., & Otzen, D. E. (2010). Functional amyloid in *Pseudomonas*. *Molecular Microbiology*, *77*(4), 1009–1020. https://doi.org/10.1111/j.1365-2958.2010.07269.x

Filloux, A., & Ramos, J.-L. (Eds.). (2014). *Pseudomonas Methods and Protocols* (Vol. 1149). Springer New York. https://doi.org/10.1007/978-1-4939-0473-0

Flemming, H.-C., & Wingender, J. (2010). The biofilm matrix. *Nature Reviews Microbiology*, *8*(9), 623–633. https://doi.org/10.1038/nrmicro2415

Flint, S. H., Ward, L. J. H., & Brooks, J. D. (1999). Streptococcus waius sp. Nov., a thermophilic streptococcus from a biofilm. *International Journal of Systematic and Evolutionary Microbiology*, *49*(2), 759–767. https://doi.org/10.1099/00207713-49-2-759

Gualdi, L., Tagliabue, L., Bertagnoli, S., Ieranò, T., De Castro, C., & Landini, P. (2008). Cellulose modulates biofilm formation by counteracting curli-mediated colonization of solid surfaces in Escherichia coli. *Microbiology*, *154*(7), 2017–2024. https://doi.org/10.1099/mic.0.2008/018093-0.

Kamimura, R., Kanematsu, H., Ogawa, A., Kogo, T., Miura, H., Kawai, R., Hirai, N., Kato, T., Yoshitake, M., & Barry, D. M., 2022. Quantitative analyses of biofilm by using crystal violet staining and optical reflection. *Materials*, *15*(19), 6727. https://doi.org/10.3390/ma15196727

Kim, S., Li, X.-H., Hwang, H.-J., & Lee, J.-H. (2020). Thermoregulation of *Pseudomonas aeruginosa* Biofilm Formation. *Applied and Environmental Microbiology*, *86*(22), e01584-20. https://doi.org/10.1128/AEM.01584-20

Liu, J., Wu, S., Feng, L., Wu, Y., & Zhu, J. (2023). Extracellular matrix affects mature biofilm and stress resistance of psychrotrophic spoilage Pseudomonas at cold temperature. *Food Microbiology*, *112*, 104214. https://doi.org/10.1016/j.fm.2023.104214

Machado S. G., Baglinière F., Marchand S., Van Coillie, E., Vanetti M. C. D., De Block J., & Heyndrickx M. (2017). The biodiversity of the microbiota producing heat-resistant enzymes responsible for spoilage in processed bovine milk and dairy products. *Frontiers in Microbiology*, *8*. https://doi.org/10.3389/fmicb.2017.00302.

Mbituyimana, B., Liu, L., Ye, W., Ode Boni, B. O., Zhang, K., Chen, J., Thomas, S., Vasilievich, R. V., Shi, Z., & Yang, G. (2021). Bacterial cellulose-based composites for biomedical and cosmetic applications: Research progress and existing products. *Carbohydrate Polymers*, *273*, 118565. https://doi.org/10.1016/j.carbpol.2021.118565

Mercier, S., Villeneuve, S., Mondor, M., & Uysal, I., 2017. Time-temperature management along the food cold chain: A review of recent developments. *Comprehensive Reviews in Food Science and Food Safety*, *16*(4), 647–667.https://doi.org/10.1111/1541-4337.12269.

Nychas G.-J. E., Skandamis P. N., Tassou C. C., & Koutsoumanis K. P. (2008). Meat spoilage during distribution. *Meat Science*, *78*(1–2), 77–89. https://doi.org/10.1016/j.meatsci.2007.06.020

Oliveira, M. M. M. D., Brugnera, D. F., Alves, E., & Piccoli, R. H. (2010). Biofilm formation by Listeria monocytogenes on stainless steel surface and biotransfer potential. *Brazilian Journal of Microbiology*, *41*(1), 97–106. https://doi.org/10.1590/S1517-83822010000100016

Parlapani F. F., Anagnostopoulos D. A., Karamani E., Mallouchos A., Haroutounian S. A., & Boziaris I. S. (2023). Growth and volatile organic compound production of *Pseudomonas* fish spoiler strains on fish juice agar model substrate at different temperatures. *Microorganisms*, *11*(1),189.https://doi.org/10.3390/microorganisms 11010189.

Paz-Méndez A., Lamas A., Vázquez B., Miranda J., Cepeda A., & Franco C. (2017). Effect of food residues in biofilm formation on stainless steel and polystyrene surfaces by *Salmonella enterica* strains isolated from poultry houses. *Foods*, *6*(12), 106. https://doi.org/10.3390/foods6120106.

Poimenidou, S. V., Chrysadakou, M., Tzakoniati, A., Bikouli, V. C., Nychas, G.-J., & Skandamis, P. N. (2016). Variability of Listeria monocytogenes strains in biofilm formation on stainless steel and polystyrene materials and resistance to peracetic acid and quaternary ammonium compounds. *International Journal of Food Microbiology*, *237*, 164–171. https://doi.org/10.1016/j.ijfoodmicro.2016.08.029.

RÖmling, U., & Rohde, M. (1999). Flagella modulate the multicellular behavior of Salmonella typhimurium on the community level. *FEMS Microbiology Letters*, *180*(1), 91–102. https://doi.org/10.1111/j.1574-6968.1999.tb08782.x

Solano, C., García, B., Valle, J., Berasain, C., Ghigo, J., Gamazo, C., & Lasa, I. (2002). Genetic analysis of *Salmonella enteritidis* biofilm formation: Critical role of cellulose. *Molecular Microbiology*, *43*(3), 793–808. https://doi.org/10.1046/j.1365-2958.2002.02802.x\

Von Neubeck, M., Baur, C., Krewinkel, M., Stoeckel, M., Kranz, B., Stressler, T., Fischer, L., Hinrichs, J., Scherer, S., & Wenning, M. (2015). Biodiversity of refrigerated raw milk microbiota and their enzymatic spoilage potential. *International Journal of Food Microbiology*, *211*, 57–65. https://doi.org/10.1016/j.ijfoodmicro.2015.07.001

Wahid, F., & Zhong, C. (2021). Production and applications of bacterial cellulose. In *Biomass, Biofuels, Biochemicals* (pp. 359–390). Elsevier. https://doi.org/10.1016/B978-0-12-821888-4.00010-1

Wang, D., Fletcher, G. C., Gagic, D., On, S. L. W., Palmer, J. S., & Flint, S. H. (2023). Comparative genome identification of accessory genes associated with strong biofilm formation in Vibrio parahaemolyticus. *Food Research International*, *166*, 112605. https://doi.org/10.1016/j.foodres.2023.112605

Wang, D., Fletcher, G. C., On, S. L. W., Palmer, J. S., Gagic, D., & Flint, S. H. (2023). Biofilm formation, sodium hypochlorite susceptibility and genetic diversity of Vibrio parahaemolyticus. *International Journal of Food Microbiology*, *385*, 110011. https://doi.org/10.1016/j.ijfoodmicro.2022.110011

Wickramasinghe N. N., Ravensdale J. T., Coorey R., Dykes G. A., & Scott Chandry P. (2019). *In situ* characterisation of biofilms formed by psychrotrophic meat spoilage pseudomonads. *Biofouling*, *35*(8), 840–855. https://doi.org/10.1080/08927014.2019.1669021

Wiedmann M., Weilmeier D., Dineen S. S., Ralyea R., & Boor K. J. (2000). Molecular and phenotypic characterization of *Pseudomonas spp*. isolated from milk. *Applied and Environmental Microbiology*, *66*(5)20852095. https://doi.org/10.1128/AEM.66.5.2085-2095.2000.

Xu Z., Liang Y., Lin S., Chen D., Li B., Li L., & Deng Y. (2016). Crystal violet and XTT assays on *Staphylococcus aureus* biofilm quantification. *Current Microbiology*, *73*(4), 474–482. https://doi.org/10.1007/s00284-016-1081-1

Zaffora, A., Di Franco, F., & Santamaria, M., 2021.Corrosion of stainless steel in the food and pharmaceutical industry. *Current Opinion in Electrochemistry*, *29*, 100760. https://doi.org/10.1016/j.coelec.2021.100760.

Zeng, G., Vad, B. S., Dueholm, M. S., Christiansen, G., Nilsson, M., Tolker-Nielsen, T., Nielsen, P. H., Meyer, R. L., & Otzen, D. E. (2015). Functional bacterial amyloid increases Pseudomonas biofilm hydrophobicity and stiffness. *Frontiers in Microbiology*, *6*. https://doi.org/10.3389/fmicb.2015.01099.

3.7 Supplementary Information

3.7.1 Composition of Tri Gene

1:100 dilutions of Tri Gene were used to wash the used coupons. The composition as follows,

1.Poly (hexamethylene biguanide) hydrochloride- 2.0%w /w

2.Benzalkonium chloride 1.25%w /w

3. Didecyldimethylammonium chloride 2.50%w /w.

Chapter 4 Characterisation of Biofilm Extracellular Polymeric Substances Matrix (EPS) Composition of Psychrotrophic Pseudomonads.

This chapter is an adaptation of material that was published as a peer-reviewed article:

Muthuraman, S., Flint, S., & Palmer, J. (2025). Characterization of the extracellular polymeric substances matrix of *Pseudomonas* biofilms formed at the air-liquid interface. *Food Bioscience*, *64*, 105918. https://doi.org/10.1016/j.fbio.2025.105918.

Preface to Chapter 4

In Chapter 3, the role of temperature and surface on the biofilm formation of pseudomonad dairy isolates was investigated. The isolates 3SM (*P. lundensis)* and 20SM *(P. cedrina*) formed strong biofilms at both ambient and cold temperatures. The biofilm formation was strongly influenced by the temperature and surface. In Chapter 4, using chemical analysis and microscopic observations, the composition of the EPS matrix of strong biofilm-forming isolates at 30°C and two cold chain temperatures, 4 and 7°C, was compared. In the dairy and meat processing industry, 7ºC represents another important temperature and is included in this study.

4.1 Introduction

Biofilms are aggregates of microbial cells attached to each other or the surface and embedded in a self-produced or acquired hydrated extracellular polymeric substance matrix (EPS). The matrix comprises polysaccharides, proteins, lipids, and extracellular DNA (eDNA) (Penesyan et al., 2021; Flemming & Wingender, 2010). Apart from these biomolecules, water is the major component of EPS. The EPS dries slowly, thus water in the EPS keeps the cells hydrated and protects them from desiccation (Or et al.,2007). EPS traps all the lysed components from the cells, and each component in the EPS has its functionality, such as adhesion, aggregation, water retention, nutrient source, and protective barrier (Karatan et al., 2009).

Pseudomonas spp., form biofilms in a wide range of environments such as dairy, poultry, meat processing, marine, and soil environments (Caldera and Franzetti 2014, Jiang et al., 2011). Each species from the genus *Pseudomonas* produces diverse polysaccharides. *P. aeruginosa* is an alginate producer, while the soil pseudomonads, such as *P. syringae* produce Levan in their extracellular matrix. Some other pseudomonads are the cellulose producers (Li et al.,2010; Osman et al.,1986; Spiers et al.,2003). Apart from these capsular polymers, there are Pel and Psl polysaccharides involved in the biofilm formation. Pel is involved in the formation of pellicles observed in *Pseudomonas* that form air-liquid interface biofilms. Psl is also a non-capsular extracellular polysaccharide that is responsible for the attachment of cells to abiotic surfaces (Coulon et al., 2010; Friedman and Kolter, 2004; Byrd et al., 2011; Ma et al., 2009).

Pseudomonas spp. produces considerable amounts of extracellular proteins, which include extracellular enzymes (Flemming & Wingender, 2010). Apart from enzymes, lectins (carbohydrate-binding proteins), DNA-binding proteins, glucan-binding proteins, and Psl-binding proteins are also found in *Pseudomonas*, *Streptococcus,* and *Glucanobacter* (Flemming & Wingender, 2010; Diggle et al.,2006). Proteins such as CdrA, LapA, and LapD, which are responsible for the adhesion to surfaces, are also present in the biofilm matrix of *P. aeruginosa* and other *Pseudomonas* (Borlee et al.,2010; Hinsa et al.,2003).

Lipids in the matrix are mostly present either as lipopolysaccharides or lipoproteins. Rhamnolipids are identified in the biofilm matrix of many pseudomonads (Read et al.,1992). Rhamnolipids can alter the surface properties by binding with the macromolecules by

hydrophilic or hydrophobic groups (Boles et al., 2005). Extracellular DNA in the matrix of *P. aeruginosa* is reported to be an intracellular connector (Otzen and Nielson 2008). This eDNA could be from the lysed cells or from cells that are actively excreting DNA into the biofilm matrix, playing a major role in the structural properties of the biofilms (Otzen and Nielson 2008).

In chapter 3, two isolates formed strong biofilms with high cell counts and crystal violet values. This chapter explores the detailed EPS composition at different temperatures and on both stainless-steel and polystyrene surfaces. The EPS composition of *P. aeruginosa* and some of the spoilage pseudomonads is well studied (Wei & Ma, 2013; Wickramasinghe et al., 2020). However, there is a lack of information on the composition of *Pseudomonas* spp. biofilm matrices in terms of polysaccharides, proteins, and eDNA at different temperatures and on different surfaces. This is important as temperature is one factor commonly used to reduce microbiological issues in the food industry.

This present study aimed to analyse the compositional differences between the surfaces and temperatures, and identify the protein molecules present in the EPS, along with their quantification. The polysaccharides quantified from previous research were soluble polysaccharides (Wickramasinghe et al., 2020; Liu et al.,2023). This present study aimed to quantify cellulose (Mann & Wozniak, 2012), which is an insoluble polysaccharide identified in the biofilms of *Pseudomonas* spp.

4.2 Materials and Methods

4.2.1 Bacterial isolates and culture conditions

Strong biofilm-forming isolates at both 30°C and 4°C, 3SM (*P. lundensis*), and 20SM (*P. cedrina*) were chosen for this study. Identifications were confirmed using PCR and 16S rRNA sequencing (Chapter 3). The stock cultures were prepared by streaking bacteria on the Tryptic soy agar (TSA, Difco™, Becton, Dickinson and Company, USA) and incubating at 30°C for 24 h. A single colony was picked and inoculated into a cryopreservation tube (Nalgene, Merck, Germany) and stored at -80°C. Fresh, overnight cultures were prepared by streaking a stock culture on a TSA agar plate, incubating at 30°C, and inoculating a single colony in the Tryptic soy broth (TSB, Difco™, Becton, Dickinson and Company, USA) overnight (18 h) at 30°C. This overnight culture was used for further experiments. The temperatures used for

biofilm formation in this study were 30°C, 7°C, and 4°C (cold storage and processing temperatures).

4.2.1.1 Biofilm formation on Polystyrene surface

Details were provided in Section 3.2.3.1, Chapter 3.

4.2.1.2 Biofilm formation on Stainless-steel coupons

Details were provided in Section 3.2.3.2, Chapter 3.

4.2.1.3 Planktonic cultures

The planktonic cultures (4 mL) were allowed to grow in the 15 mL tubes (Falcon®, Corning Incorporated, Durham, USA) for two weeks in half-strength TSB with the above-mentioned temperatures. Every 72 h, the planktonic cultures were centrifuged at 5000 g for 5 min to remove the spent media. The pellets were filled with 4 mL of fresh media and refreshed this way until the end of two weeks.

4.2.2 Biofilm and planktonic growth

The biofilm and planktonic growth were monitored every 24 h by serial 10-fold dilution with 0.85% sterile saline and plating on TSA plates. The wells and coupons were swabbed with sterile cotton swabs and swirled in 100 µL of saline. One hundred microliters (100 µL) of culture were serially diluted and plated using a drop plate on TSA plates. The cell counts were expressed as log CFU/cm^2 for biofilm cells and log CFU/mL for planktonic cells.

4.2.3 Microscopic observation

Polystyrene coupons of the same size as stainless-steel coupons and stainless-steel coupons were used for the microscopic observations. The polystyrene coupons were obtained from polystyrene microtiter plate lids and cut to the same size as stainless-steel coupons. The coupons containing biofilms were removed and washed in sterile water three times to remove the media and loosely attached cells. The coupons were air-dried before staining. The coupons were observed under an epifluorescence microscope (Nikon Eclipse Ni-L, Nikon

Instruments, USA) with suitable filters. The images were captured by NIS-elements D software (Version 6.02.01(Build 1955), Nikon Instruments, Melville, New York, USA).

4.2.3.1 Acridine Orange staining for biofilm cells and pellicles

Acridine orange (Acridine Orange stain, BDH, England) 5 mg/mL was used to stain the biofilms. The dried biofilm containing coupons was stained with 100µL of Acridine Orange for 3 min. The coupons were washed and allowed to dry. With the epi fluorescence microscope, the coupons were viewed with a TRITC filter (Excitation 532-550nm and emission 574nm). Acridine orange is membrane permeable; it stains live cells with red-orange fluorescence (Sharma et al., 2020).

The pellicles were carefully transferred to a glass slide, air dried, stained with acridine orange and observed under microscope.

4.2.3.2 Filamentous cell formation

The colonies from the TSA plates were stabbed into semisolid agar (TSB + 0.2% agar) vials to assess the filamentous cell formation by restricted motility.

4.2.3.3 Calcofluor white staining for EPS

The dried coupons were stained with 1 drop of calcofluor white stain (Fluka® calcofluor white stain, Sigma Aldrich, Canada). The stain was washed with water after a minute and allowed to dry. The calcofluor white-stained coupons were observed under an epi-fluorescence microscope with a DAPI filter (Excitation 340-360nm and emission,410 nm). Calcofluor white binds to cellulose and chitin and emits blue and white fluorescence (Wang et al., 2023b).

4.2.3.4 Pico green staining for eDNA

The dried coupons were stained with Pico green (Quant-iT^{TM} Picogreen^{TM}, Thermofisher Scientific, USA) and kept in the dark for 5 min. The stained coupons were washed with sterile water and allowed to dry in a dark room. After drying, the coupons were observed

under an epifluorescence microscope with a FITC filter (Excitation 465-490nm and emission 512nm). Pico green is membrane impermeable and emits green fluorescence with dead cells and eDNA, and the live cells look darker (Ban & Kim, 2024).

4.2.4 Isolation of EPS

The EPS isolation protocol followed here is a modified protocol from Yang et al., (2019). After 2 weeks, the 96-well plates were taken out of the incubator. The remaining media was removed by inverting the plates. The plates were washed three times to completely remove the media and planktonic cells with sterile distilled water. After washing the plates were air dried. Two hundred microlitres (200) µL of sterile distilled water was added to each well. The plates were sealed and sonicated (Bandelin Sonorex digitec, GmBH&Co, Germany) for 30 min. After sonication, the contents in the wells were transferred into 1.5 mL Eppendorf tubes (Quality Scientific Plastics, United States). The EPS contents in the Eppendorf tubes were then centrifuged at 12000*g* for 5 min in a refrigerated centrifuge (Hettich, Mikro 220R, USA). The supernatant was collected and filtered using a 0.2 µm syringe filter (Minisart, Sartorius, Germany). The supernatant was pooled into a 15 mL centrifuge tube (Falcon®, Corning Incorporated, Durham, USA) up to a volume of 3 mL. The centrifuge tubes were placed in the freeze dryer, and the collected fraction was soluble EPS.

The stainless coupons were removed from the vials and washed with sterile water. Four of the coupons were filled with 5 mL of sterile water and sonicated for 30 min. After 30 min, the coupons were vortexed vigorously to completely dissolve the visible air-liquid interface biofilms. The contents were centrifuged at 12000*g* for 5min in a refrigerated centrifuge and filtered using a 0.2µm syringe filter. Three milli litres (3 mL) of the isolated EPS was filled in centrifuged tubes and placed in the freeze dryer.

After 2 weeks, the planktonic cultures were washed with sterile distilled water three times by centrifugation at 3000*g* for 5 min to remove the TSB completely. Sterile distilled water (3 mL) was added to the cell pellets and mixed by vortex. The mixture was filled in 1 mL Eppendorf tubes and centrifuged at 12000*g* for 5 min. The supernatant collected was filtered through a 0.2 µm syringe filter. The collected cell-free supernatants (CFS) were placed in the freeze dryer for 24 h. The freeze-dried EPS were then stored in a desiccator.

4.2.5 Cellulose quantification

The extraction method defined above could only extract the soluble components of EPS from the supernatant. As cellulose is an insoluble polymer, the method was modified.

After 2 weeks of incubation, the plates were taken out from the incubator and washed to remove the media and planktonic cells. Then the wells were filled with 200 µL of water and sonicated for 30 min. The contents from the 32 wells were pooled into a centrifuge tube at a volume of 5 mL. Five millilitres (5 mL) of extraction buffer containing an 8:2:1 ratio of acetic acid, nitric acid, and distilled water was added and boiled for 30 min. The boiled contents were mixed by vortex and centrifuged at 10300*g* for 15 min. The supernatant was discarded, and the pellets were washed with 1 mL of water and 1 mL of acetone and left to dry overnight. After 24 h, the pellet was diluted with 1 mL of sulphuric acid. Cellulose standards of 30mg/mL, 50mg/mL, 75mg/mL, and 100mg/mL were prepared. Anthrone (0.2 g) was dissolved in 100 mL of sulphuric acid. Anthrone (500 µL) was added to the wells in the 48 well plates. One hundred microliters of the samples and standards were added to the wells containing anthrone. The absorbance was measured at 620nm, and the cellulose content was calculated as µg/10^8 cells (Wang et al., 2023a).

4.2.6 Polysaccharide Quantification

The phenol sulfuric acid assay described by Dubois et al., was followed with modifications (DuBois et al., 1956)

Reagents

5% Phenol	30 µL
98% Sulfuric acid	150 µL

Fifty microliters of the sample were added to a well in 96-well plates. One hundred fifty microlitres of (150 µL) of sulfuric acid were added, followed by 30 µL of phenol. The plates were shaken at room temperature for 5 min. Then, they were placed on hot plates at 90°C for 5 min and cooled for 5 min. The absorbance was read at 490nm. D-glucose was used as a standard (from 50 µg/mL to 1000 µg/mL).

4.2.7 Protein quantification

The proteins in the EPS were quantified by the Lowry assay with the following reagents (Shen, 2023)

Reagent A

2% Na_2CO_3 in 0.1N NaOH	48 mL
1% Sodium potassium tartrate	1 mL
0.5% $CuSO_4.H_2O$	1 mL

Reagent B

Folin Ciocalteau

Fifty microliters (50 µL) of sample and 1040 µL of Reagent A were added to an Eppendorf tube of 1.5 mL and left for 10 min. Reagent B (125 µL) was added and left for 30 min and the absorbance was read at 660 nm. The standard curve was prepared with Bovine Serum Albumin (BSA) from 50 to 1000 µg/mL. From the standard curve, proteins in the samples were quantified and expressed as $\mu g/10^8$cells.

4.2.8 Protein identification (LC-MS)

The freeze-dried EPS was subjected to SDS-PAGE, and the gels were stained with Coomassie brilliant blue. Protein bands of interest were excised from the gels. Pre-stained protein ladder used from 10 to 250 kDa (PAGE regular Plus Prestained Protein Ladder, Thermofisher Scientific, USA) was used. In-gel enzymatic digestion and protein identification (LC-MS/MS) were performed by the Mass Spectrometry Centre, University of Auckland (New Zealand) (Goodman et al., 2018).

4.2.9 eDNA isolation and quantification

The freshly isolated biofilm EPS and planktonic supernatant were used for eDNA quantification. Five microliters of the samples were added to the wells of 2% Agarose gels (E-gel® EX with SYBR Gold II) and visualized (E-Gel iBASE^{TM}, Invitrogen, USA). The samples were then cleaned and concentrated with a DNA clean and concentrate kit (ZYMO

research, USA) and quantified using a Nanodrop (Thermofisher Scientific, USA). Partial 16S rDNA sequencing was done at Massey genomics using Big Dye Terminator v3.1the results were analysed by Chromas Lite (version 2.6.6; Technelysium Pty Ltd, Australia), and BLAST gene bank. PCR amplification of 16S rDNA was used to confirm the identification of isolated eDNA using universal primers Bac27F (5′-AGAGTTTGATCCTGGCTCAG-3′), and 1492R (5′-TACGGYTACCTTGTTACGACTT-3′) (Flint et al., 1999).

4.2.10 Data analysis

All experiments were performed with three biological replicates and at least three technical replicates. One-way variance analysis (ANOVA) was generated to evaluate significant differences among the variables using Tukey's test, with a *p*-value below 0.05 considered as statistically significant. Data analysis was implemented using SPSS statistical software (Version 29.0.2.0; IBM®, New York, United States).

4.3 Results

4.3.1 Biofilm growth

Pseudomonads form air-liquid interface biofilms (Fig. 4.1 and 4.2). The visible biofilm formation around the air-liquid interface of the coupons and wells was observed from 24 h. Compared to 30°C, the biofilms formed at 7°C and 4°C showed thick visible biofilms in both stainless-steel and polystyrene surfaces. Pellicle formation was observed in both biofilm and planktonic cultures. The polystyrene surface started to show visible biofilms from 24h, but for the stainless-steel surface, biofilms were observed after 72 h; however, at the end of two weeks, both surfaces showed thick visible biofilms at 7°C and 4°C (Fig. 4.1 and 4.2).

(A)

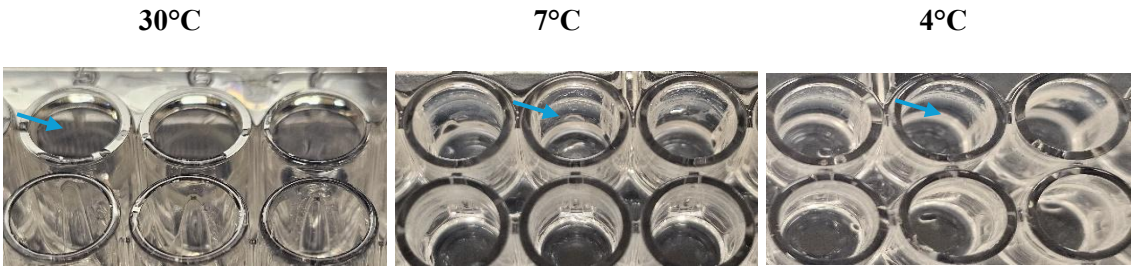

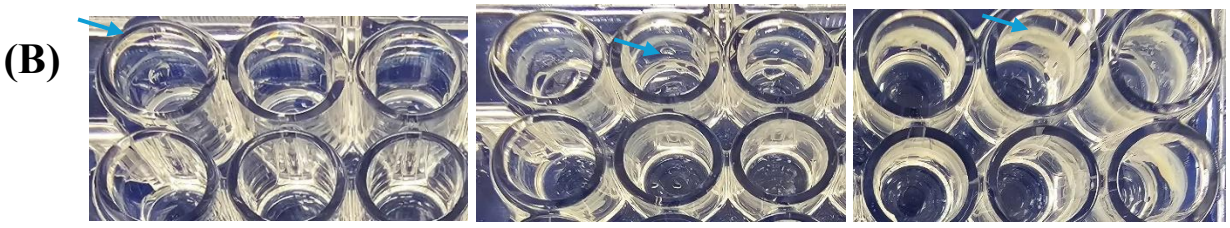

Figure 4.1 Visible biofilms on polystyrene surface at 30°C, 7°C, and 4°C at the end of two weeks. Blue arrows indicate the air-liquid interface biofilms. (A) represents the visible biofilms formed by isolate 3SM, while (B) shows the visible biofilms formed by isolate 20SM.

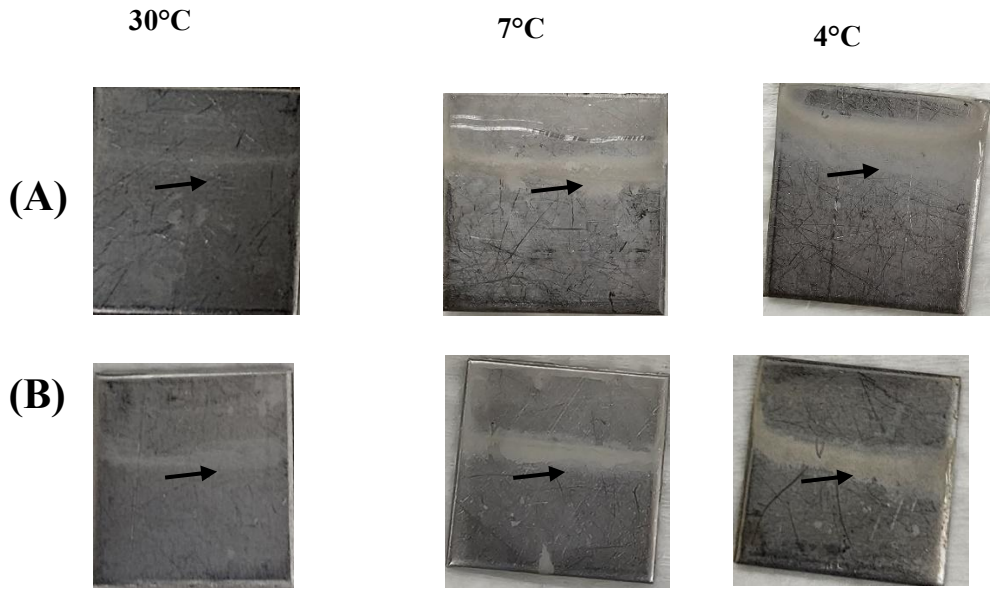

Figure 4.2 Visible biofilm formation on stainless-steel surface at 30°C, 7°C, and 4°C at the end of two weeks. Black arrows indicate the biofilm formation around the air-liquid interface. (A) shows the visible biofilms formed by isolate 3SM, while (B) shows the biofilms of isolate 20SM.

4.3.1.1 Biofilm architecture

The biofilm and planktonic cells were observed under the microscope every 24 h to monitor growth and contamination. Acridine Orange and Calcofluor White dyes were used to view the

biofilm cells, EPS, and biofilm architecture, while Pico green was used to stain the eDNA. After 24 h incubation on a polystyrene surface, large cell aggregates were seen at 4°C and 7°C, while at 30°C, few cell clusters were observed. On a stainless-steel surface, 30°C produced comparatively more cell clusters than the cold temperatures after 24 h. Cell counts also followed a similar trend (Supplementary File 4.7.1). The biofilm architecture was also different when comparing the polystyrene and stainless-steel surfaces. In the early stages, cells formed as a ringlike structure (Fig. 4.3A) on a polystyrene surface while no such patterns were observed on the stainless-steel surface. In the later days of incubation, the cell clusters (Fig. 4.3B) started growing around the ringlike structures. These observations suggest that surface characteristics influence the biofilm architecture.

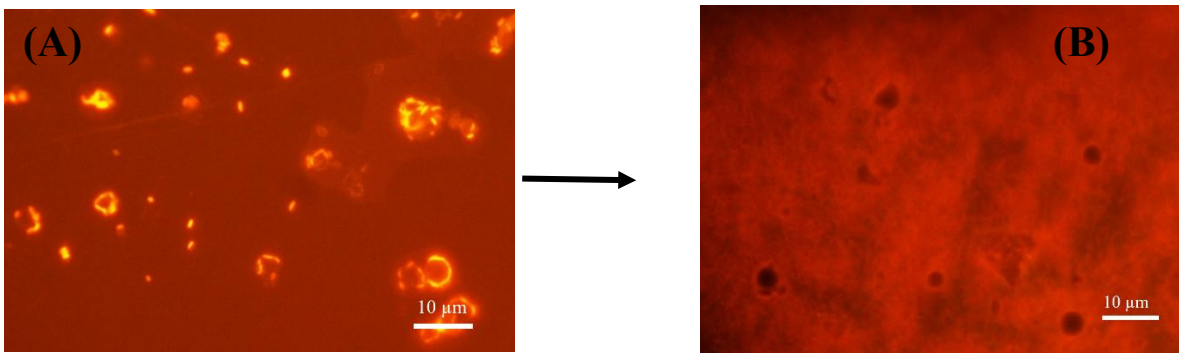

Figure 4.3 The biofilm growth on polystyrene surface, (A) Biofilm of isolate 3SM at 24h, which shows the ringlike structures, while (B) biofilm of isolate 3SM on the 14th day, which shows the cells grown around the ringlike structure (Scale bar 10µm).

4.3.1.2 Filamentous cells

Filamentous cells were observed within the biofilm structures. These cells were observed in the biofilms formed on both stainless-steel and polystyrene surfaces at 30°C, 7°C, and 4°C (Fig. 4.4 C). These filamentous cells were absent in the planktonic cultures. The EPS in the biofilms may restrict motility and cell division. This scenario was checked by growing the cells in a semi-solid medium (TSB with 0.2% agar) and observed under epifluorescence microscopy (Figs. 4.4 A and 4.4 B). There were long filaments seen in the cells grown in TSB semisolid media. These results suggest that restricting motility could be the reason for filamentous cell formation.

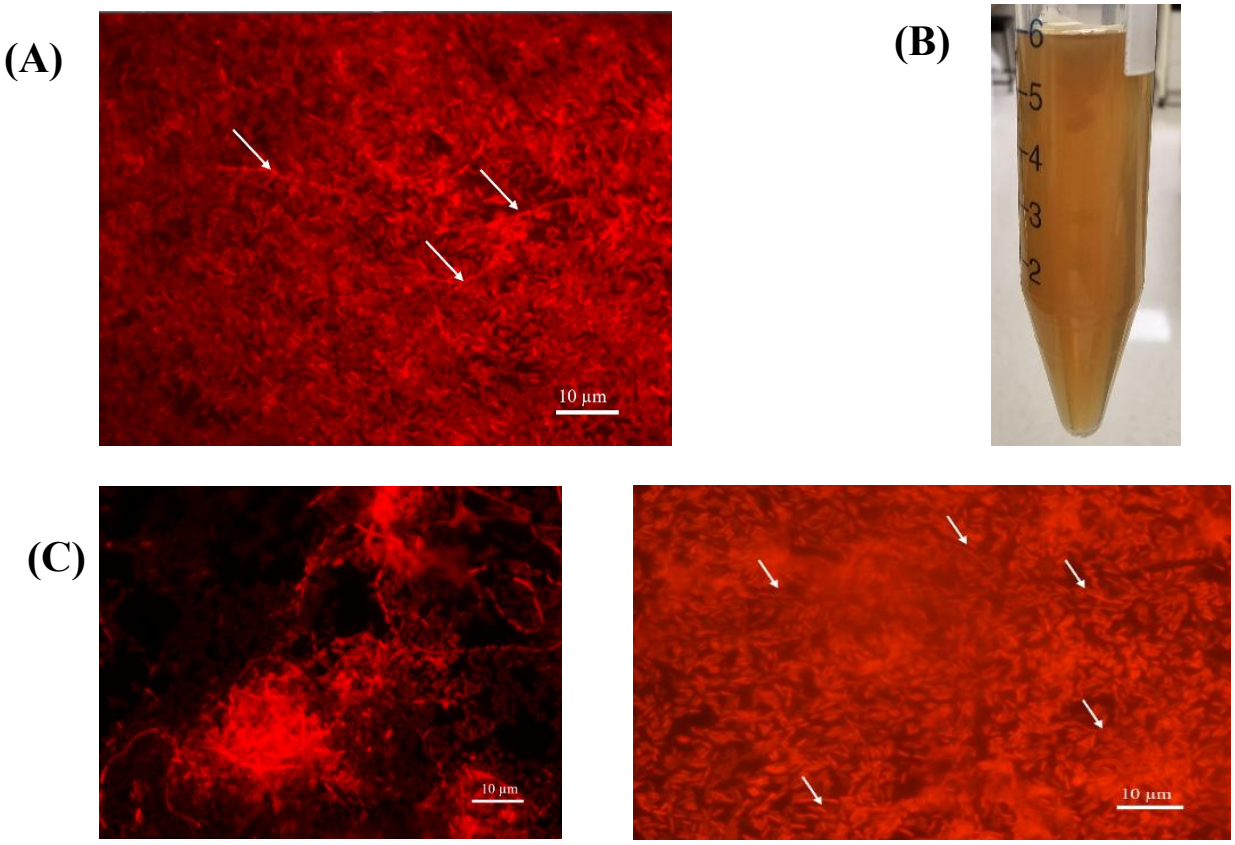

Figure 4.4 Filamentous cells in the biofilm. (A) Filamentous cells grown in a semi-solid medium,(B) Semi-solid medium (TSB with 0.2% agar) with culture (C) Biofilms grown on stainless-steel surface for the isolates 3SM (Scale bar 10µm).

4.3.1.3 Pellicles

Pellicle formation of psychrotrophic pseudomonads was observed in this study. Pellicle formation on planktonic cultures was observed after 24 h of incubation at all three temperatures in this study. Pellicles showed as tightly packed cells (Fig. 4 .5) like biofilms, while planktonic cells were not clustered. This observation also suggests that pellicle is a type of biofilm formed by pseudomonads.

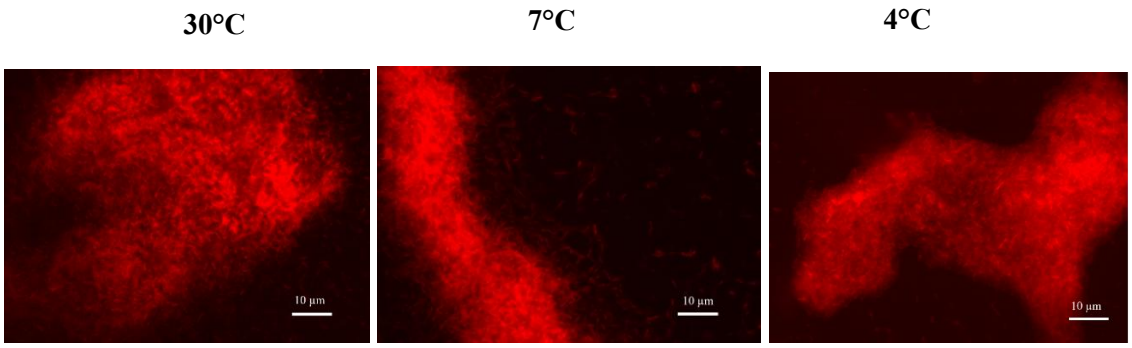

Figure 4.5 Pellicles stained with Acridine Orange at 30°C, 7°C, and 4°C from the planktonic cultures of the isolate 3SM(Scale bar 10µm).

4.3.2 Biofilm and planktonic cell enumeration

The initial inoculum for biofilms and planktonic cultures was approximately 6 log CFU/mL. Biofilm and planktonic growth were monitored every 24 h by serial dilution and plating (Data shown in supplementary file 4.7.1). The cell counts of biofilms and planktonic cultures at the end of two weeks are listed in Tables 4.1 and 4.2.

Table 4.1 Biofilm cell counts at the end of two weeks.

Bacterial Isolate	**Surface**	**Cell counts (LogCFU/cm^2)**		
		30°C	**7°C**	**4°C**
3SM (*P. lundensis*)	Polystyrene surface	7.45 ± 0.10^{a}	8.37 ± 0.23^{ab}	8.95 ± 0.13^{b}
	Stainless-steel surface	6.05 ± 0.07^{a}	6.50 ± 0.05^{b}	7.63 ± 0.15^{c}
20SM (*P. cedrina*)	Polystyrene surface	7.03 ± 0.05^{a}	8.64 ± 0.06^{b}	8.84 ± 0.10^{b}
	Stainless-steel surface	6.88 ± 0.27^{a}	7.10 ± 0.10^{ab}	7.61 ± 0.23^{b}

Table 4.2 Planktonic cell counts at the end of two weeks.

Bacterial isolate	Cell counts (log CFU/mL)		
	30°C	**7°C**	**4°C**
3SM (*P. lundensis*	7.82 ± 0.13^{b}	7.56 ± 0.09^{a}	7.56 ± 0.10^{a}
20SM (*P. cedrina)*	7.80 ± 0.17^{b}	6.92 ± 0.07^{a}	$6.86 \pm 0.29a^{a}$

Different letters above indicate significant differences ($p < 0.05$)

The planktonic cells at 30°C showed higher log CFU/mL compared to 4°C and 7°C (Table 4.2), while the biofilm cells showed higher log CFU/cm^2 at 4°C and 7°C after two weeks (Table 4.1). Notably, in the biofilm cells at 30°C, the cell counts fluctuated in response to media refreshment, and this suggests dispersion of the cells was higher at 30°C compared to 4°C and 7°C. These observations suggest that the biofilm formation of psychrotrophic pseudomonads was encouraged at 7°C and 4°C. On both stainless-steel and polystyrene surfaces, 4°C encouraged more visible biofilms and cell counts.

4.3.3 Biofilm EPS matrix composition

4.3.3.1 Quantification of Cellulose

The cellulose from the biofilm EPS was isolated and quantified from the 2-week-old biofilm cells. At all three growth temperatures, isolate 3SM produced more cellulose in the EPS than 20SM when it was allowed to grow on a stainless-steel surface. There was no significant (p >0.05) difference between the isolates for cellulose production when grown on a polystyrene surface and for the planktonic CFS. Compared to 30°C and 7°C, 4°C yielded significantly (p <0.05) higher EPS in both the isolates (Fig. 4.6 B). The isolate 3SM on stainless steel yielded 85.445 µg/10^8 cells at 30°C, while at 4°C the concentration was 417.04 µg/10^8, which is about a 4.8-fold increase. On polystyrene surfaces, isolate 3SM yielded cellulose of 9.2 µg/10^{8}cells at 30°C, while at 4°C it was 56.22 µg/10^{8}cells, a 6.2-fold increase. Isolate 20SM also followed the same trend with a 5.05-fold increase at 4°C on stainless steel and a 6.9-fold increase on a polystyrene surface at the same temperature. The temperature of 7°C yielded more cellulose than 30ºC and comparatively less cellulose than 4°C for both the isolates and

on both surfaces. There was no significant (p >0.05) difference between the temperatures for planktonic cellulose production.

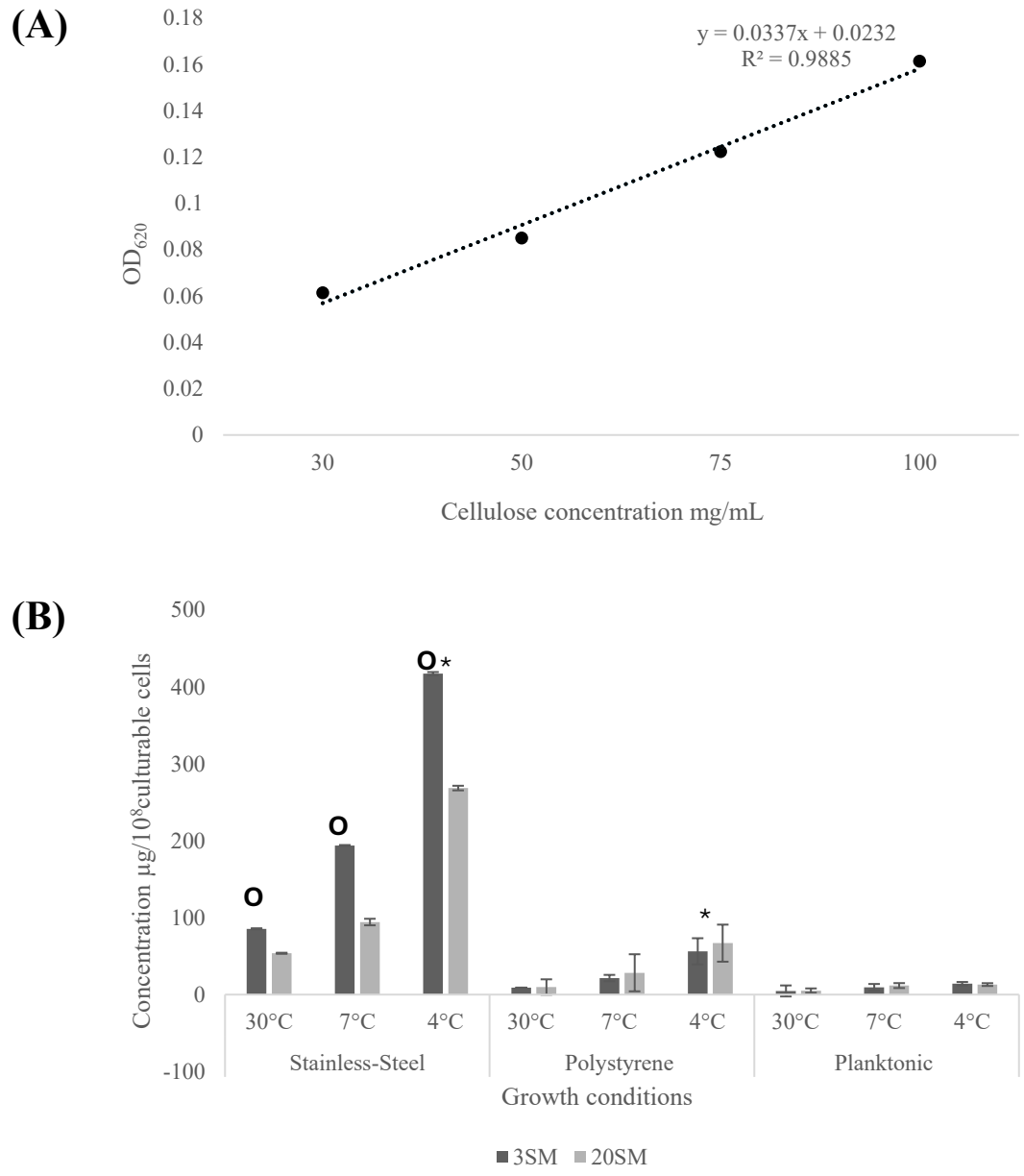

Figure 4.6 Graph A shows the standard microcrystalline cellulose curve from 30 mg/mL to 100mg/mL. Graph B shows the quantity of cellulose isolated from the EPS of biofilms and the planktonic cell-free supernatant after two weeks of incubation. Results are expressed in mean ± standard deviation. "*" indicates the significant difference between the temperatures, while "O" indicates the significant difference (p < 0.05) between the isolates.

4.3.3.2 Quantification of Polysaccharides

Polysaccharides were quantified from the EPS isolated from biofilm and planktonic cells after two weeks of incubation. When comparing the polysaccharide concentration, there was no significant difference between the isolates on either surface or planktonic CFS ($p > 0.05$). However, the biofilms grown at 4°C yielded significantly ($p < 0.01$) higher concentrations of polysaccharide than 30°C and 7°C on both polystyrene and stainless-steel surfaces (Fig. 4.7 B). The isolate 3SM on a stainless-steel surface showed around 128.9 µg/10^8cells at 30°C, while at 4°C it was 436.24 µg/10^8cells, which is about a 3.38-fold increase. For isolate 20SM at 30°C, the polysaccharide concentration was 91.02 µg/10^8cells while the same isolate at 4°C yielded about 449.9 µg/10^8cells, which is around a 4.9-fold increase. When the biofilms were allowed to form on a polystyrene surface, isolate 3SM showed a 6.5-fold increase at 4°C and 20SM showed a 4.91-fold increase at 4°C. This data suggests that biofilm formation is increasing with a decrease in temperature.

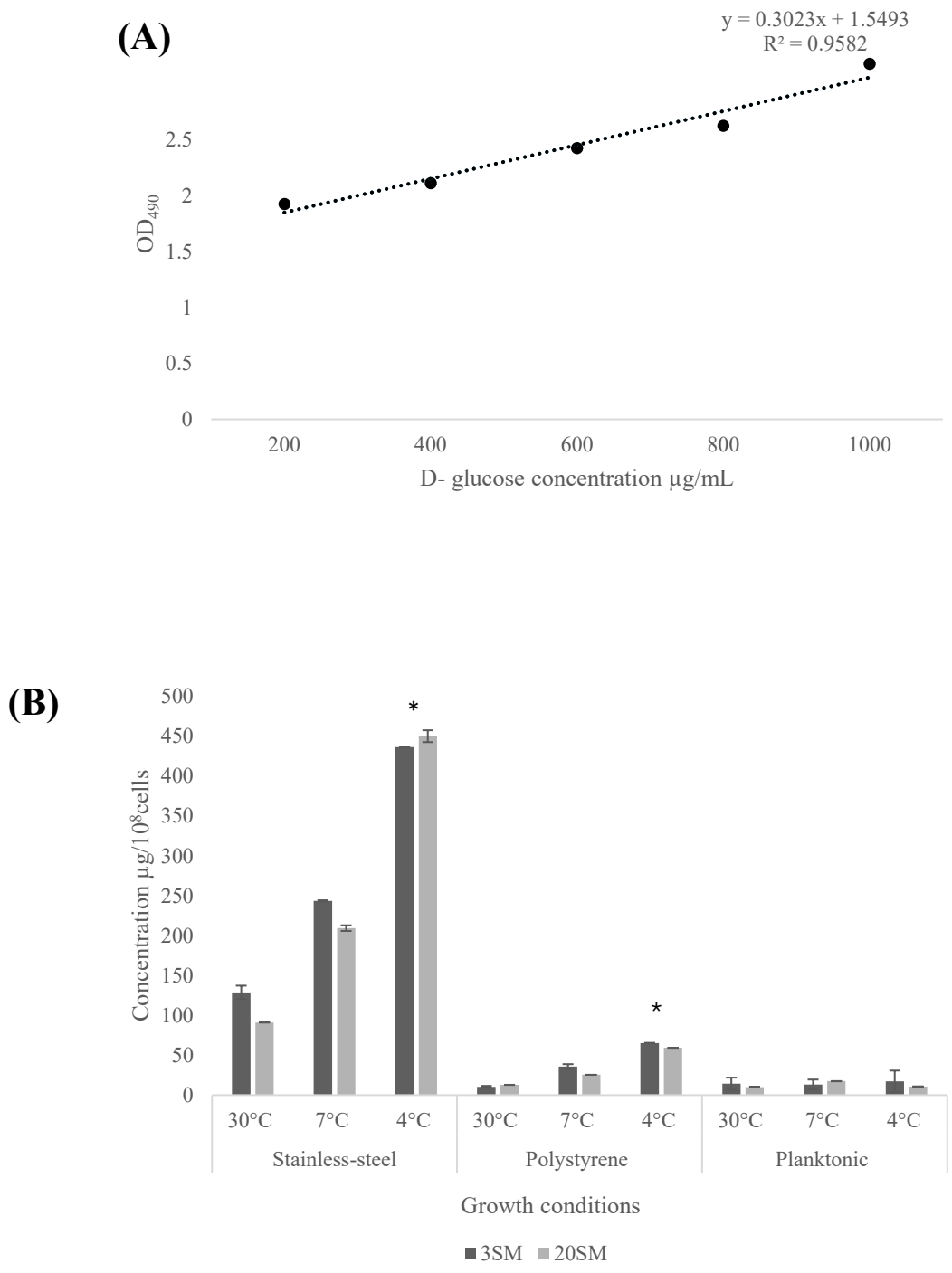

Figure 4.7 Graph A shows the standard curve for D-Glucose from 200µg/mL to 1mg/mL. Graph B shows the total polysaccharide concentration from the biofilm EPS and Planktonic cell-free supernatant. Results are expressed in mean ± standard deviation. "*" indicates the significant difference between the temperatures.

Calcofluor white enables the EPS matrix to be viewed. At 4°C and 7°C, large aggregates were seen, while at 30°C, aggregates were smaller and sparsely distributed on both stainless-steel and polystyrene surfaces (Fig. 4.8 B). At the end of two weeks, the biofilm cells were

almost covered with the EPS matrix, which can be seen with Calcofluor white staining at 4°C (Fig. 4.8A). From the microscopic observations, psychrotrophic pseudomonads produce more EPS at 4°C and 7°C compared to 30°C.

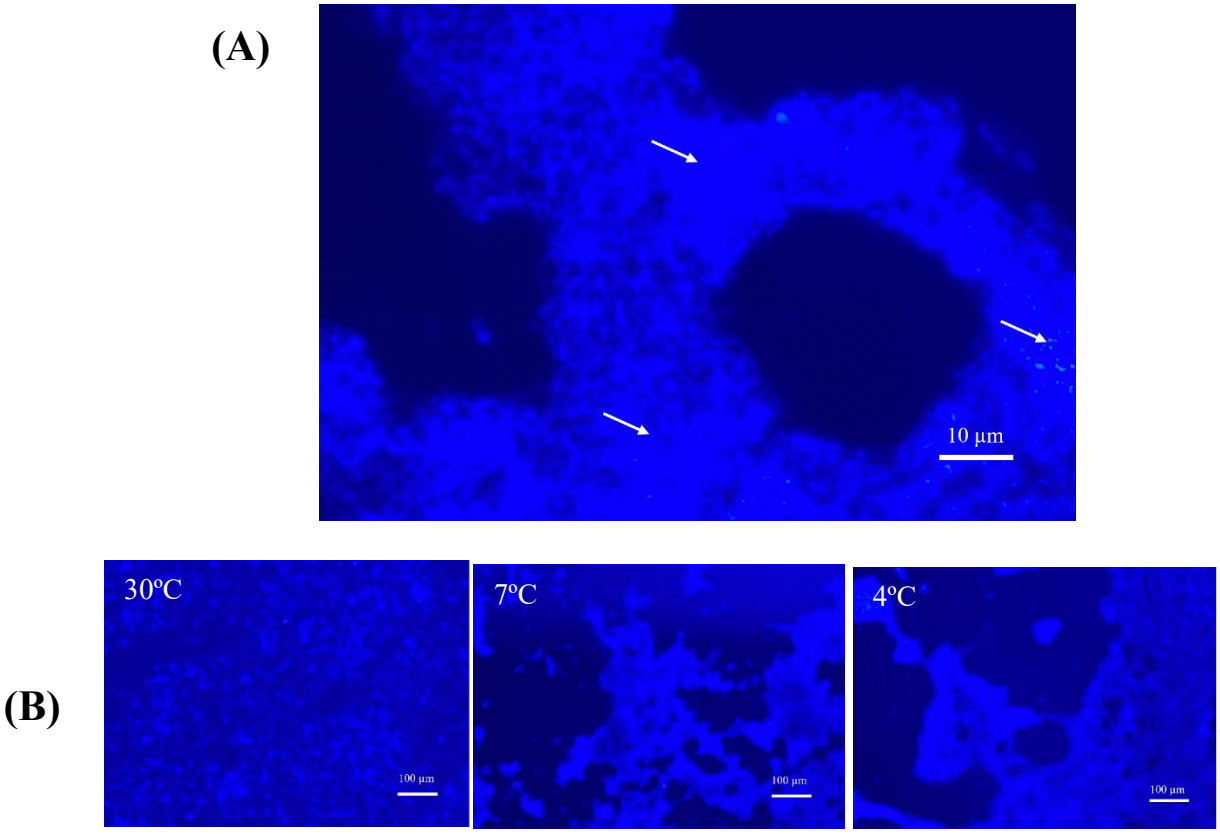

Figure 4.8 (A) Isolate 3SM on a polystyrene surface at the end of two weeks, White arrows indicate the spots where EPS entirely covered the cells(Scale bar 10µm). (B) Isolate 3SM on a polystyrene surface (Scale bar 100µm).

4.3.3.3 Quantification of eDNA

The eDNA concentrations were quantified from the biofilm and planktonic EPS after two weeks of incubation. There was no significant ($p > 0.05$) difference in eDNA concentration between the isolates grown as biofilms on polystyrene and planktonic cultures. However, the polystyrene biofilms at 4°C produced significantly higher eDNA ($p < 0.05$) than at other temperatures. Isolate 3SM yielded significantly higher eDNA ($p < 0.01$) in its biofilms than isolate 20SM (Fig. 4.9). There was a 3.42-fold increase in eDNA to approximately 15.75

ng/10^8cells observed in the biofilms on stainless steel growing at 4°C. The same isolate as a biofilm on a polystyrene surface showed a 5.28-fold increase in eDNA at 4°C compared to other temperatures. Isolate 20SM showed a 2.14-fold increase in the eDNA to approximately 2.64 ng/10^8 cells at 4°C on a stainless-steel surface. On a polystyrene surface, there was a 4.54-fold increase in eDNA observed at 4°C (Fig. 4.9). The planktonic cultures showed eDNA concentrations of less than 1ng/10^8 cells for all three temperatures tested, which supports that eDNA is a feature of biofilm characteristics. The higher concentrations of eDNA isolated from the stainless-steel biofilm EPS of isolate 3SM facilitated eDNA sequencing. The resulting sequence confirmed the presence of eDNA in the EPS.

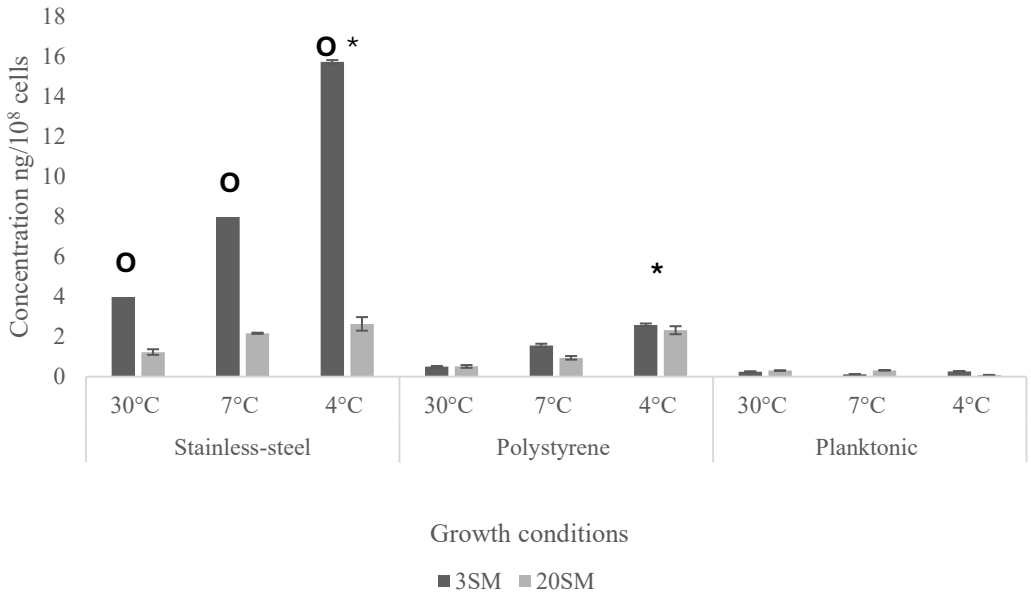

Figure 4.9 The graph here represents the concentration of eDNA present in the biofilms grown on stainless-steel and polystyrene surfaces and the planktonic cell-free supernatant. The results were expressed in mean ± standard deviation. "*" represents the significant difference between the temperatures, while "O" represents the significant difference between the isolates.

Pico green stain was used to view the eDNA in the biofilms. Pico green binds with nucleic acid and emits green fluorescence. Pico green is membrane impermeable and stains the dead

and damaged cells. The dead cells from the biofilms are green in colour while the live cells look dark (Fig. 4.10 A and 4.10 B). On the polystyrene surface, there were thread-like structures (Fig. 4.10 A) that connected the cell clusters, while on the stainless-steel surface (Fig. 4.10 B), thick grid-like channels were observed. These structures were eDNA strands that were stained by Pico green. eDNA in the biofilms was observed even at 24 h. This suggesting eDNA is important in the early stages of biofilm formation.

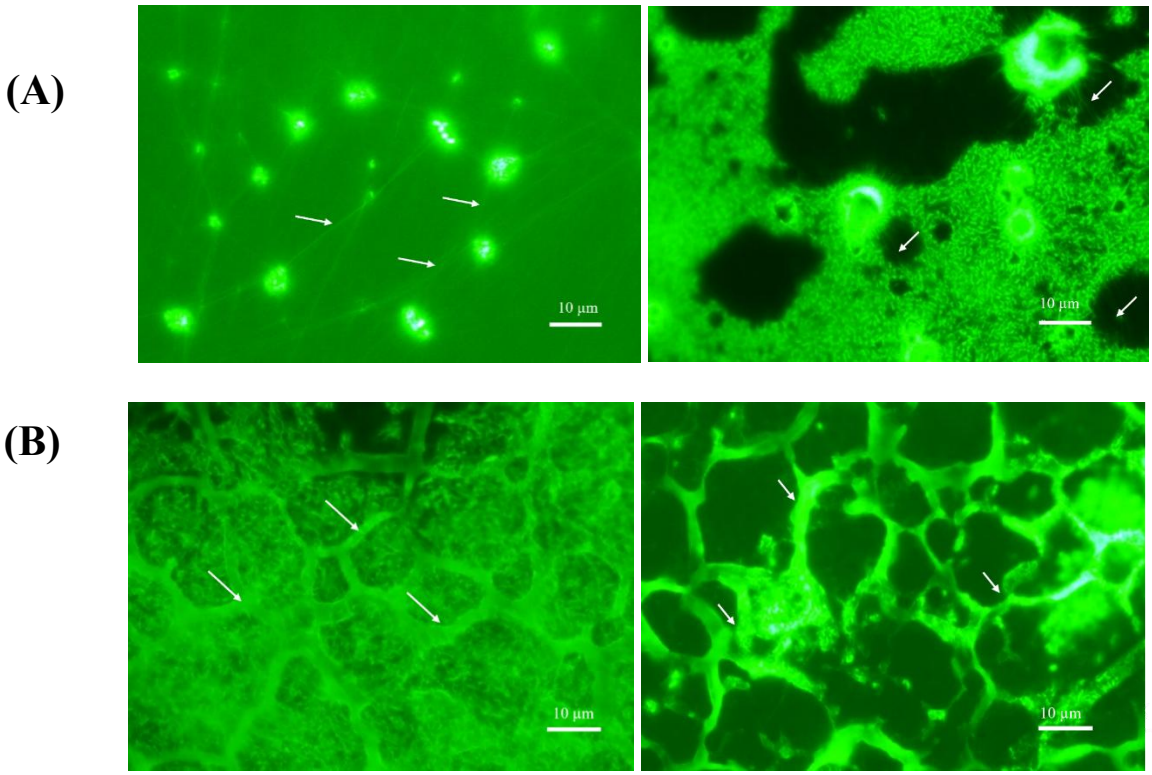

Figure 4.10 eDNA structures in biofilms. (A) eDNA forms as thread-like structures on polystyrene surfaces, (B) eDNA channels on stainless-steel surface of isolate 3SM (Scalebar 10µm).

4.3.3.4 Quantification of Proteins

The proteins were quantified from the EPS isolated from planktonic and biofilm cells after two weeks of incubation. The protein concentrations were compared, and isolate 3SM produced significantly more proteins in its EPS at 4°C and 7°C on both stainless-steel ($p < 0.01$) and polystyrene ($p < 0.05$) surfaces. There was no significant ($p > 0.05$) difference between the proteins isolated from planktonic cell-free supernatant and the biofilms grown at 30°C (Fig. 4.11 B). There was a 6.22-fold increase in proteins observed for the biofilms of isolate 3SM grown on a stainless-steel surface at 4°C, at 697.945 µg/10^8 cells, while at 30°C, total proteins were 112.55 µg/10^8 cells. Isolate 20SM on a stainless-steel surface showed a 4.93-fold increase in total proteins at 4°C at 449.9 µg/10^8 cells, while at 30°C, the total proteins were 91.02 µg/10^8 cells. Biofilms grown on polystyrene surfaces also produced more proteins at 4°C than at 7°C and 30°C. Total proteins from the EPS at 30°C were 22.63 µg/10^8 cells and increased by 5.04-fold at 4°C to 111.7 µg/10^8 cells for isolate 3SM. The total proteins at 30°C, 12.89 µg/10^8 cells, and there was a 2.41-fold increase observed at 4°C at 29.33 µg/10^8 cells. There was also a notable quantity of proteins observed from the planktonic CFS. The total protein concentrations at 7°C were higher than at 30°C and lower than at 4°C for both surfaces.

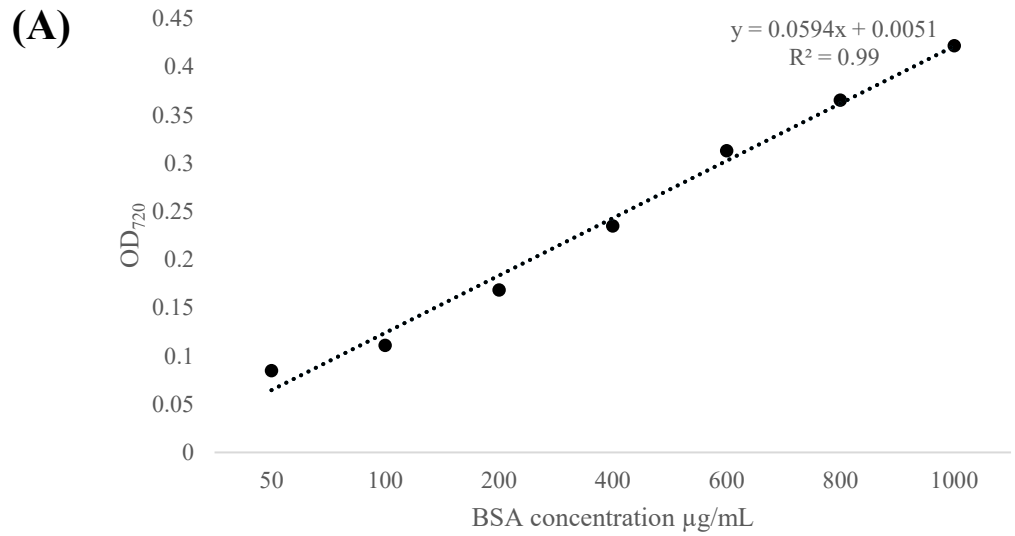

(B)

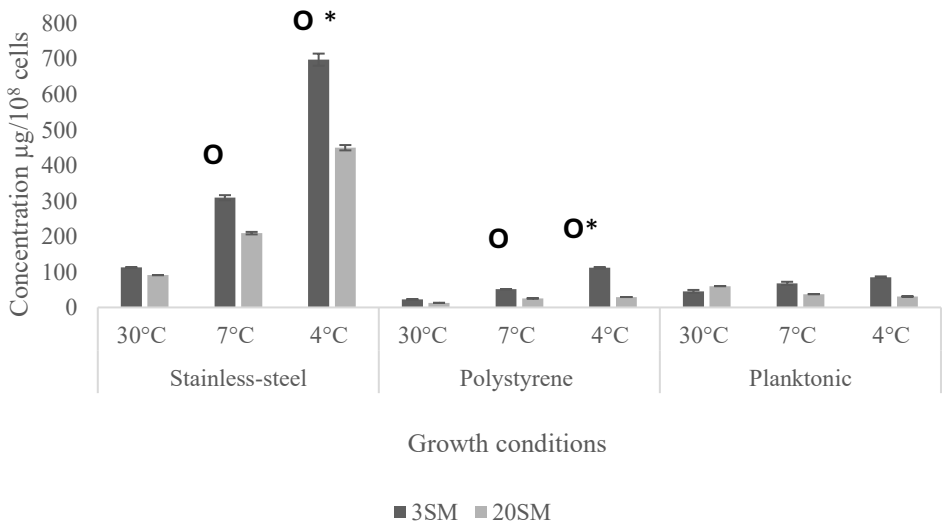

Figure 4.11 Graph A shows the standard curve for Bovine serum albumin from 50µg/mL to 1mg/mL. Graph B shows the total protein concentrations from the biofilm EPS formed on stainless-steel and polystyrene surfaces and the proteins from planktonic CFS. The results are expressed in mean ± standard deviation. "*" represents the significant difference between the temperatures, while "O" represents the significant difference between the isolates.

4.3.3.5 Protein identification

Proteins from the EPS were analysed by SDS-PAGE and Coomassie blue staining (Figure 12). The LC-MS/MS data for protein identities discussed in Table 4.3 were obtained from the proteomic analysis performed in the Mass Spectrometry Centre, University of Auckland. Protein samples were digested with trypsin and analysed on a Thermo Q Exactive mass spectrometer coupled to a nanoLC system. MS/MS spectra were searched against the UniProt database using Mascot software, with a false discovery rate of 1%.

The difference in band patterns between the isolates was observed. Isolate 3SM showed bands at 250 and 130 kDa, while for isolate 20SM, the largest band was from 75 kDa. At 35 kDa molecular weight, the isolate 20SM showed parallel bands while the isolate 3SM showed

a single band. The bands showing a molecular weight of approximately 55kDa were present in both the isolates and in both biofilm EPS and the planktonic CFS (Fig. 4.12). However, LC-MS/MS revealed that the 55kDa bands in isolate 3SM were flagellin, and in 20SM, it was Chaperonin GROEL. The proteins identified in the biofilms of isolate 3SM are listed in Table 4.3.

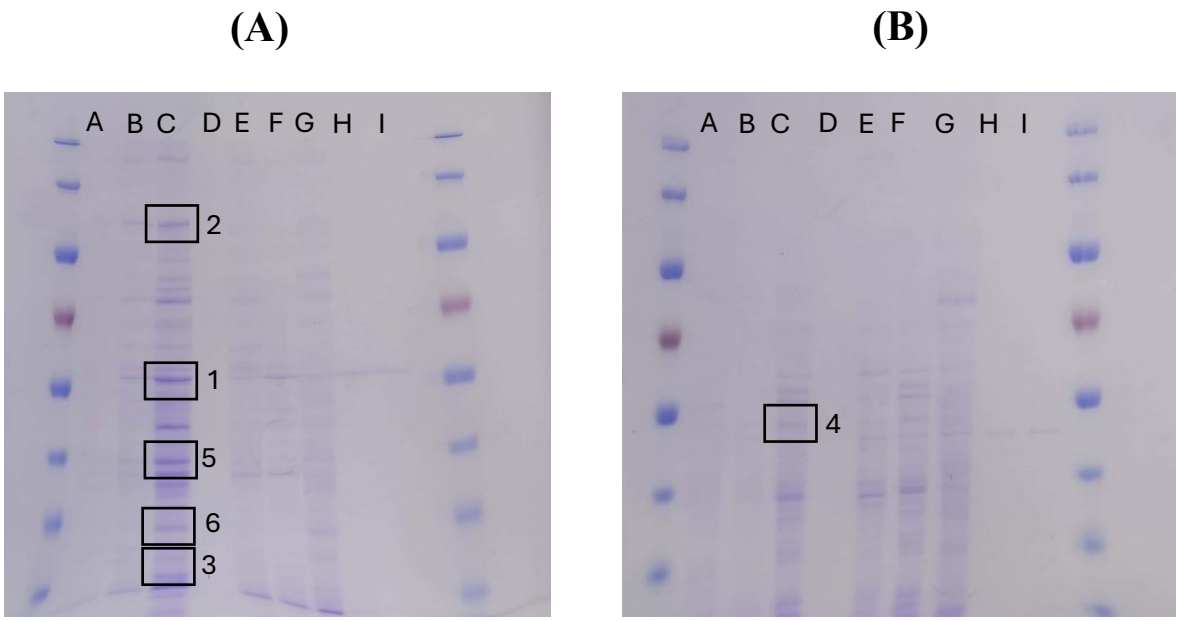

Figure 4.12 (A) represents the proteins isolated from Gel electrophoresis of isolate 3SM while (B)shows the bands from isolate 20SM. The lanes in the gels represent:

A- 30ºC stainless-steel EPS
B- 7ºC stainless-steel EPS
C- 4ºC stainless-steel EPS
D- 30ºC polystyrene EPS
E- 7ºC polystyrene EPS
F- 4ºC polystyrene EPS
G- 30ºC planktonic CFS
H- 7ºC planktonic CFS
I- 4ºC planktonic CFS

(Protein ladder range – 10-250 kDa).

Table 4.3 Proteins identified from the biofilms of 3SM and 20SM grown at 4°C on stainless-steel coupons.

No	Molecular weight(kDa)	Protein	Isolate
1	55	Flagellin	3SM
2	130	ATP-dependent Clp protease ATP-binding subunit	3SM
3	10	ABC transporter substrate-binding proteins	3SM
4	55	Chaperonin GROEL	20SM
5	35	Arginine deiminase	3SM
6	25	Branched-chain-amino-acid ABC transporter substrate-binding proteins	3SM

4.4 Discussion

The formation of biofilm on a solid substrate at an air-liquid interface is indicative of optimal microbial growth. The isolates in this study, 3SM *(P. lundensis*) and 20SM (*P. cedrina*) formed air-liquid interface biofilms. Many studies have reported biofilm formation of pseudomonads. However, only a few studies discussed biofilm formation at the air-liquid interface and its impact on food industries. In the food processing environment, an air-liquid interface can be seen in partly filled equipment, storage, piping systems, and residual liquid after cleaning (Jha et al., 2020). The air-liquid interface biofilms of *B. cereus* have a log higher cell count (log CFU/cm^2) than the submerged stainless-steel coupons. The oxygen availability causes aero taxis of the cells towards oxygen (Wijman et al., 2007). However, in the present study, isolates formed a thick air-liquid interface at 7°C and 4°C compared to 30°C. A study on the influence of temperature on biofilm formation in wastewater biofilms showed that at lower temperatures, dissolved oxygen was higher in the wastewater, which in turn altered the metabolites and encouraged the production of polysaccharides with C=O and O=C-O, which enhanced the resistance of the biofilms (Li et al., 2022).

In this present study, the planktonic cells reached a higher maximum log CFU/mL at 30°C compared with 7°C and 4°C. However, the biofilm cell counts reached a higher maximum log CFU/cm^2 at 7°C and 4°C compared with 30ºC. The temperature of growth has different effects on biofilm cells and planktonic cells of pseudomonads. The delayed log phase at 4°C was reflected in the higher cell counts (log CFU/mL) at 30°C compared to 4°C in the planktonic growth of *Pseudomonas sp.*AU10 over the 180 h of growth (García-Laviña et al., 2019). In a previous study, comparing the biofilm formation of *P. aeruginosa* at four different temperatures (20, 25, 30, and 37°C), the lowest temperature produced the most biofilm and low dispersion (Kim et al., 2020). *P. lundensis* isolated from meat showed higher biofilm biomass (CV values) and protease activity at 4°C compared with 10 and 30°C. This indicates the role of biofilm formation in food spoilage and contamination (Liu et al.,2015).

In this present study, compared to cell numbers, significantly ($p < 0.05$) higher EPS components were observed at cold temperatures. In another study on the biofilm formation of pseudomonads at 23 and 37°C, comparable cell numbers were observed at both temperatures. However, a thick air-liquid interface biofilm formation was observed at 23°C compared with 37°C (Bisht et al., 2021). The differences in the EPS production between temperatures are due to different factors. The higher C-di-GMP levels and overexpression of EPS producing genes *algD* and *pelA* are responsible for the robust biofilm formation and EPS overproduction at cold temperatures (Kim et al., 2020).

The substrate on which a biofilm forms influences the biofilm structure. In the present study, biofilm cells on both polystyrene and stainless-steel surfaces were observed with acridine orange staining, revealing a biofilm architecture that differed depending on the surface. On the polystyrene surface, the formation of ringlike structures was observed, while on the stainless-steel surface, the cells covered the surface with uneven clusters. Similar observations from a study comparing the air-liquid interface growth of *P. fluorescens* Pf1 on different surfaces, such as polypropylene, glass, and stainless-steel showed, showed the formation of weblike structures on polypropylene, while on stainless steel and glass, a heterogeneous distribution was observed (Jha et al., 2020). Polypropylene is a hydrophobic material; however, the author concludes, based on existing literature it is difficult to argue that hydrophobicity is the major reason for biofilm architecture (Jha et al., 2020).

In the present study, filamentous cells were seen with acridine orange staining on both surfaces and all temperature conditions but were absent in planktonic cells. Bacteria produce

filamentous cells as a survival mechanism against stressful environments (Khan et al., 2022). In biofilms, the filamentous cell morphology aids in the adhesion to biotic or abiotic surfaces (Khan et al., 2022). However, not all the cells form filaments, and stress was not the reason for filamentous cell formation in the present study. Some of the cells undergo morphogenesis via cell-cell communication and form filamentous cells and interconnect bacterial clusters. (Anbumani et al., 2021). Other pseudomonads, such as *P. putida,* exhibit filamentous cell morphology in the addition of phosphates and EDTA to the growth media and are reversed by the addition of Mg^{2+} ions (Jensen & Woolfolk, 1985). The filamentous cell formation is strongly influenced by the environment.

In this present study, both the isolates formed pellicles with tightly packed cells, indicating the potential of psychrotrophic pseudomonads to form pellicles. Pellicles form an air-liquid interface that acts as a substrate rather than a solid substrate. Longitudinal cross-packed cells were observed in the pellicles formed by *P. alkylphenolica* KL28, and the controlled growth of pellicle cells accumulates extracellular polymeric substances (Song et al.,2018). The thin layer observed between the cells indicates its role in pellicle flotation. Flagellum-based motility and aero taxis are essential for the pellicle formation in *P. aeruginosa* (Hölscher et al., 2015). Both Pel and Psl polysaccharides are important in the pellicle formation of pseudomonads, and the mutants failed to form pellicles (Ghafoor et al., 2011). The oxygen availability and presence of specific EPS producing genes are responsible for the pellicle formation.

This present study also highlighted similar observations where, at 30°C, the biofilm formation was with small and unevenly distributed cell clusters, while at 4°C and 7°C, larger aggregates were observed. The psychrotrophic pseudomonads produce significantly ($p < 0.05$) higher exopolysaccharides/ 10^8 cells (436- 449 µg/10^8 cells) at cold temperatures, which is confirmed with quantification of EPS components.

In this present study, higher calcofluor white fluorescence was observed at cold temperatures. Calcofluor white stains the cellulosic biomass in the biofilms, and the biofilms of *S. aureus* stained with calcofluor white showed similar structures (García-Salinas et al., 2018). More blue fluorescence was observed for the biofilms grown at 4°C, compared to 15°C and 25°C, suggesting more exopolysaccharide secretion at cold temperatures by pseudomonads (Liu et al.,2023). The significant EPS overproduction at cold temperatures may be responsible for difficulties in cleaning and removing these biofilms. This may lead to improper cleaning and

continuous contamination in the food processing environment. Liu et al. (2023) reported that the biofilms formed at 4ºC showed higher resistance to sodium hypochlorite cleaning.

In this present study, the differences in eDNA structures were observed on different surfaces. On the polystyrene surface, threadlike structures were observed, while on the stainless-steel surface, thick rope or channel-like structures were observed. The eDNA can possess different structures from amorphous mass to filamentous fibres and grid-like structures. The biofilms of *Xanthomonas citri* subsp *citri* formed on a glass surface showed amorphous eDNA structures in the early stages of biofilm formation and long fibres after 72 h of incubation (Sena-Vélez et al., 2016). After 24 h, the fibre structure is established, and the short amorphous structures around the cell clusters are newly formed (Sena-Vélez et al., 2016). The biofilms formed on stainless-steel surfaces showed grid-like structures. Similar grid-like structures are observed in the biofilms of *P. aeruginosa* (flow cell biofilms), and thin rope-like structures are observed in the biofilms of *Haemophilus influenzae* (Allsen-Holm et al.,2006; Jones et al., 2013). However, in the present study, these rope-like structures were found only on stainless-steel surfaces. This observation suggests substrate surface properties can influence the Psl production, and further studies need to confirm the link between surface and EPS production.

The dairy isolates in this study showed differences in their matrix composition. The isolate 3SM showed significantly ($p < 0.05$) higher cellulose and proteins compared to the isolate 20SM. These key differences may play a major role in their biofilm integrity and strength. However, both isolates showed similar quantities of soluble polysaccharides in their EPS matrix. The isolate 3SM produced more proteins than total polysaccharides in the EPS matrix and a higher amount of cellulose. Even though these isolates exhibited similar biofilm-forming abilities in terms of biomass and cell numbers (data not shown), the biofilm EPS matrix composition differed. In a recent study, even though there is a close taxonomic similarity between *P. fragi* and *P. lundensis,* the amounts of carbohydrates and proteins in the biofilms of these bacteria were different (Wickramasinghe et al., 2020). The information on the EPS matrix composition is essential in designing an eradication strategy. The cleaning agent needs to successfully degrade the EPS matrix, especially the exopolysaccharides, proteins, and eDNA (Wang et al., 2023c).

In the present study, flagellin was identified in the EPS matrix of isolate 3SM. This finding is similar to the observations by Jung et al. (2019) that the flagellin homologous proteins in

Vibrio vulnicus biofilms do not participate in the construction of flagellar filaments but are involved in strengthening the biofilm matrix (Jung et al., 2019).

In the present study, the same 55 kDa proteins were present in planktonic CFS and biofilm EPS. However, the functions of the flagellin protein might be different between biofilm and planktonic cells. The 55 kDa band from isolate 20SM was identified as Chaperonin GroEL. Heat shock in *E. coli* induced a three-fold increase in GroEL, indicating the chaperonin function under stress (Wagner et al., 2024). Another interesting molecule identified in the EPS of isolate 3SM was the ATP-dependent Clp protease ATP-binding subunit. The ClpP is present in the biofilms of *X. oryzae* and is responsible for pathogenicity, biofilm production, swimming ability, and EPS production (Ni et al., 2021).

Arginine deiminase system was identified in the present study in isolate 3SM. This system is found in oral biofilms of *Streptococcus mutans*, where it catabolizes the L-arginine, which can inhibit the water-insoluble exopolysaccharide production (Huang et al., 2017). In this present study, the arginine deiminase and other proteins were predominantly present in higher concentrations in the EPS isolated at 4ºC, indicating overproduction of these proteins and their role in the cold temperature-induced biofilm formation.

The ABC transport molecules identified in the present study in isolate 3SM (Table 4.3), are involved in the translocation of diverse substrates across the membranes (Thomas & Tampé, 2020). However, the present study only focused on the soluble EPS, and it needs more research in terms of bound EPS.

When grown on a stainless-steel surface, the isolate 3SM showed significantly ($p < 0.05$) higher eDNA than the isolate 20SM, notably at 4°C. In published work, *P. lundensis* shows significantly high levels of eDNA at cold temperatures, and cellular disruption and cell death at cold temperatures could be the reason for higher eDNA production (Wickramasinghe et al., 2020). Bacterial cell lysis is the major mechanism behind the eDNA release in some gram-positive and negative pathogens; however, some bacteria, such as *E. faecalis* and *Neisseria gonorrhoea,* actively secrete eDNA. In *N. gonorrhoea* biofilm, type IV pili release large quantities of eDNA (Campoccia et al., 2021). The 16s rRNA sequencing of the isolated eDNA confirmed that it is not different from genomic DNA. However, with this information, either the eDNA formed from dead cells or actively secreted into EPS cannot be concluded.

Stainless steel and polystyrene surfaces are commonly found in food processing environments. Polystyrene is mostly used for packaging, while stainless steel is a food-

contact surface (Paz-Méndez et al., 2017). In this study, the isolates formed strong biofilms on both surfaces at 4°C and 7°C. The stainless-steel surface encouraged more EPS production with approximately 7.5 log CFU/cm^2. This suggests that with fewer cells, these isolates can produce more EPS.

The reason behind the higher biofilm biomass at 4°C from Chapter 3 is the overproduction of cellulose, polysaccharides, proteins, and eDNA. On the polystyrene surface, higher cell numbers resulted in high EPS production. In contrast, on the stainless-steel surface, the cell counts were lower than on the polystyrene surface, and the EPS produced remained higher. The linkage between the surface and EPS production still needs to be explored.

4.5 Conclusion

Food spoilage by psychrotrophic pseudomonads is common in dairy and meat processing environments. Temperature is a key factor affecting the biofilm formation of psychrotrophic pseudomonads. Microscopic observations, matrix quantification, and cell count suggested that cold temperatures of 4°C and 7°C yielded higher cell counts and EPS than the biofilms formed at 30°C. Surface characteristics are also an important factor influencing these pseudomonads' biofilm architecture. Knowledge of all the key components in the EPS matrix is important for designing elimination strategies. This study attempted to find the protein molecules present in the EPS matrix. This study highlighted the compositional differences in the EPS formed by two dairy isolates, even though both formed strong biofilms under cold temperatures. However, the interaction between the EPS components needs to be studied. Overall, this study emphasized the biofilm formation and composition of psychrotrophic pseudomonads under cold temperatures, providing new insights that will help the food industry in targeting effective control measures of biofilms of these bacteria.

4.6 References

Allesen-Holm, M., Barken, K. B., Yang, L., Klausen, M., Webb, J. S., Kjelleberg, S., Molin, S., Givskov, M., & Tolker-Nielsen, T. (2006). A characterization of DNA release in *Pseudomonas aeruginosa* cultures and biofilms. *Molecular microbiology*, *59*(4), 1114–1128. https://doi.org/10.1111/j.1365-2958.2005.05008.x

Anbumani, S., Da Silva, A. M., Carvalho, I. G. B., Fischer, E. R., De Souza E Silva, M., Von Zuben, A. A. G., Carvalho, H. F., De Souza, A. A., Janissen, R., & Cotta, M. A. (2021). Controlled spatial organization of bacterial growth reveals key role of cell filamentation preceding *Xylella fastidi*osa biofilm formation. *Npj Biofilms and Microbiomes*, *7*(1), 86. https://doi.org/10.1038/s41522-021-00258-9

Ban, E., & Kim, A. (2024). PicoGreen assay for nucleic acid quantification—Applications, challenges, and solutions. *Analytical Biochemistry*, *692*, 115577. https://doi.org/10.1016/j.ab.2024.115577

Bisht, K., Moore, J. L., Caprioli, R. M., Skaar, E. P., & Wakeman, C. A. (2021). Impact of temperature-dependent phage expression on Pseudomonas aeruginosa biofilm formation. *Npj Biofilms and Microbiomes*, *7*(1), 22. https://doi.org/10.1038/s41522-021-00194-8

Boles, B. R., Thoendel, M., & Singh, P. K. (2005). Rhamnolipids mediate detachment of *Pseudomonas aeruginosa* from biofilms. *Molecular microbiology*, *57*(5), 1210-1223.doi: 10.1111/j.1365-2958.2005.04743.x.

Borlee, B. R., Goldman, A. D., Murakami, K., Samudrala, R., Wozniak, D. J., & Parsek, M. R. (2010). *Pseudomonas aeruginosa* uses a cyclic-di-GMP-regulated adhesin to reinforce the biofilm extracellular matrix. *Molecular microbiology*, *75*(4), 827-842.https://doi.org/10.1111/j.1365-2958.2009.06991.x

Byrd, M. S., Pang, B., Hong, W., Waligora, E. A., Juneau, R. A., Armbruster, C. E., ... & Swords, W. E. (2011). Direct evaluation of *Pseudomonas aeruginosa* biofilm mediators in a chronic infection model. *Infection and immunity*, *79*(8), 3087-3095.https://doi.org/10.1128/iai.00057-11

Caldera, L., & Franzetti, L. (2014). Effect of storage temperature on the microbial composition of ready-to-use vegetables. *Current Microbiology*, *68*, 133-139.https://doi.org/10.1007/s00284-013-0430-6

Campoccia, D., Montanaro, L., & Arciola, C. R. (2021). Tracing the origins of extracellular DNA in bacterial biofilms: Story of death and predation to community benefit. *Biofouling*, *37*(9–10), 1022–1039. https://doi.org/10.1080/08927014.2021.2002987

Coulon, C., Vinogradov, E., Filloux, A., & Sadovskaya, I. (2010). Chemical analysis of cellular and extracellular carbohydrates of a biofilm-forming strain *Pseudomonas aeruginosa* PA14. *PLoS One*, *5*(12), e14220.DOI: 10.1371/journal.pone.0014220

Diggle, S. P., Stacey, R. E., Dodd, C., Cámara, M., Williams, P., & Winzer, K. (2006). The galactophilic lectin, LecA, contributes to biofilm development in *Pseudomonas aeruginosa. Environmental microbiology*, *8*(6), 1095-1104.https://doi.org/10.1111/j.1462-2920.2006.001001.x.

DuBois, Michel., Gilles, K. A., Hamilton, J. K., Rebers, P. A., & Smith, Fred. (1956). Colorimetric Method for Determination of Sugars and Related Substances. *Analytical Chemistry*, *28*(3), 350–356. https://doi.org/10.1021/ac60111a017

Flemming, H.-C., & Wingender, J. (2010). The biofilm matrix. *Nature Reviews Microbiology*, *8*(9), 623–633. https://doi.org/10.1038/nrmicro2415

Flint, S. H., Ward, L. J. H., & Brooks, J. D. (1999). *Streptococcus waius* sp. Nov., a thermophilic streptococcus from a biofilm. *International Journal of Systematic and Evolutionary Microbiology*, *49*(2), 759–767. https://doi.org/10.1099/00207713-49-2-759

Friedman, L., & Kolter, R. (2004). Two genetic loci produce distinct carbohydrate-rich structural components of the *Pseudomonas aeruginosa* biofilm matrix. DOI: 10.1128/JB.186.14.4457-4465.2004

García-Laviña, C. X., Castro-Sowinski, S., & Ramón, A. (2019). Reference genes for real-time RT-PCR expression studies in Antarctic *Pseudomonas* exposed to different temperature conditions. *Extremophiles*, *23*(5), 625–633. https://doi.org/10.1007/s00792-019-01109-4

García-Salinas, S., Elizondo-Castillo, H., Arruebo, M., Mendoza, G., & Irusta, S. (2018). Evaluation of the Antimicrobial Activity and Cytotoxicity of Different Components of Natural Origin Present in Essential Oils. *Molecules*, *23*(6), 1399. https://doi.org/10.3390/molecules23061399

Ghafoor, A., Hay, I. D., & Rehm, B. H. A. (2011). Role of Exopolysaccharides in Pseudomonas aeruginosa Biofilm Formation and Architecture. *Applied and Environmental Microbiology*, *77*(15), 5238–5246. https://doi.org/10.1128/AEM.00637-11.

Goodman, J. K., Zampronio, C. G., Jones, A. M. E., & Hernandez-Fernaud, J. R. (2018). Updates of the In-Gel Digestion Method for Protein Analysis by Mass Spectrometry. *PROTEOMICS*, *18*(23), 1800236. https://doi.org/10.1002/pmic.201800236

Hinsa, S. M., Espinosa-Urgel, M., Ramos, J. L., & O'Toole, G. A. (2003). The transition from reversible to irreversible attachment during biofilm formation by *Pseudomonas fluorescens* WCS365 requires an ABC transporter and a large, secreted protein. *Molecular microbiology*, *49*(4), 905-918. DOI: 10.1046/j.1365-2958.2003.03615.x

Hölscher, T., Bartels, B., Lin, Y.-C., Gallegos-Monterrosa, R., Price-Whelan, A., Kolter, R., Dietrich, L. E. P., & Kovács, Á. T. (2015). Motility, Chemotaxis and Aerotaxis Contribute to Competitiveness during Bacterial Pellicle Biofilm Development. *Journal of Molecular Biology*, *427*(23), 3695–3708. https://doi.org/10.1016/j.jmb.2015.06.014

Huang, X., Zhang, K., Deng, M., Exterkate, R. A. M., Liu, C., Zhou, X., Cheng, L., & Ten Cate, J. M. (2017). Effect of arginine on the growth and biofilm formation of oral bacteria. *Archives of Oral Biology*, *82*, 256–262. https://doi.org/10.1016/j.archoralbio.2017.06.026

Jensen, R. H., & Woolfolk, C. A. (1985). Formation of Filaments by *Pseudomonas putida*. *Applied and Environmental Microbiology*, *50*(2), 364–372. https://doi.org/10.1128/aem.50.2.364-372.1985.

Jha, P. K., Dallagi, H., Richard, E., Benezech, T., & Faille, C. (2020). Formation and resistance to cleaning of biofilms at air-liquid-wall interface. Influence of bacterial strain and material. *Food Control*, *118*, 107384. https://doi.org/10.1016/j.foodcont.2020.107384

Jiang, Y., Gao, F., Xu, X., Ye, K., & Zhou, G. (2011). Changes in the composition of the bacterial flora on tray-packaged pork during chilled storage were analyzed by PCR-DGGE and real-time PCR. *Journal of Food Science*, *76*(1), M27-M33.doi: 10.3389/fmicb.2019.00043

Jones, E. A., McGillivary, G., & Bakaletz, L. O. (2013). Extracellular DNA within a Nontypeable Haemophilus influenzae-Induced Biofilm Binds Human Beta Defensin-3

and Reduces Its Antimicrobial Activity. *Journal of Innate Immunity*, *5*(1), 24–38. https://doi.org/10.1159/000339961

Jung, Y.-C., Lee, M.-A., & Lee, K.-H. (2019). Role of Flagellin-Homologous Proteins in Biofilm Formation by Pathogenic *Vibrio* Species. *mBio*, *10*(4), e01793-19. https://doi.org/10.1128/mBio.01793-19

Karatan, E., & Watnick, P. (2009). Signals, regulatory networks, and materials that build and break bacterial biofilms. *Microbiology and molecular biology reviews : MMBR*, *73*(2), 310–347. https://doi.org/10.1128/MMBR.00041-08

Khan, F., Jeong, G.-J., Tabassum, N., Mishra, A., & Kim, Y.-M. (2022). Filamentous morphology of bacterial pathogens: Regulatory factors and control strategies. *Applied Microbiology and Biotechnology*, *106*(18), 5835–5862. https://doi.org/10.1007/s00253-022-12128-1

Kim, S., Li, X.-H., Hwang, H.-J., & Lee, J.-H. (2020). Thermoregulation of *Pseudomonas aeruginosa* Biofilm Formation. *Applied and Environmental Microbiology*, *86*(22), e01584-20. https://doi.org/10.1128/AEM.01584-20

Klausen, M., Aaes-Jørgensen, A., Molin, S., & Tolker-Nielsen, T. (2003). Involvement of bacterial migration in the development of complex multicellular structures in Pseudomonas aeruginosa biofilms. *Molecular microbiology*, *50*(1), 61-68. DOI: 10.1046/j.1365-2958.2003.03677.x

Li, W., Siddique, M. S., Graham, N., & Yu, W. (2022). Influence of Temperature on Biofilm Formation Mechanisms Using a Gravity-Driven Membrane (GDM) System: Insights from Microbial Community Structures and Metabolomics. *Environmental Science & Technology*, *56*(12), 8908–8919. https://doi.org/10.1021/acs.est.2c01243

Li, X., Nielsen, L., Nolan, C., & Halverson, L. J. (2010). Transient alginate gene expression by *Pseudomonas putida* biofilm residents under water-limiting conditions reflects adaptation to the local environment. *Environmental microbiology*, *12*(6), 1578-1590.DOI: 10.1111/j.1462-2920.2010.02186.x

Liu, J., Wu, S., Feng, L., Wu, Y., & Zhu, J. (2023). Extracellular matrix affects mature biofilm and stress resistance of psychrotrophic spoilage *Pseudomonas* at cold temperature. *Food Microbiology*, *112*, 104214.

Liu, Y. J., Xie, J., Zhao, L. J., Qian, Y. F., Zhao, Y., & Liu, X. (2015). Biofilm Formation Characteristics of *Pseudomonas lundensis* Isolated from Meat. *Journal of Food Science*, *80*(12), M2904–M2910. https://doi.org/10.1111/1750-3841.13142

Ma, L., Conover, M., Lu, H., Parsek, M. R., Bayles, K., & Wozniak, D. J. (2009). Assembly and development of the *Pseudomonas aeruginosa* biofilm matrix. *PLoS pathogens*, *5*(3), e1000354.https://doi: 10.1371/journal.ppat.1000354.

Mann, E. E., & Wozniak, D. J. (2012). *Pseudomonas* biofilm matrix composition and niche biology. *FEMS Microbiology Reviews*, *36*(4), 893–916. https://doi.org/10.1111/j.1574-6976.2011.00322.x.

Moshynets, O.V.; Pokholenko, I.; Iungin, O.; Potters, G.; Spiers, A.J. eDNA, Amyloid Fibers and Membrane Vesicles Identified in *Pseudomonas fluorescens* SBW25 Biofilms. *Int. J. Mol. Sci.* **2022**, *23*, 15096. https://doi.org/10.3390/ijms232315096

Ni, Y., Hou, Y., Kang, J., & Zhou, M. (2021). ATP-Dependent Protease ClpP and Its Subunits ClpA, ClpB, and ClpX Involved in the Field Bismerthiazol Resistance in *Xanthomonas oryzae* pv. *Oryzae*. *Phytopathology*®, *111*(11), 2030–2040. https://doi.org/10.1094/PHYTO-01-21-0011-R

Or, D., Phutane, S., & Dechesne, A. (2007). Extracellular polymeric substances affecting pore-scale hydrologic conditions for bacterial activity in unsaturated soils. *Vadose Zone Journal*, *6*(2), 298-305.https://doi.org/10.2136/vzj2006.0080

Osman, S. F., Fett, W. F., & Fishman, M. L. (1986). Exopolysaccharides of the phytopathogen *Pseudomonas syringae* pv. glycine. *Journal of Bacteriology*, *166*(1), 66-71.https://doi.org/10.1128/jb.166.1.66-71.1986

O'Toole, G. A., & Kolter, R. (1998). Flagellar and twitching motility are necessary for *Pseudomonas aeruginosa* biofilm development. *Molecular microbiology*, *30*(2), 295-304.https://doi.org/10.1046/j.1365-2958.1998.01062.x

Otzen, D., & Nielsen, P. H. (2008). We find them here; we find them there: functional bacterial amyloid. *Cellular and molecular life sciences: CMLS*, *65*(6), 910–927. https://doi.org/10.1007/s00018-007-7404-4.

Paz-Méndez, A., Lamas, A., Vázquez, B., Miranda, J., Cepeda, A., & Franco, C. (2017). Effect of Food Residues in Biofilm Formation on Stainless Steel and Polystyrene

Surfaces by *Salmonella enterica* Strains Isolated from Poultry Houses. *Foods*, *6*(12), 106. https://doi.org/10.3390/foods6120106

Penesyan, A., Paulsen, I. T., Kjelleberg, S., & Gillings, M. R. (2021). Three faces of biofilms: A microbial lifestyle, a nascent multicellular organism, and an incubator for diversity. *Npj Biofilms and Microbiomes*, *7*(1), 80. https://doi.org/10.1038/s41522-021-00251-2

Read, R. C., Roberts, P., Munro, N., Rutman, A., Hastie, A., Shryock, T., Taylor, G. (1992). *Effect of Pseudomonas aeruginosa rhamnolipids on mucociliary transport and ciliary beating*. *Journal of Applied Physiology, 72*(6), 2271–2277. https://doi.org/10.1152/jappl.1992.72.6.2271.

Sena-Vélez, M., Redondo, C., Graham, J. H., & Cubero, J. (2016). Presence of Extracellular DNA during Biofilm Formation by *Xanthomonas citri subsp. Citri* Strains with Different Host Ranges. *PLOS ONE*, *11*(6), e0156695. https://doi.org/10.1371/journal.pone.0156695

Sharma, S., Acharya, J., Banjara, M. R., Ghimire, P., & Singh, A. (2020). Comparison of acridine orange, fluorescent microscopy, and Gram stain light microscopy for the rapid detection of bacteria in cerebrospinal fluid. *BMC Research Notes*, *13*(1), 29. https://doi.org/10.1186/s13104-020-4895-7

Shen, C.H. (2023). Quantification and analysis of proteins. In *Diagnostic Molecular Biology* (pp. 231–257). Elsevier. https://doi.org/10.1016/B978-0-323-91788-9.00002-8

Song, M., Veeranagouda Y., Ganzorig M., Lee K. (2018). Circular pellicles formed by *Pseudomonas alkylphenolica* KL28 are a sophisticated architecture principally designed by matrix substance. J Microbiol. 2018 Nov;56(11):790-797. doi: 10.1007/s12275-018-8252-7.

Spiers, A. J., Bohannon, J., Gehrig, S. M., & Rainey, P. B. (2003). Biofilm formation at the air-liquid interface by the Pseudomonas fluorescens SBW25 wrinkly spreader requires an acetylated form of cellulose. *Molecular microbiology*, *50*(1), 15-27. https://doi.org/10.1046/j.1365-2958.2003.03670.x

Thomas, C., & Tampé, R. (2020). Structural and Mechanistic Principles of ABC Transporters. *Annual Review of Biochemistry*, *89*(1), 605–636. https://doi.org/10.1146/annurev-biochem-011520-105201

Wagner, J., Carvajal, A. I., Bracher, A., Beck, F., Wan, W., Bohn, S., Körner, R., Baumeister, W., Fernandez-Busnadiego, R., & Hartl, F. U. (2024). Visualizing chaperonin function in situ by cryo-electron tomography. *Nature*, *633*(8029), 459–464. https://doi.org/10.1038/s41586-024-07843-w.

Wang, D., Fletcher, G. C., Gagic, D., On, S. L. W., Palmer, J. S., & Flint, S. H. (2023a). Comparative genome identification of accessory genes associated with strong biofilm formation in *Vibrio parahaemolyticus*. *Food Research International*, *166*, 112605. https://doi.org/10.1016/j.foodres.2023.112605

Wang, D., Fletcher, G. C., On, S. L. W., Palmer, J. S., Gagic, D., & Flint, S. H. (2023b). Biofilm formation, sodium hypochlorite susceptibility, and genetic diversity *of Vibrio parahaemolyticus*. *International Journal of Food Microbiology*, *385*, 110011. https://doi.org/10.1016/j.ijfoodmicro.2022.110011

Wang, D., Yu, J. M., Dorosky, R. J., Pierson, L. S., 3rd, & Pierson, E. A. (2016). The Phenazine 2-Hydroxy-Phenazine-1-Carboxylic Acid Promotes Extracellular DNA Release and Has Broad Transcriptomic Consequences in *Pseudomonas chlororaphis* 30-84. *PloS one*, *11*(1), e0148003. https://doi.org/10.1371/journal.pone.0148003

Wang, S., Liu, X., Liu, H., Zhang, L., Guo, Y., Yu, S., Wozniak, D. J., & Ma, L. Z. (2015). The exopolysaccharide Psl–eDNA interaction enables the formation of a biofilm skeleton in *Pseudomonas aeruginosa*. *Environmental Microbiology Reports*, *7*(2), 330–340. https://doi.org/10.1111/1758-2229.12252

Wang, S., Zhao, Y., Breslawec, A. P., Liang, T., Deng, Z., Kuperman, L. L., & Yu, Q. (2023c). Strategy to combat biofilms: A focus on biofilm dispersal enzymes. *Npj Biofilms and Microbiomes*, *9*(1), 63. https://doi.org/10.1038/s41522-023-00427-y

Wei, Q., & Ma, L. (2013). Biofilm Matrix and Its Regulation in Pseudomonas aeruginosa. *International Journal of Molecular Sciences*, *14*(10), 20983–21005. https://doi.org/10.3390/ijms141020983

Wickramasinghe, N. N., Hlaing, M. M., Ravensdale, J. T., Coorey, R., Chandry, P. S., & Dykes, G. A. (2020). Characterization of the biofilm matrix composition of psychrotrophic, meat spoilage pseudomonads. *Scientific Reports*, *10*(1), 16457. https://doi.org/10.1038/s41598-020-73612-0

Wijman, J. G. E., De Leeuw, P. P. L. A., Moezelaar, R., Zwietering, M. H., & Abee, T. (2007). Air-Liquid Interface Biofilms of *Bacillus cereus*: Formation, Sporulation, and Dispersion. *Applied and Environmental Microbiology*, *73*(5), 1481–1488. https://doi.org/10.1128/AEM.01781-06

Yang, G., Lin, J., Zeng, E. Y., & Zhuang, L. (2019). Extraction and characterization of stratified extracellular polymeric substances in *Geobacter* biofilms. *Bioresource Technology*, *276*, 119–126. https://doi.org/10.1016/j.biortech.2018.12.100.

4.7 Supplementary file

4.7.1 Cell counts over 14 days.

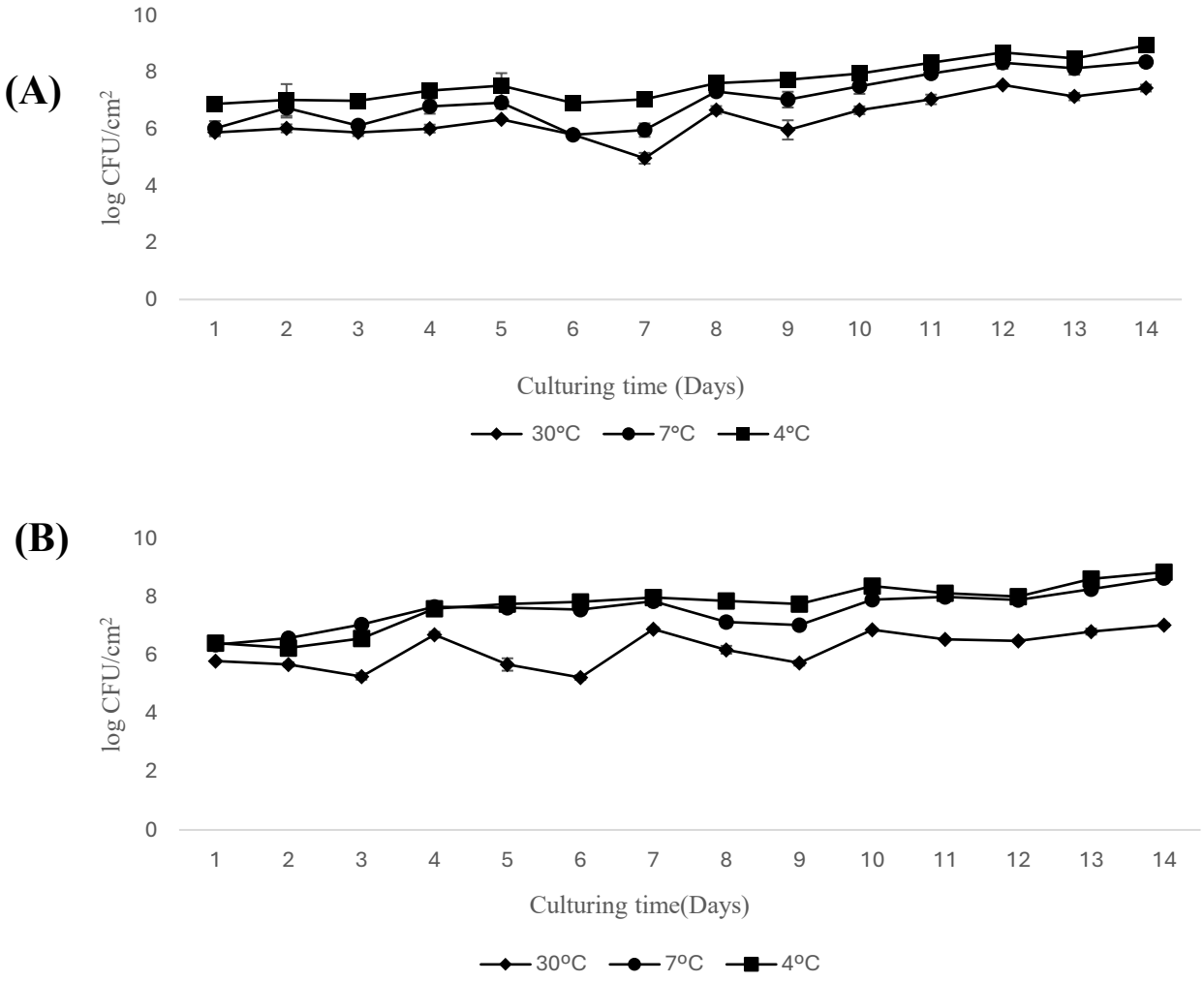

Figure 4.7.1: Cell counts from biofilms grown on polystyrene surfaces at three different temperatures 30°C, 7°C, and 4°C. (A) Isolate 3SM and (B) isolate 20SM. All results are expressed as mean±standard deviation.

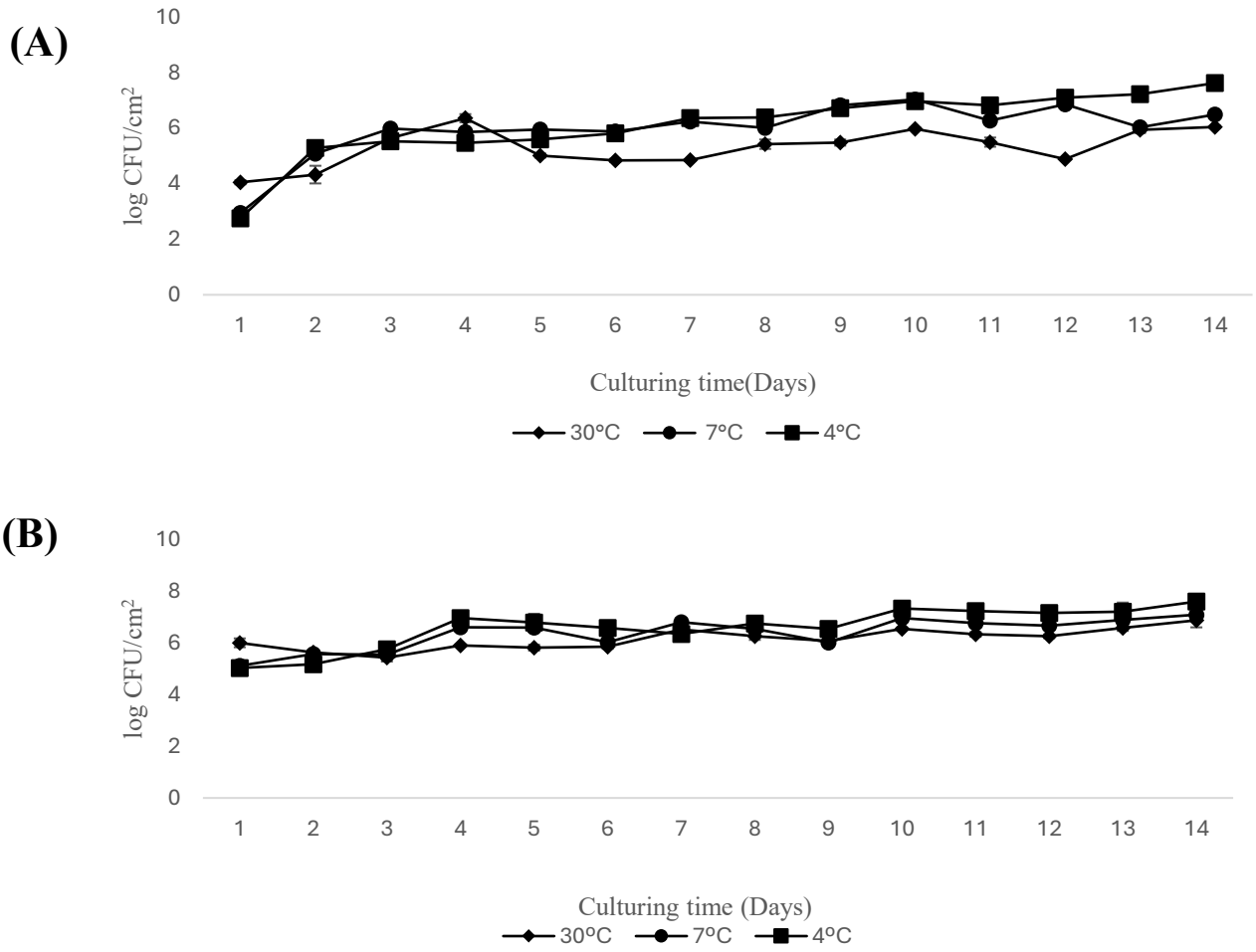

Figure 4.7.2: Cell counts from biofilms grown on stainless-steel surfaces at three different temperatures 30°C, 7°C, and 4°C. (A) Isolate 3SM and (B) isolate 20SM. All results are expressed as mean±standard deviation.

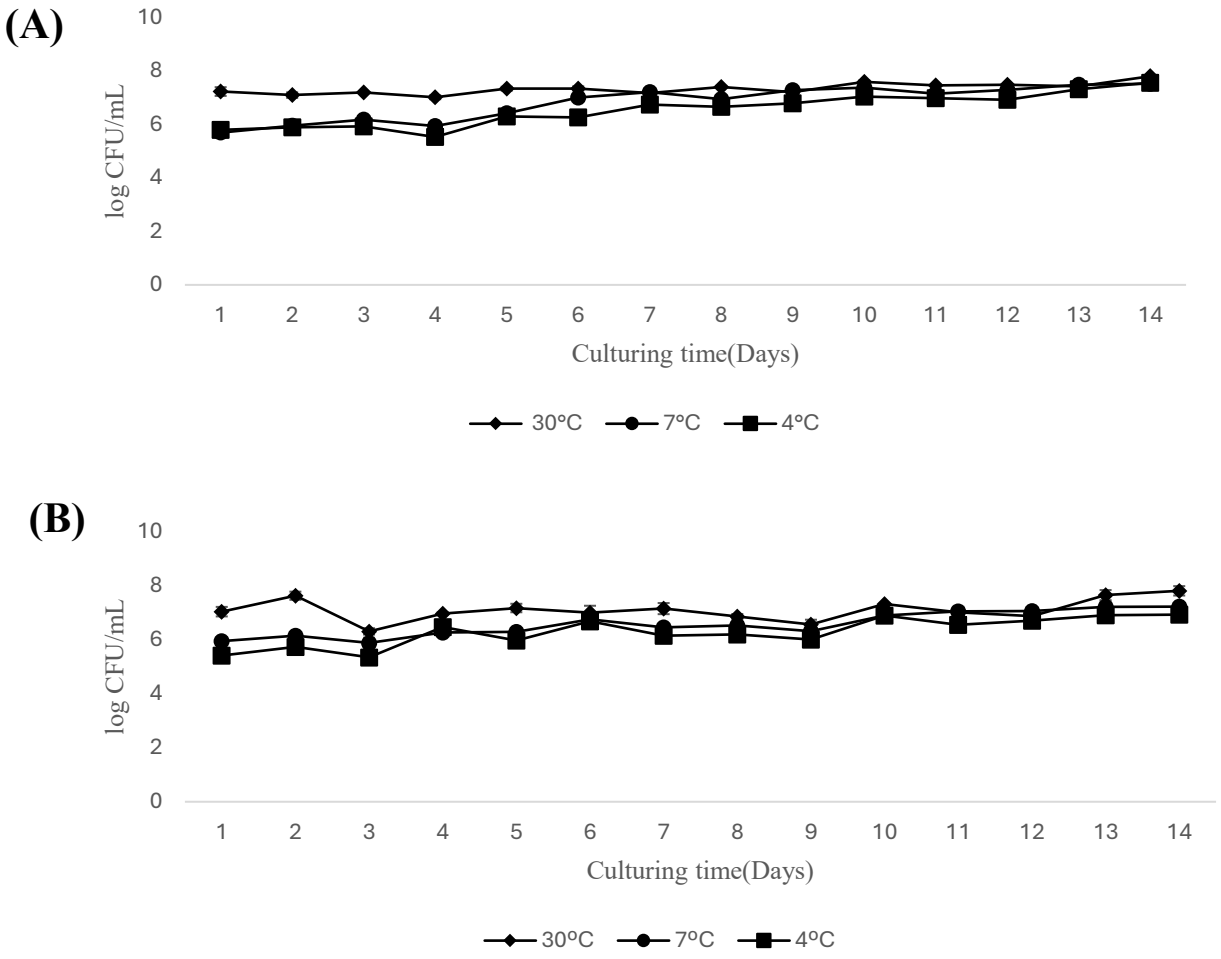

Figure 4.7.3: Cell counts from planktonic cultures grown at 30°C, 7°C, and 4°C. (A) Isolate 3SM and (B) isolate 20SM. All results are expressed as mean ± standard deviation.

4.7.1 Microscopic observations.

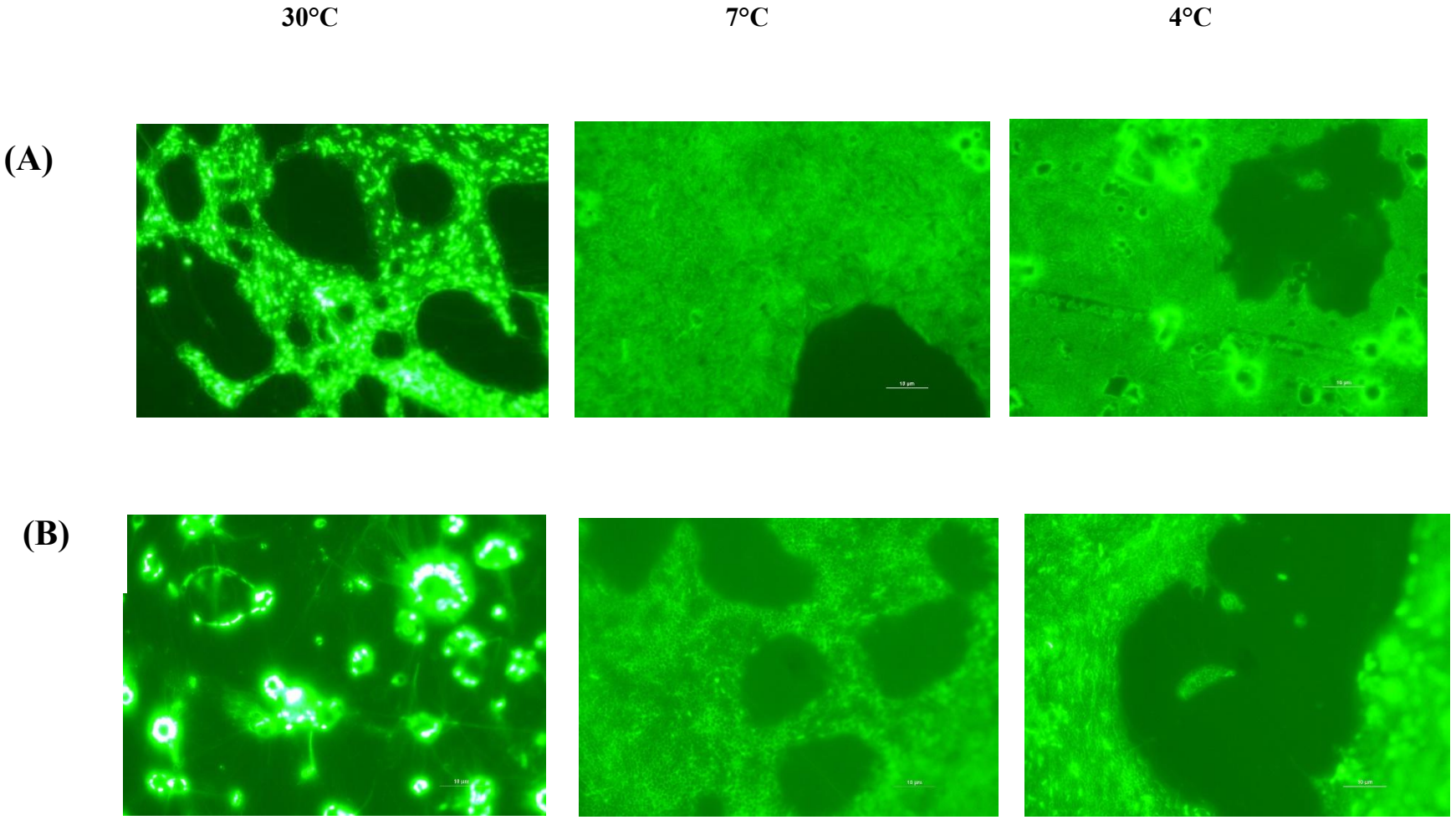

Figure 4.7.4: eDNA formed as a thread-like structure on a polystyrene surface. (A) Biofilms of 3SM on 24h and (B) on the 14th day (Scale bar 10 µm).

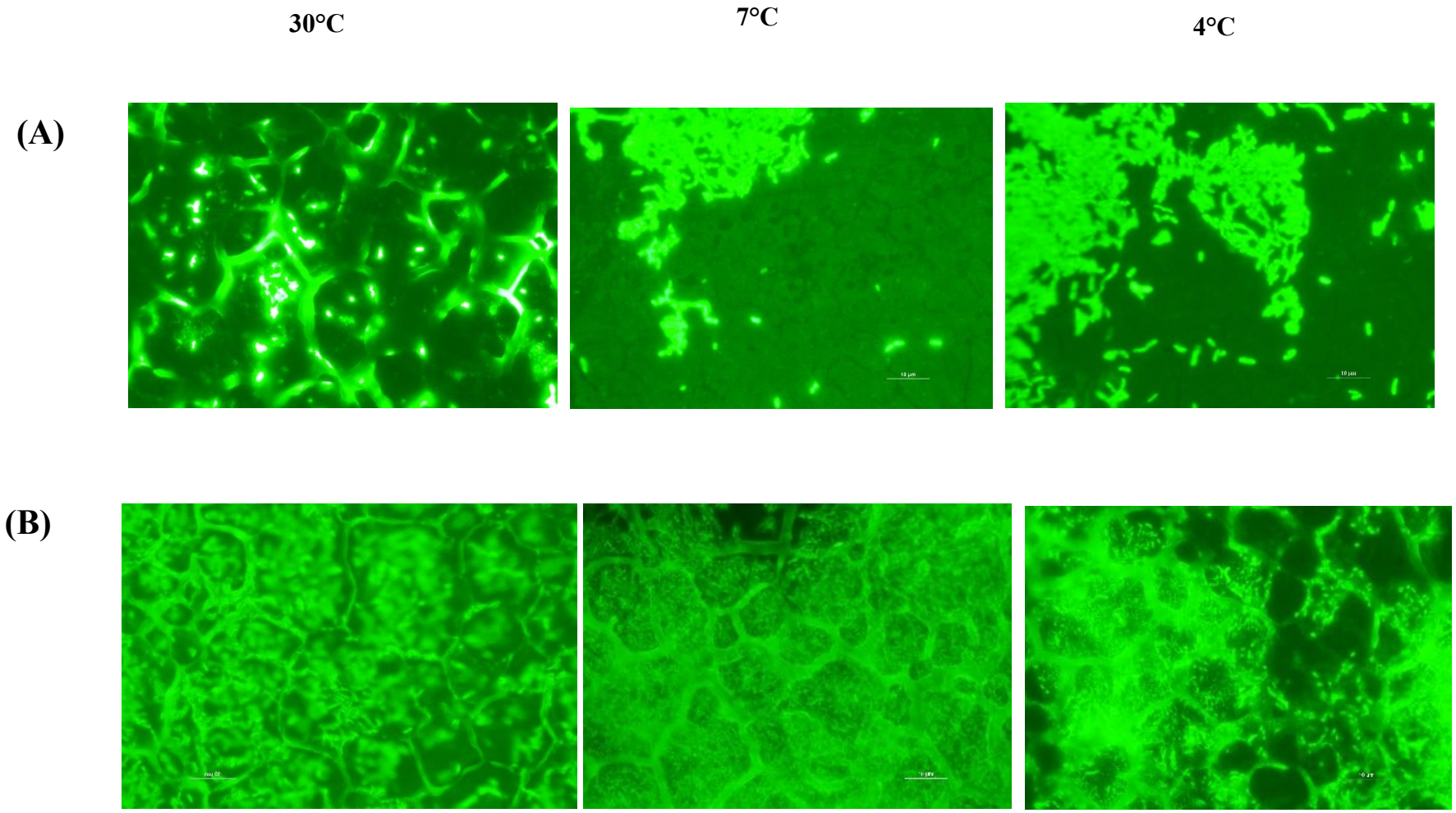

Figure 4.7.5: eDNA formed as a thread-like structure on a stainless-steel surface. (A) Biofilms of 3SM on 24h and (B) on the 14th day (Scale bar 10µm).

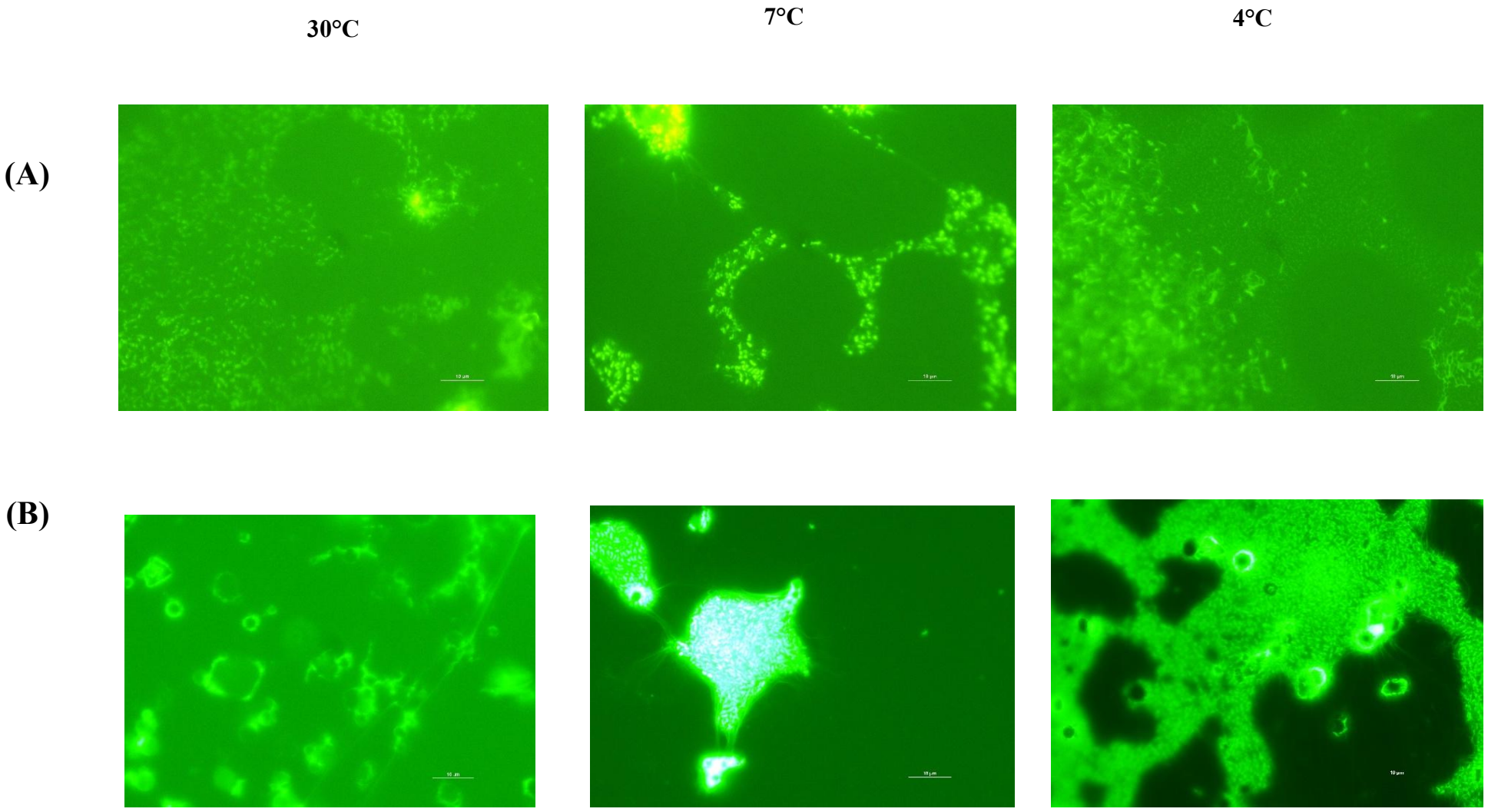

Figure 4.7.6: eDNA formed as a thread-like structure on a polystyrene surface. (A) Biofilms of 20SM on 24h and (B) on the 14th day(Scale bar 10 µm)

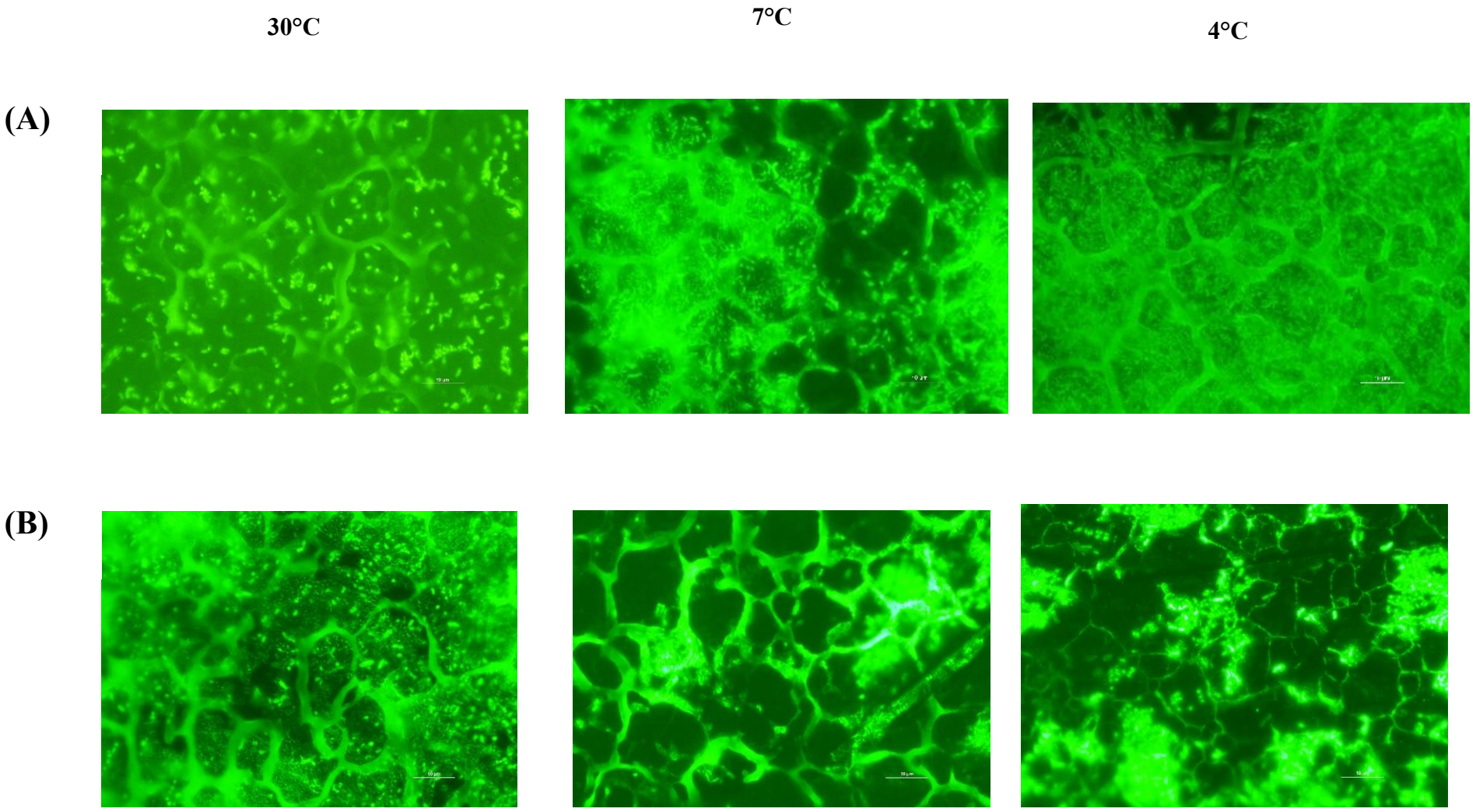

Figure 4.7.7: eDNA formed as a thread-like structure on a stainless-steel surface. (A) Biofilms of 20SM on 24h and (B) on the 14th day(Scale bar 10µm).

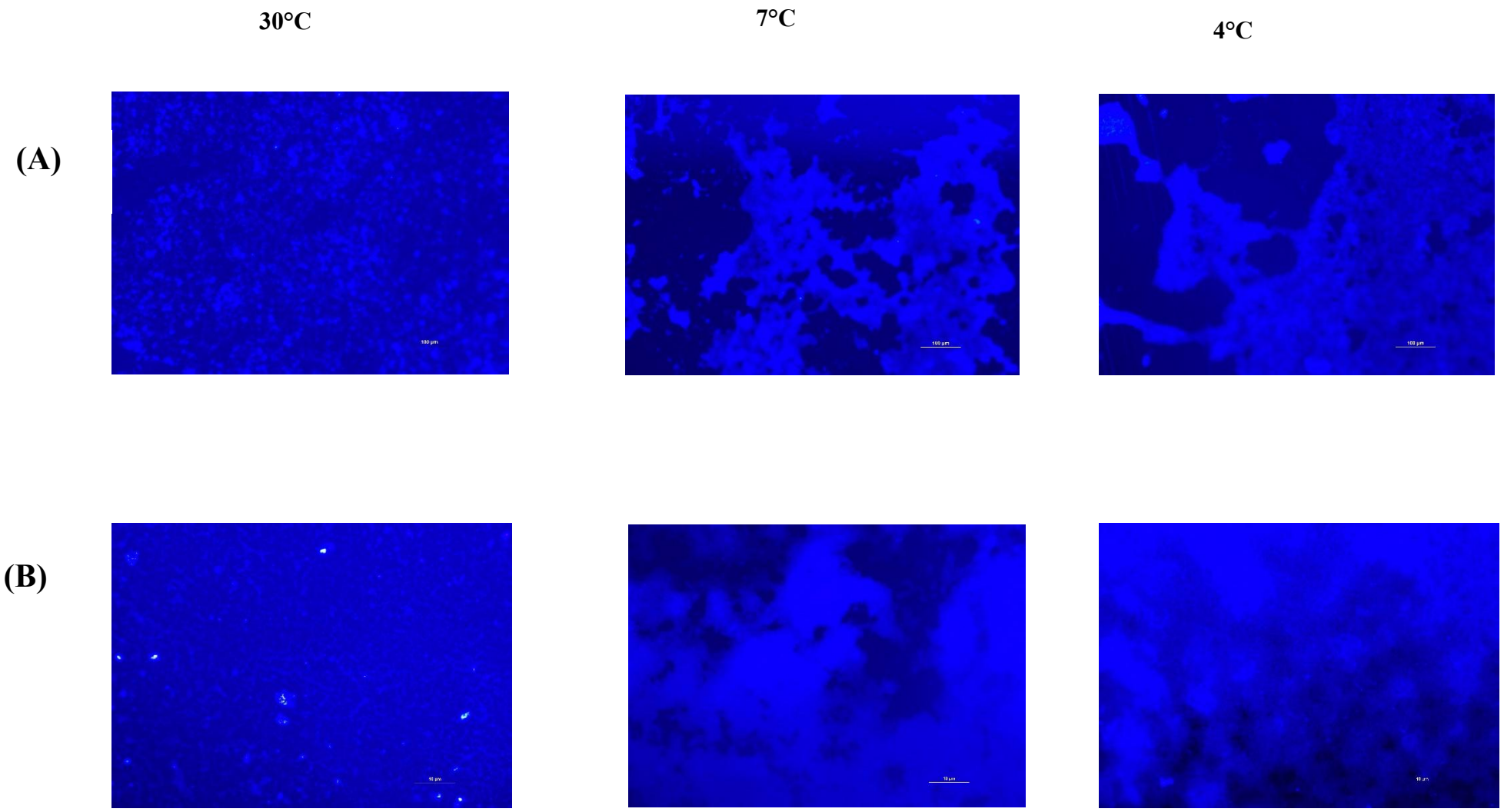

Figure 4.7.8: (A) Biofilms of 3SM on 24 h and (B) on the 14th day (Scale bar 100 µm) on the polystyrene surface.

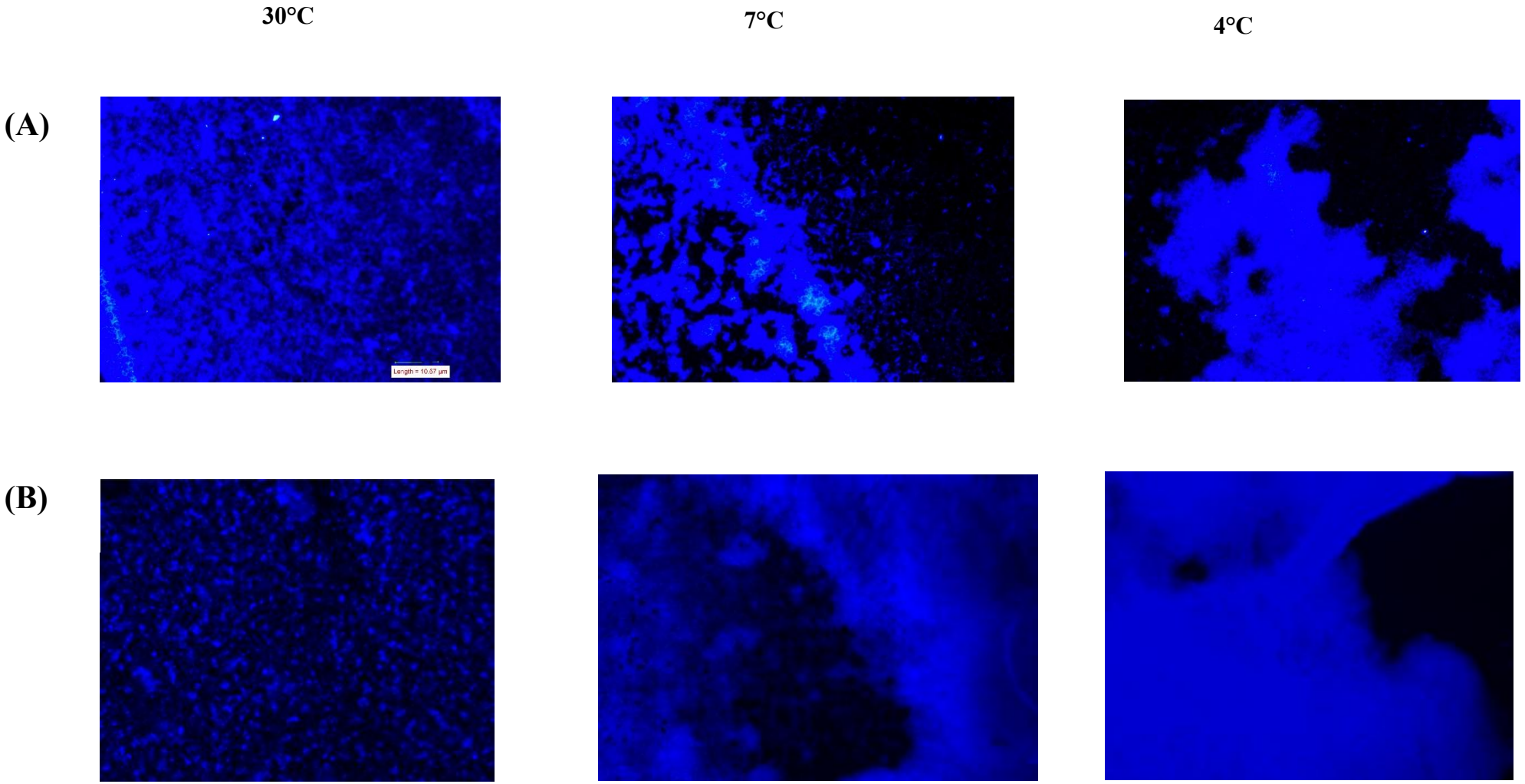

Figure 4.7.9: (A) Biofilms of 3SM on 24 h and (B) on the 14th day (Scale bar 100 µm) on the stainless-steel surface.

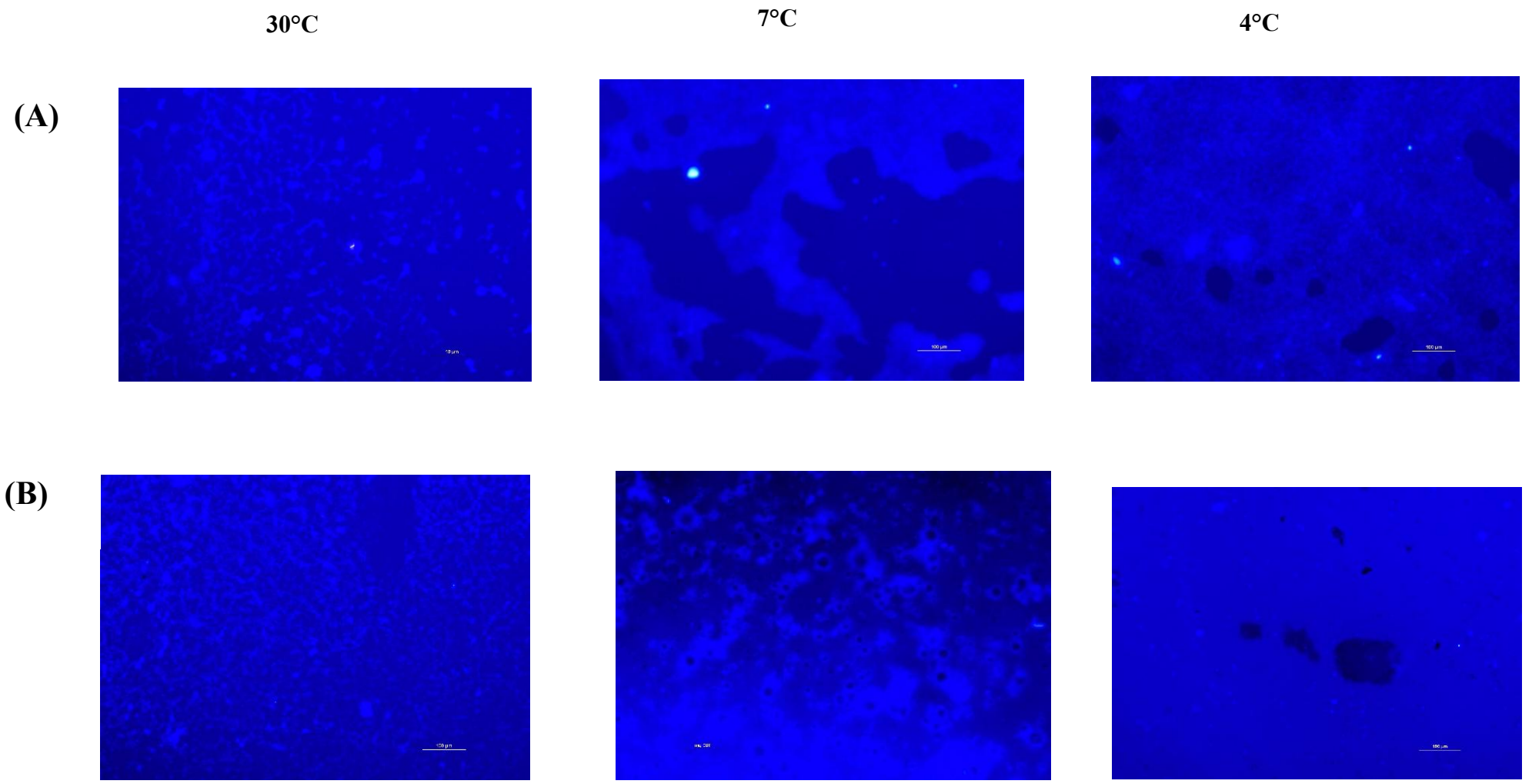

Figure 4.7.10: (A) Biofilms of 20SM on 24 h and (B) on the 14th day (Scale bar 100 µm) on the polystyrene surface.

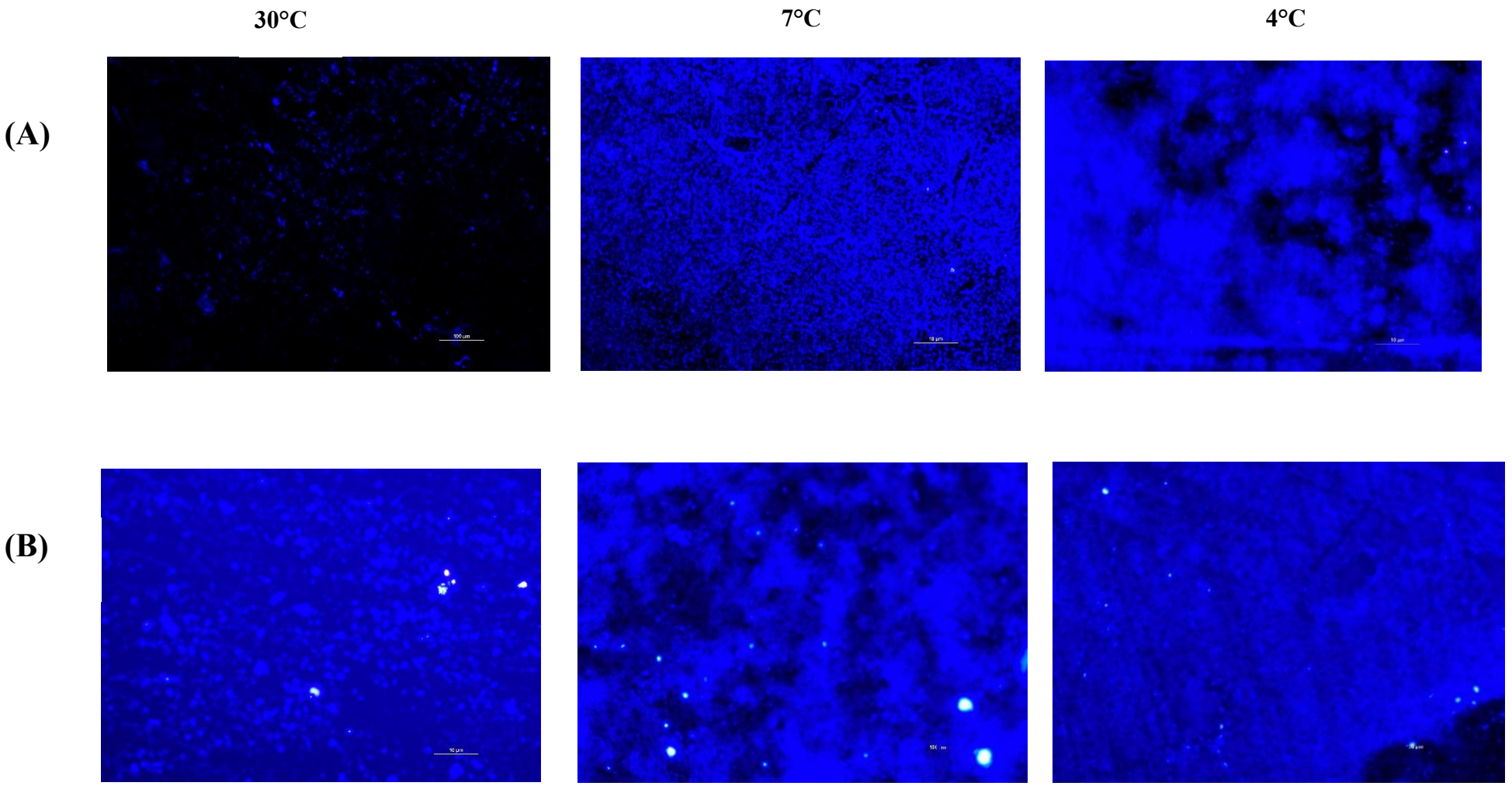

Figure 4.7.11: (A) Biofilms of 20SM on 24 h and (B) on the 14th day (Scale bar 100 µm) on the stainless-steel surface.

Chapter 5 Air-Liquid Interface Biofilm Formation of Pseudomonads.

Preface to Chapter 5

In Chapter 4, the biofilm EPS composition of two strong biofilm-forming isolates was determined at ambient temperatures of 30ºC and cold storage temperatures of 7ºC and 4ºC. The biofilms formed under cold temperatures produced more EPS components such as polysaccharides, proteins, and eDNA. The composition of EPS between the two isolates varies, even though the biofilm formation characteristics are similar. In Chapter 5, the biofilms of psychrotrophic pseudomonads were grown in a CDC reactor that allows for studying under turbulent conditions and a continuous supply of nutrients that more closely simulates a food manufacturing plant. The air-liquid interface was introduced by lifting the coupon holders, which resulted in air-liquid interface biofilm formation on the top coupons in the colder and two coupons with submerged biofilm formation. The difference in the cell counts, total polysaccharides in the EPS, the biofilm architecture, and EPS-producing genes was compared between the air-liquid interface and submerged coupons.

5.1 Introduction

Pseudomonads are common contaminants in the dairy industry, which cause spoilage by producing thermostable enzymes (Raposo et al., 2016). Pseudomonads are known for their ability to form denser biofilms at psychrotrophic temperatures (Liu et al., 2023). Pseudomonads are strong EPS (extracellular polymeric substances) producers (Wickramasinghe et al., 2020), and the EPS produced is exploitable as a public good by other weak EPS producers and pathogens (Puga et al.,2018). Pseudomonads produce large amounts of exopolysaccharides, and the biofilms of pseudomonads in the food industry are hard to remove. The EPS protects the biofilm cells from harsh sanitising and cleaning agents (Santos Rosado Castro et al., 2021).

Most of the biofilm formation studies with pseudomonads focus on the submerged biofilms (Liu et al., 2023; Wickramasinghe et al., 2020). In food industries, the air-liquid interface can be seen in tankers, silos, partly filled equipment, and stagnated water. It is important to study the biofilms at the air-liquid interface in an industrial context (Jha et al., 2020). The air-liquid interface biofilm formation is observed with pseudomonads, *Bacillus*, *E. coli*, *Vibrio*, and *Acinetobacter* (Martí et al., 2011; Hollenbeck et al., 2014). Access to both nutrients and oxygen facilitates the air-liquid interface biofilm formation (Ye et al., 2022). The interaction between the cellulose fibres, attachment factors, and lipopolysaccharides results in maintaining strong biofilms at the air-liquid interface identified in *P. fluorescens* SBW25 (Koza et al., 2009).

There are wide range of methods to study the biofilm formation, among those, the CDC biofilm reactor ®, developed by the researchers at the Centres for Disease Control and Prevention, is commonly used to study the biofilm formation and resistance to sanitizers (Mendez et al., 2020). The continuous exposure to shear stress and renewable nutrients directly mimics the natural environment or industrial conditions (Williams et al., 2019). In this study, the CDC biofilm reactor was used to generate both air-liquid interface and submerged biofilms in the same system. This system in this study closely mimics the dairy processing conditions, in terms of cold temperature, stainless-steel surface and continuous flow of nutrients.

This chapter explores the difference in the cell counts, total polysaccharides in the EPS, and biofilm architecture between the air-liquid interface (A-L) and submerged biofilms. This

study, for the first time, compared the gene expression difference of EPS producing genes between the air-liquid interface and submerged biofilms.

5.2 Materials and Methods

5.2.1 Bacterial isolates and Culture conditions

The two strong biofilm-forming isolates at cold temperatures, 3SM *(P. lundensis*) and 20SM (*P. cedrina*), and a weak biofilm-forming isolate, 44SM (*P. fluorescens*), were chosen for this study.

5.2.2 CDC reactor conditions

The CDC reactor was used to grow a week-old biofilm. The CDC biofilm reactor (CBR 90; Biosurface Technologies, USA) was used with stainless-steel coupons (304 grade with 2B finish with a total surface area of 2.26 cm^2). The coupons were passivated (cleaned with 50% nitric acid at 70°C for 30 min), sonicated for 30 min, cleaned with ethanol and Trigene, and autoclaved at 121°C. The reactor parts were assembled and autoclaved before use (reactor beaker, coupon holders, inlet and outlet tanks and connecting tubes). The entire CDC reactor was kept at 4°C. The growth media used were half-strength TSB (TSB, Difco™, Becton, Dickinson and Company, USA), which was filled in the inlet tank. The cultures were inoculated in TSB for 24 h to reach the OD_{600} of 0.05±0.15. Two percent (2%) of the overnight culture was added directly to the reactor beaker containing 400 mL of TSB (approximately 3 log CFU/mL). The flow rate of the reactor was set at 3.3 mL/min to achieve a mean residence time lower than the doubling time (Supplementary File 5.7) using a peristaltic pump. The coupon holders (Fig. 5.1) were lifted and supported about 2.5 cm to create the air-liquid interface on the top coupons (A-L), and the remaining two coupons were submerged (L1 and L2). The spent media were collected in the outlet tank (Kumar et al., 2021).

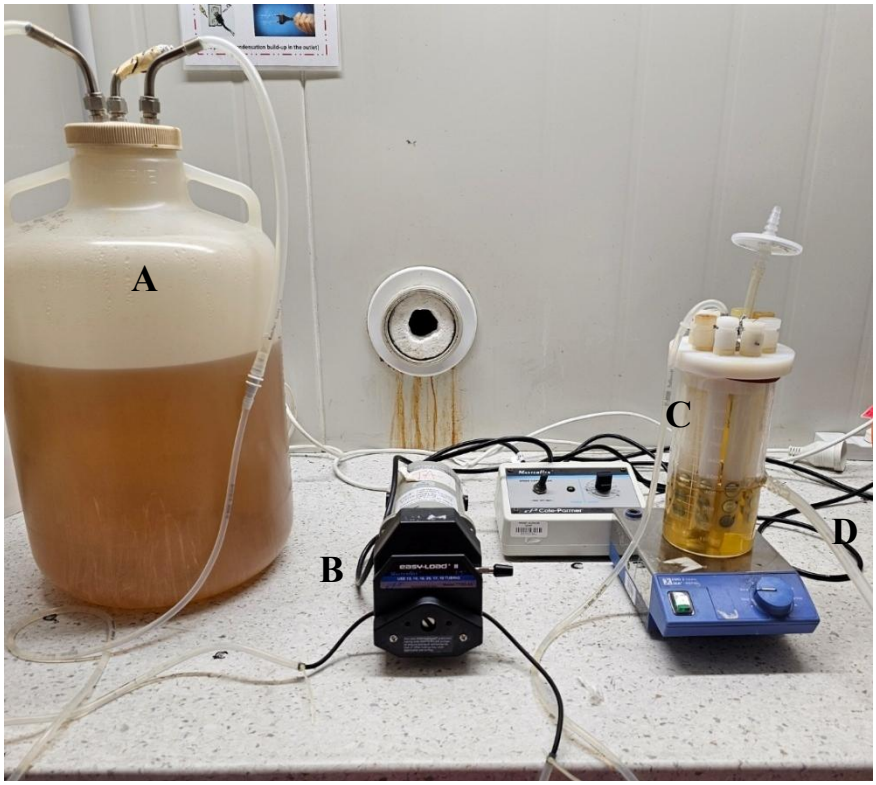

Figure 5.1 The CDC reactor setup in this study at 4ºC. The reactor parts are as follows: A- inlet tank, B- peristaltic pump, C- reactor beaker with coupons, and D- connecting pipe to outlet tank.

5.2.3 Enumeration of biofilm cells

The reactor was allowed to run for 168 h (The cell counts reached more than 7.5 log CFU/cm^2 in the continuous system, while in static, the same cell counts reached around 336 h (Chapter 4). The coupons containing holders were removed every 24 h, and a blank holder was replaced to maintain the turbulence. The removed coupons were washed with 0.85% physiological saline and transferred to the vials containing 900 µL of saline. After transferring the coupons, 1 g of sterile glass beads was added, and the vials were sonicated for 5 min. After sonication, the coupon-containing vials were mixed by vortex to remove the cells from the coupons. One hundred microlitres (100 µL) of the contents from the vials were serially diluted and plated on the TSA (TSA, Difco^{TM}, Becton, Dickinson and Company, USA) plates. The viable bacterial colonies were counted and expressed as log CFU/cm^2.

5.2.4 Quantification of Polysaccharides

After a week of incubation, the coupons containing biofilms were removed. Two coupons from the A-L, L1, and L2 coupons were added to a vial containing 2 mL of sterile distilled water. The vials containing coupons were sonicated for 30 min. After sonication, the contents were transferred to Eppendorf tubes. The Eppendorf tubes were centrifuged at 12000*g* for 5 min (Hettich, Mikro 220R, Germany). The supernatant was collected and filtered using a 0.2 µm syringe filter (Minisart, Sartorius, Germany). Two millilitres (2 mL) of the filtered supernatant were pooled into 15 mL of centrifuge tubes (Falcon®, Corning Incorporated, USA). These tubes were placed in a freeze-dryer. Total polysaccharides in the freeze-dried EPS were measured using the Phenol sulfuric acid method (DuBois et al., 1956) and D-glucose as a standard. The total polysaccharides were expressed as $\mu g/cm^2$.

5.2.5 Microscopic observations

After a week of biofilm formation, the coupons were observed under an epifluorescence (Nikon- Eclipse Ni-L, Nikon instruments, USA) microscope (Filter- TRITC) and SEM to view the biofilm architecture and the difference between the air-liquid interface coupons and submerged coupons. The SEM observations were done with JSM 6500F (Jeol, Australia) with 1000x and 5000x magnifications. The coupons were dried and carbon-coated before observing under SEM. Acridine orange (Acridine orange, BDH, England) was used for staining the coupons to view the cells and EPS under an epifluorescence microscope. The images were processed using NIS-elements D software (Version 6.02.01(Build 1955), Nikon Instruments, USA) (Muthuraman et al., 2025; Li et al., 2022).

5.2.6 Expression of EPS producing genes.

The overexpression of EPS genes such as *alg, pel*, and *psl* is responsible for the matrix overproduction at cold temperatures (Liu et al., 2023). In this present study, the difference in total polysaccharides and EPS quantity was observed between the air-liquid interface and submerged biofilms. It is important to analyse the differences in the gene expression of EPS genes to know the role of the air-liquid interface in the EPS overproduction. To confirm this

algK, pslA, bcsA, and *pelD* genes were chosen (functions of these genes are listed in supplementary file 5.7.2).

5.2.6.1 Isolation of biofilm cells

The coupons were removed after 168 h of incubation. Eight coupons for each A-L and L biofilm were added to the vials containing 4 mL of sterile distilled water and 1g of glass beads. The contents were transferred into four 1 mL Eppendorf tubes. The tubes were centrifuged at 12000 *g* for 5 min at 4ºC. The supernatant was discarded, and the cell pellets were collected and added to a single Eppendorf tube. Planktonic cultures grown at 4ºC for 18 h were centrifuged at 12000 *g* for 5 min at 4ºC to collect the cell pellets.

5.2.6.2 RNA extraction

The RNA was extracted using the Nucleospin RNA plus kit (with gDNA removal column) (Machery-Nagel, Germany) according to the manufacturer's instructions. The cell pellets were lysed with lysis buffer, washed, and isolated in sterile RNase-free water. The concentrations and purity were checked using a Genovonano spectrophotometer.

5.2.6.3 Real-time -quantitative PCR(RT-qPCR)

Real-time quantitative PCR was performed using the Light Cycler 480 (Roche Diagnostics, USA) to analyse the difference in EPS producing gene expression between the air-liquid interface and submerged biofilm cells. The primers used in this study are listed in the Table. The qPCR was performed using the Luna ® Universal One-step RT-qPCR kit (New England Biolabs, USA) according to the manufacturer's instructions. The cycling conditions were as follows: reverse transcription of RNA to cDNA at 55°C for 10 min, followed by initial denaturation at 95°C for 1 min; the amplification was performed with 40 cycles of denaturation at 95°C for 10 s, annealing at 60°C for 20 s, and extension at 60°C for 30 s.

RT-qPCR results are influenced by the differences in the nucleic acid extraction efficiency. Normalisation with internal housekeeping genes was done to reduce this variability. However, the absence of an exogenous internal standard remains a potential bias in relative gene expression measurements.

Table 5.1: Primers used for quantification of EPS producing genes

Gene	Sequence	Product Size (Bp)	Reference
pelD	F 5′-AAGAACGGATGGCTGAAGG-3′ R 5′-TTCCTCACCTCGGTCTCG-3’	250	(Ghafoor et al., 2013)
pslA	F 5’-ATCAATATCCGCTCCACGC-3’ R 5’-CTGCTGCTCTTCCCCCAGT-3’	140	(Liu et al., 2023)
bcsA	F 5’-GATTTTCGACTGCGACCACGTS- 3’ R 5’- ACATGTCGTTRCCRTCCTGCAC- 3’	150	(Gao et al., 2017)
algK	F 5’ -ATGCCTATGTATTCAGCCAAC-3’ R 5’-ATTCCTCGCCGTCTTCTTC-3’	200	(Liu et al., 2023)
16S rRNA	F: 5’- GCCCCTGGACAAAGACTGAC-3’ R: 5’CATGGTTTACGGCGTGGACTACC-3’	90	(Liu et al., 2023)

5.3 Results

5.3.1 Visible biofilm formation

The visible biofilm formation on the CDC reactor coupons was observed from 24 h. At 24 h, no visible biofilms were seen in all three coupons. After 48h, a thin visible line appeared on the air-liquid interface. At the end of 72 h, thick visible biofilms were observed on the A-L coupons, and visible aggregates started to form on L1 coupons. At the end of 144 h, compared to submerged coupons, the A-L coupons showed more dense visible biofilms (Fig. 5.2).

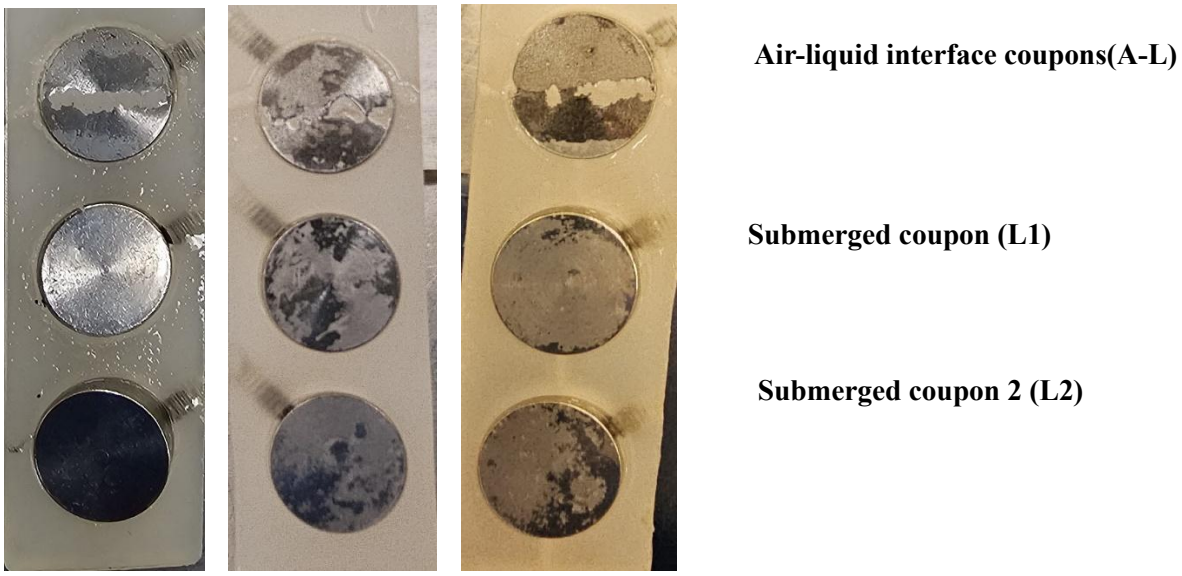

Figure 5.2 The visible biofilm formation of isolate 3SM observed on A-L, L1, and L2 coupons at 168 h at 4ºC.

5.3.2 Biofilm cell enumeration

The isolates 3SM and 20SM were allowed to form biofilms on the CDC reactor coupons with half-strength TSB. The growth was monitored every 24 h until 168 h (Fig. 5.3). At 24 h, the cell counts from the A-L coupons were around 3.20 log CFU/cm^2 for both isolates. The L1 coupon also got similar cell counts at 24 h. From 48 h, the A-L coupons dominated in terms of cell counts compared to L1 and L2. This trend continued until the end of 168 h. At 168 h, the cell counts from the A-L coupons were around 7.26 and 7.47 log CFU/cm^2 for isolates 3SM and 20SM. At 168 h, the A-L coupons showed significantly higher cell counts ($p < 0.05$) compared to L1 and L2 coupons (Fig. 5.3).

(A)

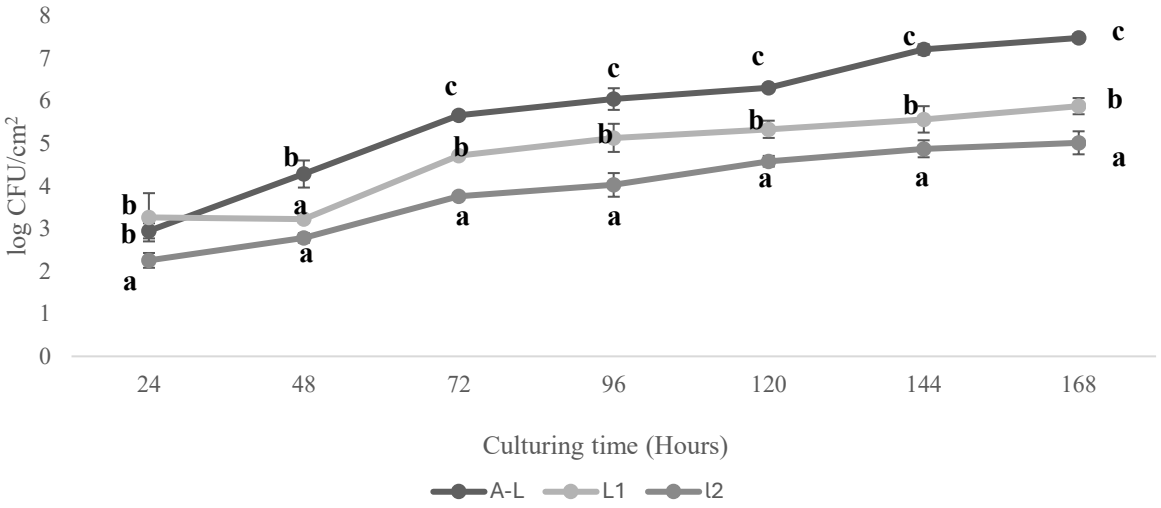

(B)

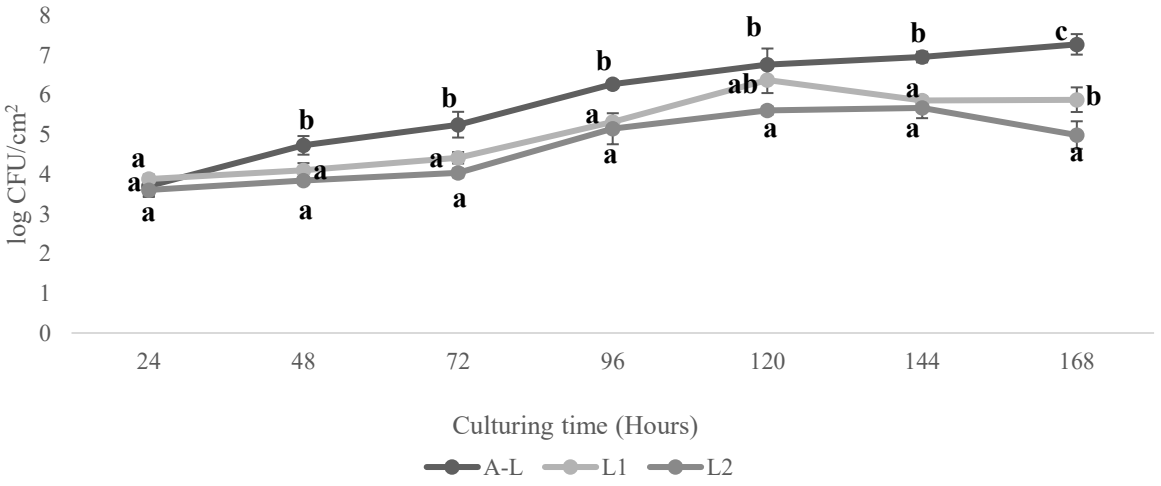

Figure 5.3 Graph A shows the cell counts from isolate 3SM over seven days. Graph B shows the cell counts from isolate 20SM. Different letters indicate significant differences ($p < 0.05$).

5.3.3 Quantification of the polysaccharides

The EPS recovered from the A-L coupons was significantly ($p < 0.05$) higher than the L1 and L2 coupons (Fig. 5.4 A). The total polysaccharides were also significantly higher ($p < 0.05$) in the biofilms formed at the A-L coupons compared to the L1 and L2 coupons (Fig. 5.4 B). This indicates the importance of the air-liquid interface in EPS production by psychrotrophic pseudomonads.

(A)

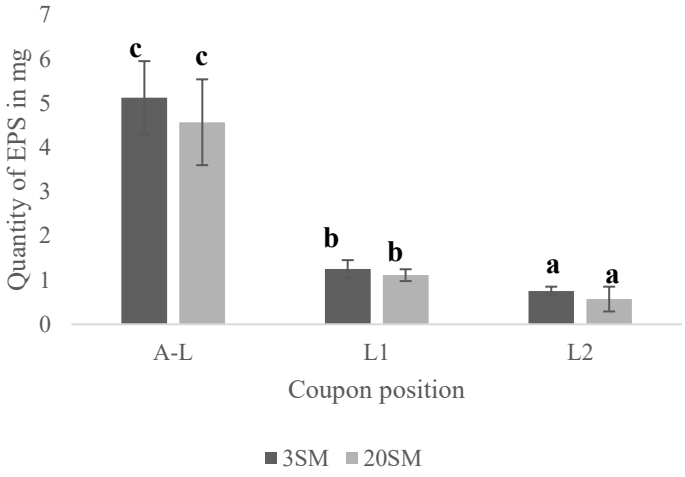

(B)

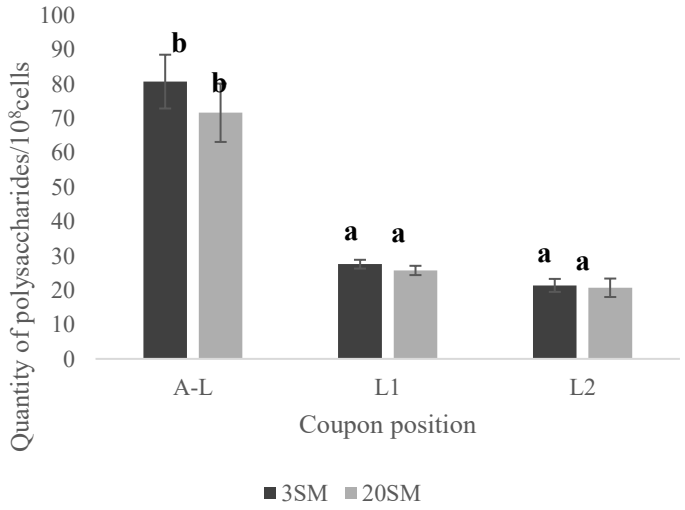

Figure 5.4 Graph A shows the quantity of EPS recovered from the A-L, L1, and L2 coupons. Graph B shows the total polysaccharides from the isolated EPS recovered from A-L, L1, and L2 coupons. Different letters indicate significant differences ($p < 0.05$).

5.3.4 Microscopic observations

With SEM observations, the biofilms produced by pseudomonads appeared as cells tightly packed together. The biofilms grown on the A-L coupons showed layers of biofilm cells; on the L1 and L2 coupons, the stainless-steel surface was often seen between cell clusters. This observation agreed with the cell counts as the biofilms grown on A-L coupons showed more cells than the L1 and L2 coupons (Fig. 5.6 A and B). With the epifluorescence microscopy, the cells on the A-L coupons were tightly packed and emitted more fluorescence compared to the L1 and L2 coupons. Filamentous cells were present in all three coupons (Fig. 5.5 A and B).

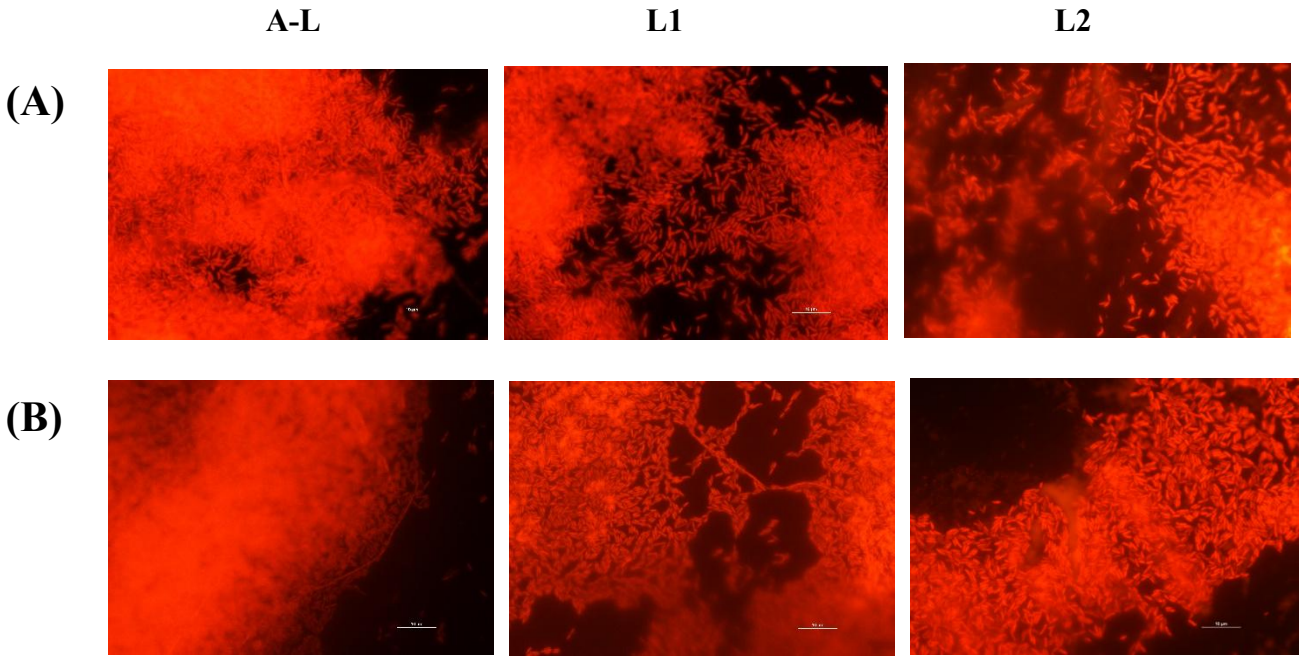

Figure 5.5: Epifluorescence microscopic images of (A) Isolate 3SM at the end of 168 h, (B) Isolate 20SM at the end of 168 h (Scale bar 10µm).

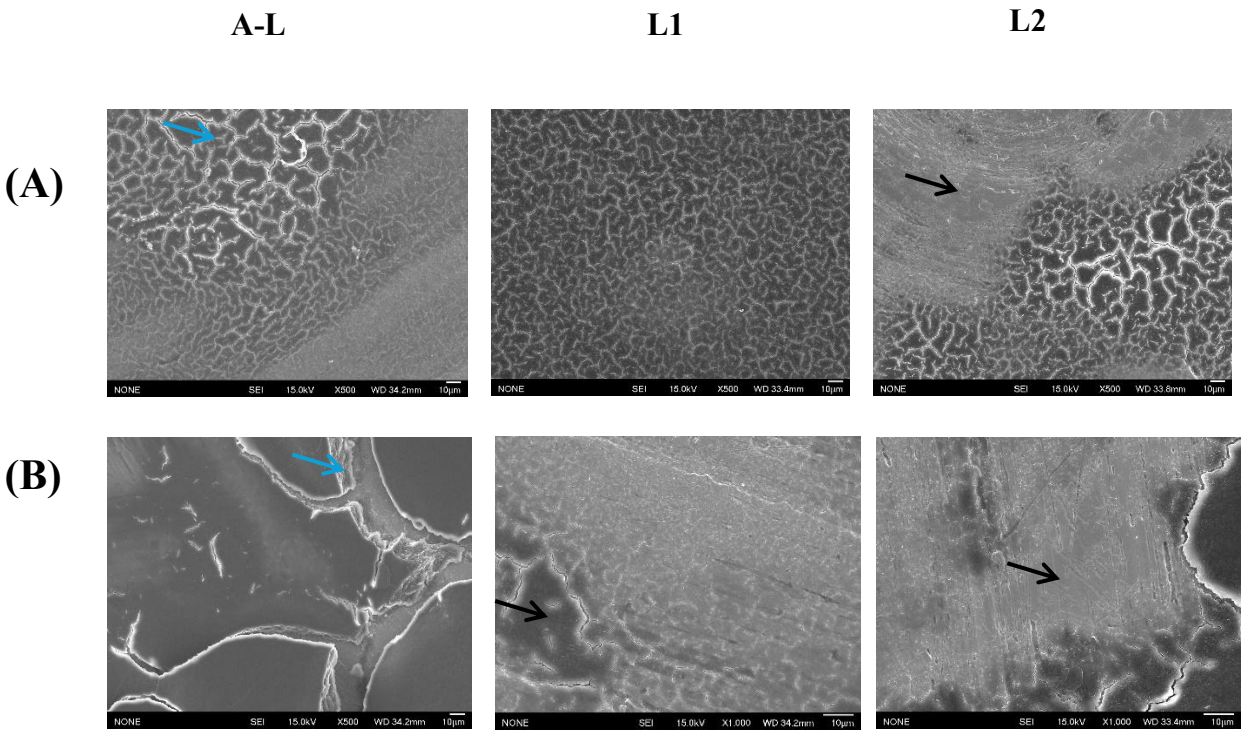

Figure 5.6 SEM images of (A) Isolate 3SM at the end of 168 h, (B) Isolate 20SM at the end of 168 h (Scale bar 10µm). Blue arrows show the layers of cells present in the air-liquid interface, and black arrows show the stainless-steel surface in the L1 and L2 coupons.

5.3.5 Expression of EPS producing genes.

The RNA extracted from L2 was lower and not sufficient for qPCR. Four EPS producing genes were compared between the A-L and L1 biofilm cells (Fig. 5.7). The capsular polysaccharide alginate-producing genes (*algK*) were highly expressed in the A-L biofilm cells. The aggregative polysaccharide cellulose-producing genes (*bcsA*) were also highly expressed in the air-liquid interface biofilm cells. There was no significant ($p > 0.05$) difference between the expression of another aggregative polysaccharide-producing gene, *pelD*, between the air-liquid interface biofilm cells and submerged biofilm cells. The *pslA*-producing genes were highly expressed in the air-liquid biofilm cells. However, the expression of *algK* and *bcsA* was significantly ($p < 0.05$) higher than *pslA*.

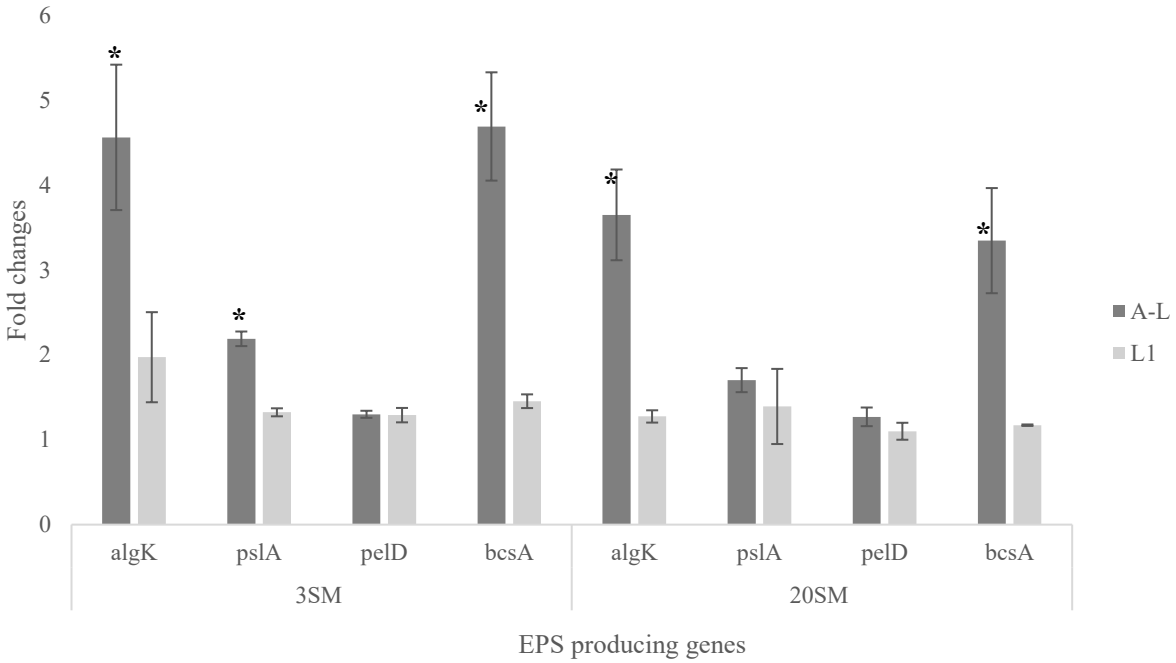

Figure 5.7 Gene expression differences in EPS producing genes between air-liquid interface and submerged biofilm cells. "*" indicates significant differences ($p < 0.05$).

5.4 Discussion

When *P. aeruginosa* biofilms are grown in a CDC reactor, the coupon position does not affect cell counts (Buckner et al., 2024). However, when the air-liquid interface was included, the cell counts were higher at the air-liquid interface coupons than at the submerged coupons. The A-L coupon attracted more cells compared with the L1 and L2. The difference between cell concentrations across the interfaces might be the differential concentrations of oxygen. The mechanism that controls the bacterial movement to the air is known as aero taxis. The aero taxis of *P. fluorescens* SBW25 (wrinkly spreaders) can reach higher oxygen microcosms using flagella-mediated swimming under a static system (Jerdan et al., 2019). In this present study, even with the continuous nutrient supply and under turbulence, the bacterial cells can still reach and colonise at the air-liquid interface and appear as a favourable niche. In published work on *B. cereus*, the air-liquid interface on stainless-steel surface produced cell counts (5.3 to 6.3 log CFU/cm^2) significantly ($p < 0.05$) higher than the submerged biofilms (4.2 log CFU/cm^2) (Wijman et al.,2007). In this present study on *Pseudomonas* spp., the A-L coupons showed significantly ($p < 0.05$) higher cell counts than submerged coupons (L1 and L2).

However, in this case the L1 and L2 coupons had the same number of cells in their biofilms. The cell concentration difference between L1 and L2 interfaces is not well understood.

This present study showed that the CDC biofilm reactor can be used to grow air-liquid interface biofilms under a continuous flow of nutrients. An air-liquid interface biofilm provides air and nutrients and encourages biofilm formation. An air-liquid interface is commonly seen in food industries in partly filled silos, vats, balance tanks, stagnant water, etc (Jha et al., 2020). It is important to study the CIP and sanitizers based on the air-liquid interface. This present study compared the cell counts and EPS quantification between the air-liquid interface coupons and submerged coupons. Compared to the submerged coupons, the air-liquid interface coupons contained more cells and EPS, representing a favourable niche for persistent biofilms during industrial processing and transport. Not only pseudomonads, but other bacteria such as *Bacillus* spp. can form air-liquid interface biofilms (Ren et al., 2024). In this present study, thick biofilm formation was observed on the coupons at the air-liquid interface compared to the submerged coupons.

In the work of Ren et al. (2024), the semi-submerged coupons showed significantly higher cell counts of *B. cereus* in both UHT milk and BHI media than in fully submerged coupons. The EPS produced is higher in the semi-submerged coupons due to the gas-liquid interface (Ren et al., 2024). In this present study, the quantity of isolated EPS and the total polysaccharides for *Pseudomonas* spp. were also higher in the A-L coupons compared to L1 and L2. This indicates the possibility of pseudomonads producing air-liquid interface biofilms with higher EPS in storage tanks and silos that are refrigerated and run under turbulent flow.

The aerotaxis mechanism needs no energy, and the energy is utilised to secrete higher EPS components (Jerdan et al., 2019). Higher EPS and polysaccharide production at the A-L coupons were observed in the present study. This study, for the first time, compared the gene expression between the air-liquid interface and submerged biofilm cells. Studies found that the EPS producing genes in pseudomonads, such as *algK* and *pslA,* are highly expressed at 4ºC, compared to 25ºC (Liu et al., 2023; Vásquez-Ponce et al., 2017). In this present study, although both biofilm cells were grown at 4ºC, there was a difference in the expression of EPS producing genes. The *algK*, *pslA*, and *bcsA* were highly expressed in air-liquid interface biofilm cells compared to submerged biofilm cells, indicating the possible EPS overproduction at the air-liquid interface. Overproduction of EPS often leads to difficulty in

cleaning and removal of these biofilms. There was no difference between the expression of *pelD* genes. Pellicle formation of these isolates was observed under static conditions (Data not shown). The higher expression of EPS genes at the air-liquid interface in this study confirms the findings of Jerden et al. (2019). In the CDC reactor, the pellicle formation was not observed. Comparing the *pelD* gene expression between the static and continuous systems is needed.

5.5 Conclusion

This chapter explored the difference between the air-liquid interface and submerged coupons. Introducing the air-liquid interface in the CDC reactor caused significantly ($p < 0.05$) higher cell numbers and EPS in the air-liquid interface biofilms compared to the submerged biofilms. The *algK* and *bcsA* genes were highly expressed in the air-liquid interface biofilm cells. Studying the biofilms at the air-liquid interface is important from an industrial point of view.

5.6 References

Buckner, E., Buckingham-Meyer, K., Miller, L. A., Parker, A. E., Jones, C. J., & Goeres, D. M. (2024). Coupon position does not affect *Pseudomonas aeruginosa* and Staphylococcus aureus biofilm densities in the CDC biofilm reactor. *Journal of Microbiological Methods*, *223*, 106960. https://doi.org/10.1016/j.mimet.2024.106960.

DuBois, Michel., Gilles, K. A., Hamilton, J. K., Rebers, P. A., & Smith, Fred. (1956). Colorimetric Method for Determination of Sugars and Related Substances. *Analytical Chemistry*, *28*(3), 350–356. https://doi.org/10.1021/ac60111a017.

Gao, J., Li, P., Du, X., Han, Z., Xue, R., Liang, B., & Wang, S. (2017). A Negative Regulator of Cellulose Biosynthesis, bcsR, Affects Biofilm Formation, and Adhesion/Invasion Ability of *Cronobacter sakazakii. Frontiers in Microbiology*, *8*, 1839. https://doi.org/10.3389/fmicb.2017.01839.

Ghafoor, A., Jordens, Z., & Rehm, B. H. A. (2013). Role of PelF in Pel Polysaccharide Biosynthesis in *Pseudomonas aeruginosa. Applied and Environmental Microbiology*, *79*(9), 2968–2978. https://doi.org/10.1128/AEM.03666-12.

Hollenbeck, E. C., Fong, J. C. N., Lim, J. Y., Yildiz, F. H., Fuller, G. G., & Cegelski, L. (2014). Molecular Determinants of Mechanical Properties of *V. cholerae* Biofilms at the Air-Liquid Interface. *Biophysical Journal*, *107*(10), 2245–2252. https://doi.org/10.1016/j.bpj.2014.10.015.

Jha, P. K., Dallagi, H., Richard, E., Benezech, T., & Faille, C. (2020). Formation and resistance to cleaning of biofilms at air-liquid-wall interface. Influence of bacterial strain and material. *Food Control*, *118*, 107384. https://doi.org/10.1016/j.foodcont.2020.107384.

Koza, A., Hallett, P. D., Moon, C. D., & Spiers, A. J. (2009). Characterization of a novel air–liquid interface biofilm of *Pseudomonas fluorescens* SBW25. *Microbiology*, *155*(5), 1397–1406. https://doi.org/10.1099/mic.0.025064-0.

Kumar, M., Flint, S., Palmer, J., Chanapha, S., & Hall, C. (2021). Influence of Incubation Temperature and Total Dissolved Solids on Biofilm and Spore Formation by Dairy Isolates of *Geobacillus stearothermophilus*. *Applied and Environmental Microbiology*, *87*(8), e02311-20. https://doi.org/10.1128/AEM.02311-20.

Li, Y., Wang, H., Zheng, X., Li, Z., Wang, M., Luo, K., Zhang, C., Xia, X., Wang, Y., & Shi, C. (2022). Didecyldimethylammonium bromide: Application to control biofilms of *Staphylococcus aureus* and *Pseudomonas aeruginosa* alone and in combination with slightly acidic electrolyzed water. *Food Research International*, *157*, 111236. https://doi.org/10.1016/j.foodres.2022.111236.

Liu, J., Wu, S., Feng, L., Wu, Y., & Zhu, J. (2023). Extracellular matrix affects mature biofilm and stress resistance of psychrotrophic spoilage *Pseudomonas* at cold temperature. *Food Microbiology*, *112*, 104214. https://doi.org/10.1016/j.fm.2023.104214.

Martí, S., Rodríguez-Baño, J., Catel-Ferreira, M., Jouenne, T., Vila, J., Seifert, H., & Dé, E. (2011). Biofilm formation at the solid-liquid and air-liquid interfaces by *Acinetobacter* species. *BMC Research Notes*, *4*(1), 5. https://doi.org/10.1186/1756-0500-4-5.

Prabhukhot, G. S., Eggleton, C. D., Kim, M., & Patel, J. (2024). Impact of surface topography and hydrodynamic flow conditions on single and multispecies biofilm formation by *Escherichia coli* O157:H7 and *Listeria monocytogenes* in presence of promotor bacteria. *LWT*, *201*, 116240. https://doi.org/10.1016/j.lwt.2024.116240.

Puga, C. H., Dahdouh, E., SanJose, C., & Orgaz, B. (2018). *Listeria monocytogenes* Colonizes *Pseudomonas fluorescens* Biofilms and Induces Matrix Over-Production. *Frontiers in Microbiology*, *9*, 1706. https://doi.org/10.3389/fmicb.2018.01706

Raposo, A., Pérez, E., De Faria, C. T., Ferrús, M. A., & Carrascosa, C. (2016). Food Spoilage by *Pseudomonas* spp.—An Overview. In O. V. Singh (Ed.), *Foodborne Pathogens and Antibiotic Resistance* (1st ed., pp. 41–71). Wiley. https://doi.org/10.1002/9781119139188.ch3.

Ren, F., Chen, Y., Yang, S., Zhang, Y., Liu, Y., Ma, Y., Wang, Y., Liu, Y., Dong, Q., & Lu, D. (2024). Characterization of emetic *Bacillus cereus* biofilm formation and cereulide production in biofilm. *Food Research International*, *192*, 114834. https://doi.org/10.1016/j.foodres.2024.114834

Santos Rosado Castro, M., Da Silva Fernandes, M., Kabuki, D. Y., & Kuaye, A. Y. (2021). Modelling *Pseudomonas fluorescens* and *Pseudomonas aeruginosa* biofilm formation on stainless steel surfaces and controlling through sanitisers. *International Dairy Journal*, *114*, 104945. https://doi.org/10.1016/j.idairyj.2020.104945.

Vásquez-Ponce, F., Higuera-Llantén, S., Pavlov, M. S., Ramírez-Orellana, R., Marshall, S. H., & Olivares-Pacheco, J. (2017). Alginate overproduction and biofilm formation by psychrotolerant *Pseudomonas mandelii* depend on temperature in Antarctic marine sediments. *Electronic Journal of Biotechnology*, *28*, 27–34. https://doi.org/10.1016/j.ejbt.2017.05.001

Wickramasinghe, N. N., Hlaing, M. M., Ravensdale, J. T., Coorey, R., Chandry, P. S., & Dykes, G. A. (2020). Characterization of the biofilm matrix composition of psychrotrophic, meat spoilage pseudomonads. *Scientific Reports*, *10*(1), 16457. https://doi.org/10.1038/s41598-020-73612-0.

Wijman, J. G., de Leeuw, P. P., Moezelaar, R., Zwietering, M. H., & Abee, T. (2007). Air-liquid interface biofilms of *Bacillus cereus*: formation, sporulation, and dispersion. *Applied and environmental microbiology*, *73*(5), 1481-1488.

Ye, Z., Silva, D. M., Traini, D., Young, P., Cheng, S., & Ong, H. X. (2022). An adaptable microreactor to investigate the influence of interfaces on *Pseudomonas aeruginosa* biofilm growth. *Applied Microbiology and Biotechnology*, *106*(3), 1067–1077. https://doi.org/10.1007/s00253-021-11746-5.

Mendez, E., Walker, D. K., Vipham, J., & Trinetta, V. (2020). The use of a CDC biofilm reactor to grow multi-strain Listeria monocytogenes biofilm. *Food Microbiology*, *92*, 103592. https://doi.org/10.1016/j.fm.2020.103592

Williams, D. L., Smith, S. R., Peterson, B. R., Allyn, G., Cadenas, L., Epperson, R. T., & Looper, R. E. (2019). Growth substrate may influence biofilm susceptibility to antibiotics. *PLOS ONE*, *14*(3), e0206774. https://doi.org/10.1371/journal.pone.0206774.

Jerdan, R., Kuśmierska, A., Petric, M., & Spiers, A. J. (2019). Penetrating the air–liquid interface is the key to colonization and wrinkly spreader fitness. *Microbiology*, *165*(10), 1061–1074. https://doi.org/10.1099/mic.0.000844.

5.7 Supplementary Information

5.7.1 Doubling time and flow rate

Doubling time of pseudomonads grown in half-strength TSB.

Isolate	Doubling time at 4°C (min)	Flow rate (mL/ min)
3SM	94.25	3.3
20SM	88.57	3.3

5.7.2 EPS producing genes in this study and their functions

EPS producing genes	Functions
pelD	Pellicle formation and aggregation of cells
pslA	Polysaccharide synthesis locus – Biofilm architecture
bcsA	Bacterial cellulose synthesis- Cellulose production and air-liquid interface biofilm formation.
algK	Alginate production -Biofilm stability and architecture
16S rRNA	Housekeeping gene

Chapter 6 Cleaning with NaOH, Footprints and Regrowth

This chapter is an adaptation of material that was published as a peer-reviewed article:

Muthuraman, S., Palmer, J., & Flint, S. (2026). Air-liquid interface biofilm formation of pseudomonads and the impact of traditional clean-in-place on biofilm removal. *Food Research International*, *226*, 118215. https://doi.org/10.1016/j.foodres.2025.118215.

Preface to Chapter 6

In Chapter 5, the difference between the air-liquid interface and submerged biofilms was analysed using cell counts, EPS quantification, microscopic observations, and gene expression. In Chapter 6, the biofilms of isolates 3SM and 20SM were treated with hot water and NaOH to study the biofilm footprints left after cleaning and their regrowth potential.

6.1 Introduction

Pseudomonads are psychrotrophic rods found in food processing environments. Pseudomonads produce thermostable enzymes and pigments that affect the food quality (Raposo et al., 2016). Pseudomonads form strong biofilms with robust EPS production at cold temperatures (Liu et al., 2023). Cellulose production in the pseudomonads is the reason behind the air-liquid interface biofilm formation (Spiers et al., 2003). The EPS of pseudomonads is made up of different polysaccharides, such as alginate, cellulose, Psl, and Pel (Mann & Wozniak, 2012). The interaction between the components in the EPS matrix keeps the biofilm architecture and integrity (Flemming & Wingender, 2010). EPS produced by pseudomonads is hard to remove due to its complex nature (Da Cruz Nizer et al., 2024). This EPS protects the cells from adverse conditions and antimicrobials.

The term “footprint” was used in the past to describe the polymeric material left on the surface after the bacterial cells are removed by shear forces or enzymes (Neu & Marshall, 1991). The bacterial cells are removed carefully from the surface, and the remaining adhesive polymers are observed with TEM and SEM, revealing that the footprint material on the surface matches the size of the cells nearby, and some are shown as clumps after cell removal due to the hydrophobic properties (Neu & Marshall, 1991).

The clean-in-place (CIP) system is designed to remove the deposits on the interior surface of the equipment without dismantling (Tirpanci Sivri et al., 2023). The conventional CIP process includes water rinse, alkali cleaning with or without acid cleaning, and sanitation (Joseph et al., 2001). This study focused on a water rinse and alkali wash without acid cleaning. This is the first study on biofilm EPS footprints left by pseudomonads after cleaning. This involved forming air-liquid interface biofilms of psychrotrophic pseudomonads under a continuous flow of nutrients at cold temperatures. This study explored the potential of biofilm EPS footprints to enhance the biofilm formation of the same isolates and a weak biofilm-forming isolate.

6.2 Materials and Methods

6.2.1 Bacterial isolates and Culture conditions

The two strong biofilm-forming isolates at cold temperatures, 3SM *(P. lundensis*) and 20SM (*P. cedrina*), and a weak biofilm-forming isolate, 44SM (*P. fragi*) were chosen for this study.

6.2.2 CDC reactor conditions

Details were provided in Section 5.2.2, Chapter 5.

6.2.3 Enumeration of biofilm cells

Details were provided in Section 5.2.3, Chapter 5.

6.2.4 Cleaning -in- Place (ClP) system

Hot water at 55°C and 1% NaOH at 70°C represents the chemical treatments used in a typical CIP system. The water and NaOH were heated on a hot plate to reach the required temperatures. Sterile distilled water was used in this experiment to prepare NaOH. The inlet tube was inserted into the beakers containing CIP chemicals (hot water and NaOH), and the temperatures of the chemicals were confirmed before connecting to the CDC reactor. The entire CDC reactor was cleaned using 1.2 litres of water and circulated for at least 3 to 4 cycles at 300 rpm to reach a Reynolds number of more than 12000. After the water rinse, 2 holders were taken out for the cell counts, and two blank holders were inserted to maintain the flow. The same steps were followed for NaOH.

6.2.4.1 Reynolds Number

The flow of the CDC reactor in this study was turbulent (Table 6.1) based on the Reynolds number. The Reynolds number was calculated by

$Re = \upsilon D_h / \eta$

(Where υ is the hydrodynamic velocity (m/s), ρ is the density of the fluid, which is 998.23 Kg/m^3, η is the kinematic viscosity 1.0023E-06 m^2/s. D_h is calculated using the outer radius (R_o) of 0.03m and the inner radius of 0.0225m (R_i) (Prabhukhot et al., 2024).

Table 6.1 Reynolds number

RPM	Reynolds number	Function	Flow
125	4239	Biofilm growth	Turbulent
300	12215	CIP	Turbulent

6.2.5 Microscopic observations

Details were provided in Section 5.2.5, Chapter 5.

6.2.6 Attenuated Total Reflection – Fourier-transform infrared spectroscopy (ATR-FTIR)

Fourier-transform infrared spectroscopy (FTIR) generates direct information about the molecular and chemical composition of the biomolecules (Gieroba et al., 2020). FTIR observations can show the differences in the intensity and height of spectral peaks, but quantitative information is not possible with FTIR (Crisp et al., 2023). The EPS from untreated coupons and cleaned coupons was tested using ATR-FTIR analysis to observe the composition of footprints left after cleaning with water and NaOH. The EPS isolation protocol was described in Section 5.2.4, Chapter 5. The control coupon that had not been exposed to biofilm was used as a control and observed directly under FTIR (Nicolet™, Thermofisher Scientific™, USA). FTIR parameters were as follows: acquisition range 2000-400 cm^{-1}, scanning times of 32 s, and resolution of 4 cm^{-1} (Li et al., 2022).

6.2.7 Regrowth of the strong biofilm formers

After CIP, the reactor was treated with hot water at pasteurization temperature (72°C) for 2 min until it reached the reactor lid to enable the inactivation of any remaining cells. Four holders were removed from the CIP-cleaned reactor, and four holders containing clean coupons were inserted, and the holders were transferred to a new reactor beaker (Fig. 6.1).

This was allowed to run at a 3.3mL/min flow rate and 125 rpm with half-strength TSB for 24 h, and after 24 h, 2% inoculum (approximately 3 log CFU/mL cells) were added to check the biofilm formation differences between untreated clean coupons and CIP-treated coupons.

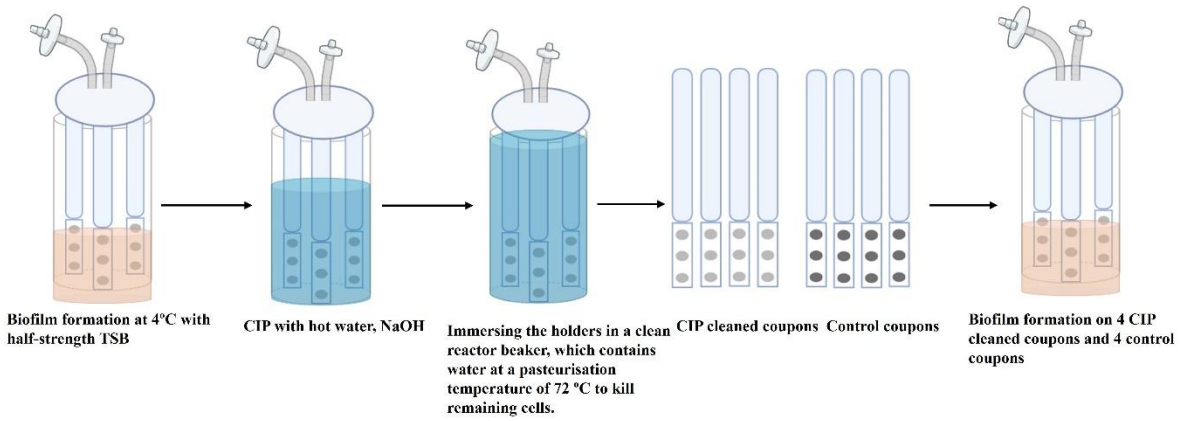

Figure 6.1 Schematic representation of the CIP process and regrowth.

6.2.8 Regrowth of the weak biofilm former

A weak biofilm former, 44SM, and a strong biofilm former, 3SM, were used in this experiment. The strong biofilm of the former 3SM was allowed to form biofilms in the CDC reactor. After a week, the CIP was done. Four CIP coupon-containing holders and four untreated clean coupons were inserted in a new CDC reactor beaker, and the weak biofilm former was inoculated at a concentration of 2% (approximately 3 log CFU/mL) of cells. The cell counts were compared between the untreated clean and CIP-cleaned coupons, and the effects of remaining EPS footprints on the biofilm formation of a weak biofilm former were analyzed.

6.2.9 Data analysis

All the experiments were performed with at least three biological and three technical replicates. One-way variance analysis (ANOVA) was generated to evaluate significant differences among the variables using Tukey's test, which had a p-value below 0.05 and was considered statistically significant. Data analysis was implemented using SPSS statistical software (Version 29.0.2.0; IBM®, USA). FTIR data were processed using Origin Pro software (Origin Pro 2025, 10.2 Origin Lab Corporation, USA).

6.3 Results

6.3.1 Cell counts after CIP

The coupons were taken out after circulating hot water and again after NaOH. Hot water at 55°C achieved around a log cell reduction in the biofilms formed by both isolates. With NaOH, the cell counts were below the detectable limit (1.7 log CFU/cm^2) for both isolates. Compared to hot water at 55°C, NaOH at 70ºC significantly ($p < 0.05$) killed the biofilm cells of psychrotrophic pseudomonads (Fig. 6.2).

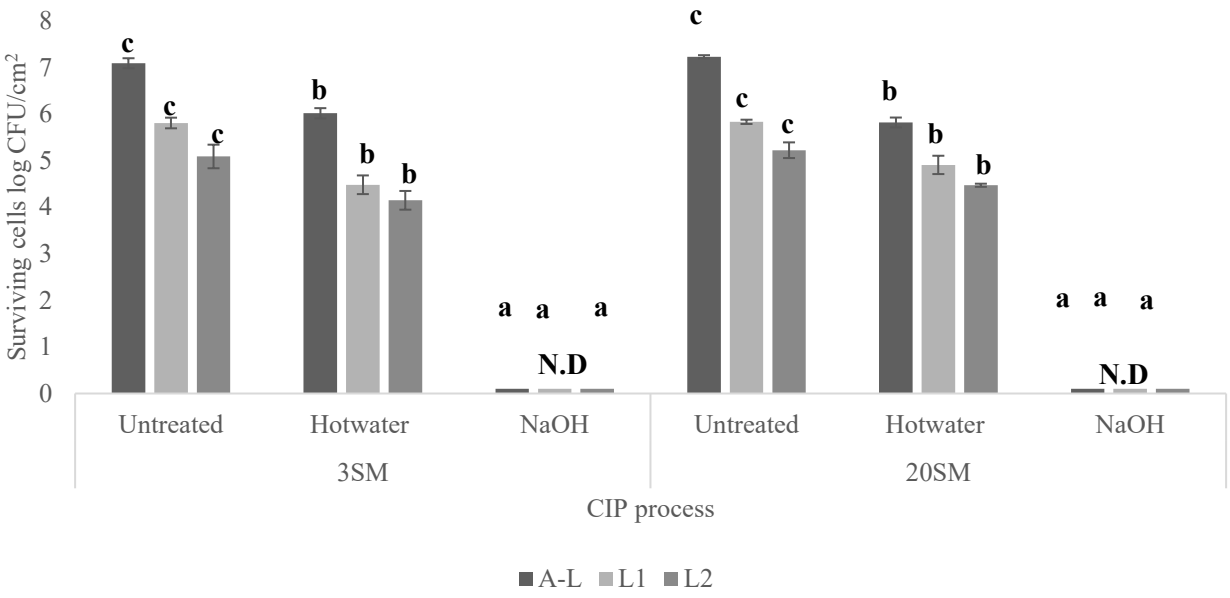

Figure 6.2 The cell counts from untreated control coupons, hot water-treated coupons (55ºC for 10 min), and NaOH-treated (70ºC for 10 min) coupons. Different letters indicate significant differences ($p < 0.05$).

6.3.2 Microscopic observations

6.3.2.1 Cleaning with 55°C water

With SEM observations, the hot water-treated coupon surfaces showed compromised upper layers on all the coupons. The cells could be seen, but not as clear as the control coupons. The biomass appeared to be smeared (Fig. 6 .3 C and D). Cell counts after hot water treatment (55ºC for 10 min) resulted in a one-log reduction. The cells after 55°C treatment stayed intact, which was confirmed by epifluorescence microscopic observations, which agreed with the cell counts (Fig. 6 .4 C and D).

6.3.2.2 Cleaning with 70°C NaOH

After introducing the NaOH to the CIP system, the coupons were free of cells, which was confirmed by the SEM observation. However, the coupons were not completely clean. NaOH crystals, along with organic matter, were present in the coupons. These were the biofilm footprints left after cleaning (Fig. 6.3 E and F). Compared to L1 and L2 coupons, the A-L coupons showed more organic materials left after cleaning. The cell counts were nondetectable (1.7 log CFU/cm^2) after cleaning with NaOH. While the acridine orange staining showed a dead and deformed mass on all three coupons (Fig. 6 .4 E and F).

A-L L1 L2

(A)

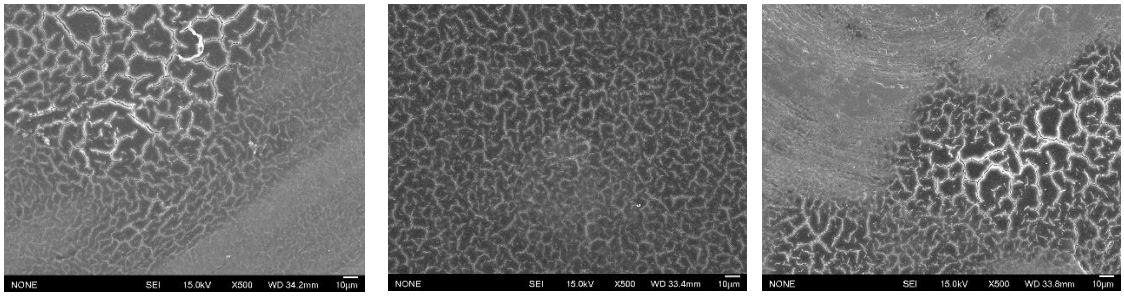

(B)

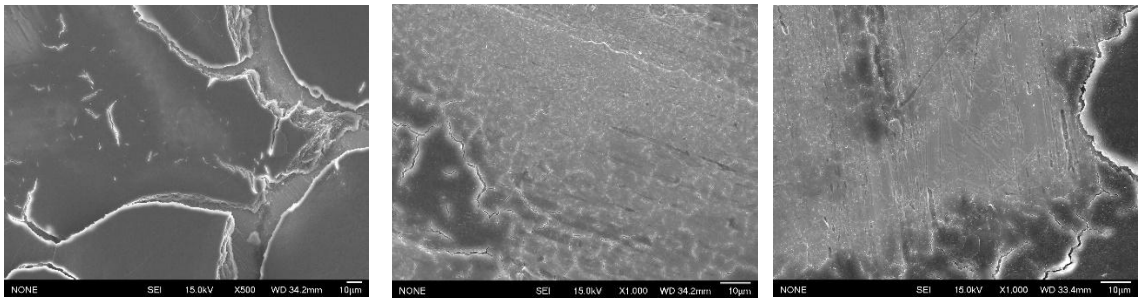

(C)

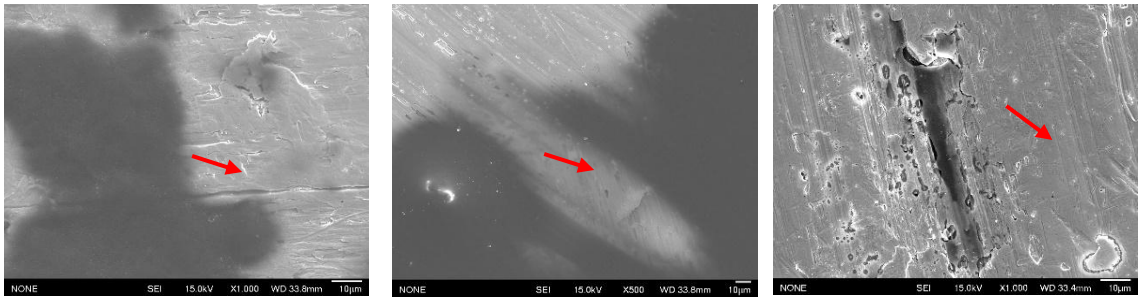

(D)

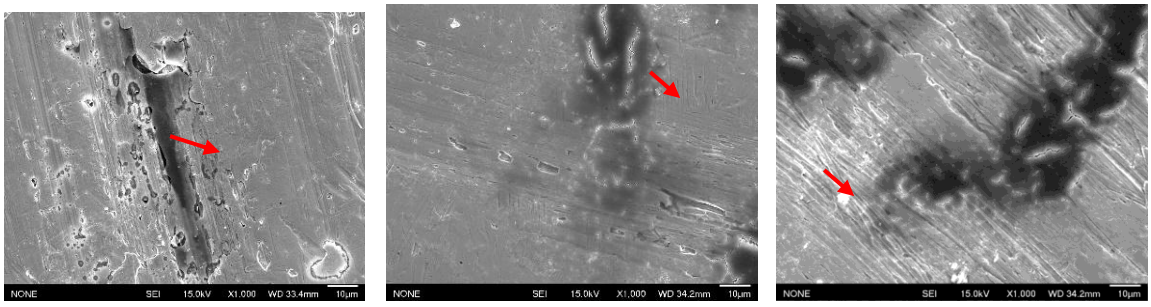

(E)

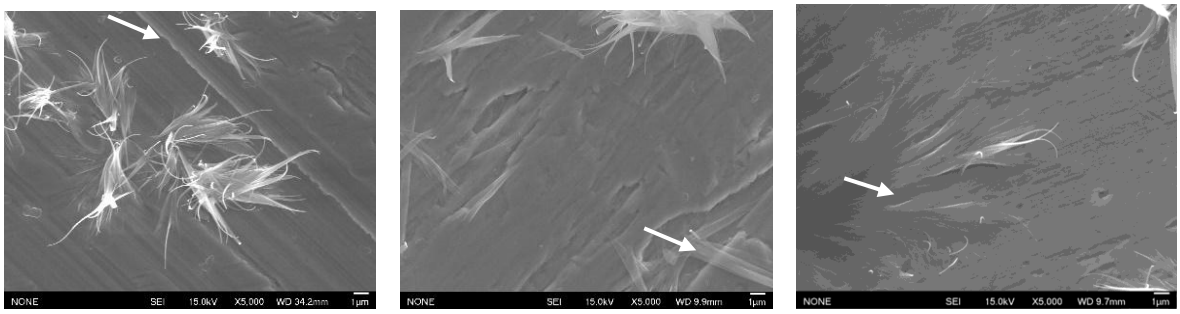

(F)

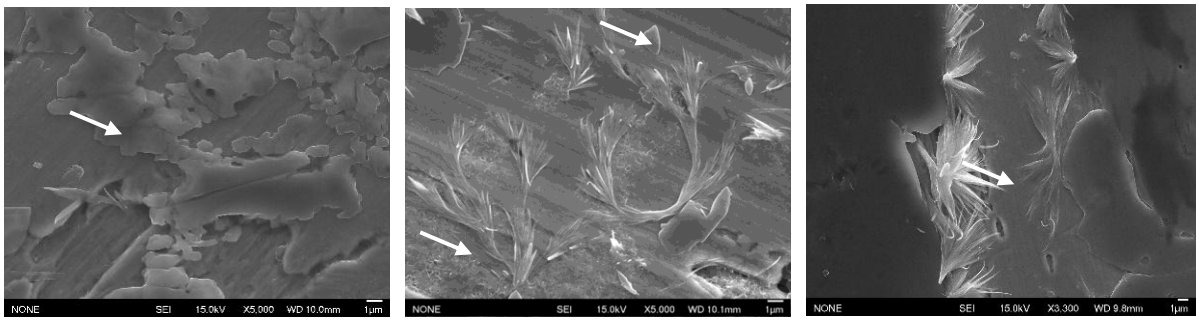

Figure 6.3 (A)& (B) SEM images of 3SM and 20SM untreated coupons, (C) & (D)SEM images of hot water-treated coupons of isolates 3SM and 20SM, and (D) & (F) SEM images of NaOH-treated coupons of isolates 3SM and 20SM. Red arrows indicate the compromised upper layer of cells after hot water treatment. White arrows indicate the biofilm footprints remaining after cleaning with hot water and NaOH.

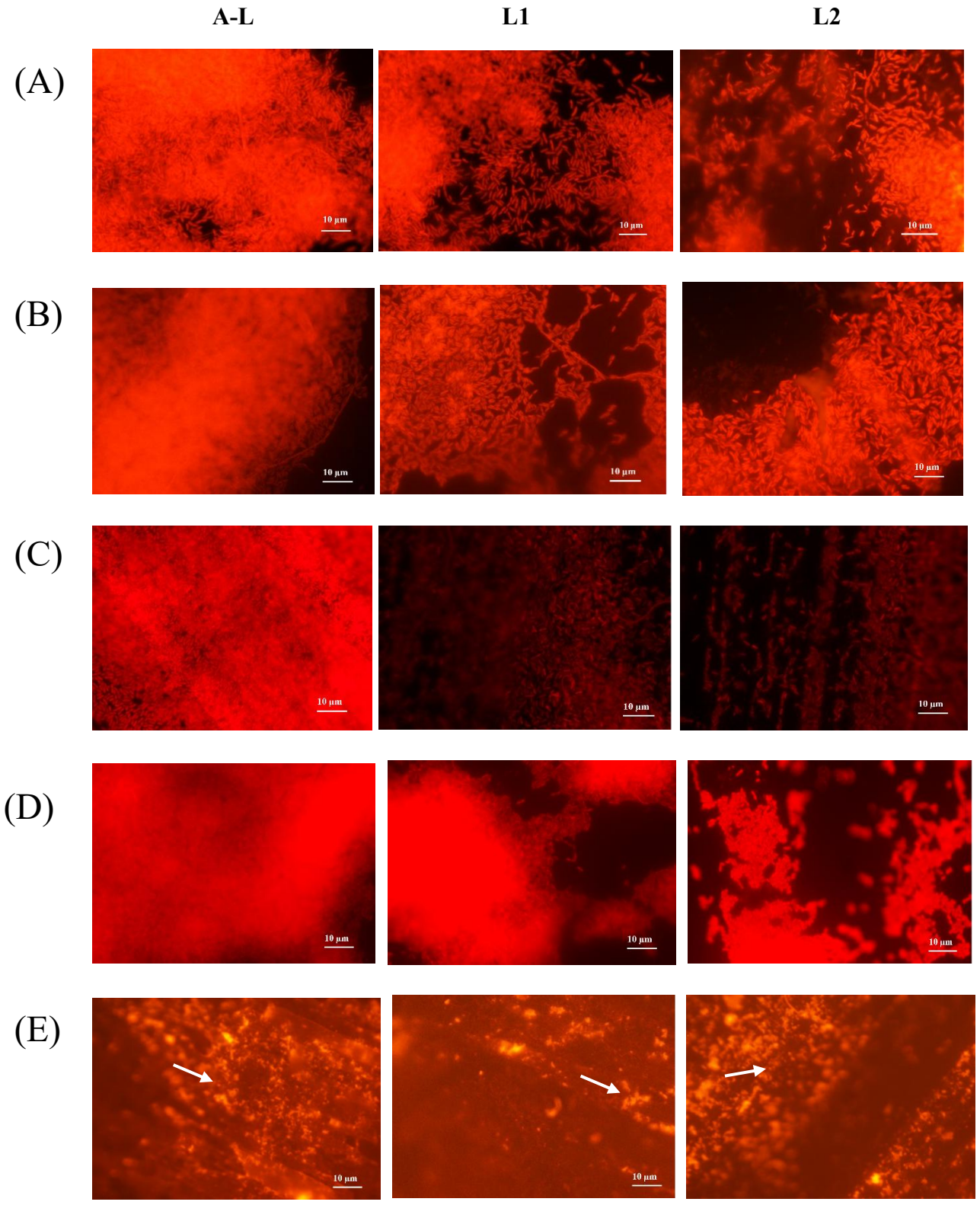
A-L
L1
L2
(A)
(B)
(C)
(D)
(E)
10 µm

(F)

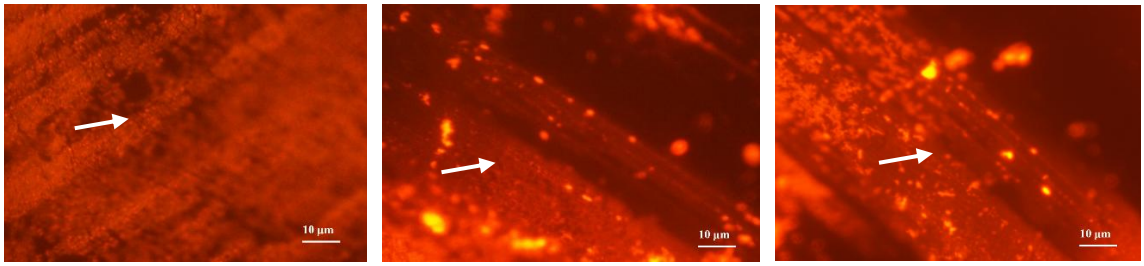

Figure 6.4 (A) & (B) epifluorescence microscopic images of 3SM and 20SM untreated coupons, (C) & (D) hot water-treated coupons of isolates 3SM and 20SM, and (E) & (F) NaOH-treated coupons of isolates 3SM and 20SM. White arrows indicate the dead and deforms cells with EPS footprints.

6.3.3 ATR-FTIR spectra on EPS isolated from untreated and cleaned coupons

The FTIR spectra for the untreated and CIP-cleaned coupons were compared to the coupon with no biofilms, which was used as a control. In the FTIR spectra, 1650 and 1540 cm-1 peaks represent the amide I and amide II bands of proteins, and 1055 cm-1 from polysaccharides (Fig. 6.5 A and B). Compared to the untreated EPS, the intensities of the respective peaks were decreased in EPS isolated from NaOH-treated coupons. With the hot water, the intensities did not decrease much; however, there were some changes in the peaks noticed. The two peaks around 1400 and 1600 cm^{-1} in the untreated EPS become inverted in the hot water-treated EPS. The CIP-cleaned coupon was not as clean as the sterile acid-cleaned stainless-steel coupon. The FTIR observation agreed with the remaining biofilm EPS footprints seen in SEM.

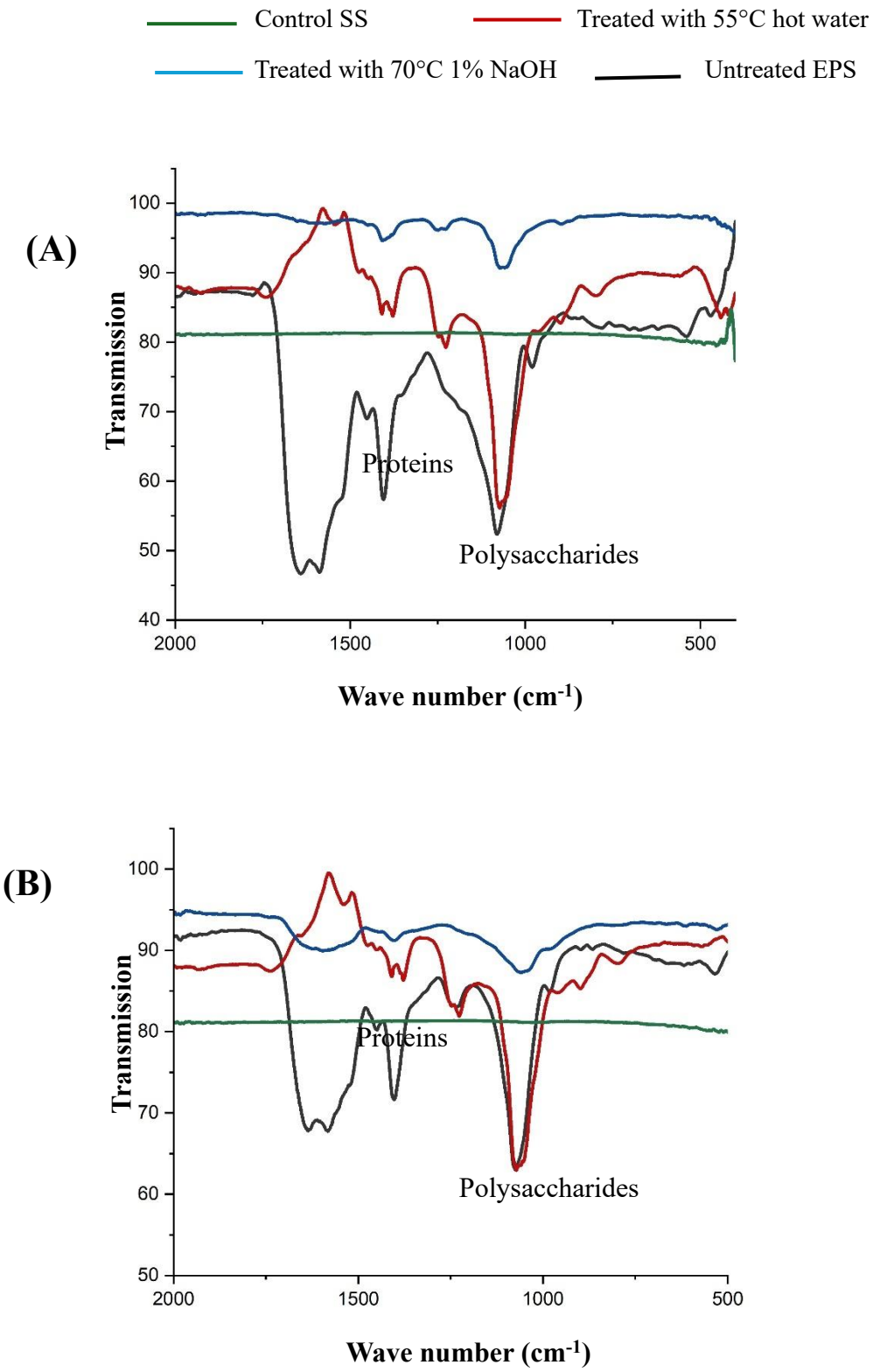

Figure 6.5 (A) ATR-FTIR images of the EPS isolated from untreated, hot water washed, and NaOH washed coupons from isolate 3SM and (B) 20SM.

6.3.4 Regrowth of the strong biofilm former after CIP cleaning

Compared to the untreated clean coupons, the CIP cleaned coupons started showing a visible air-liquid interface from 24 h of incubation, whereas in clean coupons it took 72 h to form a visible air-liquid interface (Fig. 6 .6 C). The cell counts from the CIP-cleaned coupons were significantly ($p < 0.05$) higher than the control coupons from 24 h for both isolates. The cell counts in the A-L coupons of the CIP cleaned coupons were 6.71±0.16 and 5.88±0.13 log CFU/cm^2 for 3SM and 20SM, respectively (Fig. 6.6 A and B). Whereas, in the control clean coupons, the A-L coupons yielded 3.59 ± 0.17 and 3.40 ± 0.19 log CFU/cm^2 for isolates 3SM and 20SM, respectively. The L1 and L2 coupons of the CIP cleaned group showed significantly ($p < 0.05$) higher cell counts than the control group of submerged coupons. These results suggest that the remaining footprints of biofilm EPS encouraged the cells to establish the early air-liquid interface biofilm.

(A)

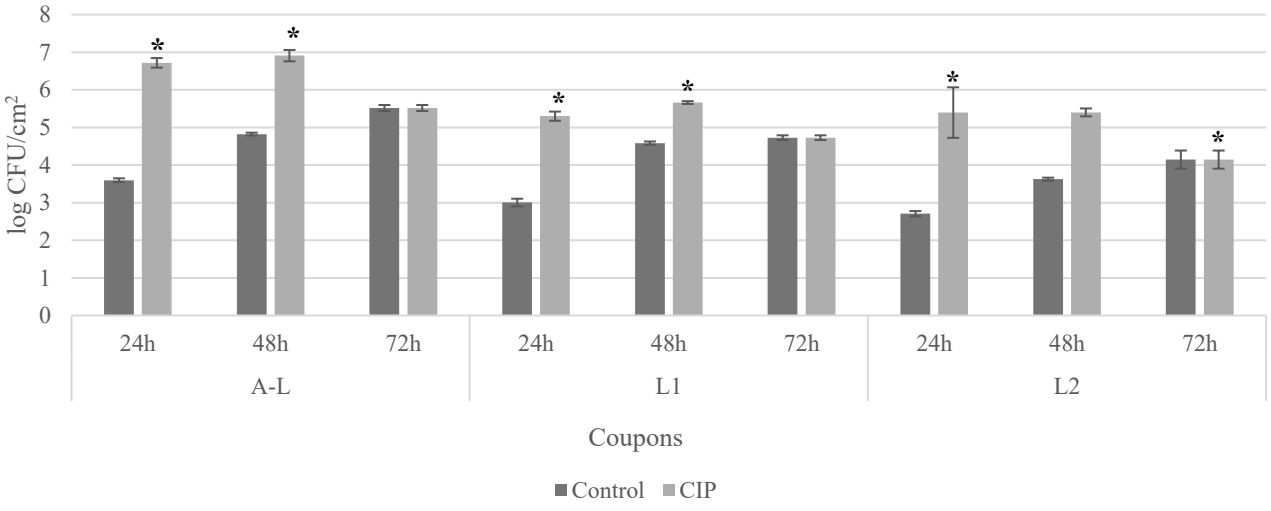

(B)

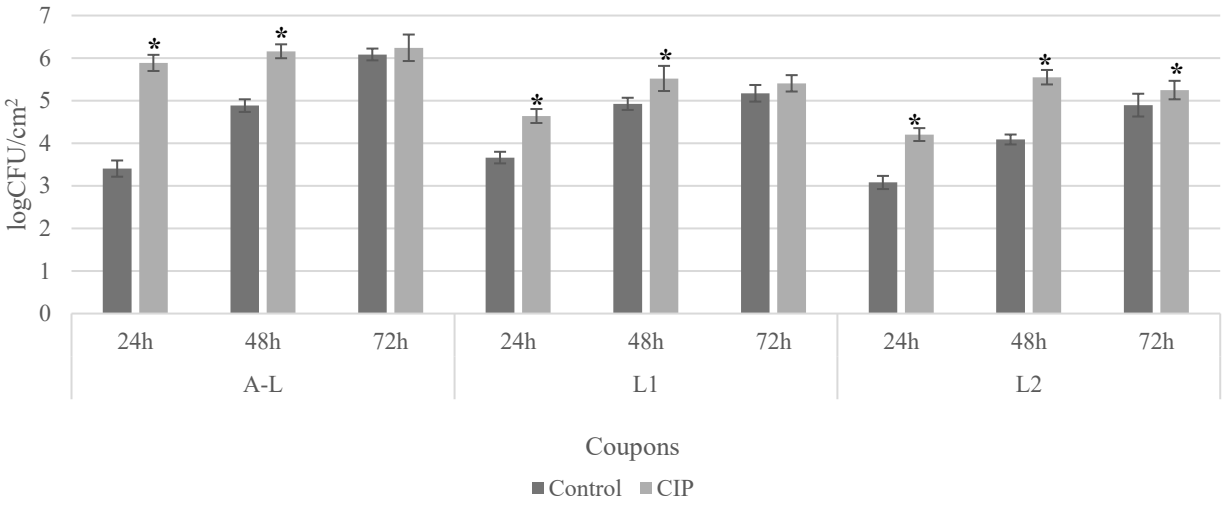

(C)

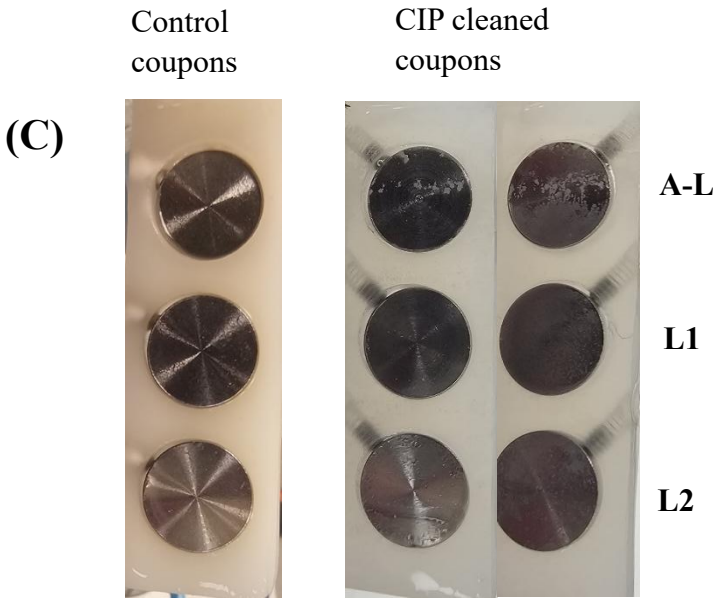

Figure 6.6 Graph A shows the regrowth of isolate 3SM after CIP cleaning, while Graph B shows the isolate 20SM after CIP cleaning. All the results were expressed as mean ± standard deviation. The symbol (*) indicate significant differences ($p < 0.05$), and (C) shows the early appearance of the air-liquid interface biofilm in the CIP-cleaned coupons of isolate 3SM.

6.3.5 Regrowth of the weak biofilm former after CIP cleaning

44SM was the weak biofilm-forming isolate chosen for this study, based on the crystal violet assay (Chapter 3). The weak biofilm former was allowed to grow for over a week on clean coupons under the same conditions as the strong biofilm former. No visible biofilm of this weak biofilm appeared in the first week at the air-liquid interface (Fig. 6.7 B). The cell counts were low at 3.92 ± 0.16, 3.25 ± 0.19, and 3.055 ± 0.17 log CFU/cm^2 for the A-L, L1, and L2 coupons, respectively (Fig. 6.7 A). The microscopic observations showed sparsely dispersed cells on all the coupons and a few clusters in the A-L coupons (Fig. 6 .7 C).

After CIP cleaning, tiny visible clusters of weak biofilm-forming cells were noted in the air-liquid interface (Fig. 6.8 C). The isolates were confirmed using the Congo red assay, where the strong biofilm formers produced pink colonies, which indicates cellulose production, and the weak biofilm former 44SM produced white colonies, indicating neither cellulose nor curli was produced (Supplementary File 6.7). The highest cell count, 5.76 ± 0.14 log CFU/cm^2 of the weak biofilm formers, was reached on the air-liquid interface at 72 h in the CIP-cleaned coupons (Fig. 6.8 A). The cell counts and microscopic observations on the CIP cleaned coupons were compared with control coupons (Fig. 6.8 B). At 24 h, the cell counts from the L1 and L2 coupons from both control and CIP cleaned coupons were below detectable limits. This indicates the influence of biofilm footprints on encouraging the biofilm formation of weak biofilm formers.

(A)

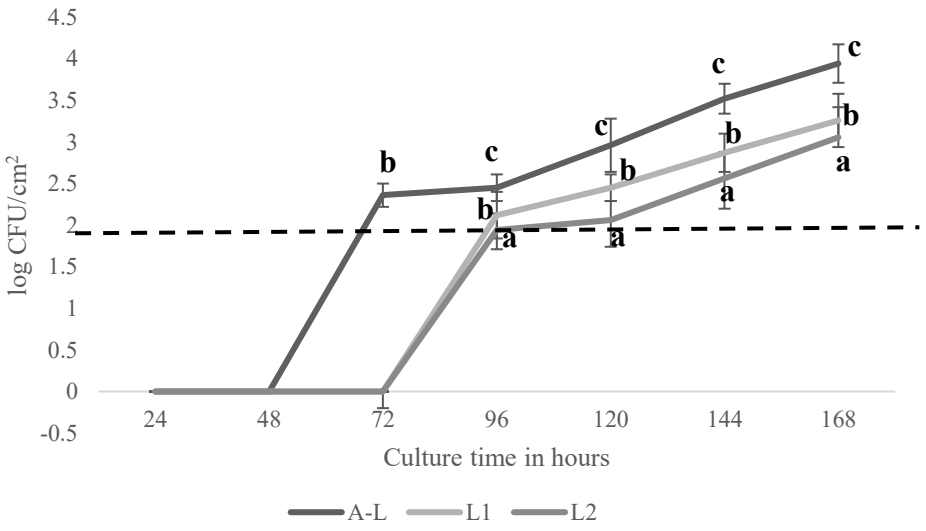

(B)

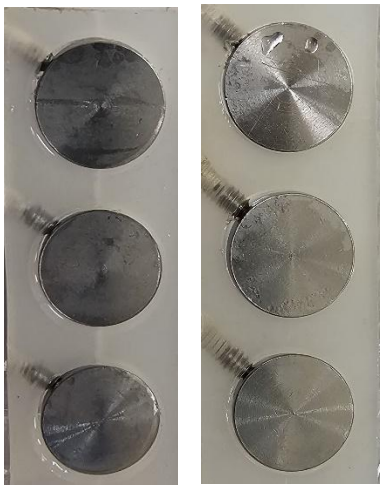

A-L

L1

L2

(C)

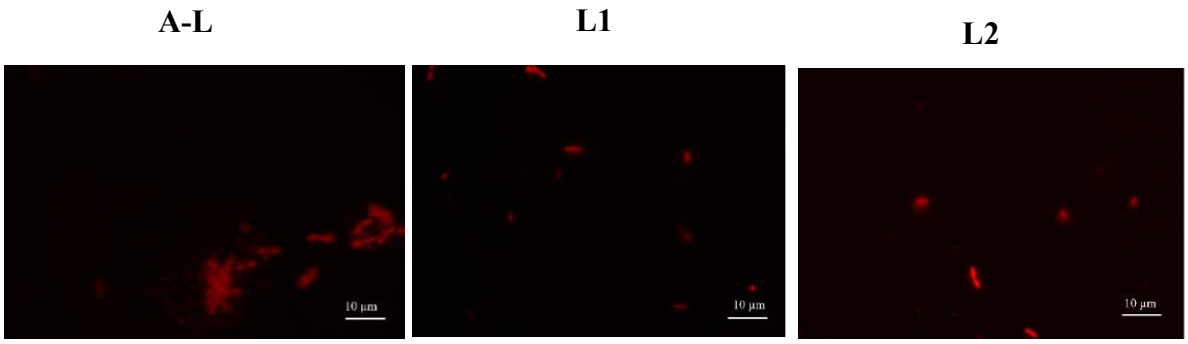

Figure 6.7 (A) shows the cell counts of the weak biofilm former 44SM on control clean coupons A-L, L1, and L2 after a week of incubation. The results are expressed as mean ± standard deviation. Different letters indicate significant differences ($p < 0.05$). (B) shows the coupons at 24 h and 48 h, showing no visible biofilm formation. (C) shows the microscopic images of the weak biofilm former 44SM after a week of incubation.

(A)

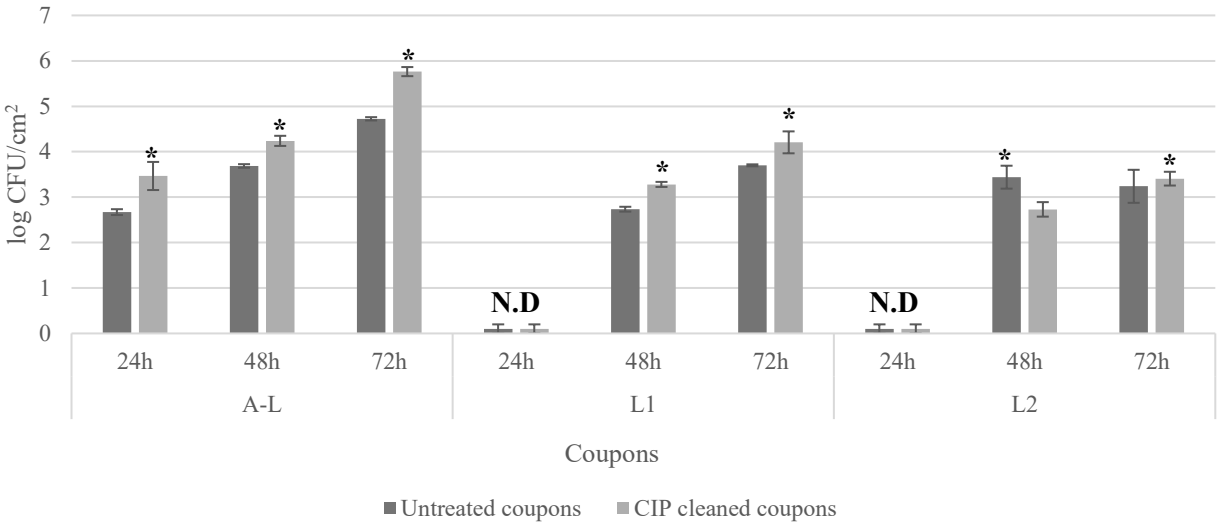

(B)

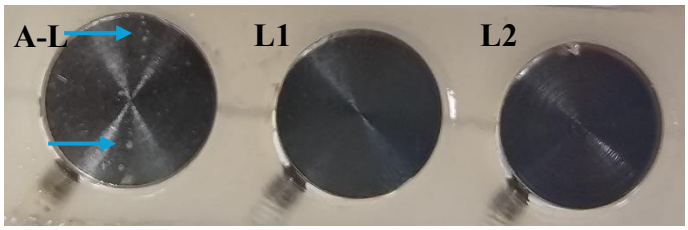

(C)

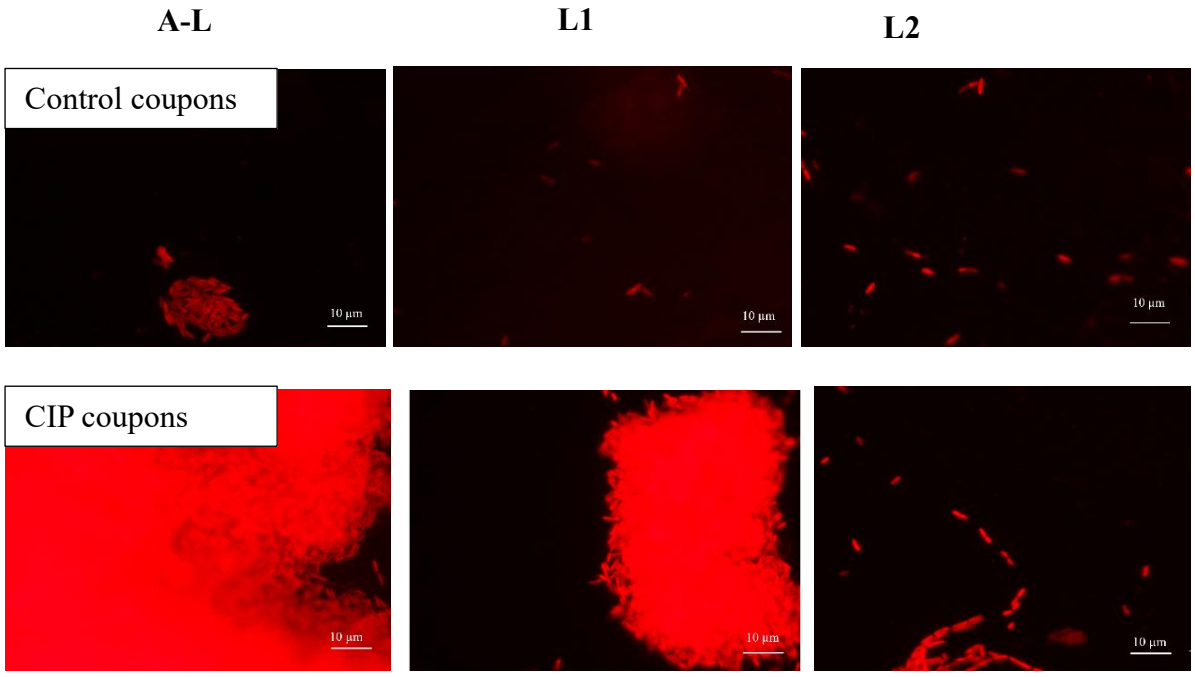

Figure 6.7 (A) shows the cell counts from the control clean coupons and CIP coupons of the weak biofilm former 44SM. All the results are expressed as mean ± standard deviation. The symbol (*) indicate significant differences($p < 0.05$). (B) Blue arrows show the appearance of

air-liquid interface biofilms on the CIP cleaned coupons. (C) Microscopic images show the biofilms formed on the control and CIP cleaned coupons.

6.4 Discussion

A study on the effects of cleaning regimes on biofilms of thermophilic bacilli on stainless steel showed that 2% caustic for 30 min at 70°C, followed by a water rinse and 1.8% HNO_3 at 75°C, removed the cells and polysaccharides effectively (Parkar et al., 2004). This study also reported that the caustic treatment alone showed 6 log cell reductions; however, the fluorescent polysaccharide remnants were observed. The present study focused on biofilm removal with water and caustic. 1% Caustic at 70°C effectively removed all the cells, but the remaining biofilm footprints were noted on the surface. The focus of this present study was to analyse the footprints rather than targeting biofilm cells. A study on treating the biofilms of *Listeria monocytogenes* with caustic and peracetic acids showed that caustic is not effective in biofilm removal with maximum concentrations, higher temperatures, and long operation time (Hashim et al.,2020). A study with multi-species biofilms noted that there are survivors even after the final sanitation step, and the traditional CIP is ineffective in removing biofilms on the reverse osmosis membranes in dairy industries (Singh & Anand, 2022). The survivors were *Bacillus* isolates that can form spores and survive post-treatments. This present study also confirmed that CIP can effectively remove the pseudomonad cells, but the EPS of the pseudomonad biofilms cannot be completely removed.

In the present study, the SEM results showed remaining EPS and NaOH crystals, revealing the ineffectiveness of alkaline CIP. The presence of NaOH crystals even after washing explains the possibility of NaOH deposits over time. A study on the removal of pseudomonad biofilms with microbubbles showed the remaining footprints of EPS with SEM observations. Subsequent treatment with microbubbles and sanitisers removed the biofilm footprints (Deng et al., 2025).

A study with cassia essential oil combined with amylase and proteinase significantly removed the viable cells of *Salmonella* and *Listeria* spp. However, the regeneration of the biofilms was observed within 24 h with high cell density, higher EPS production, and robust biofilm formation (Cervantes-Huamán et al., 2025). When the multispecies biofilm grows on titanium surfaces and is cleaned with antimicrobials, the regrowth of the biofilm appears early and aggressive (Han et al., 2019). This present study also demonstrated the early appearance of an

air-liquid interface biofilm with the strong biofilm-forming isolates, and increased the cell counts and appearance of the air-liquid interface clusters with the weak biofilm formers. This data suggests the potential of EPS footprints in the subsequent aggressive biofilm formation, which can add further burden to cleaning and sanitation in industrial processes.

In this present study with FTIR data, the CIP-cleaned coupons are not as clean as the acid-cleaned coupons. Peaks for polysaccharides and proteins can be seen after cleaning with caustic soda, which supports that the footprints cannot be removed by caustic soda. Peaks for both polysaccharides and proteins revealed that the complex nature of the EPS remains the same even after CIP. Similar observations were seen in a study treating *P. aeruginosa* biofilms with DDAB (Didecyl Dimethyl Ammonium Bromide) and SAEW (Slightly Acidic Electrolysed Water). Even if cell removal is achieved, removing EPS footprints from the surface is harder (Li et al., 2022).

The results of this study closely resemble the plate heat exchangers and drains in the dairy industry by simulating the turbulent flow. However, the air-liquid interface biofilms will not generally be observed in the plate heat exchangers. The data from submerged biofilms also confirmed the influence of footprints on the regrowth of pseudomonads. The preliminary results showed significantly ($p < 0.05$) higher cell numbers on air-liquid interface and submerged coupons under laminar flow compared to turbulent flow. These results suggest that the pseudomonad biofilms under laminar flow can form robust biofilms, and potentially, the EPS footprints from laminar flow biofilms might have similar effects. The laminar flow can be found in tankers, mixing and balance tanks in the dairy industry. However, the biofilm formation and cleaning studies of the laminar flow biofilms of pseudomonads still need to be explored.

Microbubblers are small oxygen bubbles generated by microparticles in the liquid systems (Chung et al., 2025). Due to the small size and active movement of the microparticles, the penetration into EPS and continuous generation of gas bubbles are possible inside the biofilms (Seo et al., 2018). Microbubblers have the potential to invade, deform, and displace EPS by 99.9%. Self-locomotive MnO_2-doped diatom micro-bubblers activated by hydrogen peroxide (H_2O_2) are known as SLAM. SLAM, when combined with peracetic acid (PAA) and hydrogen peroxide (H_2O_2), shows promising results against *P. aeruginosa* biofilms and prevents the regrowth over time by reducing the EPS volume (Deng et al., 2025). This

present study also focused on the EPS rather than the cells. This explains the need for more similar studies that target the EPS and cells.

This present study focused on psychrotrophic pseudomonads that can be killed with heat treatment. However, in industries, bacteria exist as multispecies community biofilms, and there might be cells that cannot be killed by heat treatment, and some of them can produce spores. There is a need for more studies to analyze the footprints in a multispecies setup, including thermophilic bacteria. This present study explored the consequences of remaining biofilm EPS footprints; however, studies targeting the removal of biofilm footprints need to be developed.

6.5 Conclusion

This study showed the reason behind the ineffectiveness of caustic soda against biofilm removal. The pseudomonads used in this study can be killed by hot water and caustic treatment. However, the remaining biofilm footprints can encourage the biofilm formation of the same isolate. The regenerated biofilm was more aggressive than the previous one. Targeting the removal of remaining biofilm footprints after the CIP process or any other antimicrobial treatments needs to be developed.

6.6 References

Cervantes-Huamán, B. R. H., Vega-Sánchez, A., Rolón-Verdún, P., Gervilla-Cantero, G., Rodríguez-Jerez, J. J., & Ripolles-Avila, C. (2025). Effect of Cinnamomum cassia essential oil combined with enzymes on the elimination and regrowth potential of *Listeria monocytogenes* and *Salmonella enterica* biofilms formed on stainless steel surfaces. *Food Control*, *172*, 111120. https://doi.org/10.1016/j.foodcont.2024.111120.

Chung, J. Y., Ahn, Y., Lee, J. H., Yang, S., Lee, S. C., Kong, H., & Chung, H. J. (2025). Microbubble-Controlled Delivery of Biofilm-Targeting Nanoparticles to Treat MRSA Infection. *Advanced Functional Materials*, 2508291. https://doi.org/10.1002/adfm.202508291

Crisp, A. R., Short, B., Rowan, L., Ramage, G., Rehman, I. U. R., Short, R. D., & Williams, C. (2023). Investigating the chemical pathway to the formation of a single biofilm

using infrared spectroscopy. *Biofilm*, *6*, 100141. https://doi.org/10.1016/j.bioflm.2023.100141.

Da Cruz Nizer, W. S., Allison, K. N., Adams, M. E., Vargas, M. A., Ahmed, D., Beaulieu, C., Raju, D., Cassol, E., Howell, P. L., & Overhage, J. (2024). The role of exopolysaccharides Psl and Pel in resistance of *Pseudomonas aeruginosa* to the oxidative stressors sodium hypochlorite and hydrogen peroxide. *Microbiology Spectrum*, *12*(10), e00922-24. https://doi.org/10.1128/spectrum.00922-24.

Deng, Y.-H., Lee, J. H., Kim, M.-J., & Kong, H. (2025). Biofilm comes back: Controlling regrowth by mitigating the cell-matrix interaction. *Chemical Engineering Journal*, *508*, 160947. https://doi.org/10.1016/j.cej.2025.160947.

Gieroba, B., Krysa, M., Wojtowicz, K., Wiater, A., Pleszczyńska, M., Tomczyk, M., & Sroka-Bartnicka, A. (2020). The FT-IR and Raman Spectroscopies as Tools for Biofilm Characterization Created by Cariogenic Streptococci. *International Journal of Molecular Sciences*, *21*(11), 3811. https://doi.org/10.3390/ijms21113811.

Han, Q., Jiang, Y., Brandt, B. W., Yang, J., Chen, Y., Buijs, M. J., Crielaard, W., Cheng, L., & Deng, D. (2019). Regrowth of Microcosm Biofilms on Titanium Surfaces After Various Antimicrobial Treatments. *Frontiers in Microbiology*, *10*, 2693. https://doi.org/10.3389/fmicb.2019.02693.

Hashim, S. T., Fakhry, S. S., & Alrubaye, H. H. (2020). Evaluation of the Effectiveness Of Treatments for Sanitizing Agents for Removal of *Listeria Monocytogenes* Biofilm. Plant archives Vol 20 ,pp 249-255.

Jha, P. K., Dallagi, H., Richard, E., Benezech, T., & Faille, C. (2020). Formation and resistance to cleaning of biofilms at air-liquid-wall interface. Influence of bacterial strain and material. *Food Control*, *118*, 107384. https://doi.org/10.1016/j.foodcont.2020.107384.

Joseph, B., Otta, S. K., Karunasagar, I., & Karunasagar, I. (2001). Biofilm formation by *Salmonella* spp. On food contact surfaces and their sensitivity to sanitizers. *International Journal of Food Microbiology*, *64*(3), 367–372. https://doi.org/10.1016/S0168-1605(00)00466-9.

Li, Y., Wang, H., Zheng, X., Li, Z., Wang, M., Luo, K., Zhang, C., Xia, X., Wang, Y., & Shi, C. (2022). Didecyldimethylammonium bromide: Application to control biofilms of

Staphylococcus aureus and *Pseudomonas aeruginosa* alone and in combination with slightly acidic electrolyzed water. *Food Research International*, *157*, 111236. https://doi.org/10.1016/j.foodres.2022.111236.

Liu, J., Wu, S., Feng, L., Wu, Y., & Zhu, J. (2023). Extracellular matrix affects mature biofilm and stress resistance of psychrotrophic spoilage *Pseudomonas* at cold temperature. *Food Microbiology*, *112*, 104214. https://doi.org/10.1016/j.fm.2023.104214.

Mann, E. E., & Wozniak, D. J. (2012). *Pseudomonas* biofilm matrix composition and niche biology. *FEMS Microbiology Reviews*, *36*(4), 893–916. https://doi.org/10.1111/j.1574-6976.2011.00322.x.

Neu, T. R., & Marshall, K. C. (1991). Microbial "footprints"—A new approach to adhesive polymers. *Biofouling*, *3*(2), 101–112. https://doi.org/10.1080/08927019109378166.

Parkar, S. G., Flint, S. H., & Brooks, J. D. (2004). Evaluation of the effect of cleaning regimes on biofilms of thermophilic bacilli on stainless steel. *Journal of Applied Microbiology*, *96*(1), 110–116. https://doi.org/10.1046/j.1365-2672.2003.02136.x.

Raposo, A., Pérez, E., De Faria, C. T., Ferrús, M. A., & Carrascosa, C. (2016). Food Spoilage by *Pseudomonas* spp.—An Overview. In O. V. Singh (Ed.), *Foodborne Pathogens and Antibiotic Resistance* (1st ed., pp. 41–71). Wiley. https://doi.org/10.1002/9781119139188.ch3.

Ren, F., Chen, Y., Yang, S., Zhang, Y., Liu, Y., Ma, Y., Wang, Y., Liu, Y., Dong, Q., & Lu, D. (2024). Characterization of emetic *Bacillus cereus* biofilm formation and cereulide production in biofilm. *Food Research International*, *192*, 114834. https://doi.org/10.1016/j.foodres.2024.114834.

Santos Rosado Castro, M., Da Silva Fernandes, M., Kabuki, D. Y., & Kuaye, A. Y. (2021). Modelling Pseudomonas fluorescens and Pseudomonas aeruginosa biofilm formation on stainless steel surfaces and controlling through sanitisers. *International Dairy Journal*, *114*, 104945. https://doi.org/10.1016/j.idairyj.2020.104945.

Seo, Y., Leong, J., Park, J. D., Hong, Y.-T., Chu, S.-H., Park, C., Kim, D. H., Deng, Y.-H., Dushnov, V., Soh, J., Rogers, S., Yang, Y. Y., & Kong, H. (2018). Diatom Microbubbler for Active Biofilm Removal in Confined Spaces. *ACS Applied*

Materials & Interfaces, *10*(42), 35685–35692. https://doi.org/10.1021/acsami.8b08643

Singh, D., & Anand, S. (2022). Efficacy of a typical clean-in-place protocol against in vitro membrane biofilms. *Journal of Dairy Science*, *105*(12), 9417–9425. https://doi.org/10.3168/jds.2022-21712.

Spiers, A. J., Bohannon, J., Gehrig, S. M., & Rainey, P. B. (2003). Biofilm formation at the air–liquid interface by the *Pseudomonas fluorescens* SBW25 wrinkly spreader requires an acetylated form of cellulose. *Molecular Microbiology*, *50*(1), 15–27. https://doi.org/10.1046/j.1365-2958.2003.03670.x.

Tirpanci Sivri, G., Abdelhamid, A. G., Kasler, D. R., & Yousef, A. E. (2023). Removal of Pseudomonas fluorescens biofilms from pilot-scale food processing equipment using ozone-assisted cleaning-in-place. *Frontiers in Microbiology*, *14*, 1141907. https://doi.org/10.3389/fmicb.2023.1141907.

6.7 Supplementary information

6.7.1. Elemental analysis of EPS and NaOH crystals.

The NaOH crystals were seen in different shapes. The elemental analysis revealed strong signals for carbon, nitrogen, and sodium. The crystals were of sodium, but carbon signals were also detected in the spots (23, 21, 13, 18) with sodium crystals. This may be due to the crystals attached to the EPS footprints. Water rinse after CIP failed to remove the EPS and NaOH crystals. The spots (17, 24, 15, and 16) showed strong C and N signals and lower Na SIGNALS. This elemental analysis confirmed the presence of organic matter and Na crystals.

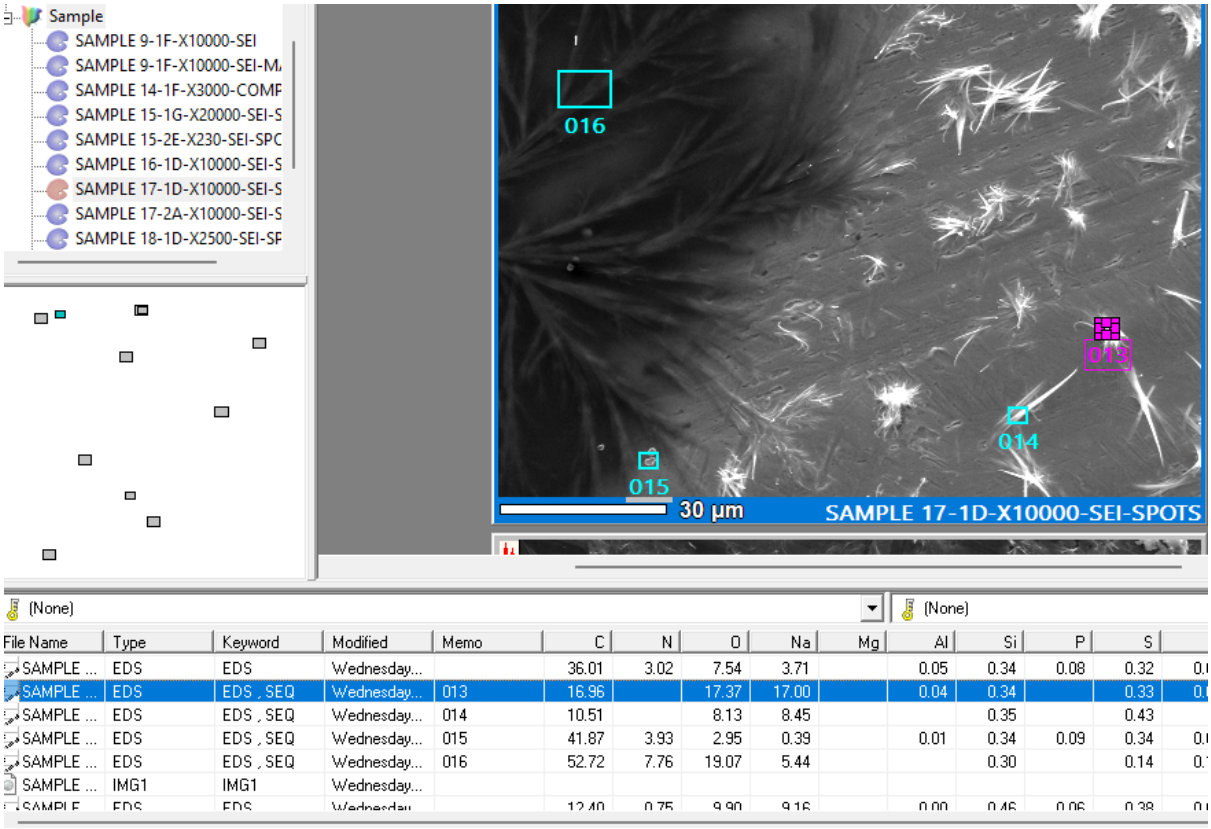

(None) (None)

File Name	Type	Keyword	Modified	Memo	C	N	O	Na	Mg	Al	Si	P	S
SAMPLE ...	EDS	EDS	Wednesday...		36.01	3.02	7.54	3.71		0.05	0.34	0.08	0.32
SAMPLE ...	EDS	EDS , SEQ	Wednesday...	013	16.96		17.37	17.00		0.04	0.34		0.33
SAMPLE ...	EDS	EDS , SEQ	Wednesday...	014	10.51		8.13	8.45			0.35		0.43
SAMPLE ...	EDS	EDS , SEQ	Wednesday...	015	41.87	3.93	2.95	0.39		0.01	0.34	0.09	0.34
SAMPLE ...	EDS	EDS , SEQ	Wednesday...	016	52.72	7.76	19.07	5.44			0.30		0.14
SAMPLE ...	IMG1	IMG1	Wednesday...										

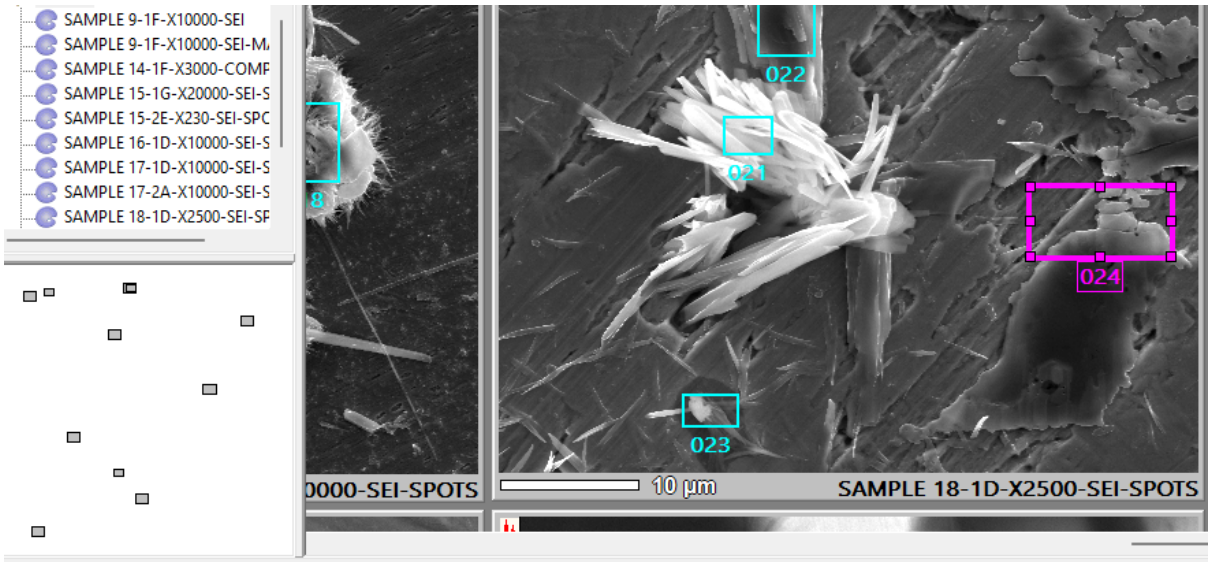

(None) (None)

le Name	Type	Keyword	Modified	Memo	C	N	O	Na	Mg	Al	Si	P	S	Cl
SAMPLE ...	IMG1	IMG1	Wednesday...											
SAMPLE ...	EDS	EDS	Wednesday...		13.48	0.96	10.22	9.39		0.03	0.51	0.04	0.37	0.05
SAMPLE ...	EDS	EDS , SEQ	Wednesday...	021	24.03		40.92	28.21			0.16		0.06	
SAMPLE ...	EDS	EDS , SEQ	Wednesday...	022	15.77		35.61	31.13			0.16		0.16	0.05
SAMPLE ...	EDS	EDS , SEQ	Wednesday...	023	18.56		8.44	9.43			0.55	0.13	0.37	
SAMPLE ...	EDS	EDS , SEQ	Wednesday...	024	12.16	1.14	0.94	0.92			0.68	0.05	0.48	

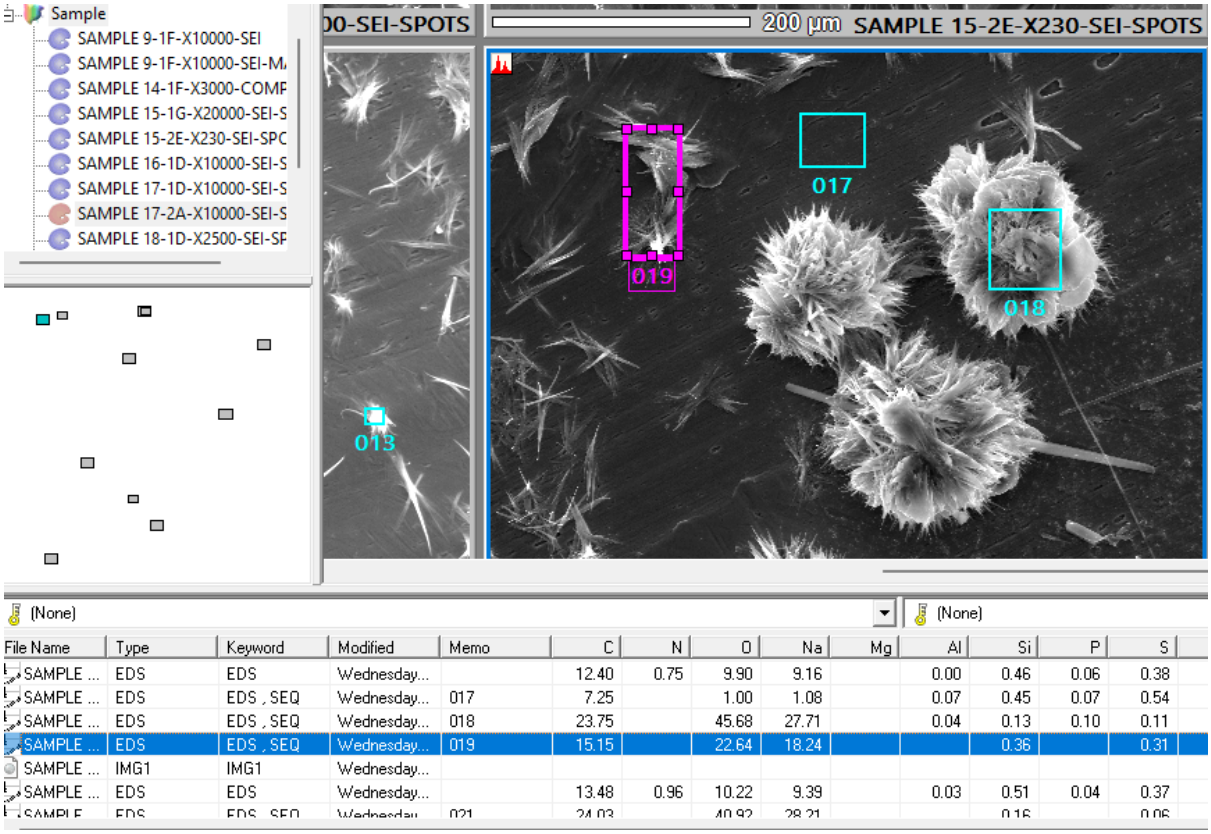

\

6.7.2 Calcofluor white staining

The remaining EPS footprints on the stainless-steel surface of isolate 3SM after NaOH cleaning.

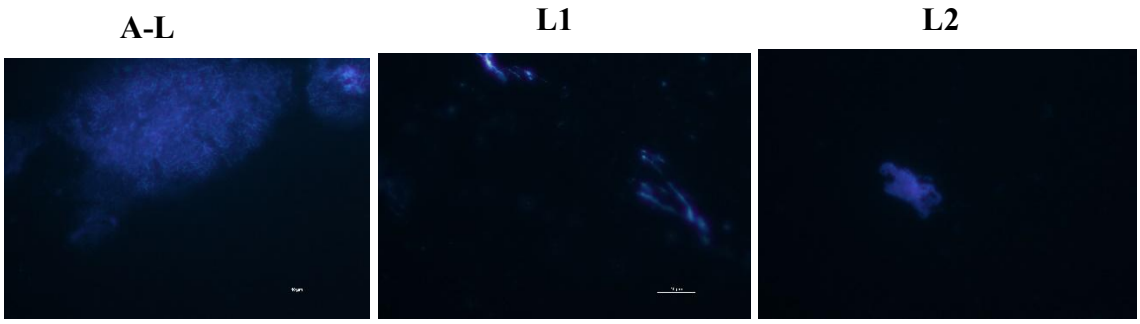

6.7.3 The control coupons that underwent CIP were included in the FTIR observations

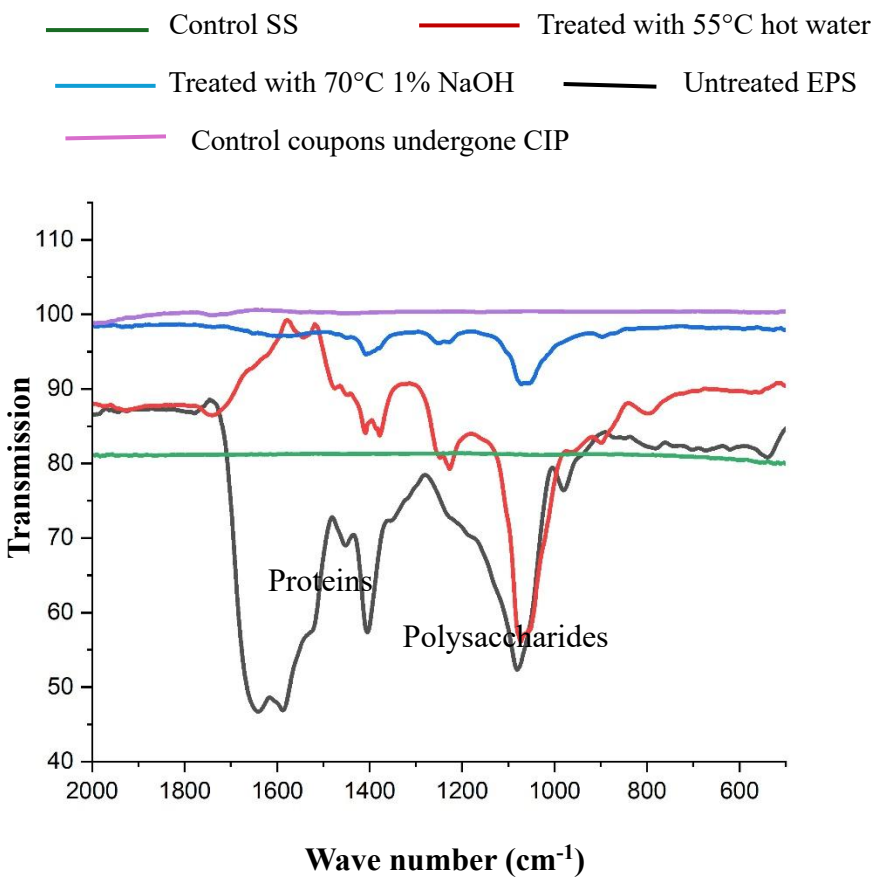

6.7.4 Congo red assay confirmation for weak biofilm formers

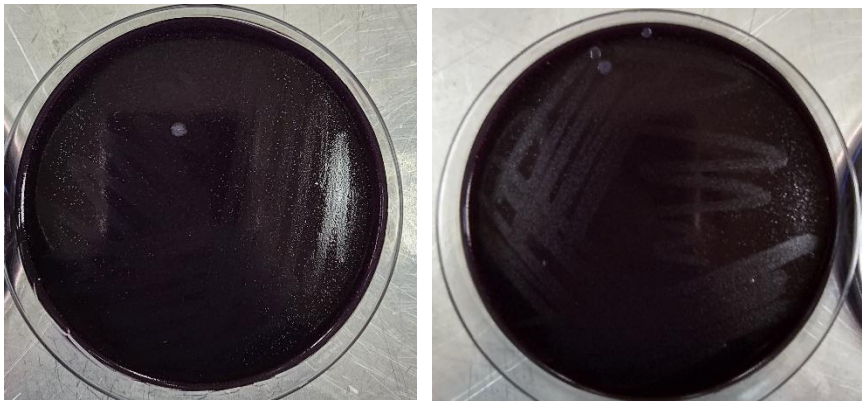

White colonies indicating neither curli not nor cellulose.

Chapter 7 Sequential Treatment of Biofilms with NaOH and Enzyme Cleaners.

This chapter is an adaptation of material that was published as a peer-reviewed article:

Muthuraman, S., Palmer, J., & Flint, S. (2026). Sequential treatment of psychrotrophic pseudomonad biofilms with sodium hydroxide and commercial enzyme cleaners. *Food Control*, *182*, 111858. https://doi.org/10.1016/j.foodcont.2025.111858.

Preface to Chapter 7

Chapter 6 explored the ineffectiveness of NaOH in biofilm removal and the effects of footprints on biofilm regrowth. In Chapter 7, the sequential application of NaOH and enzyme cleaners was tested on a 168-h-old biofilm in preventing the biofilm regrowth.

7.1 Introduction

Pseudomonads are psychrotrophic, motile, aerobic, Gram-negative rods. Pseudomonads produce various thermostable enzymes and pigments that affect the quality of dairy, poultry, and meat products (Raposo et al., 2016). The common psychrotrophic pseudomonads isolated from the cold chain are *Pseudomonas fragi*, *P. lundensis, P. fluorescens*, and *P. putida* (Nychas et al., 2008). It is well known that pseudomonads are strong biofilm formers at cold temperatures, with the extracellular polymeric substances (EPS) made up of polysaccharides, proteins, eDNA, and lipids (Flemming & Wingender, 2010). The EPS produced by pseudomonads protects the biofilm cells from adverse conditions and antimicrobials (Flemming & Wingender, 2010). Pseudomonads form biofilms at the air-liquid interface due to an increased access to oxygen, which encourages their biofilm formation. In the food processing environments, partly filled utensils, silos, tankers, and stagnated water represent the air-liquid interface where the biofilm formation by pseudomonads is higher (Jha et al., 2020).

The biofilm elimination strategies for pseudomonads, such as sanitizers (Li et al., 2022; Liu et al., 2023), cleaning chemicals (Shah & Muriana, 2021), quorum quenching molecules (Khalid et al., 2022), and cold atmospheric plasma (Lavrikova, 2025), target the biofilm cells, and the remaining biofilm EPS on the surface can attract bacteria to recolonise the surface. This remaining EPS on the surface is known as biofilm footprints (Neu & Marshall, 1991).

Enzyme cleaners can destabilise the biofilms by cleaving the polysaccharides, proteins, lipids and eDNA in the biofilm matrix (Stiefel et al., 2016). Studies have shown that proteinases, DNases, amylases, alginate lyases and cellulases are effective in dispersing biofilms (Yang et al., 2023; Kiedrowski & Horswill, 2011; Molobela et al., 2010). Enzyme cleaners are one of those strategies that target the biofilm EPS. There are many advantages, such as being environmentally friendly, targeting the EPS, and being biodegradable (Nahar et al.,2018). However, there are no bactericidal effects observed with enzyme cleaners, and dispersed cell clusters can recolonise another surface. In Chapter 6, the biofilm EPS footprints left on the stainless-steel surface after traditional CIP were observed, but the cells were eliminated. The biofilm footprints on the surface need to be eliminated to prevent regrowth. Combining the CIP and enzyme cleaners leads to targeting both biofilm cells and EPS.

This chapter focuses on eliminating both biofilm cells and EPS using traditional CIP and enzyme cleaners. This study sequentially treated the biofilms of psychrotrophic pseudomonads with hot water and NaOH, followed by commercial enzyme cleaners. The effects of enzyme cleaners on the biofilm footprints were evaluated by FTIR, microscopy, and biofilm regrowth.

7.2 Materials and methods

7.2.1 Bacterial isolates

Strong biofilm-forming isolates at cold temperatures, 3SM (*P. lundensis*) and 20SM (*P. cedrina*), isolated from the dairy environment, were chosen for this study.

7.2.2 Biofilm formation

Details were provided in Section 5.2.2, Chapter 5.

7.2.3 Treating the biofilms with enzyme cleaners.

Enduro Zyme, Dual Zyme, and Tri Zyme were the enzyme cleaners from IXOM, Australia. The composition, temperature, and pH for optimal activity are provided in Table 7.1.

Table 7.1: Enzyme cleaners used in this study

Product	Composition	Temperature	Concentration	pH
Superflux Enduro Zyme	Protease	50°C	0.5% v/v	11
Superflux Dual Zyme	Protease and Lipase			10
Superflux Tri Zyme	Protease, cellulase, and amylase			10

The 168 h old biofilms of psychrotrophic pseudomonads on the stainless-steel coupons were removed and washed with sterile distilled water. The enzymes were prepared according to

Table 1 in sterile distilled water. Five millilitres (5 mL) of the prepared enzymes were poured into the wells of the 6-well polystyrene plates (FALCON ®, Corning Incorporated, USA). The coupons were immersed in the enzyme cleaners for an hour and incubated at 50°C. After an hour, the coupons were washed with sterile distilled water and added to the vials containing 1 mL of sterile saline (0.85%). The coupons were mixed by vortex with glass beads to remove the biofilm cells. The mixture was serially diluted in sterile saline (0.85%) and plated on Tryptic Soy Agar (TSA, Difco^{TM}, Becton and Dickinson company, USA) on TSA and incubated at 30ºC for 24 h to count colonies. The cell counts were compared between the untreated control coupons and coupons treated with enzyme cleaners.

7.2.4 Treating the biofilms with NaOH and Enzyme cleaners

After 168 h of incubation, the CDC reactor was cleaned using hot water at 55°C and NaOH at 70°C (pH 12). The coupons containing holders were taken out and inserted into the beakers containing enzyme cleaners and incubated at 50°C for an hour. The remaining cells were removed from the stainless-steel coupons, and bacteria were counted as described previously. The cell counts were compared between the untreated coupons with NaOH + enzyme cleaner-treated coupons.

7.2.5 Microscopical observations

Details were provided in Section 5.2.5, Chapter 5. The control coupons, enzyme-cleaned coupons, NaOH-cleaned coupons, and NaOH + enzyme cleaners cleaned coupons were compared to evaluate the effects of enzyme cleaners in removing biofilm cells and EPS footprints.

7.2.6 Attenuated Total Reflection- Fourier Transform Infrared Spectroscopy (ATR-FTIR)

After cleaning with enzyme cleaners, the coupons were washed with sterile distilled water. The coupons were added to the vials containing 2 mL of sterile distilled water. The mixture was sonicated for 15 min at room temperature. The mixture was centrifuged to get rid of the cells and filtered through syringe filters to obtain cell-free EPS. The EPS was isolated in the same way from the untreated and the coupons treated with NaOH (Section 5.2.4, Chapter 5).

The isolated EPS was freeze-dried and observed using FTIR with the following parameters: acquisition range 2000-400 cm^{-1}, scanning times of 32 s, and resolution 4 cm^{-1} (Li et al., 2022). The acid-treated coupons were used as a negative control. The EPS isolated from the enzyme-cleaned coupons was compared with untreated and NaOH-treated EPS.

7.2.7 Regrowth after CIP+ enzymatic cleaners

The biofilms of pseudomonads were grown for 168 h. The CDC reactor was flushed with hot water at 55°C, NaOH at 70°C, at a Reynolds number >12000. The Enduro Zyme enzyme was chosen for this experiment. The enzyme cleaner was flushed (Reynolds number >12000) into the CDC reactor at 50°C for an hour. Finally, the entire coupon containing holder system was briefly submerged in the hot water at 72°C to remove any other cells in the system. Four holders containing 3 coupons each (NaOH+ Enduro Zyme treated coupons) from the CDC reactor were retained, and four holders containing acid-treated coupons (Control coupons) were added. All holders with the baffle were transferred into a new CDC reactor beaker and allowed to run for 24 h. After 24 h, the isolates of 3SM and 20SM were inoculated. The regrowth was monitored up to 72h. The cell counts from the control clean coupons and NaOH + Enduro Zyme cleaned coupons were compared to determine the effects of footprints left after NaOH + Enduro Zyme treatment.

7.2.8 Data analysis

All the experiments were performed with three biological and three technical replicates. One-way variance analysis (ANOVA) was generated to evaluate significant differences among the variables using Tukey's test, which had a p-value below 0.05 and was considered statistically significant. Data analysis was implemented using SPSS statistical software (Version 29.0.2.0; IBM®, USA). FTIR data was processed using Origin Pro software (Origin Pro 2025, 10.2 Origin Lab Corporation, USA).

7.3 Results

7.3.1 Treating the biofilms with enzyme cleaners

From 48 h to 72 h, the appearance of the air-liquid interface biofilm was observed on the A-L coupons. After 168 h of incubation in the CDC reactor, the cell counts in the A-L coupons reached the following cell counts in log CFU/cm^2: 8.1 ± 0.14 (3SM) and 7.89 ± 0.12 (20SM), and the L1 coupons reached 6.23 ± 0.11 (3SM) and 6.43 ± 0.28 (20SM). The cell counts from the L2 coupons were (log CFU/ cm^2) 4.98 ± 0.21 (3SM) and 4.57 ± 0.16 (20SM) (Fig. 7.1A and B). When comparing the results after enzyme cleaning, Enduro Zyme significantly ($p <$ 0.05) reduced the cell counts compared to the other two enzymes, Tri Zyme and Dual Zyme. The log reductions observed after treating with Enduro Zyme were 4.21 ± 0.36 and 3.79 ± 0.35 log CFU/cm^2 for the A-L coupons, 3.29 ± 0.16 and 3.4 ± 0.19 log CFU/cm^2 for L1 coupons, and 2.24 ± 0.11 and 2.4 ± 0.25 log CFU/cm^2 for the L2 coupons. The log reductions for DualZyme were 1.45 ± 0.33, 1.42 ± 0.10, and 1.55 ± 0.31 log CFU/cm^2 for A-L, L1, and L2 of isolate 3SM and 1.93 ± 0.12, 1.89 ± 0.25, and 1.13 ± 0.28 log CFU/cm^2 for A-L, L1, and L2 of isolate 20SM. After treating with Tri Zyme, the log reductions were 1.76 ± 0.24, 1.35 ± 0.10, and 1.52 ± 0.18 log CFU/cm^2 for the isolate 3SM and 1.9 ± 0.18, 1.85 ± 0.25, and 1.2 ± 0.24 log CFU/cm^2 for the isolate 20SM (Fig.7.1A and B).

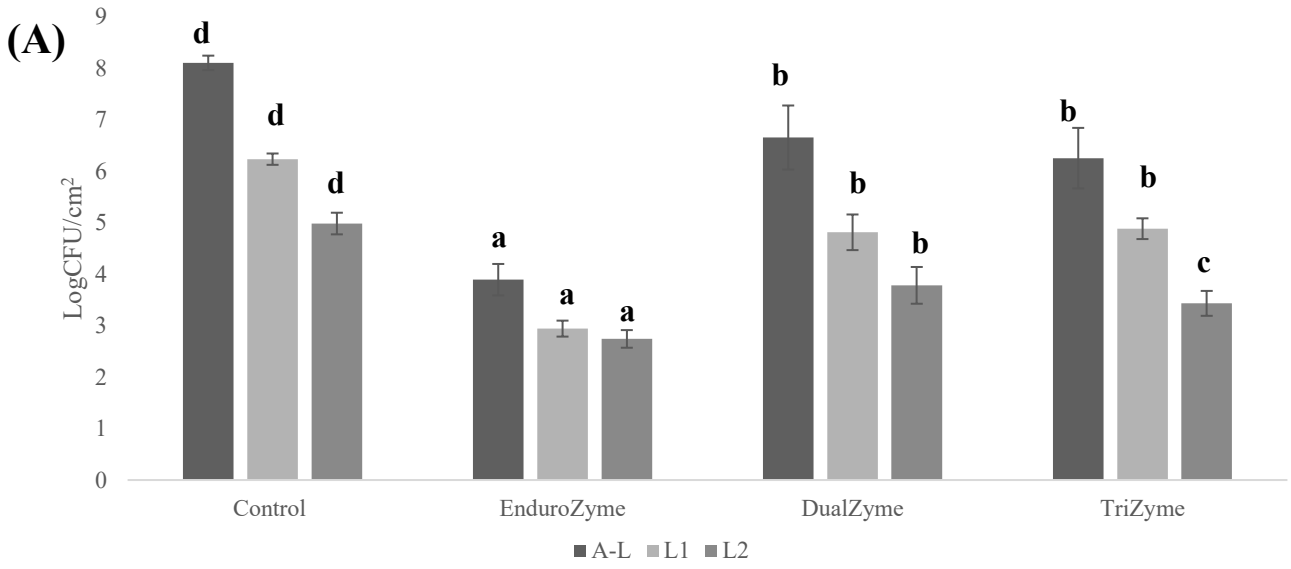

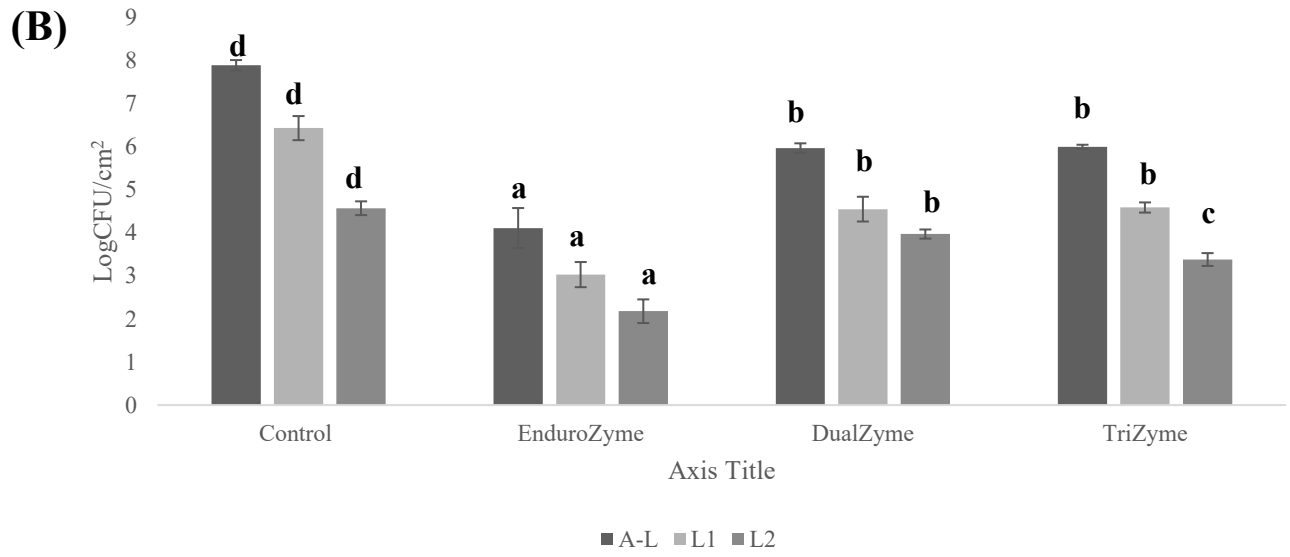

Figure 7.1 (A) Cell counts of biofilms formed by isolate 3SM after treating with commercial enzyme cleaners, (B) Cell counts of isolate 20SM biofilms after treating with commercial enzyme cleaners. All the results were expressed as mean ± standard deviation. Different letters above each bar indicate significant differences ($p < 0.05$).

The log reduction was reflected in the microscopic observations. When the biofilms of isolates were treated with the enzyme cleaners, the enduro Zyme-treated coupons showed more dispersed cells and fewer aggregates on the A-L coupons than the untreated coupons (Fig. 7.2 A and B). The coupons treated with Dual Zyme still had the biofilms with full integrity in the A-L coupons. The L1 and L2 coupons showed aggregates rather than dispersed cells (Fig. 7.2 C and D). The coupons treated with Tri Zyme had the biofilm structure and big aggregates of cells in the A-L, L1, and L2 coupons (Fig. 7.2 E and F). The cell reduction from coupons treated with Tri Zyme and Dual Zyme was not significantly (p <0.05) different and resembled the same with microscopic observations. Among the three enzyme cleaners, Enduro Zyme resulted in approximately a 4-log reduction (4.21 ± 0.36 log CFU/cm^2) and the breakdown of the biofilm structures.

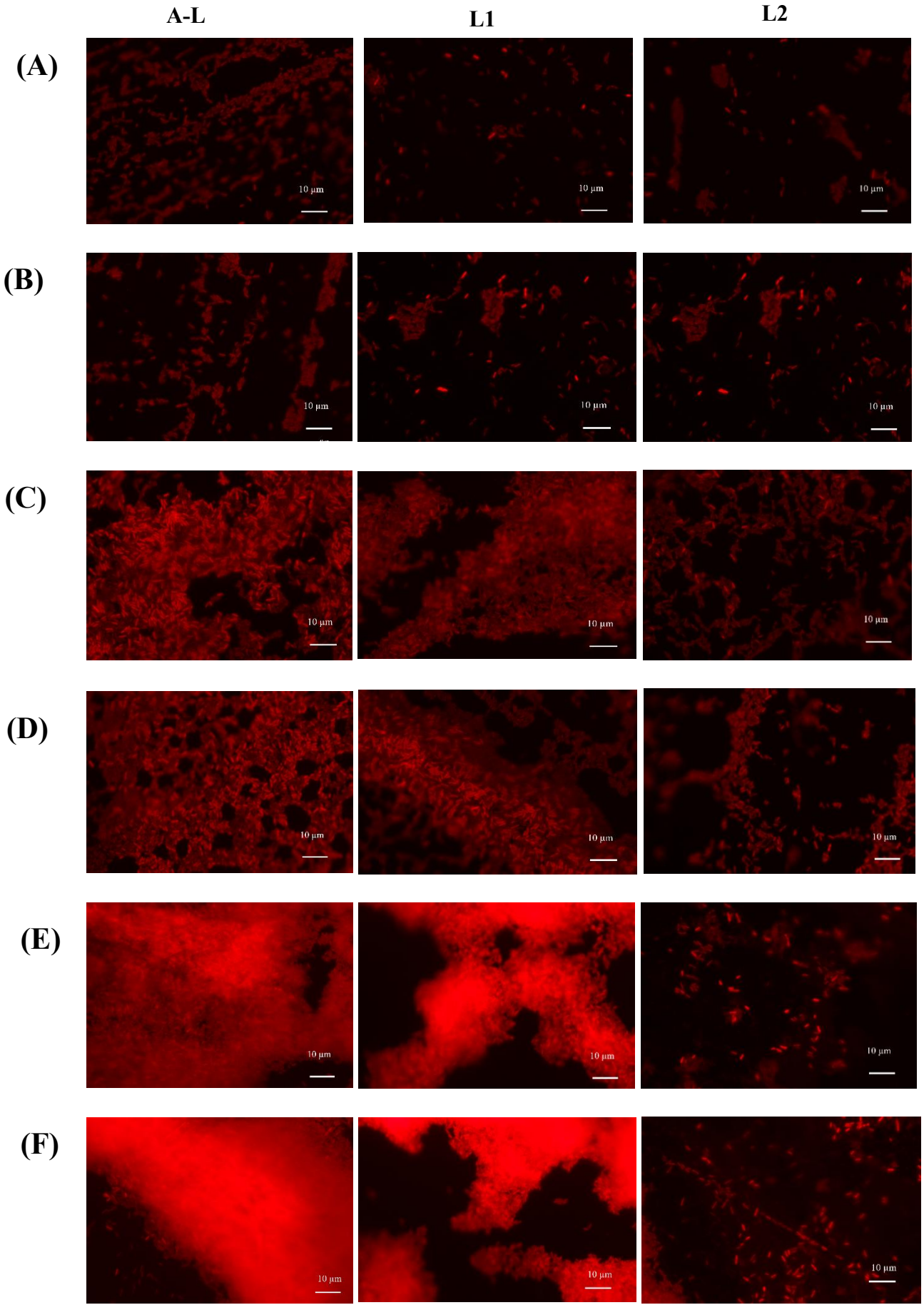
A-L
L1
L2
(A)
(B)
(C)
(D)
(E)
(F)
10 µm

Figure 7.2 (A) & (B) EnduroZyme-treated coupons of isolate 3SM and 20SM, (C) & (D) DualZyme-treated coupons of isolates 3SM and 20SM, (E) & (F) TriZyme-treated coupons of isolates 3SM and 20SM.

7.3.2 NaOH + Enzyme cleaners

From Section 7.3.1, the biofilms did not disperse after being treated with enzyme cleaners, even though the Enduro Zyme reduced the cell counts by approximately 4 log CFU/cm^2 for the A-L coupons. When the enzyme cleaners were applied after NaOH cleaning, the cell counts reduced below the detectable limit (1.7 log CFU/cm^2).

The epifluorescence microscope images showed that some fluorescence remained on the coupons treated with NaOH + DualZyme and NaOH + Tri Zyme (Fig. 7.3 C, D, E, and F). The coupons treated with NaOH + EnduroZyme were clear for both isolates (Fig. 7.3 A and B). Thus, NaOH + enzyme cleaners effectively removed biofilm EPS footprints compared to treating with enzyme cleaners alone.

The SEM observations (Fig. 7.4 (A-G)) showed that the NaOH + Enzyme-treated coupons were cleaner, and there were no cells or debris found. The NaOH Enzyme-treated coupons (Fig. 7.4 (A-F) resemble the acid-treated control coupons (Fig. 7.4 G) in appearance. The NaOH + Enzyme cleaning removed the biofilm EPS footprints from the surface of A-L, L1, and L2 coupons. The fluorescent debris seen from epifluorescence microscopy images was not seen in SEM images. The SEM images showed that the ridges of the coupons were damaged, and the furrows were clear. The topography of the surface may facilitate biofilm formation.

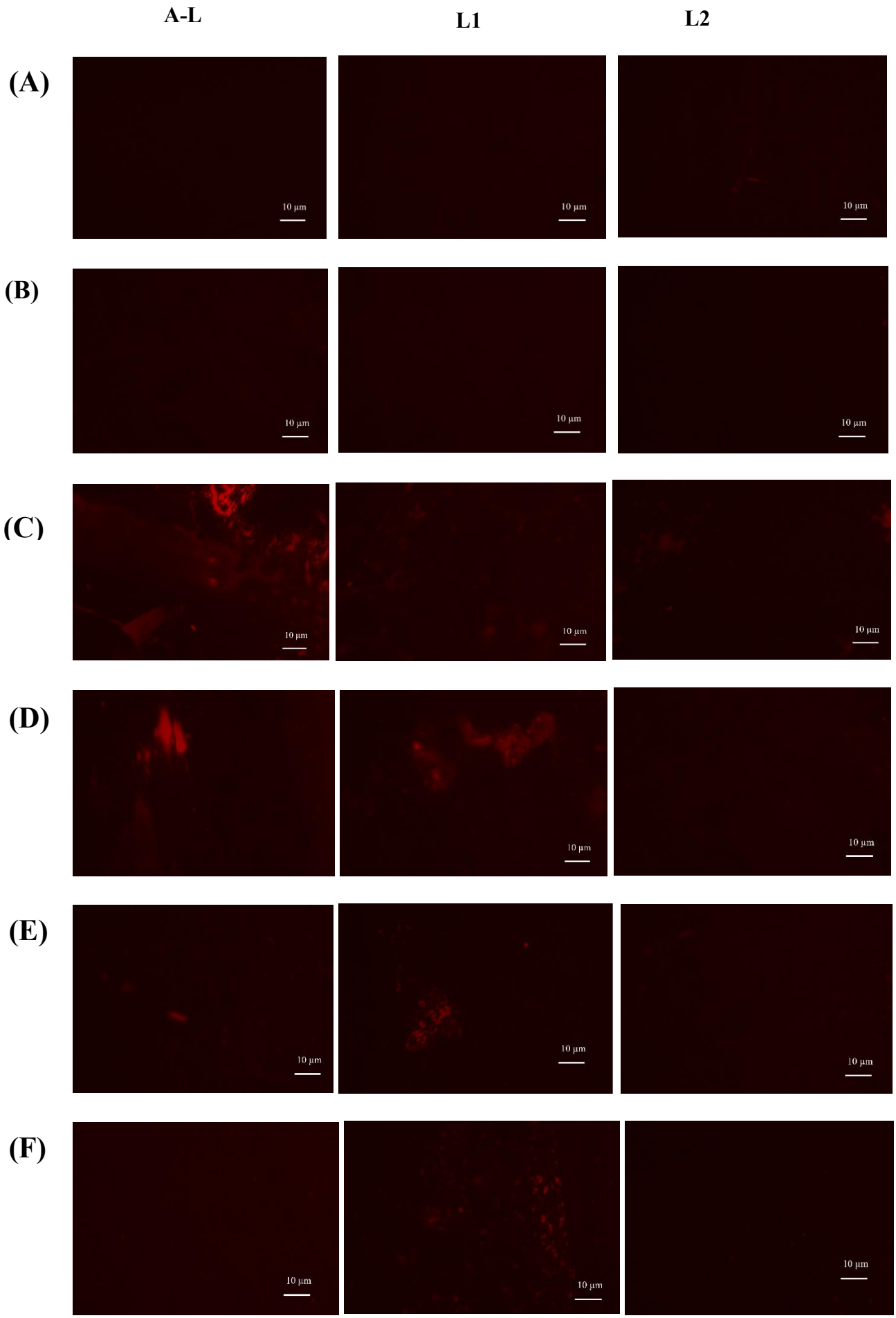
A-L
L1
L2
(A)
(B)
(C)
(D)
(E)
(F)
10 µm

Figure 7.3 Epifluorescence microscopic images of (A) & (B) NaOH + Enduro Zyme treated coupons of isolates 3SM and 20SM, (C) & (D) NaOH+Dual Zyme treated coupons of isolates 3SM and 20SM, (E) & (D) NaOH+Tri Zyme treated coupons of isolates 3SM and 20SM.

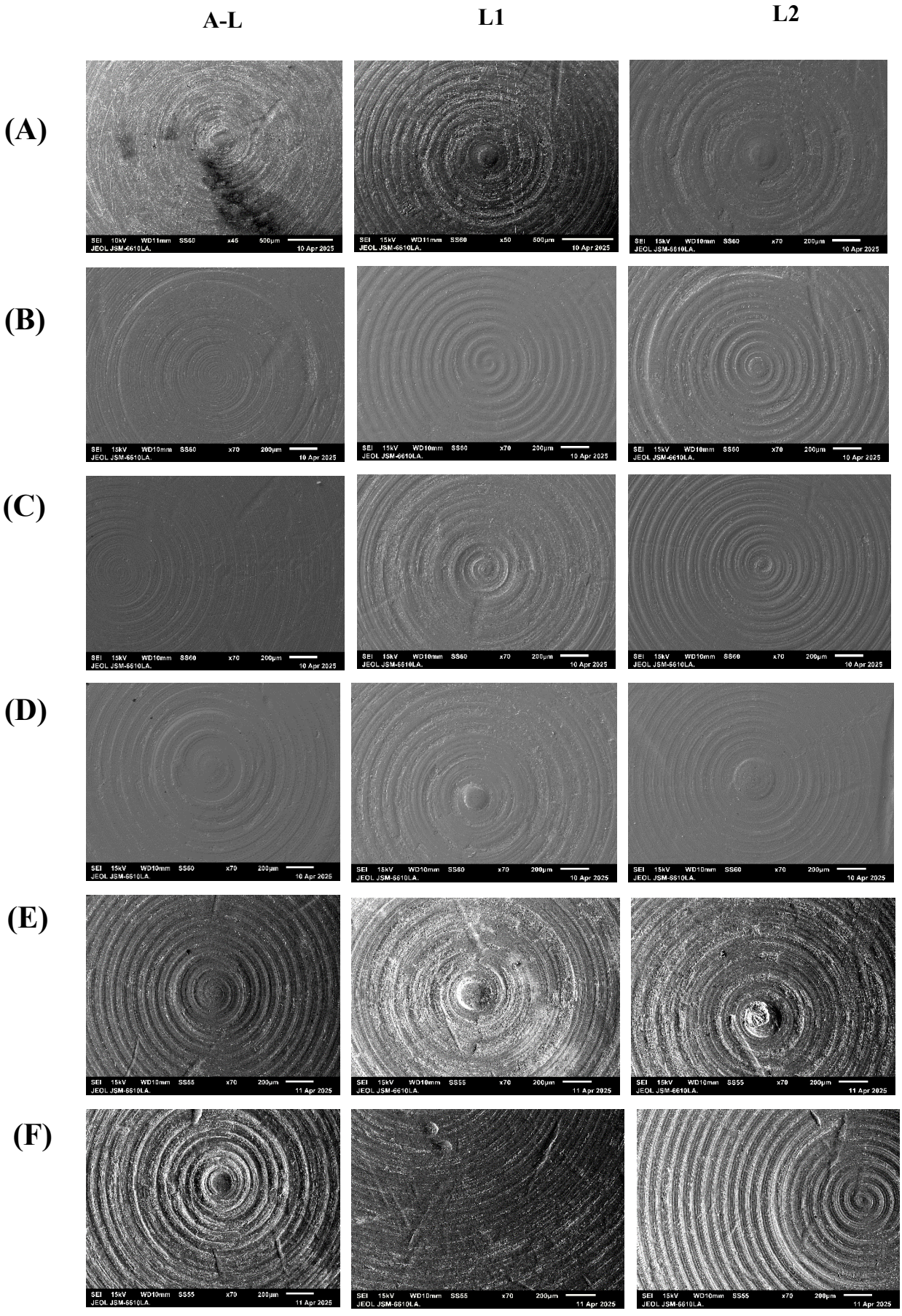
A-L
L1
L2
(A)
(B)
(C)
(D)
(E)
(F)

(G)

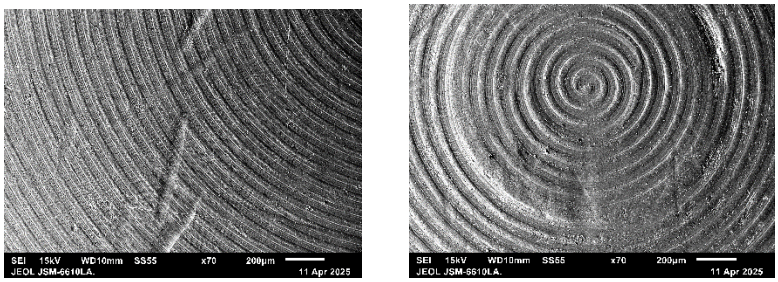

Figure 7.4 Scanning electron microscope images of (A) & (B) NaOH+ Enduro Zyme treated coupons of isolates 3SM and 20SM, (C) & (D) NaOH + Dual Zyme treated coupons of isolates 3SM and 20SM, (E) & (F) NaOH +Tri Zyme treated coupons of isolates 3SM and 20SM, (G) acid treated control coupons.

7.3.3 ATR-FTIR observations of EPS after treating with enzyme cleaners.

The EPS isolated after NaOH and NaOH + enzymes were observed under FTIR. A sterile stainless-steel coupon was used as a control. EPS isolated from the untreated biofilms was used to compare the remaining debris after NaOH and NaOH + enzymes. The amide I and amide II bands at 1650 and 1540 cm^{-1} were present in the untreated EPS. There was a less prominent peak of this wavelength present in the EPS isolated after NaOH cleaning (Fig. 7.5A and B). The peak at 1055 cm^{-1} represents the polysaccharides. This peak was still present in the EPS isolated after NaOH. The EPS isolated after NaOH+ enzymes showed the absence of the polysaccharide peaks, but there was a presence of a single protein peak (Fig. 7.5A and 5B). However, this peak was different from the one present in untreated samples. The EPS isolated after NaOH+ enzymes was not as clear as the control stainless steel. The enzymes used in the cleaning solutions might be responsible for the protein peaks. This suggests that the NaOH + enzymes leave enzyme debris after cleaning (The FTIR comparison of enzyme cleaners and the EPS isolated after treating with enzyme cleaners was added in the supplementary File 7.7).

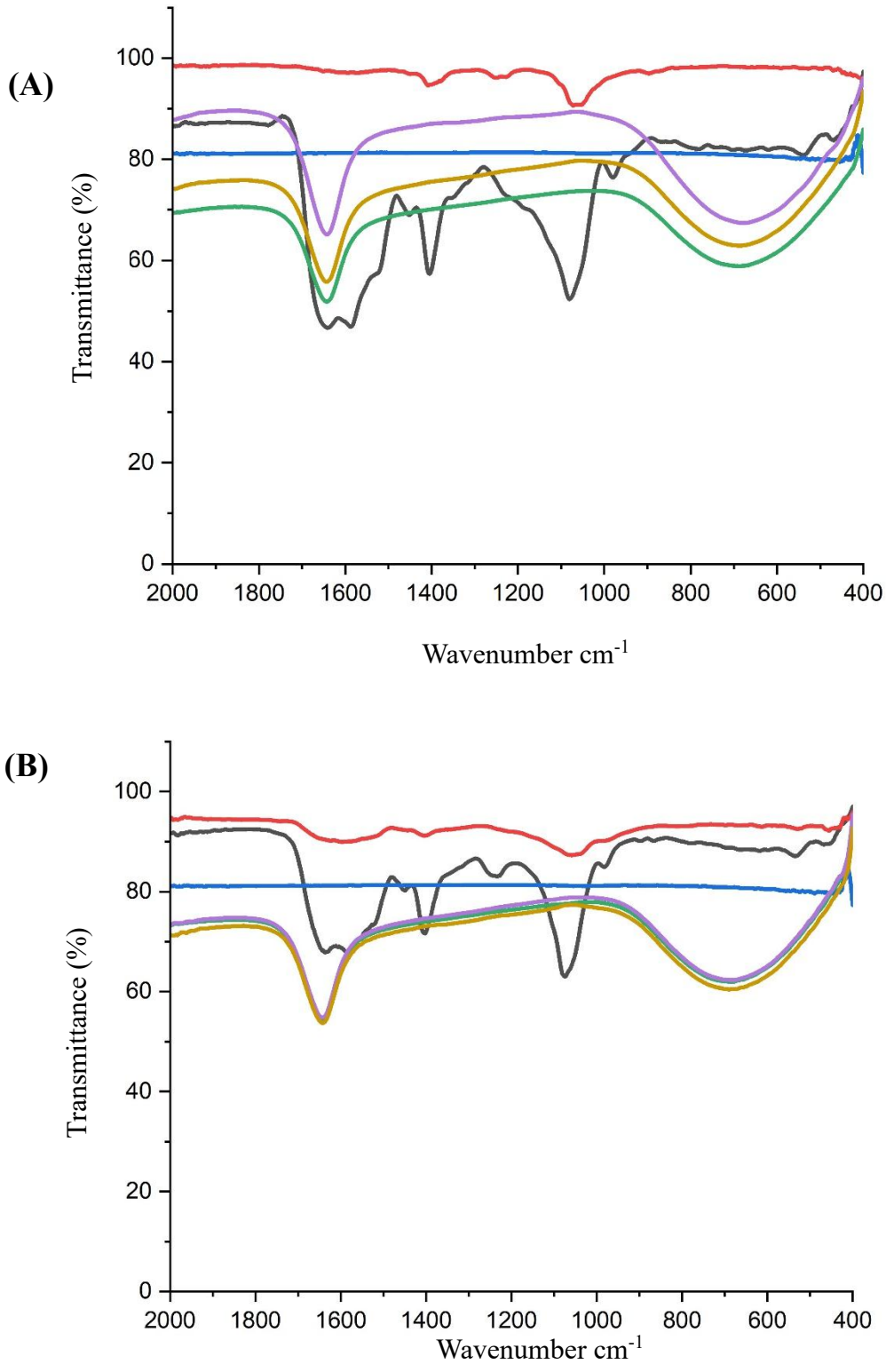
(A)
Transmittance (%)
100
80
60
40
20
0
2000
1800
1600
1400
1200
1000
800
600
400
Wavenumber cm-1
(B)
Transmittance (%)
100
80
60
40
20
0
2000
1800
1600
1400
1200
1000
800
600
400
Wavenumber cm-1
Control SS
Untreated EPS
EPS after NaOH
NaOH + Enduro Zyme
NaOH+ Dual Zyme
NaOH + Tri Zyme

Figure 7.5 ATR-FTIR images of untreated, NaOH, and NaOH+ Enzyme treated coupons of isolates (A) 3SM and (B) 20SM.

7.3.4 Regrowth

There was no appearance of air-liquid interface for both control coupons and NaOH + Enduro Zyme-treated coupons. The cell counts on the control coupons were significantly higher than the cell counts of coupons treated with NaOH + Enduro Zyme for both the isolates (Fig. 7.6 A and 7.6 B). The highest cell counts reached by isolate 3SM were 5.48 log CFU/cm^2 at the control A-L coupon (72h), while the highest cell counts for NaOH + Enduro Zyme-treated coupons were 4.84 log CFU/cm^2 at the A-L interface at 72 h (Fig. 7.6 A). For the isolate 20SM, the highest cell count reached by the control A-L coupons at 72 h was around 5.72 log CFU/cm^2, and the A-L NaOH + Enduro Zyme-treated coupon showed the highest cell count at 72h, which was 5.30 log CFU/cm^2 (Fig. 7.6 B). Compared to the isolated 3SM, 20SM established biofilms on NaOH + Enduro Zyme-treated coupons with cell counts closer to the control coupons. The NaOH + Enduro Zyme-treated coupons showed lower cell counts might be due to the adhering enzyme cleaner on the surface of the coupons, which prevented the initial adhesion of the biofilm cells.

(A)

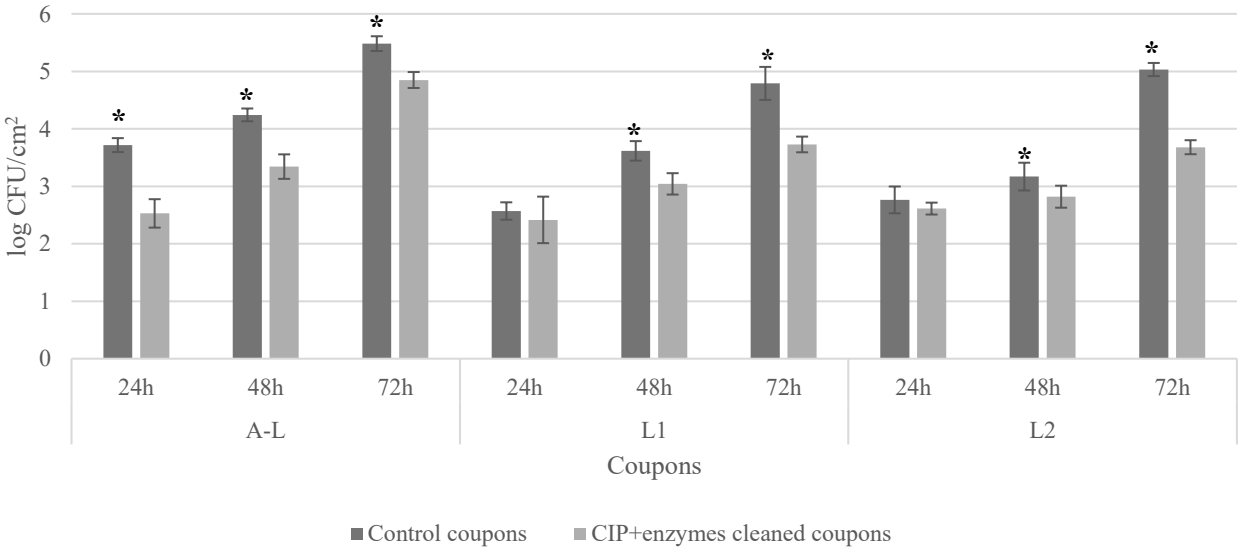

(B)

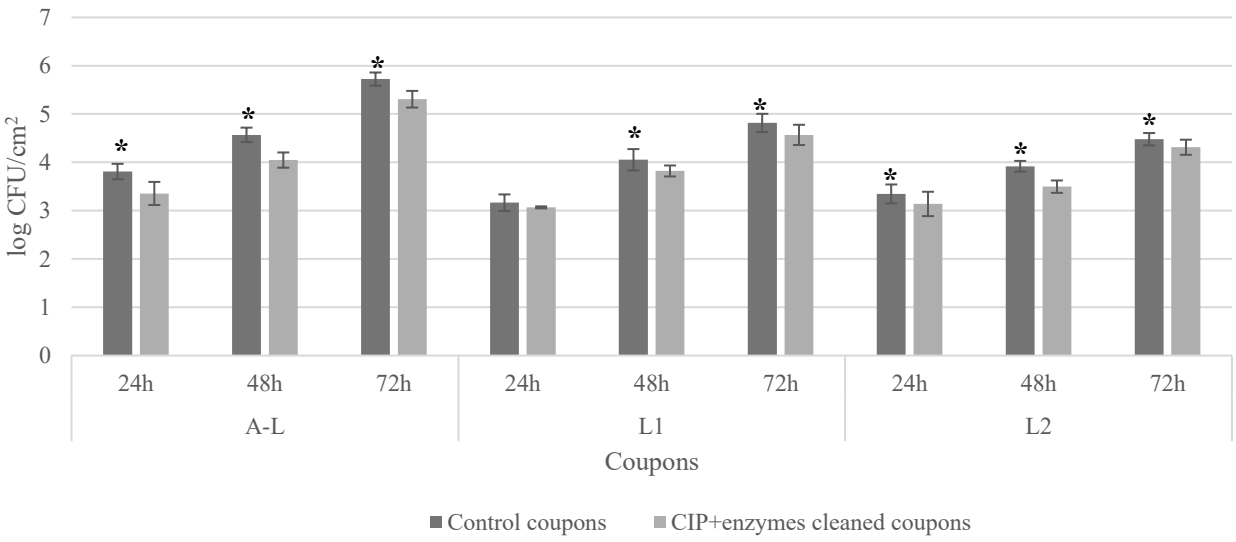

Figure 7.6 Graph (A) shows the regrowth of isolate 3SM after CIP+EnduroZyme cleaning, while graph (B) shows the regrowth of isolate 20SM. All results were expressed as mean ± standard deviation. The symbol (*) above each bar indicate significant differences ($p < 0.05$).

7.4 Discussion

In this present study, the following enzyme cleaners were compared: 1. The combination of amylase, protease, cellulase (Tri Zyme), 2. Protease and lipase (Dual Zyme), 3. Protease (Enduro Zyme). These effectively removed the biofilms. However, the enzyme cleaners could not disperse the biofilms completely. Microscopic observations showed similar results, with more dispersion seen using Enduro Zyme than with the other two enzymes. A study comparing the combination of enzyme cleaners against biofilms grown on PET and SS coupons showed that the highest removal percentage obtained was 82.9% by the formulation that consisted of amylase, protease, and lipase for the SS surface. Meanwhile, for the PET surface, the highest removal percentage was 82.6% for the same combination (Tsiaprazi-Stamou et al., 2019). However, this present study focused on the pseudomonad biofilms, and the study by Tsiaprazi-Stamou et al. (2019) was from the meat isolates, and different biofilms respond differently to the enzyme cleaners. This explains the importance of studying the biofilms in the food matrix of concern.

In this present study, when the biofilms were treated with NaOH and enzyme cleaners, the remaining cells were below the detectable limit (1.7 log CFU/cm^2). From these observations,

the application of enzyme cleaners with sanitisers or other cleaning agents is needed for effective cell reduction and possible re-colonisation of dispersed cells. In a study by Iñiguez-Moreno et al. (2021), when the alkaline protease and α-amylase (180 Modified Wohlgemuth unit/g for 30 min at 25ºC) were applied to the multispecies biofilms grown on the stainless-steel coupons, this resulted in 2- 3 log CFU/cm^2 reductions. However, when the enzyme treatment is combined with PAA (Peracetic Acid, 200mg/L for 10 min at 25ºC) and SBC (Sanicip Bio Control, 30g/L for 30 min at 25ºC), the log reduction was around 6.5 log CFU/cm^2.

In this present study, the sequential treatment using NaOH followed by enzyme cleaners resulted in a high log reduction and EPS footprint removal. In another study on multispecies biofilm removal, sequential treatment steps included alkali, surfactant 1, acid, enzyme, surfactant 2, and sanitisers (Singh & Anand, 2022). Among the tested bacteria in the multispecies consortia, around 1.13 ±0.03 log CFU/cm^2 *Bacillus* spp. cells remained. This sequential CIP treatment eliminated the *Enterococcus* spp. and *Escherichia coli*, but *Staphylococcus* spp., *Klebsiella* spp., and *Corynebacterium* spp. remained (0.05, 0.010, and 0.05 log CFU/cm^2). This observation also highlighted the use of sequential treatments in biofilm removal (Singh & Anand, 2022).

In this present study, the NaOH-treated EPS showed reduced intensities in protein and polysaccharide peaks compared to the untreated EPS. However, the FTIR observations of the EPS isolated after NaOH + Enzyme cleaners showed different peaks from the untreated EPS and NaOH-treated EPS. This data suggests that the NaOH + Enzyme cleaners removed the biofilm footprints. The different peaks most likely resulted from the enzyme cleaners, which were confirmed by the FTIR observations of the enzyme cleaners (Supplementary File 7.7).

In a study by Li et al. (2022b), the FTIR observations of *P. aeruginosa* biofilms treated with DDAB (Di Decylmethyl Ammonium Bromide) and SAEW (Slightly Acidic Electrolysed Water) showed reduced intensities compared to the untreated biofilms. The DDAB and SAEW combined treatment removes the biofilm structures of *P. aeruginosa,* and some of the small cell clusters remain on the surface (Li et al., 2022b). With a confocal microscope, the authors observed the reduction in green and blue fluorescence, which indicates the reduction in the EPS (Li et al., 2022b). In this present study, Enduro Zyme (Protease- subtilisin) was most effective among the three enzyme cleaners and resulted in around 4 log CFU/cm^2 reduction on the A-L coupons (Fig. 7.2 A &B). The coupons treated with Enduro Zyme alone

showed dispersed cells (Fig. 7.2 A &B). When combined with NaOH treatment, there was no debris when observed under an epifluorescence microscope. The Dual Zyme (Protease and lipase) and Tri Zyme (Protease, amylase, cellulase) showed some debris, which can be seen with epifluorescent microscopic images (Fig. 7.3 C-F). The SEM observations showed no cells after treating the biofilms with NaOH and enzyme cleaners. The role of NaOH here was to remove the cells, and the enzyme cleaners removed the EPS. This sequential application of NaOH and enzyme cleaners resulted in cell death and EPS reduction.

The NaOH + Enduro Zyme-treated coupons showed no debris and were chosen for the regrowth experiment. After the NaOH + Enduro Zyme treatment, the new inoculum was introduced, and the regrowth of the negative control and NaOH + Enduro Zyme-treated coupons was compared. The NaOH + Enduro Zyme-treated coupons resulted in significantly ($p < 0.05$) fewer cells compared to the control acid-treated coupons. The FTIR observations showed peaks other than EPS for the NaOH + Enzyme-treated coupons. This indicates the presence of enzymes on the surface. These enzymes could have prevented more cells from attaching to the NaOH + enzyme-treated coupons, resulting in lower cell numbers. This data suggests that the combined treatment can eliminate the mature biofilms and reduce the attachment of newer cells compared to the acid-treated coupons. Including enzyme cleaners in the CIP process would be able to control the pseudomonad biofilms under food processing conditions.

In this present study, the log difference between the control and NaOH + Enduro Zyme-treated coupons were around 0.5 to 1 log CFU/cm^2 for the isolate 3SM and 0.5 log CFU/cm^2 for the isolate 20SM. The enzyme cleaners can prevent biofilm formation. However, the interference of remaining enzymes on the food matrix needs to be considered. In the work by Li et al. (2022a), the coating of proteinase-K (45 U/mL) on the stainless-steel surface inhibited the biofilm formation by 58.6%. The difference between the control and enzyme-treated coupons was less than 2 log CFU/cm^2. However, the enzyme coating was not enough to prevent adhesion and biofilm formation completely (Li et al., 2022a).

In this present study, the cells were eliminated by NaOH and pasteurisation steps, and the remaining EPS footprints were eliminated by enzyme cleaners, resulting in less aggressive biofilm formation. Even after being treated with enzymes, the A-L coupons resulted in higher cell counts than L1 and L2, which indicates the importance of the air-liquid interface in the biofilm formation of pseudomonads. In a study by Cervantes-Huamán et al. (2025), the

Cinnamomum cassia essential oil combined with protease and amylase resulted in cell numbers lower than 1.45 log CFU/cm^2 for *Listeria monocytogenes* and *Salmonella* Typhimurium. However, the regrowth of these strains was more aggressive, suggesting the remaining debris encouraged the regrowth (Cervantes-Huamán et al., 2025).

7.5 Conclusion

The enzyme cleaners, when treated alone, cannot disperse the biofilms completely. However, when treated after the NaOH cleaning and the enzyme cleaners reduce the remaining biofilm footprints. The regrowth of the biofilms on the NaOH + Enzyme-treated coupons is reduced, indicating the effectiveness of enzyme cleaners in removing biofilm footprints. Sequential treatment with strategies targeting cells and EPS needs to be developed to prevent the biofilm regrowth on food contact surfaces. The enzyme cleaners were effective in removing the footprints. However, interaction with the food matrix, cost-effective production, and environmentally friendly cleaners need to be studied to ensure better biofilm removal.

7.6 References

Cervantes-Huamán, B. R. H., Vega-Sánchez, A., Rolón-Verdún, P., Gervilla-Cantero, G., Rodríguez-Jerez, J. J., & Ripolles-Avila, C. (2025). Effect of Cinnamomum cassia essential oil combined with enzymes on the elimination and regrowth potential of *Listeria monocytogenes* and *Salmonella enterica* biofilms formed on stainless steel surfaces. *Food Control*, *172*, 111120. https://doi.org/10.1016/j.foodcont.2024.111120.

Flemming, H.-C., & Wingender, J. (2010). The biofilm matrix. *Nature Reviews Microbiology*, *8*(9), 623–633. https://doi.org/10.1038/nrmicro2415.

Iñiguez-Moreno, M., Gutiérrez-Lomelí, M., & Avila-Novoa, M. G. (2021). Removal of Mixed-Species Biofilms Developed on Food Contact Surfaces with a Mixture of Enzymes and Chemical Agents. *Antibiotics*, *10*(8), 931. https://doi.org/10.3390/antibiotics10080931.

Jha, P. K., Dallagi, H., Richard, E., Benezech, T., & Faille, C. (2020). Formation and resistance to cleaning of biofilms at the air-liquid-wall interface. Influence of bacterial strain and material. *Food Control*, *118*, 107384. https://doi.org/10.1016/j.foodcont.2020.107384.

Khalid, S. J., Ain, Q., Khan, S. J., Jalil, A., Siddiqui, M. F., Ahmad, T., Badshah, M., & Adnan, F. (2022). Targeting Acyl Homoserine Lactones (AHLs) by the quorum quenching bacterial strains to control biofilm formation in *Pseudomonas aeruginosa*. *Saudi Journal of Biological Sciences*, *29*(3), 1673–1682. https://doi.org/10.1016/j.sjbs.2021.10.064.

Kiedrowski, M. R., & Horswill, A. R. (2011). New approaches for treating staphylococcal biofilm infections. *Annals of the New York Academy of Sciences*, *1241*(1), 104–121. https://doi.org/10.1111/j.1749-6632.2011.06281.x.

Lavrikova, A., Janda, M., Bujdáková, H., & Hensel, K. (2025). Eradication of single- and mixed-species biofilms of *Pseudomonas aeruginosa* and *Staphylococcus aureus* by pulsed streamer corona discharge cold atmospheric plasma. *Science of The Total Environment, 916*, 178184. https://doi.org/10.1016/j.scitotenv.2024.178184.

Li, Y., Dong, R., Ma, L., Qian, Y., & Liu, Z. (2022). Combined Anti-Biofilm Enzymes Strengthen the Eradicate Effect of *Vibrio parahaemolyticus* Biofilm: Mechanism on cpsA-J Expression and Application on Different Carriers. *Foods*, *11*(9), 1305. https://doi.org/10.3390/foods11091305.

Li, Y., Wang, H., Zheng, X., Li, Z., Wang, M., Luo, K., Zhang, C., Xia, X., Wang, Y., & Shi, C. (2022). Didecyldimethylammonium bromide: Application to control biofilms of *Staphylococcus aureus* and *Pseudomonas aeruginosa* alone and in combination with slightly acidic electrolyzed water. *Food Research International*, *157*, 111236. https://doi.org/10.1016/j.foodres.2022.111236.

Liu, J., Wu, S., Feng, L., Wu, Y., & Zhu, J. (2023). Extracellular matrix affects mature biofilm and stress resistance of psychrotrophic spoilage *Pseudomonas* at cold temperature. *Food Microbiology*, *112*, 104214. https://doi.org/10.1016/j.fm.2023.104214.

Molobela, I. P., Cloete, T. E., & Beukes, M. (2010). Protease and amylase enzymes for biofilm removal and degradation of extracellular polymeric substances (EPS) produced by *Pseudomonas fluorescens* bacteria.

Nahar, S., Mizan, M. F. R., Ha, A. J., & Ha, S. D. (2018). Advances and future prospects of enzyme-based biofilm prevention approaches in the food industry. *Comprehensive*

Reviews in Food Science and Food Safety, 17(6), 1484–1502. https://doi.org/10.1111/1541-4337.12382.

Neu, T. R., & Marshall, K. C. (1991). Microbial "footprints"—A new approach to adhesive polymers. *Biofouling*, *3*(2), 101–112. https://doi.org/10.1080/08927019109378166.

Nychas, G.-J. E., Skandamis, P. N., Tassou, C. C., & Koutsoumanis, K. P. (2008). Meat spoilage during distribution. *Meat Science*, *78*(1–2), 77–89. https://doi.org/10.1016/j.meatsci.2007.06.020.

Prabhukhot, G. S., Eggleton, C. D., Kim, M., & Patel, J. (2024). Impact of surface topography and hydrodynamic flow conditions on single and multispecies biofilm formation by *Escherichia coli* O157:H7 and *Listeria monocytogenes* in presence of promotor bacteria. *LWT*, *201*, 116240. https://doi.org/10.1016/j.lwt.2024.116240.

Raposo, A., Pérez, E., De Faria, C. T., Ferrús, M. A., & Carrascosa, C. (2016). Food Spoilage by *Pseudomonas* spp.—An Overview. In O. V. Singh (Ed.), *Foodborne Pathogens and Antibiotic Resistance* (1st ed., pp. 41–71). Wiley. https://doi.org/10.1002/9781119139188.ch3.

Shah, K., & Muriana, P. (2021). Efficacy of a Next Generation Quaternary Ammonium Chloride Sanitizer on *Staphylococcus* and *Pseudomonas* Biofilms and Practical Application in a Food Processing Environment. *Applied Microbiology*, *1*(1), 89–103. https://doi.org/10.3390/applmicrobiol1010008.

Singh, D., & Anand, S. (2022). Efficacy of a typical clean-in-place protocol against in vitro membrane biofilms. *Journal of Dairy Science*, *105*(12), 9417–9425. https://doi.org/10.3168/jds.2022-21712.

Stiefel, P., Mauerhofer, S., Schneider, J., Maniura-Weber, K., Rosenberg, U., & Ren, Q. (2016). Enzymes Enhance Biofilm Removal Efficiency of Cleaners. *Antimicrobial Agents and Chemotherapy*, *60*(6), 3647–3652. https://doi.org/10.1128/AAC.00400-16

Tsiaprazi-Stamou, A., Monfort, I. Y., Romani, A. M., Bakalis, S., & Gkatzionis, K. (2019). The synergistic effect of enzymatic detergents on biofilm cleaning from different surfaces. *Biofouling*, *35*(8), 883–899. https://doi.org/10.1080/08927014.2019.1666108.

Wang, S., Zhao, Y., Breslawec, A. P., Liang, T., Deng, Z., Kuperman, L. L., & Yu, Q. (2023). Strategy to combat biofilms: A focus on biofilm dispersal enzymes. *Npj Biofilms and Microbiomes*, *9*(1), 63. https://doi.org/10.1038/s41522-023-00427-y.

Wickramasinghe, N. N., Hlaing, M. M., Ravensdale, J. T., Coorey, R., Chandry, P. S., & Dykes, G. A. (2020). Characterization of the biofilm matrix composition of psychrotrophic, meat-spoilage pseudomonads. *Scientific Reports*, *10*(1), 16457. https://doi.org/10.1038/s41598-020-73612-0.

Yang, S., Wang, Y., Ren, F., Li, Z., & Dong, Q. (2023). Applying enzyme treatments in Bacillus cereus biofilm removal. *LWT*, *180*, 114667. https://doi.org/10.1016/j.lwt.2023.114667.

7.7 Supplementary File

7.7.1 ATR-FTIR observations of enzyme cleaners, and EPS isolated after cleaning with enzyme cleaners.

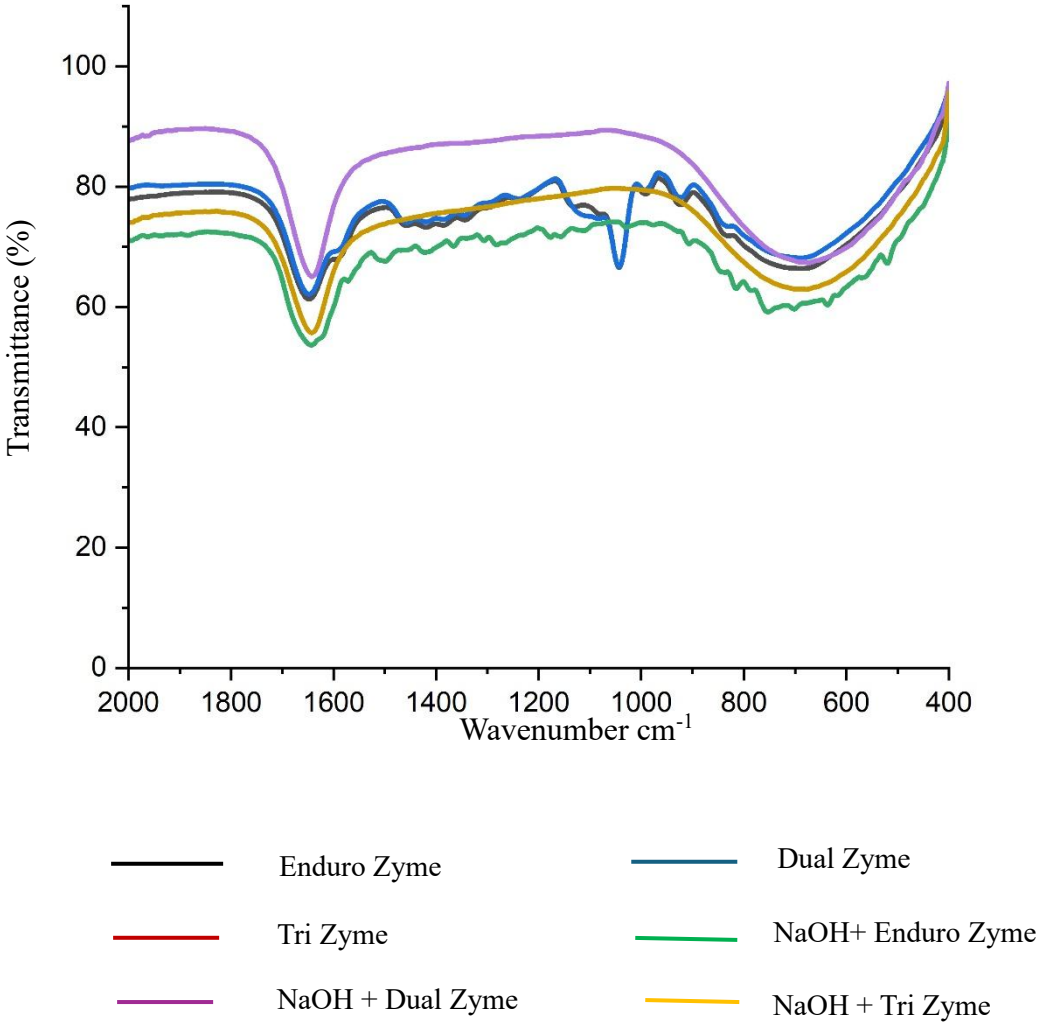

Chapter 8 Final Discussion

8.1 Final discussion

Pseudomonads are common and persistent psychrotropic spoilage bacteria in chilled food environments. The ability to form biofilms at low temperatures makes them difficult to control. From the literature, these bacteria produce robust biofilm EPS at cold temperatures (Liu et al., 2023, Wickramasinghe et al.,2020). However, this thesis demonstrates heterogeneity in biofilm formation, EPS matrix characteristics, and responses to cleaning and sanitation compared to previous studies. This present study collectively reveals how variability between isolates, surface characteristics, environmental conditions, including temperature and nutrient flow and finally how incomplete EPS removal supports the recurrence of these pseudomonad biofilms.

Chapter 3 emphasises the species-dependent biofilm formation of *Pseudomonas* species, though the isolates were obtained from the same source. Only two isolates form strong biofilms at both 30°C and 4°C, indicating that cold tolerance does not correlate with robust biofilm formation. The CRA revealed different EPS phenotypes among the isolates, and CRA is usually compared for the clinical isolates. This study expands the diversity of EPS in dairy-associated pseudomonads. These classical assays need to be combined with the crystal violet assay and cell counts to ensure biofilm formation. This study confirms the temperature-driven biofilm formation of these psychotropic pseudomonads, independent of surface type and nutrient conditions.

Another highlight from Chapter 3 is the difference in the biofilm formation between the surface types. The biofilm biomass observations from the crystal violet assay and cell counts provide very limited information on the EPS. Chapter 4 focused on the differences in the biofilm EPS composition and architecture between these two commonly observed surfaces in the food processing environments. The cells to EPS ratio was higher in the biofilms formed on the stainless-steel surfaces compared to the polystyrene surfaces. The adhered cells were higher on the polystyrene surfaces. However, the EPS quantity per cell was much higher on the stainless-steel surfaces. This chapter also confirms the temperature-driven biofilm formation of pseudomonads by comparing the cold temperatures to 30°C. Even the small difference in the temperatures of 4 and 7°C resulted in a huge difference in the EPS secretion. These insights reinforce the importance of studying these biofilms under realistic conditions to tackle these biofilms.

The comparison between air-liquid interface and submerged biofilms revealed that the air-liquid interface is a more favourable niche to colonise and form biofilms. In Chapter 5, the air-liquid interface exhibited higher cell count, EPS production, and significant upregulation of *alg K* and *bcs A* genes compared with submerged biofilms. The microscopical observations confirmed that the air-liquid interface is favoured for the adhesion and EPS production, and it occurred in the reactor even when it's not designed for this purpose. This finding highlights the critical gap in biofilm research methodologies, as submerged systems often lead to misinterpretation of the complexity of these biofilms in industrial settings.

The limitations of the CIP process are illustrated in Chapters 6 and 7. With water and NaOH, these cells can be killed, but these biofilms persist. The microscopical observations and FTIR revealed the underlying mechanisms, which are the EPS footprints left by these biofilms after CIP. The application of enzyme cleaners in Chapter 7 strengthens the findings that removal of protein and polysaccharide moieties from the surface results in reduced re-colonisation or regrowth compared to the acid-treated surfaces with no biofilm. These findings highlight the need to evaluate the sequential cleaning based on the long-term impact on cleaning and recolonisation of these biofilms.

Together, this study illustrates the complex biofilm-forming behaviour of psychotropic pseudomonads. The biofilm formation of these dairy isolates is highly variable and strongly influenced by temperature and surface conditions. This study stresses that the air-liquid interface is a high-risk site for biofilm formation of these isolates, and targeting both biofilm cells and EPS is a key to controlling consistent contamination by these isolates. These insights provide a foundation for designing more effective sanitation approaches and for future research that aims to disrupt the full biofilm life cycle in cold food-processing environments.

8.2 Limitations

1. Pseudomonads are psychrotrophic bacteria. However, not all the pseudomonads in this study formed strong biofilms. The strong biofilm formers are identified as cellulose producers. The importance of cellulose production at the air-liquid interface is well studied (Spiers et al., 2003; Koza et al., 2009). More dissolved oxygen at the psychrotrophic temperatures encourages the production of polysaccharides (Li et al.,

2022). The links between oxygen availability, cellulose production, and robust biofilm formation need to be studied at the molecular level.

2. This study analysed biofilm formation (Chapter 3), biofilm EPS composition (Chapter 4), NaOH, and enzyme cleaners for biofilm removal (Chapters 6& 7) with half-strength TSB as a medium. However, in food manufacturing, the growth medium for the biofilms is food debris. The role of food debris in the EPS matrix composition is still not answered. In a study with *Listeria monocytogenes* and its resistance to quaternary ammonium compounds, utilising salmon broth as a growth medium for biofilm, there was reduced penetration by QAC and more resistance compared to TSB (Tryptic Soy Broth) medium (Pang et al., 2019). In another study with *P. aeruginosa* and *L. monocytogenes,* chicken juice was used as a growth medium, and it supported the biofilm formation of *Pseudomonas* and resisted the biofilm formation of *Listeria* (Dong et al., 2022).
3. This study explored the pathway of EPS footprints acting as an attachment site for upcoming bacteria. However, the changes in the expression of EPS producing genes during footprint-mediated biofilm formation still need to be explored.
4. This study focused only on pseudomonads. Biofilms exist as multispecies communities in natural environments. In this situation, the contribution to building the EPS and providing public goods can play a major role in biofilm development. Some of the studies identified that pseudomonads contribute to the biofilm thickness and stress tolerance (Lee et al., 2017; Periasamy et al., 2015). Most of the polymicrobial studies focused on submerged biofilm formation. Studying these biofilms at the air-liquid interface can benefit industries where the air-liquid interface is commonly observed. Few multispecies biofilms focused on biofilm formation at cold temperatures; more studies are needed on biofilm formation at cold chain temperatures.
5. Typical NaOH cleaning eliminated the cells in the biofilm footprints chapter (Chapter 6). However, some bacteria can produce spores that survive high temperatures and cleaning chemicals. In this situation, the spores, heat-resistant cells, and biofilm EPS footprints together lead to different results. This study did not include a spore-forming bacterium, nor did it study its regrowth along with pseudomonad EPS footprints.
6. The regrowth was assessed only once after NaOH and NaOH enzyme cleaners. In a food processing environment, cleaning is ongoing. The cleaning and regrowth need to be monitored periodically to know the dynamics of these biofilms.

7. This study focused on mature biofilms, grown for over a week. This represents regions, such as T junctions, where access to cleaning chemicals is difficult, and it is undisturbed (Anand et al., 2014). However, there is a need to consider a shorter growth period with regular cleaning and regrowth over several cycles to understand the dynamics of cleaning and regrowth.
8. This study compared the air-liquid interface and submerged biofilms (Chapter 5). However, pellicles are also air-liquid interface biofilms that lack physical support (Dragoš et al., 2018). The mechanism behind pellicle formation needs to be studied. Pellicle formation in the present study was noticed only with static biofilms, not in the continuous biofilms. Few studies compare the pellicles and submerged biofilm formation. In *B. cereus* biofilms, the pellicles are formed from the submerged biofilm cells after oxygen depletion (Sanchez-Vizuete et al., 2022). Molecular mechanisms of this transition need to be studied.
9. This study identified that EPS footprints left by strong biofilm formers can support the biofilm formation of the weak isolates. Studying the biofilm formation of these isolates together would simulate natural conditions in which various cell types coexist.
10. This study explored the EPS matrix composition and identified the differences between temperatures. However, the rheological aspects of EPS were not studied.

8.3 Future work

1. Source of eDNA- autolysis or active secretion

Rationale: Different eDNA structures were identified in this study. However, with the sequencing data, it is hard to confirm whether the eDNA in these biofilms is derived from dead cells or actively secreted into them.

Objectives: To understand the mechanism of eDNA formation.

Approaches:

Using fluorescent probes to track the eDNA from 0h to the mature biofilm stage.

2. Molecular mechanisms behind air-liquid interface biofilms

Rationale: The air-liquid interface encourages higher EPS production, but the molecular pathways need to be studied.

Objective: To identify the key genes and molecular pathways involved in the air-liquid interface biofilm formation.

Approaches: Comparing the air-liquid interface and submerged biofilms in terms of proteomics and transcriptomics.

Validate the candidate genes by knockouts.

3. EPS can enhance the recolonisation

Rationale: The EPS footprints can enhance the biofilm formation of new colonisers. However, in this present study, the footprints are what is left after cleaning with NaOH crystals and enzymes. It is important to study the effects of EPS alone without any possible residual NaOH or enzymes.

Objectives: To determine the regrowth of the isolates' EPS free from NaOH or other chemicals.

Approaches:

Alternate approaches, such as sonication or heat treatment, to eliminate the cells and analyse the recolonisation.

The gene expression changes need to be studied during EPS mediated regrowth.

8.4 Final conclusions

Pseudomonads are common psychrotrophic spoilage bacteria that can form biofilms at psychrotrophic temperatures. This study identified two strong biofilm formers at both 4 and 30ºC, and both are cellulose producers. The EPS production was higher at 4ºC and 7ºC, compared to 30ºC. This is an important consideration for the food industry that relies on refrigeration to control microbial contamination. The substrate surface can modify the biofilm architecture, shown by the formation of eDNA as channels on the stainless-steel surface and threadlike structures on the polystyrene surface. This may influence biofilm control. This study also identified that pseudomonads form strong biofilms at the air-liquid interface, another likely implication for biofilm control. Compared to submerged coupons, the air-liquid interface encouraged higher cell counts, EPS production, and biofilm thickness. The EPS producing genes are more upregulated in the air-liquid interface biofilms than in submerged biofilms. Typical NaOH cleaning was simulated in the laboratory using hot water and sodium

hydroxide, leaving EPS footprints on both A-L and submerged coupons. The EPS footprints encouraged aggressive biofilm formation and the early appearance of biofilm growth at the air-liquid interface when a new inoculum was introduced. The EPS footprints encouraged the biofilm formation of both strong and weak biofilm formers. Sequential cleaning with NaOH and enzyme cleaners removes the biofilm footprints. Sequential applications targeting both cells and the EPS need to be developed. This study has demonstrated the importance of EPS produced by pseudomonads in biofilm persistence.

8.4 References

Anand, S., Singh, D., Avadhanula, M., & Marka, S. (2014). Development and Control of Bacterial Biofilms on Dairy Processing Membranes. *Comprehensive Reviews in Food Science and Food Safety*, *13*(1), 18–33. https://doi.org/10.1111/1541-4337.12048

Behzadi, P., Gajdács, M., Pallós, P., Ónodi, B., Stájer, A., Matusovits, D., Kárpáti, K., Burián, K., Battah, B., Ferrari, M., Doria, C., Caggiari, G., Khusro, A., Zanetti, S., & Donadu, M. G. (2022). Relationship between Biofilm-Formation, Phenotypic Virulence Factors and Antibiotic Resistance in Environmental Pseudomonas aeruginosa. *Pathogens*, *11*(9), 1015. https://doi.org/10.3390/pathogens11091015

Buckner, E., Buckingham-Meyer, K., Miller, L. A., Parker, A. E., Jones, C. J., & Goeres, D. M. (2024). Coupon position does not affect Pseudomonas aeruginosa and Staphylococcus aureus biofilm densities in the CDC biofilm reactor. *Journal of Microbiological Methods*, *223*, 106960. https://doi.org/10.1016/j.mimet.2024.106960

Campoccia, D., Montanaro, L., & Arciola, C. R. (2021). Tracing the origins of extracellular DNA in bacterial biofilms: Story of death and predation to community benefit. *Biofouling*, *37*(9–10), 1022–1039. https://doi.org/10.1080/08927014.2021.2002987

Chung, J., Eisha, S., Park, S., Morris, A. J., & Martin, I. (2023). How Three Self-Secreted Biofilm Exopolysaccharides of Pseudomonas aeruginosa, Psl, Pel, and Alginate, Can Each Be Exploited for Antibiotic Adjuvant Effects in Cystic Fibrosis Lung Infection. *International Journal of Molecular Sciences*, *24*(10), 8709. https://doi.org/10.3390/ijms24108709

Dong, Q., Sun, L., Fang, T., Wang, Y., Li, Z., Wang, X., Wu, M., & Zhang, H. (2022). Biofilm Formation of Listeria monocytogenes and Pseudomonas aeruginosa in a

Simulated Chicken Processing Environment. *Foods*, *11*(13), 1917. https://doi.org/10.3390/foods11131917

Dragoš, A., Martin, M., Falcón García, C., Kricks, L., Pausch, P., Heimerl, T., Bálint, B., Maróti, G., Bange, G., López, D., Lieleg, O., & Kovács, Á. T. (2018). Collapse of genetic division of labour and evolution of autonomy in pellicle biofilms. *Nature Microbiology*, *3*(12), 1451–1460. https://doi.org/10.1038/s41564-018-0263-y

Dueholm, M. S., Petersen, S. V., Sønderkær, M., Larsen, P., Christiansen, G., Hein, K. L., Enghild, J. J., Nielsen, J. L., Nielsen, K. L., Nielsen, P. H., & Otzen, D. E. (2010). Functional amyloid in *Pseudomonas*. *Molecular Microbiology*, *77*(4), 1009–1020. https://doi.org/10.1111/j.1365-2958.2010.07269.x

Koza, A., Hallett, P. D., Moon, C. D., & Spiers, A. J. (2009). Characterization of a novel air–liquid interface biofilm of Pseudomonas fluorescens SBW25. *Microbiology*, *155*(5), 1397–1406. https://doi.org/10.1099/mic.0.025064-0

Lee, K., Lee, K.-M., Kim, D., & Yoon, S. S. (2017). Molecular Determinants of the Thickened Matrix in a Dual-Species Pseudomonas aeruginosa and Enterococcus faecalis Biofilm. *Applied and Environmental Microbiology*, *83*(21), e01182-17. https://doi.org/10.1128/AEM.01182-17

Li, W., Siddique, M. S., Graham, N., & Yu, W. (2022). Influence of Temperature on Biofilm Formation Mechanisms Using a Gravity-Driven Membrane (GDM) System: Insights from Microbial Community Structures and Metabolomics. *Environmental Science & Technology*, *56*(12), 8908–8919. https://doi.org/10.1021/acs.est.2c01243

Liu, J., Wu, S., Feng, L., Wu, Y., & Zhu, J. (2023). Extracellular matrix affects the mature biofilm and stress resistance of psychrotrophic spoilage Pseudomonas at cold temperature. *Food Microbiology*, *112*, 104214. https://doi.org/10.1016/j.fm.2023.104214

Mann, E. E., & Wozniak, D. J. (2012). *Pseudomonas* biofilm matrix composition and niche biology. *FEMS Microbiology Reviews*, *36*(4), 893–916. https://doi.org/10.1111/j.1574-6976.2011.00322.x

Pang, X., Wong, C., Chung, H.-J., & Yuk, H.-G. (2019). Biofilm formation of Listeria monocytogenes and its resistance to quaternary ammonium compounds in a simulated

salmon processing environment. *Food Control*, *98*, 200–208. https://doi.org/10.1016/j.foodcont.2018.11.029

Periasamy, S., Nair, H. A. S., Lee, K. W. K., Ong, J., Goh, J. Q. J., Kjelleberg, S., & Rice, S. A. (2015). Pseudomonas aeruginosa PAO1 exopolysaccharides are important for mixed species biofilm community development and stress tolerance. *Frontiers in Microbiology*, *6*. https://doi.org/10.3389/fmicb.2015.00851

Sanchez-Vizuete, P., Dergham, Y., Bridier, A., Deschamps, J., Dervyn, E., Hamze, K., Aymerich, S., Le Coq, D., & Briandet, R. (2022). The coordinated population redistribution between Bacillus subtilis submerged biofilm and liquid-air pellicle. *Biofilm*, *4*, 100065. https://doi.org/10.1016/j.bioflm.2021.100065

Sauer, K. (Ed.). (2017). *c-di-GMP Signaling: Methods and Protocols* (Vol. 1657). Springer New York. https://doi.org/10.1007/978-1-4939-7240-1

Singh, D., & Anand, S. (2022). Efficacy of a typical clean-in-place protocol against in vitro membrane biofilms. *Journal of Dairy Science*, *105*(12), 9417–9425. https://doi.org/10.3168/jds.2022-21712

Spiers, A. J., Bohannon, J., Gehrig, S. M., & Rainey, P. B. (2003). Biofilm formation at the air–liquid interface by the *Pseudomonas fluorescens* SBW25 wrinkly spreader requires an acetylated form of cellulose. *Molecular Microbiology*, *50*(1), 15–27. https://doi.org/10.1046/j.1365-2958.2003.03670.x

Wickramasinghe, N. N., Hlaing, M. M., Ravensdale, J. T., Coorey, R., Chandry, P. S., & Dykes, G. A. (2020). Characterization of the biofilm matrix composition of psychrotrophic, meat-spoilage pseudomonads. *Scientific Reports*, *10*(1), 16457. https://doi.org/10.1038/s41598-020-73612-0.

Appendices

Appendix I. Statement of contribution- Chapter 2

MASSEY UNIVERSITY
TE KUNENGA KI PŪREHUROA
UNIVERSITY OF NEW ZEALAND

GRADUATE RESEARCH SCHOOL

STATEMENT OF CONTRIBUTION
DOCTORATE WITH PUBLICATIONS/MANUSCRIPTS

We, the student and the student's main supervisor, certify that all co-authors have consented to their work being included in the thesis and they have accepted the student's contribution as indicated below in the Statement of Originality.	
Student name:	Srinithi Muthuraman
Name and title of main supervisor:	Steve Flint
In which chapter is the manuscript/published work?	Chapter 2
Describe the contribution that the student and members of the supervisory team have made to the manuscript/published work:[1] Srinithi Muthuraman: Conceptualization,Writing- original draft, review, and editing; Steve Flint & Jon Palmer: Supervision, Writing- review and editing.	
Please select one of the following three options:	
○ The manuscript/published work is published or in press Please provide the full reference of the research output:	
◉ The manuscript is currently under review for publication Please provide the name of the journal: Food Bioscience	
○ It is intended that the manuscript will be published, but it has not yet been submitted to a journal	
Student's signature:	Srinithi Muthuraman Digitally signed by Srinithi Muthuraman Date: 2025.06.09 13:17:05 +12'00'
Main supervisor's signature:	Steve Flint Digitally signed by Steve Flint Date: 2025.06.12 09:39:56 +12'00'
This form should be placed at the beginning of each relevant thesis chapter.	

[1] Refer to the Massey University Publishing and Authorship guidelines (OneMassey for staff, Stream for students) and/ or Contributor Roles Taxonomy (CRediT) guidelines for guidance.

Appendix II. Statement of contribution- Chapter 3

MASSEY UNIVERSITY
TE KUNENGA KI PŪREHUROA
UNIVERSITY OF NEW ZEALAND

GRADUATE RESEARCH SCHOOL

STATEMENT OF CONTRIBUTION DOCTORATE WITH PUBLICATIONS/MANUSCRIPTS

We, the student and the student's main supervisor, certify that all co-authors have consented to their work being included in the thesis and they have accepted the student's contribution as indicated below in the Statement of Originality.

Student name:	Srinithi Muthuraman
Name and title of main supervisor:	Steve Flint
In which chapter is the manuscript/published work?	Chapter 3

Describe the contribution that the student and members of the supervisory team have made to the manuscript/published work:[1]

Srinithi Muthuraman: Conceptualization, Investigation, formal analysis, Writing- original draft, review, and editing; Steve Flint & Jon Palmer: Supervision, Writing- review and editing.

Please select one of the following three options:

○ The manuscript/published work is published or in press

Please provide the full reference of the research output:

◉ The manuscript is currently under review for publication

Please provide the name of the journal:

International Journal of Foodscience and Technology.

○ It is intended that the manuscript will be published, but it has not yet been submitted to a journal

Student's signature:	Srinithi Muthuraman Digitally signed by Srinithi Muthuraman Date: 2025.06.09 13:15:54 +12'00'	Main supervisor's signature:	Steve Flint Digitally signed by Steve Flint Date: 2025.06.12 09:40:21 +12'00'

This form should be placed at the beginning of each relevant thesis chapter.

[1] Refer to the Massey University Publishing and Authorship guidelines (OneMassey for staff, Stream for students) and/ or Contributor Roles Taxonomy (CRediT) guidelines for guidance.

Appendix III. Statement of contribution- Chapter 4

MASSEY UNIVERSITY
TE KUNENGA KI PŪREHUROA
UNIVERSITY OF NEW ZEALAND

GRADUATE RESEARCH SCHOOL

STATEMENT OF CONTRIBUTION
DOCTORATE WITH PUBLICATIONS/MANUSCRIPTS

We, the student and the student's main supervisor, certify that all co-authors have consented to their work being included in the thesis and they have accepted the student's contribution as indicated below in the Statement of Originality.

Student name:	Srinithi Muthuraman
Name and title of main supervisor:	Steve Flint
In which chapter is the manuscript/published work?	Chapter 4

Describe the contribution that the student and members of the supervisory team have made to the manuscript/published work:[1]

Please select one of the following three options:

- (●) **The manuscript/published work is published or in press**
  Please provide the full reference of the research output:
  Srinithi Muthuraman: Writing -original draft, review, and editing; Steve Flint& Jon Palmer: Supervision, Writing-review and editing.
- ( ) **The manuscript is currently under review for publication**
  Please provide the name of the journal:
- ( ) **It is intended that the manuscript will be published, but it has not yet been submitted to a journal**

Student's signature:	Srinithi Muthuraman Digitally signed by Srinithi Muthuraman Date: 2025.06.09 12:41:41 +12'00'	Main supervisor's signature:	Steve Flint Digitally signed by Steve Flint Date: 2025.06.12 09:41:11 +12'00'

This form should be placed at the beginning of each relevant thesis chapter.

[1] Refer to the Massey University Publishing and Authorship guidelines (OneMassey for staff, Stream for students) and/ or Contributor Roles Taxonomy (CRediT) guidelines for guidance.

Appendix IV. Statement of contribution- Chapters 5&6

MASSEY UNIVERSITY
TE KUNENGA KI PŪREHUROA
UNIVERSITY OF NEW ZEALAND

GRADUATE RESEARCH SCHOOL

STATEMENT OF CONTRIBUTION DOCTORATE WITH PUBLICATIONS/MANUSCRIPTS

We, the student and the student's main supervisor, certify that all co-authors have consented to their work being included in the thesis and they have accepted the student's contribution as indicated below in the Statement of Originality.

Student name:	Srinithi Muthuraman
Name and title of main supervisor:	Steve Flint
In which chapter is the manuscript/published work?	Chapter 5&6

Describe the contribution that the student and members of the supervisory team have made to the manuscript/published work:[1]

Srinithi Muthuraman: Conceptualization, Investigation, formal analysis, Writing- original draft, review, and editing; Steve Flint & Jon Palmer: Supervision, Writing- review and editing.

Please select one of the following three options:

- ○ The manuscript/published work is published or in press
  Please provide the full reference of the research output:
- ◉ The manuscript is currently under review for publication
  Please provide the name of the journal:
  Food Research International.
- ○ It is intended that the manuscript will be published, but it has not yet been submitted to a journal

Student's signature:	Srinithi Muthuraman Digitally signed by Srinithi Muthuraman Date: 2025.06.09 13:10:16 +12'00'	Main supervisor's signature:	Steve Flint Digitally signed by Steve Flint Date: 2025.06.12 09:41:39 +12'00'

This form should be placed at the beginning of each relevant thesis chapter.

[1] Refer to the Massey University Publishing and Authorship guidelines (OneMassey for staff, Stream for students) and/ or Contributor Roles Taxonomy (CRediT) guidelines for guidance.

Appendix V. Statement of contribution- Chapters 5&7

MASSEY UNIVERSITY
TE KUNENGA KI PŪREHUROA
UNIVERSITY OF NEW ZEALAND

GRADUATE RESEARCH SCHOOL

STATEMENT OF CONTRIBUTION
DOCTORATE WITH PUBLICATIONS/MANUSCRIPTS

We, the student and the student's main supervisor, certify that all co-authors have consented to their work being included in the thesis and they have accepted the student's contribution as indicated below in the Statement of Originality.

Student name:	Srinithi Muthuraman
Name and title of main supervisor:	Steve Flint
In which chapter is the manuscript/published work?	Chapter 5&7

Describe the contribution that the student and members of the supervisory team have made to the manuscript/published work:[1]

Srinithi Muthuraman: Conceptualization, Investigation, formal analysis, Writing- original draft, review, and editing; Steve Flint & Jon Palmer: Supervision, Writing- review and editing.

Please select one of the following three options:

- ○ The manuscript/published work is published or in press
  Please provide the full reference of the research output:
- ○ The manuscript is currently under review for publication
  Please provide the name of the journal:
- ◉ It is intended that the manuscript will be published, but it has not yet been submitted to a journal

Student's signature:	Srinithi Muthuraman Digitally signed by Srinithi Muthuraman Date: 2025.06.09 13:20:29 +12'00'	Main supervisor's signature:	Steve Flint Digitally signed by Steve Flint Date: 2025.06.12 09:42:03 +12'00'

This form should be placed at the beginning of each relevant thesis chapter.

[1] Refer to the Massey University Publishing and Authorship guidelines (OneMassey for staff, Stream for students) and/ or Contributor Roles Taxonomy (CRediT) guidelines for guidance.